Skolkovo Institute of Science and Technology

DEVELOPMENT OF THERMODYNAMIC MODELS FOR PHASE EQUILIBRIA OF WATER-ICE-GAS-HYDRATE IN AQUEOUS SOLUTIONS OF INHIBITORS AND IN POROUS MEDIA

Doctoral Thesis

by

DARIA SERGEEVA

DOCTORAL PROGRAM IN PETROLEUM ENGINEERING

Supervisor
Dr. Vladimir Istomin

Moscow - 2021

I hereby declare that the work presented in this thesis was carried out by myself at Skolkovo Institute of Science and Technology, Moscow, except where due acknowledgement is made, and has not been submitted for any other degree.

Candidate (Daria Sergeeva)

Supervisor (Dr. Vladimir Istomin)

Abstract

The thesis is devoted to phase equilibria of gas hydrates in porous media (pore water in the soils and sediments) and hydrate inhibitors in field systems. Literature review was presented for physicochemical properties and thermodynamics of gas hydrates. The new approach for thermodynamic consistency and checking of the experimental data was proposed. The smoothed reference data of the equilibria "gas – ice – hydrate" and "gas – liquid water – hydrate" were obtained. A simple correlation between three phase equilibria of gas hydrates with ice and supercooled water has been established. The technique for gas pressure influence on freezing temperature of pore water in frozen soils as well as on unfrozen water amount was developed (external gas pressure, salinity pore water and its activity, gas solubility in pore water were taken into account). As example, the thermodynamic model of increasing gas pressure during the freezing of closed gas-saturated talik was considered (modeling of crater formation at permafrost zone). The analytical dependencies are proposed for calculation of the of non-clathrate water content (pore water in equilibrium with gas hydrates) depending on the gas pressure from the known data on the pore water activity in the samples of soils at atmospheric pressure. The calculations of non-clathrate water for hydrate-containing samples of kaolinite clay showed a good agreement with the experimental contact method.

The application of hydrate inhibitors also is an important topic of the thesis. It has been developed more general correlations, which connect water activity with the temperature shift ΔT of hydrate formation in aqueous inhibitor solutions (at fixed fugacity/pressure) as well as the fugacity/pressure shift of hydrate formation (at fixed temperature). The properties of mixed inhibitor "methanol + magnesium chloride" were studied by experimental and calculation methods. On the base of obtained experimental data, it was established two reliable correlations for mixed inhibitors influence on hydrate formation. The properties of mixed "kinetic + thermodynamic" inhibitors on the examples of "PVP + NaCl" and "PVP + $MgCl_2$" solutions were studied. The experimental data on water activity at these mixed inhibitors were obtained.

The hydrate control at the Yarakta oil and gas condensate fields located in East Siberia was analyzed. A technique for calculating the methanol consumption, which take into account the formation water producing by the wells and risk of the halite precipitation, has been developed. Also, the heat-insulated in-field pipeline operation of the Yamburg gas field (Cenomanian horizons) in winter season was discussed. The cases were revealed when there is no ice or hydrate operation regime inside the gas stream, nevertheless, ice/hydrate can be deposited on the internal wall of the pipe.

Publications

Journal publications:

1. **Sergeeva D.**, Istomin V., Chuvilin E., Bukhanov B., Sokolova N., Influence of hydrate-forming gas pressure on equilibrium pore water content in soils, *Energies*, 2021, 14(7), 1841, https://doi.org/10.3390/en14071841, Impact Factor: 3.085.
2. **Sergeeva D.**, Krapivin V., Istomin V., Dolgaev S., Prokopov A., Kwon V., Gerasimov Yu., Monoethylene glycol as a gas hydrate inhibitor: thermodynamic analysis, *Vesti gazovoy nauki*, Moscow, 2 (47), 2021, pp. 156-164, RINTS.
3. Salikhov R., Chertovskikh E., Gilmutdinov B., Lebedeva I., Shabanov A., Istomin V., Kwon V., Krapivin V., **Sergeeva D.**, Improving the efficiency of measures to prevent hydrate formation at the Yaraktinskoye oil-gas-condensate field, *Oil Industry Journal*, № 9, 2020, pp. 50-54, https://doi.org/10.24887/0028-2448-2020-9-50-54, WoS/Scopus indexed journal.
4. Istomin V., Chuvilin E., **Sergeeva D.**, Bukhanov B., Badetz Ch., Stanilovskaya Yu., Thermodynamics of freezing soil closed system saturated with gas and water, *Cold Regions Science and Technology*, 2019, doi.org/10.1016/j.coldregions.2019.102901. Impact Factor: 2.767.
5. Chuvilin E., Davletshina D., Bukhanov B., Grebenkin S., Istomin V., **Sergeeva D.**, Badetz Ch., Stanilovskaya Yu., Effect of gas composition and pressure on pore water freezing point in gas-saturated sediments: an experimental study, *Earth's Cryosphere*, 2019, v. XXIII, № 5, pp. 49–57, (in Russian), doi.org/10.21782/KZ1560-7496-2019-5(49-57), indexed in Scopus, Russian, Impact factor RINTS 1.199.
6. Semenov A., Stoporev A., Mendgaziev R., Gushchin P., Khlebnikov V., Yakushev V., Istomin V., **Sergeeva D**., Vinokurov V., Synergistic effect of salts and methanol in thermodynamic inhibition of sII gas hydrates, *Journal of Chemical Thermodynamics*, Volume 137, October 2019, pp. 119-130, doi.org/10.1016/j.jct.2019.05.013. Impact Factor: 2.290.

7. Stoporev A., Semenov A., Medvedev V., Mendgaziev R., Istomin V., **Sergeeva D.**, Manakov A., Vinokurov V., Formation and agglomeration of gas hydrates in gas – organic liquid – water systems in a stirred reactor: Role of resins/ asphaltenes/ surfactants, *Journal of Petroleum Science and Engineering*, Volume 176, May 2019, pp. 952-961, doi.org/10.1016/j.petrol.2019.02.002. Impact Factor 2.886.
8. Istomin V., Chuvilin E., **Sergeeva D.**, Buhkanov B., Stanilovskaya Yu., Badetz C., Influence of composition and external gas pressure on ice and hydrate formation in gas–saturated pore solutions, *Oil&Gas Chemistry*, №2, 2018, pp. 33-42, (In Russ.) RINTS, doi.org/10.24411/2310-8266-2018-10206.
9. **Sergeeva D.**, Kudiyarov G., Features of the operation of the infield gas gathering systems of the Cenomanian deposits of the Yamburg OGCF in the presence of hydrate or ice deposits, *Transport and storage of oil products and hydrocarbons*, 2018, pp. 33-42, (In Russ.) RINTS, doi.org/10.24411/0131-4270-2018-10506.
10. **Sergeeva D.**, Istomin V., Thermodynamics of methane hydrate, *Proceedings of the Skoltech Energy PhD Seminar*, Moscow, 2018, pp. 30-38.

Conference proceedings:

1. Krapivin V., **Sergeeva D.**, Istomin V., Dolgaev S., Prokopov A., Kwon V., Gerasimov Yu., The features of monoethylene glycol rationing as a hydrate formation inhibitor, Gazprom «VNIIGAZ» III Conference, Current Research Issues Oil and Gas Formation Systems (SPRS-2020), September 23-24, 2020, pp. 28.
2. Istomin V., Chuvilin E., **Sergeeva D.**, Buhkanov B., Stanilovskaya Yu., Badetz C., Thermodynamic calculation of freezing temperature of gas-saturated pore water in talik zones, 5th European Conference on Permafrost (EUCOP 2018) – Book of Abstracts, 23 June - 1 July 2018 Chamonix, France, 2018, pp. 480–481.

3. Kudiyarov G., Istomin V., Egorichev A., Stonozhenko I., Rotov A, **Sergeeva D.**, Peculiarities of the in-field gas gathering systems at the latest stage of the development of cenomanian deposit Yamburgskoye gas field, SPE-187736-MS, SPE-187736-RU, *SPE Russian Petroleum Technology Conference*, 16-18 October 2017, Moscow, Russia, doi.org/10.2118/187736-MS.
4. **Sergeeva D.**, Istomin V., "Hydrate equilibria of pure gases: thermodynamic correction of experimental data", abstract, 10th International Conference on Gas Hydrates (ICGH10), June 21-26, 2020, Singapore, submitted (postponed to July 2023).
5. Istomin V., Chuvilin E., **Sergeeva D.**, Bukhanov B., Sokolova N., Merkulova M., Mahankali V., "Influence of gas pressure on the equilibrium pore water content in hydrate bearing sediments", abstract, 10th International Conference on Gas Hydrates (ICGH10), June 21-26, 2020, Singapore, submitted, (postponed to July 2023).
6. Semenov A., Mendgaziev R., Stoporev A., Khlebnikov V., **Sergeeva D.**, Istomin V., "Methane hydrate phase equilibria and ice freezing point measurements for methanol and magnesium chloride aqueous solutions", abstract, 10th International Conference on Gas Hydrates (ICGH10), June 21-26, 2020, Singapore, submitted, (postponed to July 2023).

Acknowledgments

I would like to thank my research supervisor Prof. Vladimir Istomin, for his patient guidance, his constructive suggestions through the research has taught me a lot.

I would also like to thank my PhD committee members – Prof. Mikhail Spasennykh, Dr. Evgeny Chuvilin for their advice, assistance, and support in doing the research.

I would also like to express my appreciation to the staff and PhD-students of the hydrate group: Dr. Boris Buhanov, Dr. Natalia Sokolova, Maria Karelskaya and Valentina Ekimova for their guidance and help in doing the experimental part of the thesis. I would also like to extend my thanks to Dr. Pavel Zobov and Dr. Sergey Antonov for their help in conducting some experiments.

I extend my gratitude to Skolkovo Institute of Science and Technology for the grand opportunity to learn from all these splendid people.

I would like to thank Jury committee members – Prof. Bahman Tohidi, Prof. Boris Balakin, Prof. Sergey Stanchits, Prof. Dimitri Pissarenko, Dr. Vyacheslav Pimenov and Dr. Alexander Shandrygin for their comments and recommendations on how to improve my work.

Last but not least, a special thanks to my fellow student buddies, my family and friends for their support and encouragement through my study.

Table of Contents

List of Figures

List of Tables

Chapter 1. Introduction

1.1. Relevance. Statement of the problem

At present, the giant gas fields in Western Siberia of Russia are moving to the late stage of development, and new gas and gas condensate fields with low reservoir temperatures (the fields of South Yakutia and the Yamal Peninsula) are being put into operation. In this connection, new features arise in the operation of wells and gas gathering systems: hydrate formation in the bottomhole formation zone, hydrate depositing in wellbores, ice formation in in-field pipelines, etc. When developing deposits in Yamal Peninsula, geological risks arise, which may be associated with the presence of gas hydrates in the geological section. For example, a new geocryological phenomenon has appeared: gas emissions (blow up) with the formation of large-diameter craters.

For the development of adequate technological solutions for prevention of hydrate formation in the wellbores and gas-gathering systems, it is advisable to provide a detailed thermodynamic and hydrodynamic analysis of the possible mechanisms for the formation and decomposition of hydrates. It is necessary to develop new thermodynamic models for the description of phase equilibria in gas-saturated soils and sediments, as well as in gas production systems at Northern conditions.

1.2. Goal

Further development of thermodynamic models for the description of the phase equilibria of hydrocarbon systems with aqueous phases and gas hydrates in free volume and in porous media (for modeling of geocryological processes and for developing more effective techniques for gas hydrate control during gas recovery).

1.3. Objectives

1. To carry out the analysis of thermodynamic consistency of the known experimental data on the three-phase equilibrium of gas hydrates (individual gases) and to prepare the smoothed data on phase equilibria and properties of several gas hydrates. To establish a correlation between three phase equilibria of gas hydrates with ice and with supercooled water.

2. To develop a technique for calculation of the phase equilibria in the system "pore mineralized water – gas – gas hydrate – ice" for soils and sediments.

3. To calculate the influence of gas pressure on the unfrozen and non-clathrate water content in soil systems and compare the results to the experimental data.

4. To carry out the experimental and thermodynamic modeling of hydrate formation in aqueous solutions of mixed hydrate inhibitors (salts + methanol, thermodynamic inhibitor + water-soluble polymer).

5. To improve the technique of the hydrate control at wellbores of the Yarakta oil and gas condensate field and in-field pipelines at the Yamburg gas fields.

6. To develop a model of hydrate deposition on the inner wall of the pipeline in the case of hydrate-free thermodynamic regime of the gas stream at the Yamburg in-field pipelines.

1.4. Novelty

New approach for thermodynamic consistency of experimental data on phase equilibria of gas hydrates. It makes possible to smooth out the experimental data, as well as to improve the determination of hydrate numbers and the positions of lower quadrupole points. Smoothed data on phase equilibria "ice (water) – gas – hydrate" for methane, nitrogen, ethane, propane, CO_2 and isobutane are presented.

Detailed thermodynamic consideration of gas pressure effect on the unfrozen and non-clathrate water contents in soils or sediments. Deriving of some new thermodynamic correlations for gas pressure influence on equilibrium water content. Comparison of the thermodynamic

models with experimental data (non-clathrated water content in kaolinite clay). Calculation of pressure increasing during a closed gas-saturated talik freezes. Obtained correlations may be also used for calculations of pressure influence on hydrate inhibitor's phase equilibrium (at fixed temperature).

New experimental data on physico-chemical properties and phase equilibria of mixed hydrate inhibitors: "methanol + magnesium chloride" and "salts ($MgCl_2$, NaCl) + polyvinylpyrrolidone" systems. Based on experimental data some simple and reliable thermodynamic correlations for temperature shifts of hydrate equilibrium for mixed thermodynamic inhibitors. Such correlations were already used in practice for thermodynamic calculations of mixed inhibitor (like methanol + brine) at Yarakta oil and gas field.

1.5. Outline of the Thesis

Chapter 2 offers a literature review for physicochemical properties and thermodynamics of gas hydrates.

Chapter 3 provides the approach for thermodynamic consistency and checking of the known experimental data was proposed. The smoothed experimental data of the equilibria "gas – ice – hydrate" and "gas – liquid water – hydrate" are obtained, which allow to provide more accurate thermodynamic calculation of enthalpies, hydrate numbers and the position of the quadruple points. A simple correlation between three phase equilibria of gas hydrates with ice and with supercooled water was presented.

Chapter 4 presents the technique for determination of gas pressure influence on pore water freezing temperature in frozen soils and on the amount of the unfrozen water (shift of the unfrozen water curve by affecting the gas pressure). Also the thermodynamic model for increasing gas pressure during the freezing of closed gas-saturated talik (as a new natural phenomena) is presented.

Chapter 5 describes the proposed dependences for calculations of the of non-clathrate water content depending on the gas pressure from the known data on of the pore water activity in the soil samples at atmospheric pressure. The thermodynamic calculation is presented for hydrate-containing samples of kaolinite clay showed a sufficiently good agreement between the results obtained by the proposed technique and by the experimental contact method.

Chapter 6 deal with the properties of mixed hydrate inhibitors. The mixed reagents "methanol + magnesium chloride", "PVP + NaCl", "PVP + $MgCl_2$" were studied by experimental and calculation methods as possible promising inhibitors.

Chapter 7 contains practical applications on the hydrate control at wellbores of the Chayandiskoe and Yarakta oil and gas condensate fields as well as in-field pipelines at the Yamburg gas fields.

Chapter 2. Gas hydrates. Directions in modern research. Problematic issues

Gas hydrates are crystalline compounds formed under certain thermobaric conditions from water (water solution, ice, water vapor) and low molecular weight gases. Gas hydrates looks like ice or snow. The area of their thermodynamic stability includes both negative and positive temperatures (Celsius).

Gas hydrates belong to the clathrate compounds (from the Latin "clathratus", which means "to put in a cage"), in which water molecules form an ice-like frame (known as a host subsystem) formed by hydrogen bonds, and this framework contains molecule-sized cavities (cells or cages). These cavities serve as hosts for atoms or molecules of lower molecular weight compounds (known as guest molecules or guest subsystems). Hydrates are described by the general formula M·*n*H2O, where M – means a mole of the hydrate-forming gas (or a mole of a multicomponent mixture of gases); *n* is the hydrate number characterizing the composition of the hydrate (the number of moles of water to one mole of gas or a gas mixture) and *n* is not constant and depends on the conditions for the hydrate formation.

Both individual hydrates (for example, methane hydrate) and mixed hydrates (for example, natural gas hydrates) are known. The crystal structure of the hydrates of the two most widespread hydrates was initially established by crystallochemical modeling [1], followed by X-ray diffraction and neutron diffraction analysis [2, 3], and neutron diffraction analysis [4]. There are some reviews on the crystal structures of gas hydrates, reporting the sizes of the individual cells of hydrate structures with different guest molecules along with the temperature data (see a recent review by [5]).

Gas hydrates are classified into two main categories: natural and technogenic hydrates.

Natural gas hydrates are accumulations of gases in a "solid state" in the Earth, both in a dispersed form and deposit-forming (where the deposits are either continental or sub-aquatic). We also include to the natural hydrate category the hydrates that are formed in the bottomhole zone of wells during the development of low-temperature gas and gas condensate reservoirs

(over-Cenomanian gas deposits in Western Siberia and gas condensate fields in the South Yakutia).

Technogenic hydrates are hydrates, which formed under certain temperature and pressure conditions in operating the gas production and gas-oil systems. They are considered as a technological complication that must be either prevented or mitigated through elimination of the consequences of gas hydrate deposition.

2.1. Gas hydrate background

Gas hydrates have been studied for a long time. A recent attempt at compiling and reviewing all existing studies was made by Professor A.M. Mastepanov in his historical monograph [6]. However, this historical review is mostly written from the point of view that gas hydrates firstly an energy resource. It should be pointed that there are significant gaps in the monograph [6] in description of hydrate' physicochemical properties. Due to our sphere of interest, the following sections of the review are limited to the consideration of only the studies investigating the physicochemical properties of gas hydrates.

The first gas hydrate was presumably observed in 1778 by J. Priestley. He discovered "anomalous ice" when cooling saturated aqueous solutions of sulfur dioxide. Surprisingly, this ice was formed at positive temperatures and sank in aqueous solutions of SO_2 [7]. The first scientific description of gas hydrates (chlorine hydrate) was given by G. Davy in 1811 [8]. Michael Faraday [9] also studied chlorine hydrate. He was the first to define the yellowish precipitate obtained by Davy as a crystalline compound of chlorine and water and to determine approximately its composition by the mass balance during the hydrate decomposition into gas and water.

For a long time, research on gas hydrates was fundamental and led by chemists, since gas hydrates initially had no practical meaning. The practical need for gas hydrate research emerged as late as in the 1930s in the United States, when the first gas condensate fields were put into

operation. Gas lines from gas condensate wells began to be clogged with "ice or snow" at positive Celsius temperatures (which at the time did not have a scientific explanation). The first paper on this technological problem was published by Hammerschmidt [10]. He proposed chemical methods for preventing hydrate formation in pipelines of raw gas using antifreeze liquids (methanol and other aqueous solutions). Soon after he named the antifreeze substances as inhibitors, the term started to spread in the literature, despite being not scientifically corrected. Soviet researches first encountered the technogenic hydrates in 1947-1948, during the launch of the first long distance gas pipeline "Saratov-Moscow". The gas pipeline was built to ensure a reliable gas supply to Moscow (it was the world's second biggest gas main pipeline, following the one built in the USA in 1943). The implementation of this project was directly supervised by the Russia government. After hydraulic tests the water remained in the pipeline, and when it was filled with natural gas under high pressure in winter season the gas hydrate plugs were formed. Local oil and gas specialists have never seen such a phenomenon in their practice. An analysis of the emergency was carried out. The examination was attended by the future professor and Lenin Prize winner P.A. Tesner[1], who had a chemistry background. He found that the cause of the emergency was quite natural due to the formation of gas hydrate plugs, so the pipeline builders avoided penalties.

As for the possibility of natural gas hydrate existence in the form of its accumulations or deposits, this hypothesis was first expressed by the famous Moscow oil professor I.N. Strizhov[2]

Then, in the 1950s, the hypothesis of the presence of gas hydrate deposits in the permafrost zone was developed by N.V. Chersky[3] and M.P. Mokhnatkin.

[1] Professor P. A. Tesner lived for almost a whole century, and had a very bright and creative life, spoke several foreign languages, followed foreign chemical literature. In the 60s he was the CEO of VNIIGAZ.

[2] Strizhov I.N. from 1934 to 1939 worked in the city of Ukhta and taught part-time at the Ukhta mining and oil technical school. The teaching staff of the technical school was highly qualified. Strizhov I.N. taught oil and gas business at the technical school and, among other lectures, talked about the possibility of the formation of gas hydrates in the earth's crust in the permafrost regions

[3] Nikolai Vasilievich Chersky (later - Academician of the Russian Academy of Sciences), being the chairman of the Yakutsk filiation of the Siberian branch of the Academy of Sciences (in 1964-1988), paid much attention to gas hydrate problems. It is interesting to note that Acad. N.V. Chersky was a reviewer of the world's first monograph on natural gas hydrates, published in 1992 by V.A. Istomin. and Yakushev V.S. [13]. Recently, the specialized pipe-laying vessel currently working on laying the Nord Stream-2 gas pipeline was named after N.V. Chersky

Later, specialists from the Moscow Petroleum Institute (now Gubkin Russian State University of Oil and Gas) Trebin F.A. and Makogon Y.F. for the first time conducted laboratory experiments on obtaining hydrates in porous media. In 1969, the Messoyakhskoye gas field was launched with the main purpose of converting the Norilsk mining and processing plant from coal to gas. The thermobaric regime of the gas field was close to the three-phase equilibrium "gas – water – hydrate". It is very likely that in the initial period of the field development, the upper productive layer of gas reservoir contained methane hydrates. It is worth noting that the Norilsk geological department of the Gazprom was initially supervised by Ginsburg G.D., later collaborating with Soloviev V.A. wrote the world's first specialized monograph on marine gas hydrates [11]. The English version of this monograph was published in Norway (1996).

In 1970, the State Committee for Science and Technology of the USSR recognized the scientific work "The property of solid-state natural gases in the earth's crust to form gas hydrate deposits" as scientific discovery (authors: V.G. Vasiliev, Yu.F. Makogon, F.A. Trebin, N.V. Chersky, A.A. Trofimuk) [12].

In the second half of the twentieth century physicists and chemists continued their research activity. In particular, unique experimental equipment was constructed, allowing obtaining the phase diagrams of gas hydrates, including high-pressure conditions (initially in the pressure range from 5 to 15 kbar, then - up to 100 kbar). This research direction was pioneered by the group of Professor Yu.A. Dyadin, who worked at the Institute of Inorganic Chemistry of the SB of RAS. The theoretical models of hydrates were developed by the to be professor V.R. Belosludov together with Yu.A. Dyadin and with their younger co-workers (see details below). Prof. Dyadin and his co-workers later discovered a new gas hydrate structure with a single type of hydrate cavities.

However, the undisputed leader of the physical and chemical research of gas hydrates at the time was Professor Davidson at the Canadian National Research Center in Ottawa. The fact that such outstanding scientists as Tse, Ratcliffe, Ripmeister, Handa worked under his

supervision speaks for itself. This research team discovered new properties of hydrates using modern physical and chemical methods such as neutron diffraction, NMR, Raman spectroscopy, calorimetry and dielectric measurements. In particular, they demonstrated that nitrogen forms the hydrate type II structure contrary to previous assumptions about the type I structure.

As for the experimental study of the phase diagrams of various gases and their mixtures, the Institute of Organic Synthesis and the Moscow Oil Institute in Russia began to actively pursue research in the area in the 50-70s. The well-known experts S.Sh. Byk and V.I. Fomina became the undoubted leaders of the thermodynamics of gas hydrates in Russia. In the USA that role belonged to Donald Katz, who led the team studying the phase equilibria of hydrates. As soon as in 1946, the first systematic monograph on hydrate phase diagrams was published, focusing on gas hydrate systems that were of interest to the actively developing gas industry [14]. In the 50-70s, the physicochemical research on the phase equilibria of hydrocarbon systems was carried out by the well-known expert-experimenter prof. Riki Kobayashi from Rice University, USA. Professor Kobayashi had trained a number of PhDs, the most famous of which was Prof. E. Dendy Sloan who later wrote an extensive monograph on gas hydrates (which has already undergone three editions). Until very recently, E. Dendy Sloan (now retired) worked actively at the Colorado School of Mines (Golden, Colorado). His most famous students are Carolyn Koh and Amadeu Sum, who currently run two gas hydrate laboratories at the Colorado School of Mines. There was also a great contribution to the experimental research of phase equilibria in the 80-90s made by an American Scientist Prof. Holder with his students. Later Prof. Holder worked as a dean of the Pittsburgh University. At the same time in Canada, Ng and Robinson carried out some precision experiments primarily on methanol influence on hydrate equilibria (up to the methanol concentrations of 85 wt%). Ng and Robinson's company was later integrated with Schlumberger company. All these studies are described in detail in the monograph by Sloan [15]. Another outstanding contribution was made by a Canadian professor Bishnoi in the 80-90s. He formulated the basic principles for modern research on the kinetics of

gas hydrates formation and decomposition. The most famous of his students is Prof. Peter Englezos. In recent years, professors B. Tohidi, D. Richon, A. Chapoy, A. H. Mohammadi and their colleagues have shown a particular activity in experimental studies of the gas hydrate thermodynamics. Professor Bahman Tohidi also made a significant contribution to the educational process at Skoltech: he developed the "Gas Hydrates and Flow Assurance" course and was the first lecturer. Also in recent years the experimental studies of thermodynamics and kinetics of gas hydrates are continued in Gubkin university in collaboration with Skoltech and VNIIGAZ.

Among the calorimetrists of the 70-90-time period, the Japanese professor Niroshi Suga is the paramount figure. Not only he studied the thermophysical properties of hydrates, but also he discovered a number of subtle effects in ice-like systems: the "order-disorder" transitions in the proton subsystem of ices and hydrates, as well as the influence of some additives on these transitions [16]. The achievements of a Canadian scientist A. Handa are also worth mentioning - his thermophysical experiments on hydrates of the 80s are still considered as standard [17]. Presently, the calorimetric research of gas hydrates is actively pursued at Gazprom VNIIGAZ LLC and at Academic Institute of Oil and Gas Problems in Moscow.

During the recent 10-15 years numerous interesting scientific groups emerged in China, South Korea, India, and Singapore. Each group is actively engaged in physical and chemical research, and it is difficult to summarize their research results. Groups in Singapore, Yokohama, Sapporo, Tsukuba, Beijing and others are actively working in the field of gas hydrate phase equilibria. The specialists from Germany and Japan showed promising results in the area of structural studies of hydrates and ice.

It should be especially noted that over the past three decades, the interest in research in the field of natural gas hydrates has been actively maintained throughout the world. This is due to the prospects for their production as a promising unconventional gas source. According to the available estimates made by various authors, the global gas content in hydrates ranges from

$2.0 \cdot 10^{14}$ to $7.6 \cdot 10^{18}$ m^3. The greatest interest in natural gas hydrates is currently shown by countries that do not have sufficient (or none at all) natural gas resources. First of all, this applies to Japan, South Korea, India and especially now to the PR China.

The reasons for the interest in natural and technogenic gas hydrates are analyzed in detail in the work of V.A. Istomin et al. [18]. Further directions are summarized in another study by Istomin [19]. The role of Russian studies of natural and technogenic gas hydrates with an emphasis on the achievements of VNIIGAZ specialists, including the pivotal stages of the discovery of marine hydrate deposits, is presented in [20].

Because the research of natural gas hydrates lies slightly outside the scope of our research activity, we will further limit our discussion only to the topic of technogenic gas hydrates. We would also like to note that the current state of the problem of technogenic hydrate formation prevention is outlined in a number of monographs [21, 22].

Let us highlight the most relevant areas of the current research in the field of technogenic hydrates:

- studies of thermodynamics and kinetics of the mixed thermodynamic hydrate formation inhibitors;
- studies of the kinetics and thermodynamics of low-dosage inhibitors, especially mixed inhibitors (low-dosage + thermodynamic inhibitors);
- prevention of technological complications when using monoethylene glycol as a hydrate formation inhibitor in offshore gas pipelines;
- prevention of hydrate formation in the gas producing wells in new fields of Eastern Siberia;
- optimization of the regeneration systems of hydrate inhibitors, taking into account the strong mineralization of their waste solutions.

The direction of the development of new hydrate inhibitors is led by a chemist M. Kelland, who wrote numerous articles and a monograph [23], as well as comprehensive reviews on the problem [24, 25].

The analysis of some studies in this area on the subject of our research is presented below in Chapters 6 and 7.

2.2. Brief description of the physicochemical properties of gas hydrates

A number of reviews on the physicochemical properties of gas hydrates have been published, including hydrates in porous media [26-28]. Therefore, below we will highlight only the main points.

One volume of gas hydrate can contain up to 160 volumes of methane. The density of natural gas hydrates is lower than the density of water and ice (for methane hydrate about 900 kg/m^3). With an increase in temperature and a decrease in pressure, the hydrate decomposes into gas and water with heat absorption. The decomposition of the hydrate in a closed volume leads to a significant increase in pressure.

Hydrates are characterized as having high electrical resistance, and conducting acoustic waves. Unlike hexagonal ice, hydrates have an abnormally low thermal conductivity (for methane hydrate at 273 K, the thermal conductivity coefficient is five times lower than that of ice). From a physical point of view, this is due to the specific scattering of acoustic phonons of the host subsystem by guest molecules. The phenomenon of low thermal conductivity is mainly characteristic of amorphous substances, and at present the same phenomenon has been discovered and is being actively studied for nanocomposites.

Up to now, more than twenty solid phases of water built on hydrogen bonds are known - hexagonal and cubic ices, more than a dozen types of high-pressure ices, two amorphous phases of water at low temperatures, as well as clathrate and semi-clathrate ice-like structures, see for instance the website of prof. Chaplin (http://www1.lsbu.ac.uk/water/water_structure_science).

As described above, the hydrate structure implies that water molecules form a framework (host subsystem) with cavities of molecular size. The cavities in hydrates (which can be represented as polyhedrons, at the vertices of which are oxygen atoms, and the edges represent

hydrogen bonds) are 12-, 14-, 15-, 16- and 20-hedrons, denoted by D, D`, T, T`, P, H, E, respectively (see Figure 2.1 [21]). A dodecahedron (D-cavity or pentagondodecahedron) turns out to be energetically most favorable, since the angle between hydrogen bonds is almost the same as the tetrahedral one and is ~108˚. The twelve-sided cavities D and D 'are usually called small cavities, and the rest (T, T', P, H, E) are called large. Small cavities can be considered as quasi-spherical, while large cavities deviate noticeably from a spherical shape and they are more like ellipsoids (the large E-cavity is especially different from a spherical shape). Figure 2.2 [https://en.wikipedia.org/wiki/Methane_clathrate] shows a methane molecule in a small D-type cavity (the methane molecule is in a cell formed by 20 water molecules, and it oscillates around the center of the cavity and rotates almost freely).

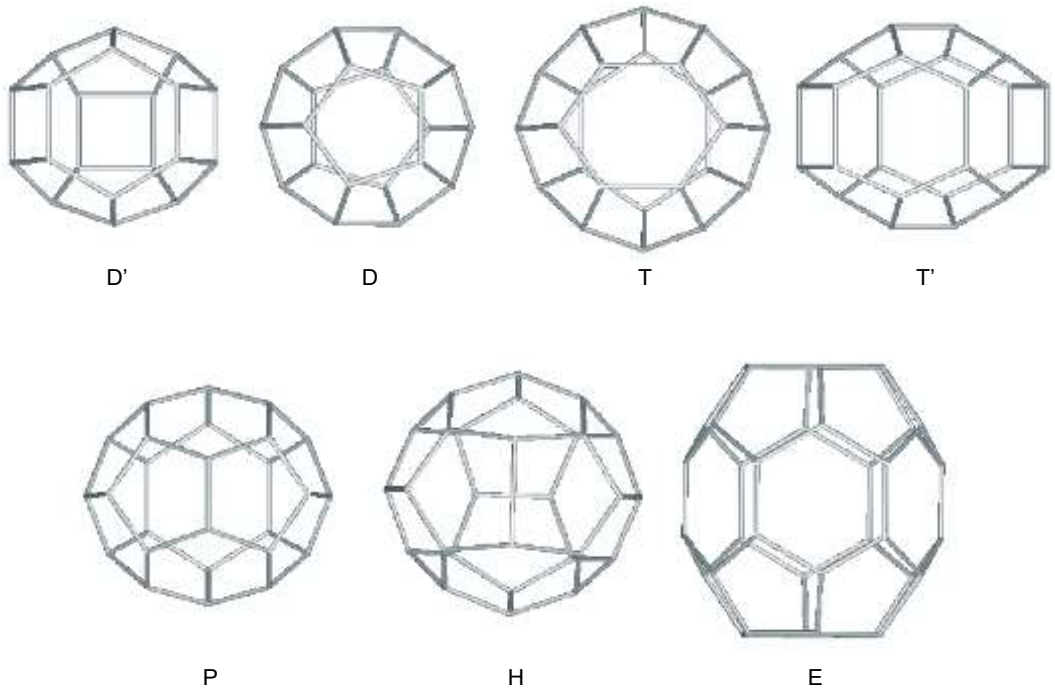

Figure 2.1 Cavities in water clathrate frameworks: D'[$4^3 5^6 6^3$], D [5^{12}], T [$5^{12}6^2$], T' [$4^2 5^8 6^4$], H [$5^{12}6^3$], P [$5^{12}6^4$], E [$5^{12}6^8$] (m^n - means n faces with m edges)

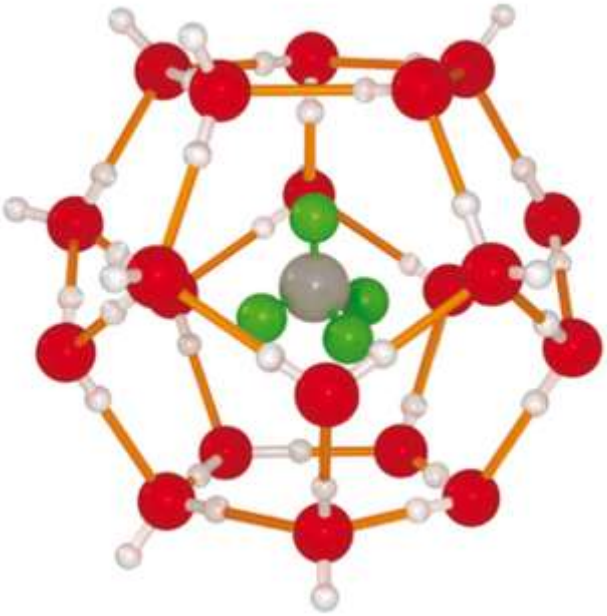

Figure 2.2 A methane molecule in a small D-type cavity

The cavities of the ice-like clathrate frame can contain both molecules with a small van der Waals radius (CH_4, Ar, H_2S molecules - in all types of cavities; C_2H_6, CO_2 molecules - starting from T-cavities), as well as larger molecules (C_3H_8, i-C_4H_{10}, n-C_4H_{10} located in H-cavities. Very large molecules, such as methylcyclohexane, can only be located in E-cavities.

Six ice-like clathrate structures with the aforementioned types of cavities are known to date, but only three are of practical interest. More specifically, these are two cubic structures KC-I and KC-II (hereinafter we call them structures I and II) and the H-structure, which is rarely formed in the oil systems. The unit cells of these three structures are shown in Figure 2.3 [15]. Natural hydrates, as well as technogenic hydrates in gas production systems, are characterized by two cubic structures, which we will consider in this work.

In clathrate hydrates KC-I, the unit cell contains 46 water molecules, which form two small (D) and six large cavities (T). In clathrate hydrates KC-II, there are 136 water molecules per unit cell, 16 small (D) and 8 large cavities (H). In GS-III hydrates, there are five small cavities (D and D') per one large cavity E (this type of cavities can only be filled with a suitable shape with large molecules).

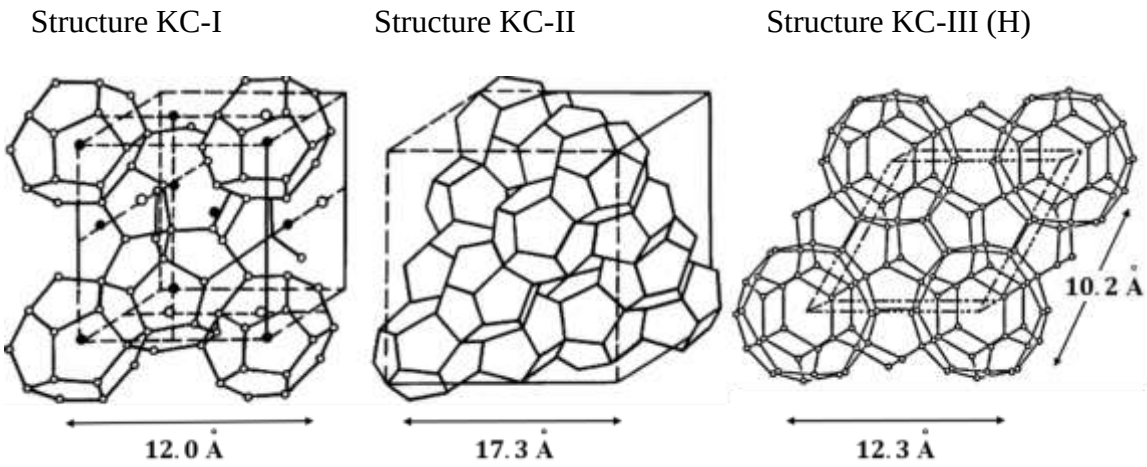

Figure 2.3 Unit cells of the three main gas hydrate structures

It should also be noted that the cavities in the hydrate frames can be only partially filled with gas molecules, and the degrees θ_1, θ_2 of filling small and large cavities are determined both by the intermolecular interaction of guest molecules with water molecules, and by thermodynamic conditions. In many cases of practical importance, the nonstoichiometry of the hydrate is sufficiently small; therefore, in some cases, it may not be taken into account. Thus, propane and iso-butane hydrates form hydrates KC-II, which are described by the general formula $M \cdot 17\ H_2O$ (large cavities are almost completely filled, and small ones are unfilled), and methane hydrate are described by the formula $CH_4 \cdot 6.1H_2O$ (large cavities are almost completely filled, and small ones are about 90% filled).

Individual gases CH_4, CO_2, H_2S, Xe, CF_4, C_2H_6, C_2H_4 form hydrates of the KC-I structure, and the gases Ar, Kr, O_2, N_2, C_3H_8, i–C_4H_{10} of the KC-II structure. At the same time, cyclopropane, depending on thermodynamic conditions, forms both KC-I and KC-II hydrates. It is interesting that n-C_4H_{10}, can be included in the composition of a mixed hydrate of structure II, but an individual n-C_4H_{10} hydrate has not been obtained (its production is unlikely based on the thermodynamic considerations, although the possibility of its existence at very low temperatures cannot be completely ruled out).

Hydrates of natural gases formed from multicomponent hydrocarbon mixtures can form hydrates of both structures depending on the gas phase composition. Hydrates KC-I are common

for natural gases of gas fields (with propane and isobutane content less than 0.3-0.6 mol%), as well as gases containing a significant amount of non-hydrocarbon components (hydrogen sulfide and carbon dioxide). The formation of KC-II hydrates is typical for natural gases of gas condensate fields. For mixed gases (including natural gases), a number of intermediate situations are possible, when a hydrate of structure I is formed in one temperature range, and structure II at other temperatures.

The composition of an individual hydrate is set by the hydration number *n* according to the formula $M \cdot nH_2O$, the molar fraction x of the gas in the clathrate phase according to the formula $(1\text{-}x) \cdot H_2O \cdot x \cdot M$, and the degrees θ_1, θ_2 of filling small and large cavities in the host lattice. Strictly speaking, hydrates are compounds of a variable composition (nonstoichiometric compounds), while *n*, θ_1, θ_2 depend on temperature and pressure. The filling degrees can formally vary from zero to one. The indicated methods of specifying the hydrate composition are interconnected by algebraic relations

$$n = \frac{1-x}{x}; \quad n^I = \frac{23}{\theta_1^I + 3 \cdot \theta_2^I}; \quad n^{II} = \frac{17}{2 \cdot \theta_1^{II} + \theta_2^{II}}. \qquad (1)$$

2.3. Metastable states of gas hydrates

In the context of the thesis, it is necessary to discuss the problem of metastable states of gas hydrates.

First of all, we note the effect of self-preservation of gas hydrates, discovered and initially studied in 1986-1988 in the Moscow gas hydrate group - E.D. Ershov, V.S. Yakushev, E.M. Chuvilin, V.A. Istomin, etc. [29, 30]. The effect consists in a delayed decomposition of methane hydrate (and some other hydrates) under negative temperatures when the pressure in the hydrate chamber is released. The hydrate surface initially decomposes into supercooled water, and then the supercooled water film crystallizes. A similar effect was observed simultaneously in 1986 by Handa et.al in the calorimetric cell [31].

The first work on the thermodynamic analysis of the effect was done by Yakushev and Istomin in 1990 [32]. Then were investigated possible modifications of the self-preservation effect, namely, the so-called forced preservation effect (with an extension of its conditions to positive Celsius temperatures, possible when a layer of one hydrate covers a layer of another). Such scenarios were analyzed in the papers [33-36] by V.A. Istomin.

The effect of self-preservation was also extended to natural gas hydrates and hydrates in porous media (see the first works [37-42] on this direction).

A thermodynamic interpretation and explanation of the self-preservation effect, as well as a detailed analysis of the studies completed by 2006, are given in the comprehensive review [43]. Eventually, more details of the effect's mechanism were uncovered [44, 45]. Later, the effect was extended to oil systems [46].

To summarize, the number of publications exploring the effect of self-preservation has exceeded one hundred, also several theses have already been written (A.S. Stoporev, V.A. Vlasov, etc.) on the topic.

In the context of our thesis, the concept of a metastable equilibrium "gas – supercooled water – hydrate" plays an important role. The first computational work devoted to predicting this metastable equilibrium appeared only in 2006 [47], it was presented at the hydrate conference in London [48]. This metastable equilibrium was first studied experimentally in the Tyumen group of A.N. Nesterov with the active participation of V.A. Istomin [49, 50]. These works present notable achievements in the thermodynamics of metastable gas hydrates.

A more detailed thermodynamic analysis of calculation methods for the metastable equilibrium "gas – supercooled water – hydrate" is presented in Chapter 2 and 4 of the thesis.

2.4. Thermodynamic models of the gas hydrate phase

We focus on the improvement of thermodynamic modeling of gas hydrate equilibria with pure water, pore water, ice, aqueous solutions of inhibitors, taking into account the applied

aspects of thermodynamic calculations. Therefore, below we discuss in detail the thermodynamic gas hydrate models obtained within the framework of statistical thermodynamics. At the same time, we do not touch upon the aspects of modeling gas hydrates with the methods of molecular and/or lattice dynamics.

The classical thermodynamic model of the gas hydrate phase (the Van der Waals (grandson) - Platteu and Barrer - Stewart model) was developed in 1957-1959 with the application of methods of statistical thermodynamics (see, for example, the discussion in [40, 51]). The following assumptions were made when developing the model:

- the empty hydrate lattice (the host subsystem) is metastable (which does not hold true at temperatures near 273 K, see below),
- the hydrate lattice retains its unit cell volume, i.e. practically does not distort when it is filled with different guest molecules (this assumption is not entirely correct, but it is partially justified by the neglecting of the interaction between the guest molecules),
- there is no interaction between guest molecules (due to they are located in different cavities, and therefore interact through a layer of water molecules, i.e. such interactions in the first approximation can be neglected, see above),
- no more than one molecule is located in each cavity (the assumption is valid for moderately high gas pressures and starts to be violated at pressures above 30-40 MPa for small molecules like nitrogen, oxygen, hydrogen),
- the cavity filling is considered as volumetric sorption, therefore, similarly to the lattice adsorption models, some of the cavities remain vacant,
- clathrate hydrate is considered as a solid solution, and the components of this solution (water and gases) can be assigned with their chemical potentials.

The assumptions listed above imply that when the hydrate is in equilibrium with the gas phase, the degree of cavity filling is connected to the fugacity of the hydrate-forming gas through the Langmuir isotherm.

As shown by recent studies [52] using the method of vacuuming gas hydrates with small molecules, hydrate lattices without gas molecules can actually exist at very low (helium) temperatures and low pressures as a highly metastable host frame with respect to hexagonal ice. It means that new metastable crystalline modifications of ice were obtained (the experiment was carried out through vacuum desorption of atoms and molecules of small size from clathrate hydrates). Their properties have not yet been investigated from the thermodynamic point of view. For example, it can be hypothesized that, upon heating, these empty hydrate frames decompose at a certain temperature by the spinodal mechanism (spinodal decomposition) with a transition to amorphous ice or other intermediate and metastable phases of ice (like cubic ice). Therefore, the validity of the assumption of the thermodynamic model about the metastability of an empty hydrate lattice near 273 K is unlikely. But even if this assumption is physically incorrect in the temperature range near 273 K, it should be noted that the use of labile states as standard states does not contradict to the thermodynamics of solutions (as some extrapolations from the area of a metastable state).

The discussed classical model of the gas hydrate phase is in essence very simplified: one can draw an analogy of this model with the thermodynamic model of ideal liquid solutions. In addition to the classical thermodynamic model of the gas hydrate phase, more complex versions have been developed in the literature, for example, taking into account a) the interaction of guest molecules with each other (guest-guest interaction) [53-56], b) the lattice distortions of the gas hydrate frames associated with the filling of cavities [57], and c) the possibility of each cavity to be filled by several guest molecules [58].

The mentioned more advanced thermodynamic models of gas hydrates have not yet become widespread, because in most practical cases it is sufficient to use the classical thermodynamic model. This is due to the partial compensation of factors unaccounted for in the classical model, for example, of two oppositely directed effects - distortion of the host lattice and the interaction of guest molecules with each other.

It is worth noting once again that despite the successful description of thermodynamic characteristics, the theory of Van der Waals-Platteeuw and Barrer-Stewart is simplified and does not fully agree with experimental data. In particular, it is not suitable for very high gas pressures due to the possibility of filling of one cavity with several molecules at once.

Within the scope of our work, the classical model of the gas hydrate phase will be used, which is quite sufficient to describe the phase equilibria of gas hydrates in various practical situations.

According to the thermodynamic model of the van der Waals-Platteu and Barrer-Stewart clathrate hydrate (for details, see, for example, [40]), the chemical potential of water $\mu_h(T,P)$ in the hydrate phase is written as follows

$$\mu_h(T,P) = \mu_h^0(T,P_0) - \nu_1 RT\ln(1+C_1 f) - \nu_2 RT\ln(1+C_2 f) + V_h \cdot (P-P_0). \quad (2.1)$$

Or alternatively

$$\mu_h = \mu_h^0(T,P_0) + \nu_1 RT\ln(1-\theta_1) + \nu_2 RT\ln(1-\theta_2) + V_h \cdot (P-P_0),$$

where: quantities θ, C and f are connected through the Langmuir isotherm $\theta = \frac{Cf}{1+Cf}$ (the model assumes that gas molecules are sorbed by the gas hydrate lattice in accordance with the Langmuir isotherm); T – temperature, K; P – external pressure exerted on the hydrate phase, MPa; $P_0 = 0.101325$ MPa; V_h – the molar volume of water in the hydrate phase (22.61 cm^3/mol for structure I and 23.06 cm^3/mol for structure II); $\mu_h^0(T,P_0)$ – the chemical potential of water in the empty hydrate lattice at pressure P_0 and temperature T; $\mu_h(T,P)$ – the chemical potential of water in a hydrate lattice partially filled with guest molecules at pressure P and temperature T; R – the universal gas constant, $R = 8.3146\ \text{J}/(\text{mol}\cdot\text{K})$; $C_1 = C_1(T), C_2 = C_2(T)$ – are the Langmuir constants for large and small cavities (depending only on temperature), respectively; θ_1, θ_2 – degrees of filling of small and large cavities of the hydration structure, respectively; ν_1 and ν_2 – crystal chemical constants (for structure I we have $\nu_1 = 1/23$, $\nu_2 = 3/23$, and for structure II - $\nu_1 = 2/17$, $\nu_2 = 1/17$).

The gas phase is described by a selected equation of state (now it is common to use the CPA equation of state), from which the fugacities of the gas phase components are determined. The liquid phase is considered as an aqueous solution containing dissolved gas, salts and hydrate inhibitors (also this aqueous solution may be in porous media).

The solubility of gas in water can be determined by the Krichevsky-Kazarnovsky equation [59], or computed from the equation of state.

2.5. Analysis of experimental data on phase equilibria of gas hydrates. Problematic aspects

Studies of the formation and destruction of gas hydrates in natural and laboratory conditions are of great importance for the reliable functioning of various production processes and for environmental protection. Tables 2.1-2.7 provide a summary of studies on hydrate equilibria for pure gases: methane, ethane, cyclopropane, propane, isobutane, nitrogen and carbon dioxide. The hydrates of these gases are of high interest in the context of our work.

Table 2.1 Experimental data on methane hydrate

Author	Year	Temperature range, K	Pressure range, MPa	Number of points
Roberts et al.	1940	273.2-286.7	2.641-10.804	4
Deaton and Frost	1946	262.4-285.9	1.793-9.784	18
Chueh et al.	1973	241.5-273.15	0.896-2.620	4
Falabella et al.	1975	148.8-191.3	0.005-0.090	5
Song et al.	1989	274.7-284.4	2.688-8.099	6
Adisasmito et al.	1991	273.4-286.4	2.68-10.57	11
Deng et al.	1993	274.9-284.8	3.00-9.00	5
Dickens et al.	1994	276.1-285.4	3.45-9.58	7
Makogon et al.	1994	190.2-262.4	0.825-1.798	6
Hutz et al.	1996	274.6-285.3	3.021-9.35	7
Mei et al.	1996	274.2-285.2	2.96-8.96	12
Nixdorf et al.	1997	273.5-284.0	2.716-7.925	15
Smelik et al.	1997	273-284.5	2.482-8.356	6

Hachikubo et al.	2002	268.4-271.3	2.324-2.527	2
Nakamura et al.	2003	274.2-284.8	2.92-8.55	15
Nesterov et al.	2005	275.1-300.1	3.17-54.53	26

Table 2.2 Experimental data on ethane hydrate

Author	Year	Temperature range, K	Pressure range, MPa	Number of points
Roberts et al.	1940	260.8-288	0.294-6.84	23
Deaton and Frost	1946	263.5-282.6	0.313-1.558	17
Reamer et al.	1952	279.9-287.4	0.972-3.299	4
Galloway et al.	1970	277.6-282.5	0.814-1.551	3
Falabella	1975	200.8-240.4	0.008-0.098	4
Holder and Hand	1982	278.8-282	0.95-1.45	4
Heng-Joo et al.	1985	288-290.6	3.33-20.34	8
Avlonitis et al.	1988	277.8-287.1	0.848-3.082	10
Englezos and Bishnoi	1991	274.3-283	0.548-1.637	6
Song et al.	1994	288.6-303.7	3.421-4.714	4
Nixdorf and Oellrich	1997	273.7-287.6	0.499-3.244	15
Nakano et al.	1998	290.4-293.9	19.48-45.370	15
Clarke and Bishnoi	2000	274.1-280.6	0.487-1.087	4
Morita et al.	2000	298-317.5	89.00-355.0	15
Yang et al.	2002	277.3-278.5	51.00-151.0	3
Kim et al.	2003	277.3-278.5	10.10-20.10	3
Ohmura	2008	244.9-275.9	0.112-0.658	33
Long et al.	2010	280.1-285.6	1.11-2.32	5
Maekawa	2012	276.6-287.5	0.73-3.22	9
Buleiko et al.	2017	272.8-289.3	0.463-14.7	89

Table 2.3 Experimental data on propane hydrate

Author	Year	Temperature range, K	Pressure range, MPa	Number of points
Deaton et al.	1946	261.2-277.0	0.100-0.386	19
Reamer et al.	1952	274.3-278.8	0.241-2.046	6

Platteeuw et al.	1959	270.1	0.150	1
Robinson et al.	1971	274.3-278.9	0.207-0.552	5
Verma et al.	1974	273.9-278.3	0.188-0.552	5
Goddard	1981	247.9-262.1	0.048-0.099	8
Holder et al.	1982	245.1-270.8	0.039-0.151	5
Kubota et al.	1984	273.2-283.6	0.172-0.659	27
Patil	1987	273.6-277.9	0.207-0.501	5
Englezos et al.	1993	274.2-278.3	0.208-0.545	6
Song et al.	1994	281.9-299.6	0.621-0.897	4
Nixdorf et al.	1997	273.5-278.5	0.186-0.567	10
Mooijer-van den Heuvel et al.	2002	276.8-278.5	0.368-0.547	9
Mooijer-van den Heuvel	2004	275.4-303.5	0.590-1.110	13

Table 2.4 Experimental data on iso-butane hydrate

Author	Year	Temperature range, K	Pressure range, MPa	Number of points
Holder et al.	1982	241.4-269.5	0.018-0.091	10
Rouher et al.	1969	266.3-276.1	0.122-0.175	32
Wu, Bing-Jin. et al.	1976	275.4-275.8	0.226-14.27	6
Buleiko et al.	2018	234.8-275.3	0.009-7.46	44

Table 2.5 Experimental data on cyclopropane hydrate

Author	Year	Temperature range, K	Pressure range, MPa	Number of points
Hafemann et al.	1969	237.2-289.4	0.009-0.566	21
Parrishl	1972	289.36	0.558	1
Dharmawardhana et al.	1980	273.2-280.2	0.064-0.176	30
Suzuki et al.	2001	278.5-314.2	0.4-344	47

Table 2.6 Experimental data on nitrogen hydrate

Author	Year	Temperature range, K	Pressure range, MPa	Number of points
Cleeff et al.	1960	269.2-290.7	10.943-92.206	31
Marshall et al.	1964	277.6-305.5	24.931-328.88	14
Nixdorf et al.	1997	273.7-277.3	16.935-24.092	5
Sugahara et al.	2002	285.6-300.5	55.00-219.00	15
Mohammadi et al.	2003	274.5-283.0	19.093-45.355	3

Table 2.7 Experimental data on CO_2 hydrate

Author	Year	Temperature range, K	Pressure range, MPa	Number of points
Deaton et al.	1946	273.8-282.9	1.324-4.323	19
Unruh et al.	1949	277.2-288.1	2.041-5.171	13
Von Stackelberg	1949	249.2-273.2	0.101-1.246	2
Larson et al.	1955	256.8-285.0	0.545-4.695	61
Takenouchi et al.	1965	283.2-292.7	4.500-186.20	15
Miller et al.	1970	151.5-192.5	0.0005-0.022	8
Robinson et al.	1971	273.9-283.3	1.379-4.468	7
Vlahakis et al.	1972	263.0-288.0	2.645-5.076	100
Falabella et al.	1975	194.5-218.2	0.025-0.104	4
Robinson et al.	1985	279.6-283.9	2.740-14.360	9
Song et al.	1987	251.7-304.2	0.690-7.390	36
Adisasmito et al.	1991	274.3-282.9	1.420-4.370	9
Dholabhai et al.	1993	273.7-279.0	1.340-2.520	4
Ohgaki et al.	1993	273.4-289.4	1.338-5.216	59
Komai et al.	1997	278.1-283.0	1.900-4.100	3
Yoon et al.	1997	275.4-283.3	1.560-4.520	5
Nakano et al.	1998	289.7-292.1	104.00-494.00	22
Fan et al.	1999	273.6-283.6	1.310-12.870	15
Wendland et al.	1999	271.1-304.6	1.026-7.411	24
Fan et al.	2000	274.7-279.7	1.500-2.780	3
Hachikubo et al.	2002	263.2-278.0	0.774-2.204	11

Zhang	2003	274.0-279.3	1.647-5.580	9
Mohammadi et al.	2005	277.5-282.5	2.048-4.020	3
Yasuda and Ohmura	2008	244.5-269.4	0.364-1.628	10
Mohammadi and Richon	2009	264.5-271	0.78-1.05	4
Fray et al.	2010	172.3-182.4	0.0045-0.0099	3
Nagashima et al.	2016	199.1-247.1	0.0343-0.4066	8

Despite the fact that there is a significant amount of experimental data that covers most of the temperature range, there are still gaps where experimental data is missing. The range of temperatures close to 273.15 K is particularly important for the study of the thermodynamics of gas hydrates. Moreover, in many cases, the lower and upper quadrupole points are inaccurately determined. In a number of cases, it is difficult to reliably determine the hydrate numbers (especially, according to the Forcran method at the lower quadrupole point) and the enthalpies of hydrate decomposition (due to the error of derivative dP/dT computation near 273 K) from the available experimental curves of three-phase equilibria. Therefore, it is appropriate to develop methods for thermodynamic interpolation and extrapolation (in order to eliminate systematic errors), and for smoothing the experimental curves with their subsequent thermodynamic post-analysis (i.e. refinement and correction of the phase diagrams of gas hydrates).

2.6. Analysis of software (HydraFLASH, etc.) and computation methods

For the purposes of the current study, there are two main available for us software packages for simulation of gas hydrate behavior:

1. The Istomin - Kwon's hydrate software, developed in 1994-1996 [60]. Henceforth, for brevity, we will call it the VNIIGaz program.

2. HydraFLASH [61]. This is a Hydrafact Limited software (Skoltech has an unlimited software license).

The simulators operate through solving the systems of transcendental equations describing the equilibria of coexisting phases. The equilibrium conditions are derived from the equality of the chemical potentials of the components of the system. The equations are usually solved using Newton's method.

In our study we also use the cubic-order equations of state of the multicomponent gas phase. In HydraFLASH, it is recommended to use the CPA equation of state, since it adequately describes the equilibria of hydrocarbons with polar components. The Istomin-Kwon's software package uses the author's modification of the Redlich-Kwong equation of state.

Aqueous solutions of hydrate formation inhibitors are described both by the CPA equation and by using various empirical models of liquid solutions (van Laar, Danon, Pitzer and their modifications).

The gas hydrate phase is described by the classical thermodynamic model of Van der Waals and Platteu (see discussion above) with an appropriate choice of parameters for fitting the experimental data on three-phase equilibria of gas hydrates (each software package uses its own parameterization). The Istomin-Kwon's program also describes the thermodynamics of hexagonal ice and supercooled water. HydraFLASH uses the Kihara interaction potential between water and guest molecules to calculate the Langmuir constants. The user needs to select the potential parameters describing experimental hydrate curves (mainly for pure gases). The Istomin-Kwon's program offers the functionality for the user to directly select the Langmuir constants of large and small cavities of various gases. This selection was made based on a set of experimental data that included gas mixtures, NMR and other spectroscopic data of the degrees of cavity filling. The direct parameter selection made it possible to improve the computations of the gas compositions in the gas hydrate phase as well as of the degrees of cavity filling (which is especially important for small cavities in clathrate structures).

Using these software packages, it is possible to calculate hydrate equilibrium conditions for pure gases, their mixtures in equilibrium with ice, water, and aqueous solutions of inhibitors.

HydraFLASH additionally computes the activity of water in aqueous solutions of inhibitors, their freezing points, and the density of solutions, as well as the effect of the hydrate inhibitor.

Applicably to our problems, the advantage of the HydraFLASH software is the large selection of hydrate inhibitors and the possibility of considering their various mixtures, as well as the possibility of calculating the activity of water in solutions. To obtain the hydrate numbers and degrees of filling of the clathrate cavities of each of the components of the gas mixture we used the Istomin-Kwon's software. Also we applied Istomin-Kwon's software to calculate two-phase equilibria of the type "multicomponent gas mixture – gas hydrate (or ice, water and supercooled water)". So, both programs are used in our calculations. It is important to note that both packages yield close results for computing the three-phase equilibria "gas – pure water – hydrates".

We also used the software package developed by the National Institute of Standards and Technology (NIST). This program REFPROP [62], developed by NIST, calculates the thermodynamic and transport properties of industrially important fluids and their mixtures. REFPROP is based on the most accurate pure fluid and mixture models currently available. It implements three models for the thermodynamic properties of pure fluids: equations of state explicit in Helmholtz energy, the modified Benedict-Webb-Rubin equation of state, and extended corresponding states (ECS) model. Mixture calculations employ a model that applies mixing rules to the Helmholtz energy of the mixture components; it uses a departure function to account for the departure from ideal mixing. Viscosity and thermal conductivity are modeled with either fluid-specific correlations, an ECS method, or in some cases the friction theory method.

Below we present examples of the calculated hydrate numbers and degrees of filling of large and small cavities of gas hydrate structures (Table 2.8, 2.9), computed using the Istomin-Kwon's program. We will refer to this data in the following chapters.

Table 2.8 Hydrate numbers and degrees of filling for some gases at the equilibrium between gas, water (supercooled water) and a hydrate

Gas		Hydrate numbers and degrees of filling at temperature, K						
		258.15	263.15	268.15	273.15	278.15	280.15	283.15
methane	n	6.370	6.238	6.131	6.047	5.979	5.956	5.925
	θ_1	0.770	0.812	0.848	0.878	0.904	0.913	0.926
	θ_2	0.947	0.959	0.968	0.975	0.981	0.983	0.985
ethane	n	7.929	7.857	7.804	7.766	7.739	7.730	7.719
	θ_2	0.967	0.976	0.982	0.987	0.991	0.992	0.993
propane	n	17.049	17.024	17.012	17	17	-	-
	θ_2	0.997	0.999	0.999	~1	~1	-	-
i-butane	n	17.049	17.049	17.012	17	-	-	17.049
	θ_2	0.997	0.997	0.999	1	-	-	0.997
nitrogen	n	7.042	6.684	6.407	6.184	5.994	-	7.042
	θ_1	0.722	0.783	0.835	0.880	0.921	-	0.722
	θ_2	0.969	0.977	0.984	0.989	0.993	-	0.969
CO_2	n	6.788	6.595	6.430	6.288	6.17	6.12	6.788
	θ_1	0.508	0.578	0.646	0.709	0.768	0.791	0.508
	θ_2	0.960	0.970	0.977	0.983	0.987	0.989	0.960

Table 2.9 Hydrate numbers and degrees of filling for some gases at the equilibrium between gas, ice and a hydrate

Gas		Hydrate numbers and degrees of filling at temperature, K		
		258.15	263.15	268.15
methane	n	6.013	6.026	6.04
	θ_1	0.892	0.886	0.881
	θ_2	0.978	0.977	0.975
ethane	n	7.750	7.756	7.761
	θ_2	0.989	0.989	0.988
propane	n	17.004	17.005	17.005
	θ_2	~1	~1	~1
i-butane	n	17.004	17.005	17.005

	θ_2	~1	~1	~1
nitrogen	n	6.189	6.209	6.230
	θ_1	0.879	0.875	0.870
	θ_2	0.989	0.988	0.988
CO_2	n	6.265	6.289	6.312
	θ_1	0.720	0.709	0.698
	θ_2	0.984	0.982	0.982

Chapter 3. Thermodynamics of gas hydrates

In this chapter we present a thermodynamic analyses of the literature data on three phase hydrate equilibria. Firstly, we consider the correlation between three phase equilibria with ice and with supercooled water at temperatures below 273 K. Secondly, we develop the technique for checking the thermodynamic consistency of experimental points for three phase equilibria "gas – water (or ice) – hydrate". The proposed approach allows smoothing more correctly the experimental data for different gases and as a result to receive recommended reference data. The focus was on gas hydrates of pure gases - methane, ethane, propane, iso-butane, carbon dioxide and nitrogen as the main components of natural gases. These data may be used for more correct calculation of hydrate numbers and enthalpies of decomposition. Smoothed reference data are used in subsequent chapters for description of hydrate equilibria in porous media (soils, sediments) and in the aqueous solutions of mixed inhibitors.

In chapter 2 (see Tables 2.1 - 2.7) references for three phase equilibria "gas – ice – gas hydrate" and "gas – water – gas hydrate" are presented. It should be noted that in many cases, the experiments were performed with insufficient accuracy. Therefore, the thermodynamic analysis is needed for selection of reliable experimental data.

Research objectives in the chapter are:

- to establish the correlation between three phase equilibria with ice and with supercooled water at temperatures below 273 K;

- to propose a new technique for checking the thermodynamic consistency of the experimental data on hydrate three-phase equilibria of some hydrate-forming gases;

- to present the smoothed experimental data of the equilibria "gas – ice – hydrate" and "gas – liquid water – hydrate" for some gases.

3.1. Traditional approach for processing of experimental data on hydrate equilibria

Three-phase equilibria of "gas – water – hydrate" and "gas – ice – hydrate" are of practical interest. The main component of the natural gases is methane. So, we start the analysis of the

experimental data for methane hydrates.

A large number of experimental studies have been devoted to the study of methane hydrate formation in free volume. Experiments on pure methane hydrate began since 1940 [63]. Five equilibrium points were obtained in the temperature range 262.4 ÷ 270.9 K at a pressure range of 1.793 ÷ 2.392 MPa. Later the data of the hydrate equilibrium of pure methane both at negative temperatures in Celsius (Figure 3.1) were published [14, 64-67], and positive temperatures (Figure 3.2) [14, 63, 68-77] as summarized in Table 2.1 (see chapter 2).

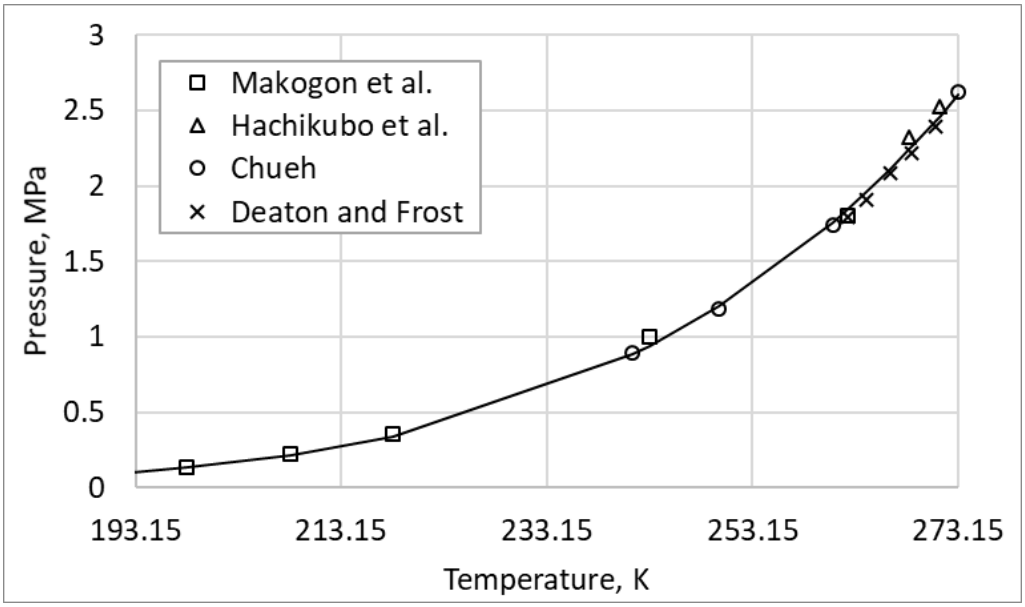

Figure 3.1 Literature experimental data on "methane – ice – hydrate" equilibrium

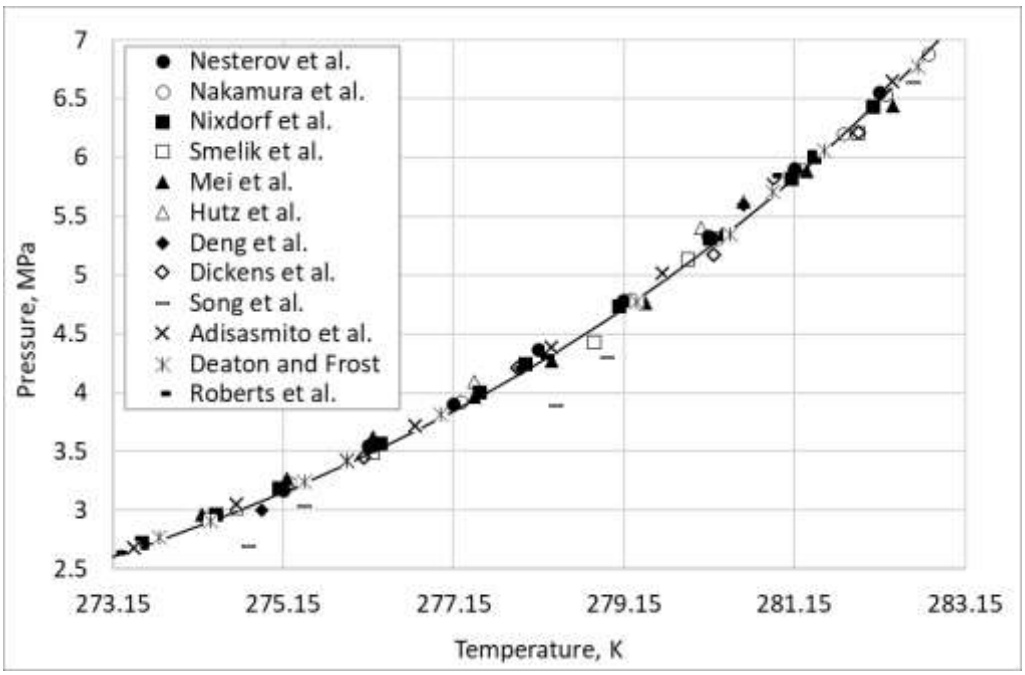

Figure 3.2 Literature experimental data on "methane – water – hydrate" equilibrium

The first question is how to smooth out the experimental data? The dependence of pressure on temperature is usually described by the empirical equation

$$\ln P = A + \frac{B}{T} + C \cdot \ln T. \qquad (3.1)$$

In this equation pressure in MPa (or kPa) and temperature in K. The equation describes the curves on three phase equilibrium in a large temperature range. Instead P may be also used gas fugacity f. From the approximations (3.1) it is possible to calculate thermodynamic values: enthalpy of hydrate decomposition and hydrate number n at lower quadrupole point.

If we neglect the solubility of gas in water and water in gas for the molar enthalpy of gas hydrate decomposition ΔH into gas and water (or ice), the following relation can be obtained

$$\Delta H = \Delta V T \frac{dP}{dT}\ , \qquad (3.2)$$

where ΔV – change in the volume of the system upon decomposition of a mole of hydrate phase on water (ice) and gas. The derivative dP/dT is taken along the three-phase equilibrium line at the considered temperature. Thus, in these assumptions the ordinary Clausius–Clapeyron relation is formally valid. Note that the Clausius–Clapeyron relation describes a two-phase equilibrium in a single-component system, while in our case there is a three-phase equilibrium in

a two-component system. Strictly speaking, we should be used the Gibbs generalization of the Clausius–Clapeyron relation for three phase equilibria of two-component system (the Gibbs equation take into account solubility of gases in water and water in gases).

At lower quadruple point we may write two Clausius–Clapeyron relations for decomposition enthalpy to ice ΔH_i and to liquid water ΔH_w. By using circular process, we may obtain hydrate number *n*

$$n = \frac{\Delta H_w(T_q) - \Delta H_i(T_q)}{\Delta h} = \frac{T_q\left(\left(\frac{dP}{dT}\right)\Big|_{(w)} \cdot \Delta V_{hw} - \left(\frac{dP}{dT}\right)\Big|_{(i)} \cdot \Delta V_{hi}\right)}{\Delta h} \quad (3.3)$$

where $n -$ hydrate number, $T_q -$ temperature in the lower quadrupole point, Δh - the enthalpy of ice melting to water at quadruple point (very close to $\Delta h(T_0) = 6008$ J/mol). $\Delta V_{hw} = V_h - V_w$, $\Delta V_{hi} = V_h - V_i$ – the difference between the molar volume of water in hydrate and molar volume of water or ice, respectively.

To find the hydrate number and enthalpies near 273.15 K, it is necessary to approximate the data (Table 2.1 (chapter 2)). Using all literature data and equation 3.3 hydrate number $n = 8.12$ was obtained [78]. This hydrate number for methane is not realistic. According to the degrees of occupation and calorimetric data, *n* is close to 6÷6.5. We assume that the derivatives $\frac{dP}{dT}$ are not estimated sufficiently correctly (the slopes of the equilibrium lines around quadrupole point are not determined reliably) and first of all it is necessary to check the experimental data from a thermodynamic point of view.

Some mistakes of the experimental data around 273.15 K may be connected to the additional physical effects: overheating of ice, melting of polycrystalline ice in the range of temperatures, supercooling of water, influence of the surface. Thus, it is necessary to develop a thermodynamic method for rejecting and smoothing of experimental data, with an emphasis on the data near the lower quadrupole point. With this goal in mind, we firstly investigate the correlation between the lines of three-phase equilibrium with ice and with supercooled water.

3.2. Correlation between three phase equilibria "gas – supercooled water – hydrate" and "gas – ice – hydrate"

Below, we discuss the line of metastable equilibrium "gas – supercooled water – hydrate" and the correlation with the line of stable equilibrium "gas – ice – hydrate".

As mentioned in chapter 2, direct experimental data for the line of metastable equilibrium "gas – supercooled water – hydrate" were firstly obtained by Mel'nikov, Nesterov, Reshetnikov, and Istomin for methane, carbon dioxide, and propane hydrates [49, 50]. So it is interesting to establish correlation between these equilibriums.

Below three cases are considered: large cavities are almost completely filled with guest molecules, while small cavities remain vacant; both types of cavities are strongly filled; and the degree of filling of small cavities may be varying, while large cavities are highly filled.

3.2.1. Hydrates with filled only large cavities in clathrate structures

For this case, the three-phase equilibrium lines: "gas – ice – hydrate" and "gas – supercooled water – hydrate" are very strongly correlated with each other (see discussion below). It means that from the data on one equilibrium it is possible with high accuracy to obtain the another equilibrium at least in the temperature range 253 - 273 K.

Let's take the temperature T below the lower quadrupole point. The pressure and fugacity of gas on the lines of three-phase equilibrium will be denoted by $P_w^{(eq)}$, $f_w^{(eq)}$ for equilibrium with supercooled water and $P_{ice}^{(eq)}$, $f_{ice}^{(eq)}$ for hydrate equilibrium with ice, respectively.

Chemical potential of water in the hydrate phase (in this case $C_2 f \gg 1$, the approximation $1 + C_2 f \approx C_2 f$ is used)

$$\mu_h(T,P) = \mu_h^0(T,P_0) - \nu_2 RT\ln(1 + C_2 f) + V_h \cdot (P - P_0) \approx$$

$$\approx \mu_h^0(T,P_0) - \nu_2 RT\ln(C_2 f) + V_h \cdot (P - P_0). \qquad (3.4)$$

Chemical potential of supercooled water with dissolved gas, depending on pressure and temperature

$$\mu_w(P,T) = \mu_w{}^0(P_0,T) + RT\ln\left(1 - x_g\right) + \bar{V}_w \cdot (P - P_0). \quad (3.5)$$

Chemical potential of ice (gases do not dissolve in ice)

$$\mu_{ice}(P,T) = \mu_{ice}{}^0(P_0,T) + V_{ice} \cdot (P - P_0). \quad (3.6)$$

It should be pointed that a detailed discussion of the chemical potentials of water in hydrate, supercooled water and ice phases is presented in the following chapters 4 and 5.

Equating the chemical potentials according to relations (3.4) and (3.6), we obtain the equation for the equilibrium line "gas – ice – hydrate"

$$\mu_h^0(T,P_0) - \nu_2 RT\ln\left(C_2 f_{ice}^{(eq)}\right) + V_h \cdot \left(P_{ice}^{(eq)} - P_0\right) =$$

$$= \mu_{ice}{}^0(P_0,T) + V_{ice} \cdot \left(P_{ice}^{(eq)} - P_0\right)$$

or

$$\nu_2 RT\ln\left(C_2 f_{ice}^{(eq)}\right) = \Delta\mu_{hi}^0(T,P_0) + \Delta V_{hi} \cdot \left(P_{ice}^{(eq)} - P_0\right), \quad (3.7)$$

where $\Delta\mu_{hi}^0(T,P_0)$ - the difference in the chemical potentials of water in hydrate and ice, $\Delta V_{hi} = V_h - V_{ice}$ – the difference between the molar volume of water in hydrate and molar volume of ice.

Similarly, from (3.4) and (3.5), we obtain the equation of the equilibrium line "gas – supercooled water – hydrate"

$$\mu_h^0(T,P_0) - \nu_2 RT\ln\left(C_2 f_w^{(eq)}\right) + V_h \cdot \left(P_w^{(eq)} - P_0\right) =$$

$$= \mu_w{}^0(P_0,T) + RT\ln(1 - x_g) + \bar{V}_w \cdot \left(P_w^{(eq)} - P_0\right)$$

or

$$\nu_2 RT\ln\left(C_2 f_w^{(eq)}\right) = \Delta\mu_{hw}^0(T,P_0) - RT\ln(1 - x_{g,w}) + \Delta V_{hw} \cdot \left(P_w^{(eq)} - P_0\right) \quad (3.8)$$

Thus, we have obtained two equations in the framework of our assumptions. If subtract Eq. (3.6) from Eq. (3.5), then the thermodynamic correlation is obtained

$$\nu_2 RT\ln\left(\frac{f_{ice}^{(eq)}}{f_w^{(eq)}}\right) = \Delta\mu_{wi}^0(T,P_0) +$$

$$+\Delta V_{hi}\cdot\left(P_{ice}^{(eq)}-P_0\right)-\Delta V_{hw}\cdot\left(P_w^{(eq)}-P_0\right)+RT\ln(1-x_{g,w}). \quad (3.9)$$

The Eq. 3.9 is connected to two phase equilibriums under consideration. The equation applicable with high precision to the following gases: ethane, propane, isobutane, cyclopropane (and mixtures thereof).

The left side of relation (3.9) contains the ratio of fugacity (for propane and isobutane, this is practically the pressure ratio, since the hydrate formation pressures for these gases are very low). The right side contains the known value $\Delta\mu_{wi}^0(T,P_0)$

$$\Delta\mu_{wi}^0(T,P_0)=6008\cdot\left(1-\frac{T}{T_0}\right)-36.93\cdot\left(T\cdot\ln\frac{T}{T_0}+(T_0-T)\right),$$

(this equation was discussed in chapter 4) and the correction terms that take into account the change in molar volumes and the gas solubility in supercooled water at pressure $P_w^{(eq)}$.

For propane and iso-butane the correction terms can be neglected, then we may get the simplified relation

$$\nu_2 RT\ln\left(\frac{f_{ice}^{(eq)}}{f_w^{(eq)}}\right)=\Delta\mu_{wi}^0(T,P_0)=6008\cdot\left(1-\frac{T}{T_0}\right)-36.93\cdot\left(T\cdot\ln\frac{T}{T_0}+(T_0-T)\right)$$

or

$$\nu_2 RT\ln\left(\frac{P_{ice}^{(eq)}}{P_w^{(eq)}}\right)=6008\cdot\left(1-\frac{T}{T_0}\right)-36.93\cdot\left(T\cdot\ln\frac{T}{T_0}+(T_0-T)\right). \quad (3.10)$$

For $\Delta\mu_{wi}^0(T,P_0)$ also can be also used the relation

$$\Delta\mu_{wi}^0(T,P_0)=\mathrm{RT}\ln\frac{p_w}{p_i}, \quad (3.11)$$

where p_w- saturated vapor pressure of supercooled water, p_i- saturated ice vapor pressure (see Table 3.1).

Table 3.1 Saturated vapor pressure of supercooled water and ice at temperatures below zero Celsius [79]

Temperature, K	Saturated water steam pressure, Pa 10^2	
	p_w	p_i
273.15	6.1121	6.1115

273.16	6.116	6.116
268.15	4.218	4.018
263.15	2.866	2.560
258.15	1.914	1.653
253.15	1.256	1.033
248.15	0.808	0.633
243.15	0.560	0.380
238.15	0.315	0.224

As for equation (3.10), it should be noted that the lower the temperature *T*, the slightly worse the assumption about the close to unity degree of filling of large cavities (3.6) is fulfilled, especially for equilibrium with supercooled water. However, our estimates show that at least in the range 258-273 K, relation (3.7) is quite acceptable.

Using (3.10), the equilibrium line "propane – supercooled water – hydrate" were obtained. For this purpose, the above smoothed data on the three-phase equilibrium "propane – ice – hydrate" were used. The Figure 3.3 and Table 3.2 shows a rather good agreement with the experimental data [49].

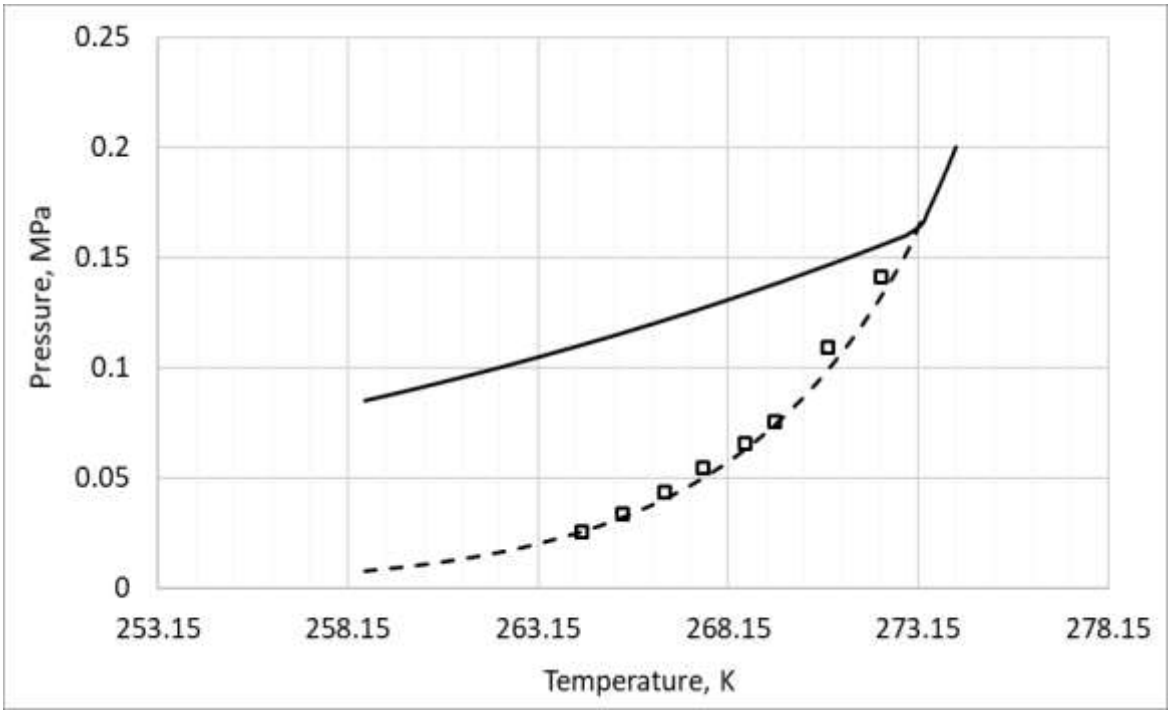

Figure 3.3 Equilibrium lines: "propane – ice – hydrate (solid line)", "propane – supercooled water – hydrate (dash line)", experimental data [49] (squares on the graph)

Table 3.2 Equilibrium line calculation "propane – supercooled water – hydrate" by formula (3.10) and comparison with experimental data [49]

Temperature (K)	Equilibrium line pressure "propane – ice hydrate" (MPa)	Equilibrium line pressure "propane – supercooled water – hydrate" (MPa)	
		Calculation by formula (3.8)	Mel'nikov's data
252.93	0.065	0.00225	0.00186
254.47	0.07	0.00313	0.00269
255.92	0.075	0.00428	0.00379
257.29	0.08	0.00574	0.00521
258.58	0.085	0.00757	0.00704
259.81	0.09	0.00985	0.00933
260.99	0.095	0.01265	0.01219
262.11	0.1	0.01607	0.01571
263.19	0.105	0.02019	0.01998
264.23	0.11	0.02513	0.02513
265.22	0.115	0.03100	0.03128
266.18	0.12	0.03793	0.03856
267.11	0.125	0.04607	0.04713
268.00	0.13	0.05556	0.05711
268.87	0.135	0.06660	0.06874
269.71	0.14	0.07936	0.08217
270.52	0.145	0.09401	0.09755
271.31	0.15	0.11083	0.11519
272.08	0.155	0.12997	0.13518
272.83	0.16	0.15179	0.15791

3.2.2. Hydrates with strongly filled both types of cavities in clathrate structures

Repeating the previous conclusion, we may get the correlation of two equilibriums under consideration (compare with Eq. (3.9))

$$(\nu_1 + \nu_2)\, RT \ln\left(\frac{f_{ice}^{(eq)}}{f_w^{(eq)}}\right) = \Delta\mu_{wi}^0(T, P_0) +$$

$$+\Delta V_{hi} \cdot \left(P_{ice}^{(eq)} - P_0\right) - \Delta V_{hw} \cdot \left(P_w^{(eq)} - P_0\right) + RT\ln(1 - x_{g,w}). \quad (3.12)$$

This relationship seems to be sufficiently true for methane and nitrogen gas hydrates.

Using (3.12), the equilibrium line "methane – supercooled water – hydrate" were obtained. For this purpose, the smoothed data on the three-phase equilibrium "methane – ice – hydrate" were used. The Figure 3.4 and Table 3.3 shows a good agreement with the experimental data [49].

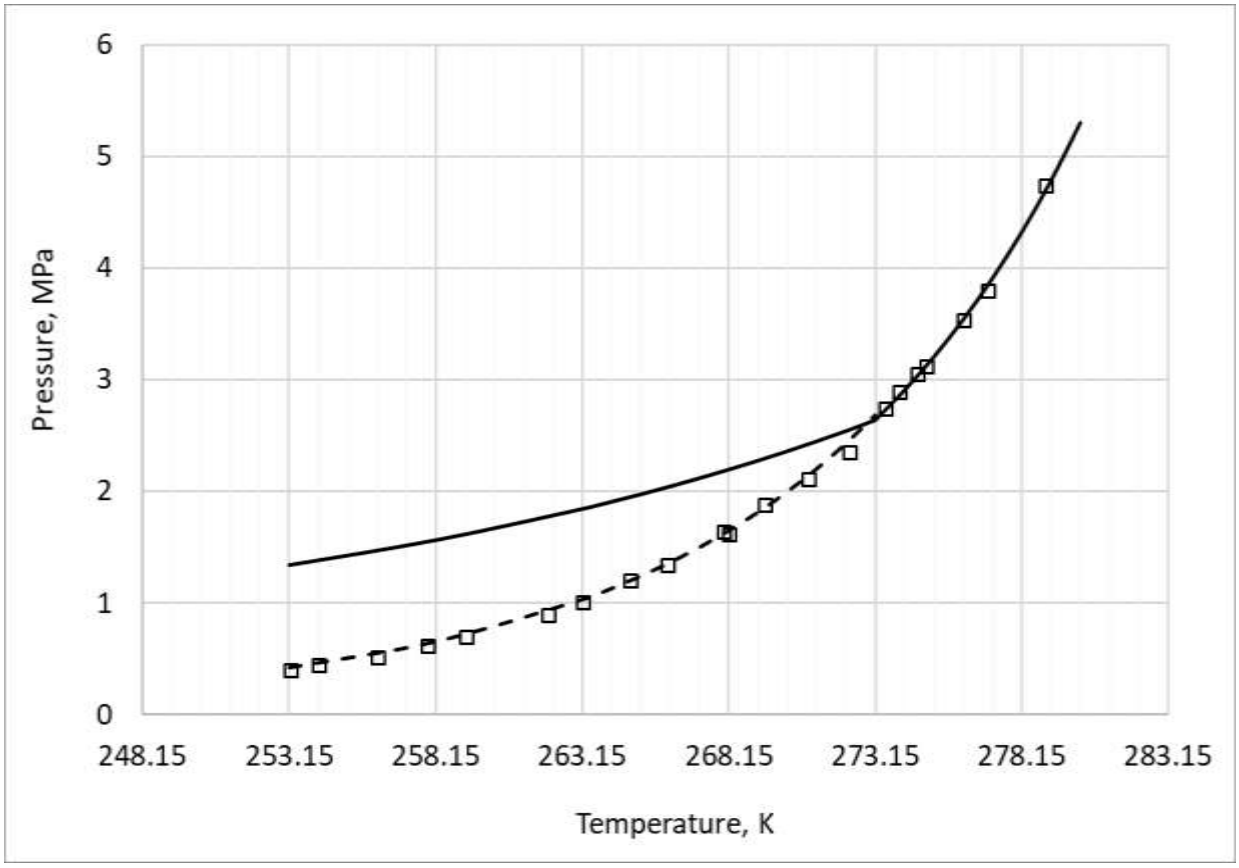

Figure 3.4 Equilibrium line: "methane – ice – hydrate (solid line)", "methane – supercooled water – hydrate (dash line)", experimental data [49] (squares on the graph)

Table 3.3 Equilibrium line calculation "methane – supercooled water – hydrate" by formula (3.12) and comparison with experimental data [49]

Temperature, K	Pressure at the equilibrium line "methane – ice hydrate", MPa	Pressure at the equilibrium line "methane – supercooled water – hydrate", MPa	
	Smoothed exp. data)	Calculation by formula (3.12)	Mel'nikov's data
253.15	1.337	0.42	0.387
258.15	1.561	0.653	0.637
263.15	1.840	1.029	1.028
264.15	1.905	1.129	1.129
265.15	1.972	1.240	1.239
266.15	2.042	1.362	1.359
267.15	2.115	1.497	1.489
268.15	2.192	1.646	1.631
269.15	2.273	1.811	1.784
270.15	2.357	1.996	1.952
271.15	2.445	2.200	2.133
272.15	2.538	2.427	2.330

We see good agreement of the predictive calculation according to formula (3.12) with experimental data at the level of 1-2% in terms of pressure.

Above, we consider the correlation between two types of equilibria at temperature below the lower quadrupole point. Also, we may obtain the similar correlation at temperature above lower quadrupole point. In this case, we restore the hypothetical line "gas – superheated ice – hydrate" (or prolong the line "gas – ice – hydrate" to positive on Celsius temperatures by using the data from the line "gas – water – hydrate").

The result of the previous two sections are of interest in studies of the thermodynamics of self-preservation effect, mentioned in the review of chapter 2. Also, we may use the obtained correlations ((3.9) and (3.12)) for checking of thermodynamic consistency and smoothing of

experimental data for hydrates with strongly filled large cavities when small cavities are empty (and for the case when both large and small cavities are strongly filled).

3.2.3. Hydrates with strongly filled large cavities in clathrate structure and small cavities is not fully filling

If we make only the assumption about the filling of large cavities close to unity, then we may get the following equation

$$\nu_1 RT\ln\left(\frac{1+C_1(T)\,f_{ice}^{(eq)}}{1+C_1(T)f_w^{(eq)}}\right)+\nu_2 RT\ln\left(\frac{f_{ice}^{(eq)}}{f_w^{(eq)}}\right)=\Delta\mu_{wi}^0(T,P_0)+$$

$$+\Delta V_{hi}\cdot\left(P_{ice}^{(eq)}-P_0\right)-\Delta V_{hw}\cdot\left(P_w^{(eq)}-P_0\right)+RT\ln(1-x_{g,w}), \qquad (3.13)$$

where

$$\Delta\mu_{wi}^0(T,P_0)=6008\cdot\left(1-\frac{T}{T_0}\right)-36.93\cdot\left(T\cdot\ln\frac{T}{T_0}+(T_0-T)\right).$$

We see, that the Langmuir constant C_1 remains in this equation (in comparison with Eq. 3.12).

The equation (3.13) may be used for carbon dioxide hydrate, but not for calculation of the equilibrium line with supercooled water from equilibrium line with ice (because we need the knowledge the Langmuir constant C_1 due to varying of small cavities filling).

But if we assume that both lines of three-phase equilibrium are known, then we can obtain the temperature dependence of the Langmuir constant from equation (3.13), and, accordingly, the temperature dependence of the filling degree of a small cavity. The experimental data on equilibrium "CO_2 – supercooled water – hydrate" was published in the paper [50].

Table 3.4 Equilibrium line "CO_2 – ice – hydrate" and equilibrium line "CO_2 – supercooled water – hydrate" using Mel'nikov's [50] and Ohmura's [80] experimental data

T	P_{ice}, MPa smoothed Ohmura data	P_w, MPa smoothed Mel'nikov data	C_1	θ_1
243.15	0.3493	0.0387	0.9654	0.036
248.15	0.4249	0.0687	0.7985	0.052
253.15	0.5168	0.1220	0.6690	0.075
258.15	0.6286	0.2167	0.5543	0.106
263.15	0.7646	0.3848	0.4172	0.135

Here $\theta_1 = \frac{C_1 f}{1+C_1 f}$ along "CO_2 – supercooled water – hydrate" equilibrium line.

Thus, it is possible to determine directly of the temperature dependence of the Langmuir constant C_1 in a small cavity for CO_2 from experimental data on two three-phase equilibria for CO_2 hydrate.

3.3. The technique for processing of the experimental data (thermodynamic consistency and smoothing)

In the processing of experimental data on the thermodynamic equilibria of gas hydrates, we face the situation where there is insufficient data in the positive or negative temperatures on Celsius, the data is very scattered or there is not enough data in the range of interest. As a result, not only the equilibrium lines but the lower or upper quadrupole points are not precisely defined.

So we must develop a sufficiently correct thermodynamic technique, which allow to reveal the thermodynamic inconsistency of the experimental data and then smooth them out more correctly.

By using previous results, below we propose some approaches for simultaneous treatment of experimental data both at negative or positive on Celsius temperatures. This technique is fit for gases like propane, iso-butane, ethane (when only large cavities are filled) and for methane and nitrogen hydrates (when both large and small cavities are filled). As for carbon dioxide

hydrate, the traditional approach for processing of experimental data on hydrate equilibria may be only used (due to numerous experimental data with sufficiently good quality).

During treatment of the experimental data for ethane, propane and iso-butane we may use the following approach: to convert experimental points (by Eq.3.9) from the line "gas – ice – hydrate" to the line "gas – supercooled water – hydrate" and then to use the traditional approach for smoothening of the data (similar as in the section 3.1). And at the final stage - to convert the smoothed line "gas – supercooled water – hydrate" to smoothed line "gas – ice – hydrate" by Eq. 3.9. During processing of the experimental data for methane and nitrogen hydrates we may use the same approach by Eq. 3.12.

Also, we may use a specially constructed parameter m, which is continuous when we transfer from equilibrium with ice to equilibrium with liquid water

$$m = \ln f + \frac{1}{(\nu_1+\nu_2)RT}\Delta V_{hi}(P - P_0), T < T_{Q1}, \quad (3.14)$$

$$m = \ln f + \frac{1}{(\nu_1+\nu_2)RT}(\Delta\mu^0_{wi}(T) + \Delta V_{wh}(P - P_0) + RT\ln(1 - x)), T \geq T_{Q1}, \quad (3.15)$$

where T_{Q1} – lower quadrupole point temperature.

Detailed discussion for choosing the parameter *m* is presented in our paper obtained [78].

And at the end of this section we give some comments for improving lower quadrupole point, which is the point of coexistence of four phases: water (gas-saturated water solution), ice, hydrate-forming gas and gas hydrate.

Firstly, it should be noted that in most cases the quadrupole point is very close to 273 K and therefore its exact location is mainly of methodological interest. A noticeable shift of the quadrupole point from 273 K is due to two factors: the high solubility of the gas in water and the high dissociation pressure of the hydrate-forming gas. These gases are: carbon dioxide and nitrogen. The quadrupole point also shifts noticeably for mixtures with these gases and mixtures of carbon dioxide + methane and nitrogen + methane.

The traditional experimental method for determining the position of the lower quadrupole point is to conduct experiments on hydrate dissociation at positive and negative Celsius temperatures, i.e. obtaining equilibrium lines "gas – ice – hydrate" and "gas – water – hydrate". The intersection of these lines gives P, T-coordinates of the lower quadrupole point. The disadvantage of the traditional approach to finding the lower quadrupole point is that near 273 K there is a low accuracy of experimental data, therefore, when two experimentally found three-phase equilibrium lines P, T intersect, the coordinates of the quadrupole point can be determined with not sufficiently accuracy. An example of recent precision but extremely laborious studies on the study of the line "CO_2 – ice – hydrate" is given in the recent paper [81], in which correctly obtain the position of the quadrupole point for CO_2 hydrate.

Also note that the quadrupole point is the point where three lines of three-phase equilibrium intersect: two hydrate curves (with water and with ice) and the equilibrium line "gas – gas saturated water – ice". A significant drawback of the above methodological approach is that the third equilibrium line "gas – gas-saturated water – ice" is not used in the experimental determination of the quadrupole point. It is important to emphasize that if we take directly the experimental data on two lines of hydrate equilibria (without any thermodynamic processing) and add this third line, then, of course, instead of crossing these three lines at a single point, we will get an intersection triangle (three points of pairwise intersections will not merge into one point due to errors of experimental data).

Thus, to clarify the coordinates of the lower quadrupole point, it is advisable to use the third equilibrium line "gas – gas saturated water – ice", while preliminary thermodynamic processing of the hydrate lines must be carried out beforehand and thereby to eliminate the errors of experimental data near 273 K. It is easy to see that the intersection of the gas – ice – hydrate equilibrium line with the gas – gas-saturated water – ice line gives more correctly the coordinates of the quadrupole point.

The line "gas – gas saturated water – ice" was specially studied in Chapter 4. The equation for this line is

$$6008 \cdot \left(1 - \frac{T_{fr}}{T_0}\right) - 36.93 \cdot \left(T \ln \frac{T_{fr}}{T_0} + \left(T_0 - T_{fr}\right)\right) = -RT_{fr} \ln(b), \qquad (3.16)$$

$$b = a \cdot \left(1 - x_g\right) \cdot \exp\left(-\frac{\Delta V \cdot (P - P_0)}{RT_{fr}}\right).$$

where $T_0 = 273.15\ K$, T_{fr} – freezing temperature of a gas-saturated water solution under gas pressure.

Note that equation (3.16) was obtained for a more general case: the presence of not only a dissolved gas, but also an inhibitor of hydrate formation (for example, salts, methanol, etc.) is taken into account in water. This line is in P, T - coordinates almost vertical (with a slight slope to the left), i.e. its use makes it possible to improve the temperature of the quadrupole point.

The intersection of the above two equilibrium lines gives the improved coordinates of the quadrupole point. It is important to note that the equilibrium line "gas – ice – hydrate" (with a small slope in P, T - coordinates) allows minimizing the pressure error at the quadrupole point, and the line "gas – gas saturated water – hydrate" (with a large slope in P, T - coordinates) allows to minimize the temperature error.

3.4. An example of the proposed technique for checking thermodynamic consistency and smoothing experimental data

Let's consider the technique with parameter m for methane hydrate as example. Remember that m is continuous function of temperature. Clarification of the temperature T_{Q1} at the lower quadrupole point is not required, since for methane T_{Q1} is very close to 273.15.

Figure 3.5 illustrates that all experimental data points lie on one curve without any break. After that, we find new smoothed values for pressure and temperature, and may calculate hydrate number. Figure 3.6 shows two variants of the curves that were obtained by processing the experimental data in two different ways.

Using the proposed method, we obtain intersection of the curves of methane – ice – hydrate and methane – water – hydrate at 273.15 K, a more correct slope of the curves near the point 273.15 K, and more correct hydrate number $n = 6.3$.

So, the new processing method was proposed, which allows checking the thermodynamic consistency of the experimental data. This method allows identifying areas where experimental data are unreliable and to smooth them. Smoothed data can give more correct values of the decomposition enthalpies to ice and water, a correct value of the quadrupole point, and a more correct hydrate number at the quadrupole point.

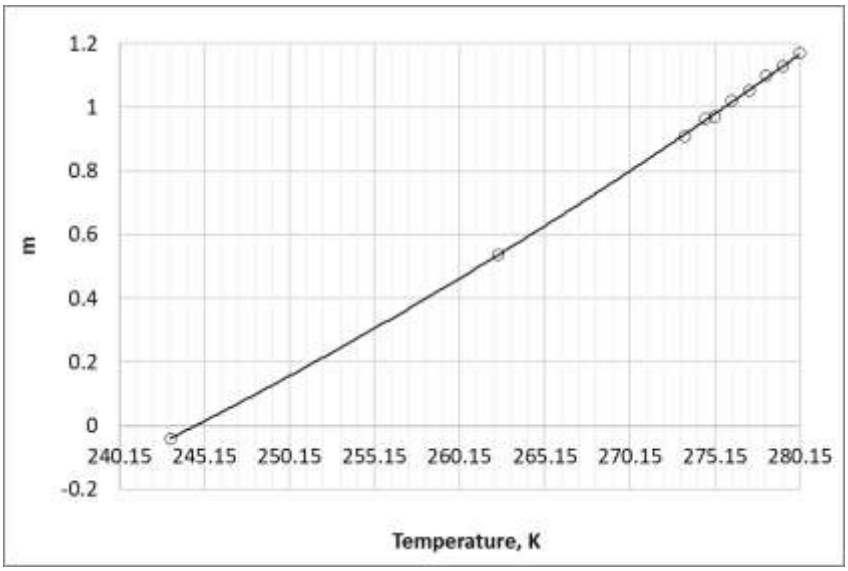

Figure 3.5 Experimental data (three-phase equilibrium of the gas – water (ice) – hydrate system) in coordinates m and T

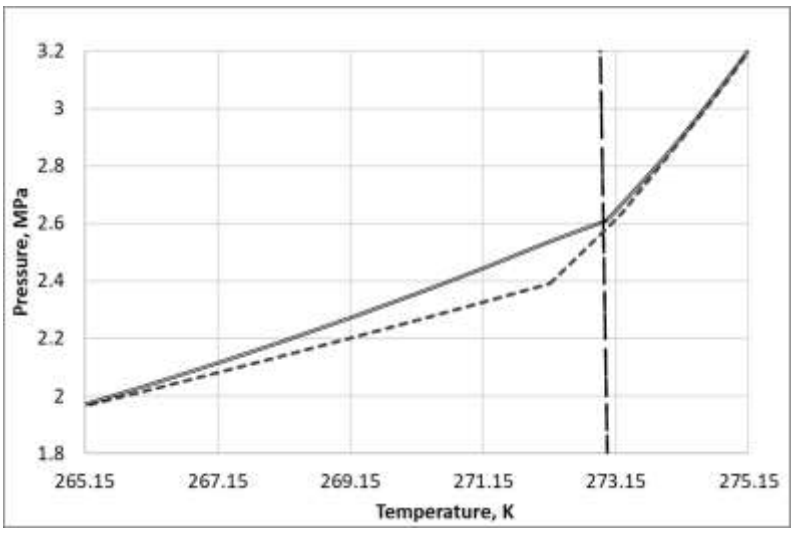

Figure 3.6 Three-phase equilibrium of the gas – water (ice) – hydrate system. Smoothed experimental data: dash line - using (3.1), solid line - using (3.14-3.15)

3.5. Recommended smoothed data on three-phase equilibria of gas hydrates for individual gases

According to the previous technique for processing of experimental data (methane, nitrogen, ethane, propane and isobutane), we obtained the standardized smoothed data on three-phase equilibria "gas – ice – hydrate" for hydrates of pure gases. Tables 3.5-3.6 for gases with strongly filled both types with cavities in clathrate structures, Tables 3.7-3.9 for gases with filled only large cavities in clathrate structures. These smoothed data also allow to obtain the conditions of metastable equilibrium "gas – supercooled water – hydrate". For gases filling only large cavities in clathrate structures (ethane, propane, iso-butane, and cyclopropane), this calculation technique actually will be sufficiently precise. And for gases that strongly fill both types with cavities, this calculation technique may be a good estimation at least in the temperature range 260-273 K. It should be pointed that such metastable equilibria may be calculated by using the Istomin - Kwon software [60], but as usual in other software there are no option for calculation of this metastable equilibrium.

Table 3.5 Recommended data of the equilibria "gas – ice – hydrate" and "gas – liquid water – hydrate" for methane

T, K	P, MPa	T, K	P, MPa	T, K	P, MPa	T, K	P, MPa
243.15	0.9952	266.15	2.0417	273.15	2.6344	280.15	5.3059
248.15	1.146	267.15	2.1152	274.15	2.904	281.15	5.8889
253.15	1.3308	268.15	2.1921	275.15	3.2035	282.15	6.5451
258.15	1.5584	269.15	2.2725	276.15	3.5369	283.15	7.2822
263.15	1.8402	270.15	2.3568	277.15	3.9084	288.15	12.7150
264.15	1.9045	271.15	2.445	278.15	4.3232	293.15	22.5750
265.15	1.9715	272.15	2.5375	279.15	4.7866		

Table 3.6 Recommended data of the equilibria "gas – ice – hydrate" and "gas – liquid water – hydrate" for nitrogen

T, K	P, MPa	T, K	P, MPa	T, K	P, MPa	T, K	P, MPa
243.15	7.2532	270.15	14.034	273.65	17.329	279.15	27.388
248.15	7.9947	271.15	14.467	274.15	18.084	280.15	29.656
253.15	8.9161	271.65	14.69	274.65	18.869	281.15	32.067
258.15	10.0584	271.77	14.744	275.15	19.686	282.15	34.621
263.15	11.472	272.15	15.235	276.15	21.412	283.15	37.318
268.15	13.222	272.65	15.905	277.15	23.269		
269.15	13.62	273.15	16.602	278.15	25.26		

Low quadruple point for nitrogen is T=271.77 K, P=14.713 MPa.

Table 3.7 Recommended data of the equilibria "gas – ice – hydrate" and "gas – liquid water – hydrate" for ethane

T, K	P, MPa	T, K	P, MPa	T, K	P, MPa	T, K	P, MPa
243.15	0.1125	269.15	0.3912	273.4	0.4837	280.15	1.126
248.15	0.1443	270.15	0.4095	273.65	0.4988	281.15	1.2815
253.15	0.1843	271.15	0.4285	273.9	0.5144	282.15	1.4615
258.15	0.2343	271.65	0.4383	274.15	0.5305	283.15	1.6711
263.15	0.2966	272.15	0.4483	274.65	0.5643	284.15	1.9171
264.15	0.3107	272.4	0.4534	275.15	0.6003	285.15	2.2092
265.15	0.3255	272.65	0.4586	276.15	0.6796	286.15	2.5628

266.15	0.3409	272.9	0.4637	277.15	0.7699	287.15	3.0045
267.15	0.3570	273.122	0.4684	278.15	0.8729	287.65	3.276
268.15	0.3738	273.15	0.4690	279.15	0.9907		

Upper quadruple point for ethane is T=287.77 K, P=3.348 MPa.

Table 3.8 Recommended data of the equilibria "gas – ice – hydrate" and "gas – liquid water – hydrate" for isobutane

T, K	P, MPa	T, K	P, MPa	T, K	P, MPa	T, K	P, MPa
243.15	0.0180	258.15	0.0479	267.15	0.0808	272.15	0.1058
248.15	0.0207	260.15	0.0541	268.15	0.0854	272.65	0.1086
253.15	0.0253	263.15	0.0645	269.15	0.0902	273.15	0.1114
258.15	0.0289	264.15	0.0683	270.15	0.0952	273.65	0.1246
263.15	0.0351	265.15	0.0723	271.15	0.1004	274.15	0.1394
264.15	0.0398	266.15	0.0765	271.65	0.1030	274.65	0.1559

Upper quadruple point for isobutane is 274.97 K, pressure 0.1673 MPa.

Table 3.9 Recommended data of the equilibria "gas – ice – hydrate" and "gas – liquid water – hydrate" for propane

T, K	P, MPa	T, K	P, MPa	T, K	P, MPa	T, K	P, MPa
243.15	0.03634	267.15	0.12825	272.65	0.16601	275.15	0.26263
248.15	0.04812	268.15	0.13453	272.9	0.16793	276.15	0.32752
253.15	0.06313	269.15	0.14106	273.15	0.16986	277.15	0.40965
258.15	0.08202	270.15	0.14785	273.4	0.17931	278.15	0.51459
263.15	0.10554	271.15	0.15491	273.65	0.18931	278.49	0.55644
264.15	0.11088	271.65	0.15854	273.9	0.19988		
265.15	0.11643	272.15	0.16224	274.15	0.21106		
266.15	0.12223	272.4	0.16412	274.65	0.23539		

Upper quadruple point for propane is 278.49 K, pressure 0.5567 MPa.

The recommended data for CO_2 hydrate were processed as follows: experimental data for negative Celsius temperatures were taken from an article by Japanese scientists [82], experimental data from our work [83] were taken for positive temperatures.

Table 3.10 Recommended data of the equilibria "gas – ice – hydrate" and "gas – liquid water – hydrate" for CO_2

T, K	P, MPa	T, K	P, MPa	T, K	P, MPa	T, K	P, MPa
243.15	0.3365	267.15	0.8887	273.15	1.2453	279.15	2.5447
248.15	0.4205	268.15	0.9208	273.65	1.3166	280.15	2.8942
253.15	0.5195	269.15	0.9537	274.15	1.3929	281.15	3.3005
258.15	0.6350	270.15	0.9875	274.65	1.4748	282.15	3.7736
263.15	0.7683	271.15	1.0220	275.15	1.5626	283.13	4.5
264.15	0.7972	271.65	1.0396	276.15	1.7578		
265.15	0.8269	272.15	1.1166	277.15	1.9831		
266.15	0.8574	272.65	1.1788	278.15	2.2433		

Low quadruple point for carbon dioxide is 271.72 K, pressure 1.03 MPa.

Upper quadruple point for carbon dioxide is 283.13 K, pressure 4.5 MPa.

3.6. Conclusions

In the chapter the thermodynamic analyses of three phase hydrate equilibria were performed.

Firstly, we obtained a simple thermodynamic correlation between three phase equilibria with ice and with supercooled water at temperatures below 273 K (the similar correlation also exist at temperature above 273 K for calculating the hypothetic equilibrium line "gas – superheated ice – hydrates"). This correlation works good for ethane, propane, isobutane, nitrogen and methane hydrates.

Secondly, we proposed a new technique for checking the thermodynamic consistency and smoothing of the experimental data for such hydrate-forming gases.

And the third, we presented the smoothed experimental data of the equilibria "gas – ice – hydrate" and "gas – liquid water – hydrate" for some gases. This data may be used for calculations of hydrate decomposition enthalpies to ice and to liquid water, as well as hydrate numbers and the position of quadruple point.

Chapter 4. Phase equilibria "pore water – gas – ice" in the soils. Thermodynamic description and some applications

The unfrozen water content in frozen rocks (soils) play an important role on their physical, physicomechanical, thermophysical and geophysical properties (see for review [84-89]). Recently researchers from Skoltech hydrate team were proposed a rapid potentiometric method for determining the temperature dependence of unfrozen water content in frozen soils. The potentiometric method includes the experimental determination of pore water activity at positive in Celsius (near room) temperature and atmospheric pressure and then the thermodynamic calculation of unfrozen water content at negative (Celsius) temperature. The theoretical foundations of this rapid method are described in detail in some papers [90, 91]. The application of the potentiometric method makes it possible to carry out the numerous determinations of pore water content during a short time in frozen soils.

At present it is essential to expand the potentiometric method for assessing the effect of the gas component in frozen soils and the unfrozen water content. The problem of gases in permafrost has several aspects, including gas emission from deep horizons, which are presented in a classical review paper by Are [92]. Recently a new geological phenomenon - crater formations in permafrost area – also is connected with gases in frozen rocks. A natural phenomenon has been discovered in the zone of continuous permafrost in the north of Western Siberia, where gas outbursts from shallow permafrost produce craters as large as tens of meters in diameter and 30-60 m deep [93-96].

From a thermodynamic point of view, the influence of free gases and gases, dissolved in pore water, practically has never been treated before, except for a few theoretical and experimental works on freezing temperature estimation. Thermodynamic calculations were performed previously to gas saturated water in sub-ice Lake Vostok in Antarctica [97, 98] under a hydrostatic pressure of 35-40 MPa. Experimental studies were focused on pore fluids with dissolved gases (primary, carbon dioxide and methane) and gas hydrates [99-101].

So, the main idea of the chapter is the thermodynamic study of gas pressure influence on the amount of the unfrozen mineralized pore water in frozen soils (rocks). Thermodynamic description below addresses the equilibrium in the system "free gas – pore water with salts and dissolved gases – ice" for freezing gas-saturated soils. Calculations are performed for the freezing temperature of pore fluids containing gases like methane, carbon dioxide, nitrogen, and their mixtures.

First, some remarks concerning the influence of hydrostatic pressure on phase equilibrium "pore water – ice", which is a special case of the problem under consideration. It is well known that the melting temperature of ice depends on hydrostatic pressure: pressurized ice melts at a lower temperature because ice is less dense than water (hence, the molar volume of frozen water exceeds that of liquid water). Thus, the ice–water thermodynamic equilibrium in the *P-T* coordinates slopes to the left. A shift of melting temperature from 273.15 K to 272.15 K requires an external pressure of ~13.5 MPa. The slope at 273.15 K (*dP/dT* derivative) can be found from the Clausius-Clapeyron equation, which includes the enthalpy of ice melting, as well as the ice-water molar volume difference. The melting temperature of hexagonal ice as a function of pressure was measured long ago by Bridgman [102] till a pressure of 210 MPa and a temperature of -22 °C.

4.1. Phase equilibrium of "gas – pore water – ice" in the soil systems

The phase equilibrium of the system "aqueous solution (water with dissolved gases and salts) – gas – ice" exposed to pressure of gas (or a gas mixture) is found using quality in equilibrium of pore water (μ_w) in the soil sample and ice (μ_{ice}) chemical potentials. It leads to an equation that relates temperature and pressure at the equilibrium of three phases: ice, water with dissolved gases and salts, and gas.

In the general case, the chemical potential of pore water $\mu_w(P,T)$ containing also gases and salts is

$$\mu_w(P,T) = \mu_w{}^0(P_0,T) + RT\ln(1-x_g) + RT\ln(a) + \bar{V}_w \cdot (P-P_0), \qquad (4.1)$$

where P is the external pressure (gas pressure in our case) applied to the thermodynamic system, MPa; P_0= 0.101325 MPa is the atmospheric pressure; T is the temperature, K; $T_0 = 273.15$ K; $\mu_w{}^0(P_0,T)$ is the chemical potential of pure water at the atmospheric pressure P_0 and the temperature T ($\mu_w{}^0(P_0,T)$ at $T < T_0$ is the chemical potential of supercooled water as metastable phase). The molar fraction of dissolved gases x_g is

$$x_g = \sum_{i=1}^{N} x_i,$$

where x_i is the molar fraction of the i-th gas in a mixture; R is the universal gas constant (8.3146 J/mol K); a is the water activity in a saline pore fluid (electrolyte) at the atmospheric pressure P_0; and $\bar{V}_w$ is the partial molar volume of water in the fluid, cm^3/mol. Note that equation (4.1) is approximate and implies the joint effect of dissolved gases and salts on the chemical potential of pore water. This assumption is valid to a high accuracy at low salinity (within 30-40 g/L) and at high contents of pore moisture. The activity a of pure water at atmospheric pressure, including its salinity, may be measured experimentally. Also, it may be calculated if we measure the activity of pore water a_1 without salinity and bulk water a_2 with salinity by using the approximate equation $a \approx a_1 \cdot a_2$. This relation stems from the assumption that the two factors contribute approximate additively to the chemical potential of pore water, so the activities are multiplied. At high water contents in a freezing talik, a_1 is ~1. For hydrophilic porous materials $a_1 < 1$ and depends on its water content.

Previously the dependence of a_1 was investigated experimentally when studied the behavior of unfrozen water [91] and hydrate formation [90] in porous materials. The variable x_g in (4.1) refers to equilibrium gas solubility in water and can be found using the equation of Krichevsky-Kazarnovsky [59], with empirical temperature-dependent solubility coefficients and partial molar volumes of dissolved gases. Furthermore, gas solubility can be calculated with modeling software using phase equations for multi-component mixtures. Note also that the

equilibrium gas solubility depends neither on salinity nor on the pore space structure. The former effect is described approximately by the empirical equation of Sechenov [103] and the latter one remains poorly constrained.

Another assumption is that the partial molar volume of water $\bar{V}_w$ in the pore fluid almost coincides with molar volume V_w of pure water. This assumption is valid to a high accuracy for fluids that contain dissolved gases and moderate amount of salts (within 40-50 g/L). Water, with its assumed ~1 g/cm^3 density and 18.015 g/mol molecular weight, has the partial molar volume V_w = 18.015 cm^3/mol. A more exact equation for the water molar volume [104] includes the effects of temperature and external pressure, but they can be neglected within the ranges of practical interest (263-273 K and up 3-4 MPa).

The chemical potential of ice as a function of temperature and pressure $\mu_{ice}(P,T)$ is

$$\mu_{ice}(P,T) = {\mu_{ice}}^0(P_0,T) + V_{ice} \cdot (P - P_0), \qquad (4.2)$$

where ${\mu_{ice}}^0(P_0,T)$ is the ice chemical potential at atmospheric pressure P_0 and temperature T; V_{ice} is the molar volume of ice, cm^3/mol, which is 19.65 cm^3/mol, assuming an ice density of 0.917 g/cm^3. The pressure and temperature dependence of the ice partial molar volume [104] can be neglected, as in the case of water. Equation (4.2) does not include solubility of gas in ice. It can be accounted for by adding the term $RT\ln(1 - x_{ice})$, where x_{ice} is the molar content of gas in ice (found empirically as a function of gas pressure). However, gases, except for hydrogen, helium, and neon, cannot dissolve in ice because their molecules (atoms) are larger than channels in the hexagonal ice structure. The gases under consideration (CH_4, CO_2, N_2, and methane homologues) are almost insoluble in ice, and the respective term is omitted in (4.2).

The difference between the chemical potentials of water ${\mu_w}^0(P_0,T)$ and ice ${\mu_{ice}}^0(P_0,T)$ at atmospheric pressure is

$$\Delta\mu^0(P_0,T) = {\mu_w}^0(P_0,T) - {\mu_{ice}}^0(P_0,T).$$

Its temperature dependence at P_0 is given by the Gibbs-Helmholtz equation

$$\frac{d(\Delta\mu^0(P_0,T)/T)}{dT} = -\frac{\Delta h(T)}{T^2}.$$

The water-ice enthalpy difference is

$$\Delta h(T) = h_w(T) - h_{ice}(T) = \Delta h(T_0) + \Delta c \cdot (T - T_0).$$

The enthalpy of ice melting $\Delta h(T_0)$ at $T = 273.15$ K and $P = P_0$ is assumed to be 6008 J/mol [105]; other published enthalpy values differ from one another at $T = 273.15$ K for ~0.1 % on average. The water-ice heat capacity difference Δc depends on temperature. This dependence is however negligible for the narrow temperature range around 273.15 K (from 263.15 to 278.15 K), i.e., $\Delta c = 36.93$ J/mol at T_0 [105].

With the above assumptions, integration of the Gibbs-Helmholtz equation leads to a temperature dependence of the difference between water and ice chemical potential

$\Delta\mu^0(P_0,T) = \mu_w{}^0(P_0,T) - \mu_{ice}{}^0(P_0,T)$ at $P = P_0$:

$$\Delta\mu^0(P_0,T) = \Delta h(T_0) \cdot \left(1 - \frac{T}{T_0}\right) - \Delta c \cdot \left(T\ln\frac{T}{T_0} + (T_0 - T)\right) =$$

$$= 6008 \cdot \left(1 - \tfrac{T}{T_0}\right) - 36.93 \cdot \left(T \cdot \ln\tfrac{T}{T_0} + (T_0 - T)\right). \quad (4.3)$$

$\Delta h(T_0)$ and Δc are assumed to be 6008 J/mol and 36.93 J/mol K, respectively.

The pore water, containing dissolved gases and salts, reaches thermodynamic equilibrium with ice at the gas pressure P when

$$\mu_w(P,T) = \mu_{ice}(P,T). \quad (4.4)$$

Using equations (4.1) and (4.2), we obtain from (4.4) that

$$\mu_w{}^0(P_0,T) + RT\ln(1 - x_g) + RT\ln a + \bar{V}_w \cdot (P - P_0) =$$

$$= \mu_{ce}{}^0(P_0,T) + V_{ice} \cdot (P - P_0)$$

or

$$\mu_w{}^0(P_0,T) - \mu_{ice}{}^0(P_0,T) = V_{ice} \cdot (P - P_0) - RT\ln(1 - x_g) -$$

$$-RT\ln a - \bar{V}_w \cdot (P - P_0).$$

Since $\Delta\mu^0(P_0,T) = \mu_w{}^0(P_0,T) - \mu_{ice}{}^0(P_0,T)$, taking into account (4.3), we obtain

$$6008 \cdot \left(1 - \frac{T}{T_0}\right) - 36.93 \cdot \left(T \ln \frac{T}{T_0} + (T_0 - T)\right) =$$

$$= V_{ice} \cdot (P - P_0) - RT \ln(1 - x_g) - RT \ln a - \bar{V}_w \cdot (P - P_0)$$

With transformed right-hand side, the latter equations become

$$6008 \left(1 - \frac{T}{T_0}\right) - 36.93 \left(T \ln \frac{T}{T_0} + (T_0 - T)\right) =$$

$$= \Delta V \cdot (P - P_0) - RT \ln\left(a \cdot \left(1 - x_g\right)\right) =$$

$$= -RT \ln[a \cdot \left(1 - x_g\right) \cdot \exp\left(-\frac{\Delta V \cdot (P - P_0)}{RT}\right)], \quad (4.5)$$

where $\Delta V = V_{ice} - \bar{V}_w$.

Given that $T = T_{fr}$, where T_{fr} is the freezing temperature (K) of gas-bearing pore water, equation (4.5) eventually becomes

$$6008 \cdot \left(1 - \frac{T_{fr}}{T_0}\right) - 36.93 \cdot \left(T \ln \frac{T_{fr}}{T_0} + \left(T_0 - T_{fr}\right)\right) = -RT_{fr} \ln(b), \quad (4.6)$$

where $b = a \cdot \left(1 - x_g\right) \cdot \exp\left(-\frac{\Delta V \cdot (P - P_0)}{RT_{fr}}\right)$.

Equation (4.6) allows calculating the freezing temperature of a pore water fluid containing dissolved gases and salts ($T = T_{fr}$) at a specified gas pressure $P \geq P_0$. Thus, it is applicable to pore water rich fluid at different gas pressures, gas compositions, and salinities.

In the specific case at $a = 1$ and $x_g = 0$, equation (4.6) describes the well known liquid water - ice equilibrium under hydrostatic pressure. If the external pressure is produced by gas, equation (4.6) have to solve jointly with equation for equilibrium solubility of gas in water x_g (like Krichevsky-Kazarnovsky equation). Note that equation (4.6) describes the relation between $T = T_{fr}$ and P irrespective of thermodynamic equilibrium between water and gas. Thus, the equation (4.6) also applicable to pore water fluids, which is undersaturated or oversaturated with respect to gas.

It should be pointed that the differentiation of (4.6) along the equilibrium line gives a generalized Calusius-Clapeyron equation, which becomes the common equation for the water-ice equilibrium under hydrostatic pressure in the case of pure water free from gas and salts.

Below we discuss some possible applicability of the equation (4.6) for freezing gas saturated talik and influence of gas pressure on unfrozen water content.

4.2. Freezing of gas-saturated soils and the thermodynamic calculations of equilibrium in the system "gas – salt water – ice"

Let's consider the closed talik, containing in its porous space some free gases and pore water. While the talik is freezing, the pore water is freezing to ice and the gas pressure is increasing. So, during the freezing process, the increasing of the pressure may continue up to the achievement of the equilibrium "gas – pore water – ice" at a given temperature or up to the pressure when the hydrate forming process is beginning. The scenario of pressure buildup in a freezing closed talik with high content of pore gas may be generally as follows. First, a closed talik forms under a thermokarst lake and becomes saturated with gas. When the lake becomes shallower, the talik begins to freeze up, first from below and from the sides and then also from above as the lake shrinking progresses. The confined freezing produces an increasingly pressurized lens saturated with gas and water, and thus causes heaving of frozen soils above the talik. The arising frost mound explodes (like hydraulic fracture), provided that the volumetric content of pore gas is high enough. Pore gas in a freezing talik may either be released from microbial decaying organic matter or from dissociating relict gas hydrates, or it may come from greater depths through highly permeable zones.

As the closed talik freezes up, the pressure of gas (of whatever origin) increases due to:

- cryogenic concentration or expulsion of gas inward of the shrinking talik, while the volume of free gas reduces;
- decrease in molar volume of water converted to ice during freezing;

- increase in the content of free gas at the account of dissolved gas released during freezing of liquid pore water.

In the absence of free gas, even minor volume reduction in a freezing water-saturated closed system leads to rapid pressure increase. In such systems would rather produce frost mounds (pingoes) than explosive craters [106]. The pore gas in sub-lake taliks consists mainly of methane, with minor carbon dioxide and nitrogen, and occasional traces of heavier methane homologs [92, 107, 108]. Correspondingly, the model below simulates a talik system with pore fluids containing methane, carbon dioxide, nitrogen, and their mixtures. Freezing of increasingly pressurized gas and water-saturated soil has not widely studied before. A single relevant model we know concerns freezing of a closed water-gas volume [109].

Thermodynamic calculations are applied below to different cases of practical interest. Equation (4.6) includes equilibrium gas solubilities in pressurized conditions, at temperatures near 273 K. Pressure and temperature-dependent gas solubility in water (aqueous solutions) can be found with the existing software using equations of state for fluids, which describe phase equilibrium in hydrocarbon systems, as well as some correlations [103] following Henry's law in its generalized thermodynamic formulation [59]. The available published data on gas solubility refer to temperatures above 25 °C, and the Henry's law solubility constants have to be extrapolated to the range of our interest (from -10 to 0 °C), which may cause up to 5–10% error. Extrapolation may be more successful with recent empirical data on gas solubility at low pressures and at temperatures from 5 to 15 °C, i.e., within the subhydrate *P*-*T* domain. The behavior of pressure-dependent solubility is modeled for a CH_4+CO_2 mixture at 0 °C (Figure 4.1) and at 10 °C (Figure 4.2).

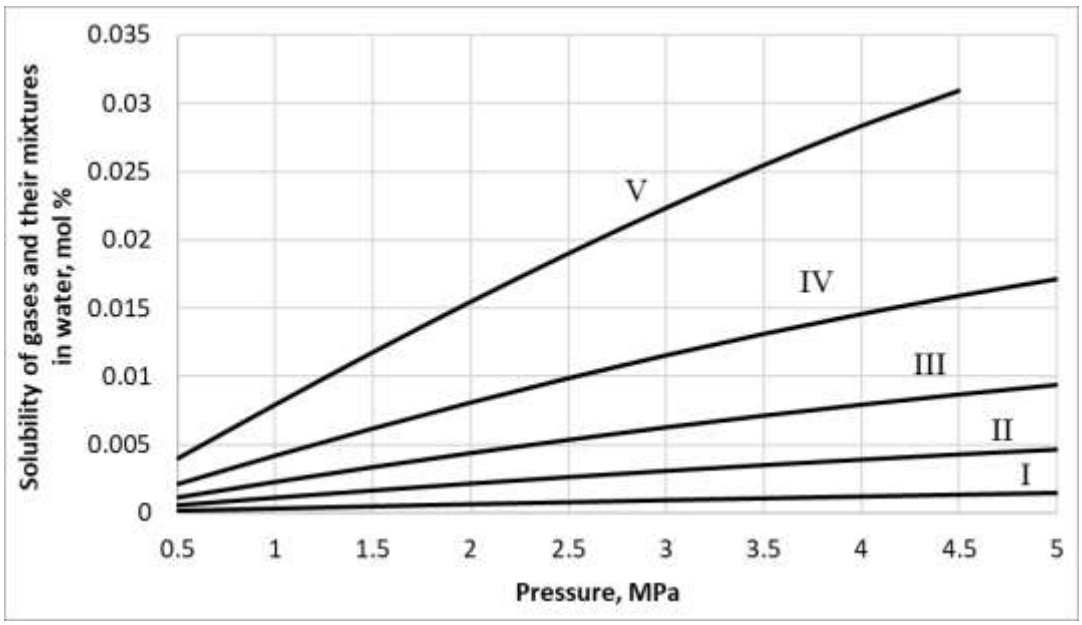

Figure 4.1 Pressure-dependent solubility of gases (methane, carbon dioxide) and their mixtures in water at 0 °C. Curves from I to V correspond to different gas phase compositions: 100 % CH_4 (I), 75 % CH_4 + 25 % CO_2 (II), 50 % CH_4 + 50 % CO_2 (III), 25 % CH_4 + 75 % CO_2 (IV), 100 % CO_2 (V)

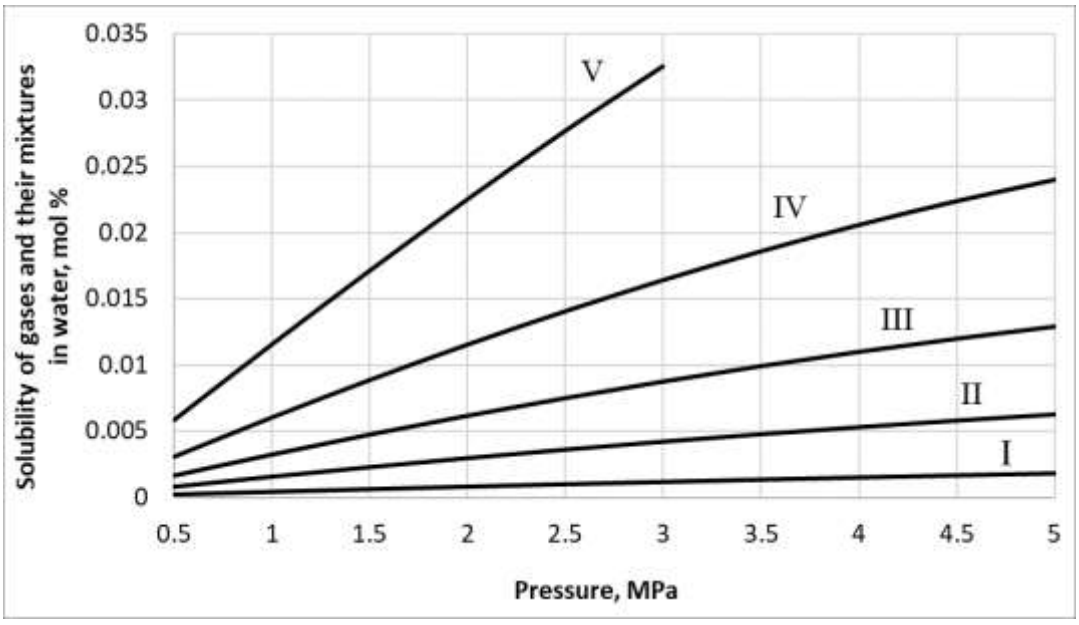

Figure 4.2 Pressure-dependent solubility of gases (methane, carbon dioxide) and their mixtures in water at 10 °C. Curves from I to V correspond to different gas phase compositions: 100 % CH_4 (I), 75 % CH_4 + 25 % CO_2 (II), 50 % CH_4 + 50 % CO_2 (III), 25 % CH_4 + 75 % CO_2 (IV), 100 % CO_2 (V)

The same calculations are performed for pressures corresponding to hydrate stability, i.e., the model includes the metastable equilibrium "gas-bearing water – gas – ice" in the zone of

possible hydrate formation. Further calculations constrain the conditions of gas hydrate formation for methane, carbon dioxide, nitrogen, and their mixtures that form cubic hydrates I, using a thermodynamic model [60]. The curves of three-phase equilibrium "gas – water – hydrate" and "gas – ice – hydrate" for methane, carbon dioxide, nitrogen, and their mixtures (Figures 4.3-4.4) show that methane and carbon dioxide form hydrates near 273 K at ~2.6 MPa and ~1.2 MPa, respectively. Then the freezing temperature of gas-bearing pore fluids is estimated using equation (4.6), taking into account gas solubility at T <0 °C and hydrate formation conditions.

The *P-T* diagram (Figure 4.5) covers the zone of possible hydrate formation, i.e., the zone of metastable equilibrium (as if no hydrate formed); the equilibrium for a four-phase system including hydrate is marked by dots.

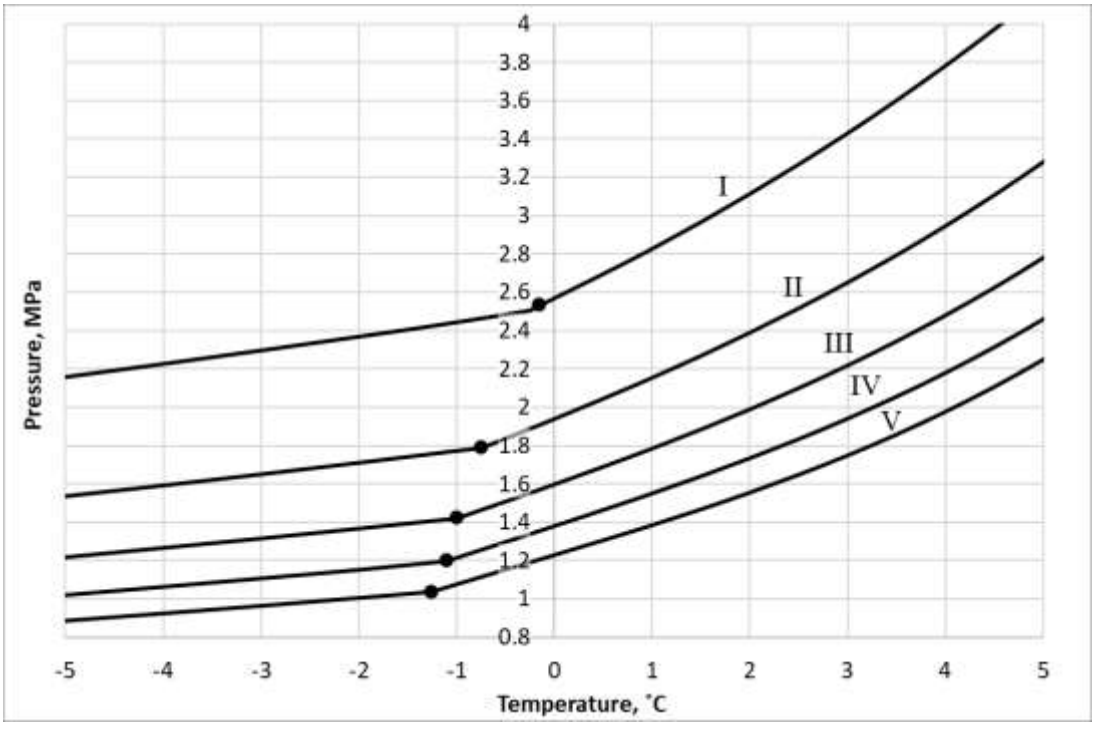

Figure 4.3 Three-phase equilibria "gas – water (ice) – hydrate I" for methane, carbon dioxide and their mixtures. Curves from I to V correspond to different gas phase compositions: 100 % CH_4 (I), 75 % CH_4 + 25 % CO_2 (II), 50 % CH_4 + 50 % CO_2 (III), 25 % CH_4 + 75 % CO_2 (IV), 100 % CO_2 (V). Dots show four-phase equilibrium "gas – water – ice – hydrate"

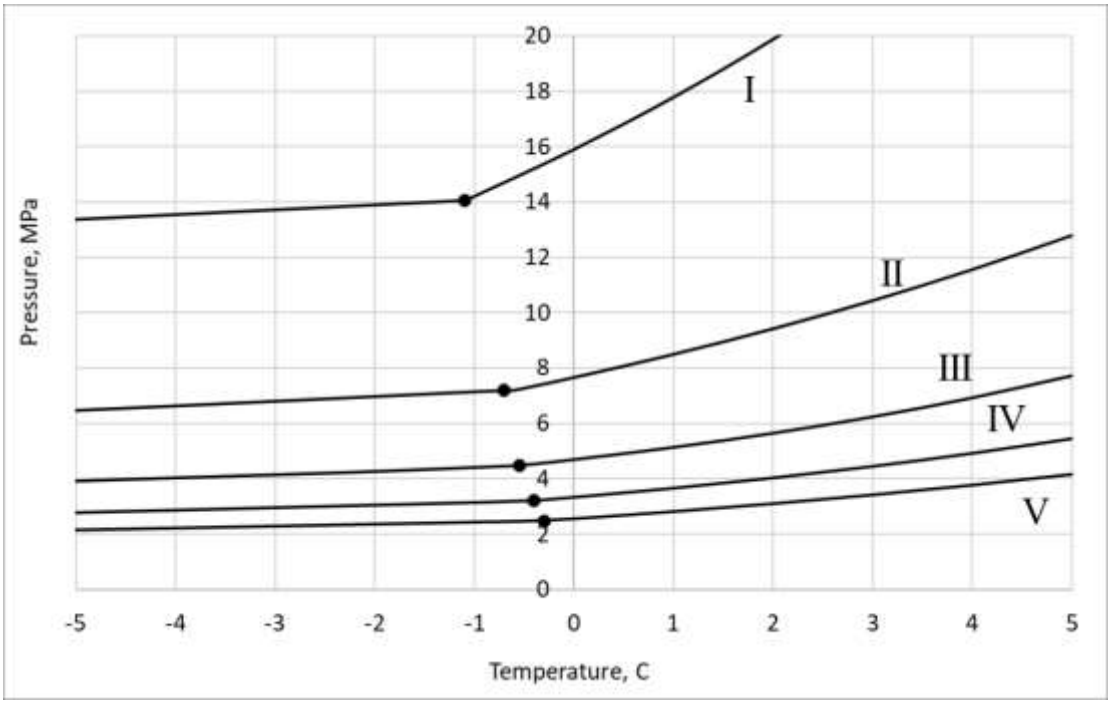

Figure 4.4 Three-phase equilibrium "gas – water (ice) – hydrate I" for methane, nitrogen and their mixtures. Curves from I to V correspond to different gas phase compositions: 100 % N_2 (I), 25 % CH_4 + 75 % N_2 (II), 50 % CH_4 + 50 % N_2 (III), 75 % CH_4 + 25 % N_2 (IV), 100 % CH_4 (V). Dots show four-phase equilibrium "gas – water – ice – hydrate"

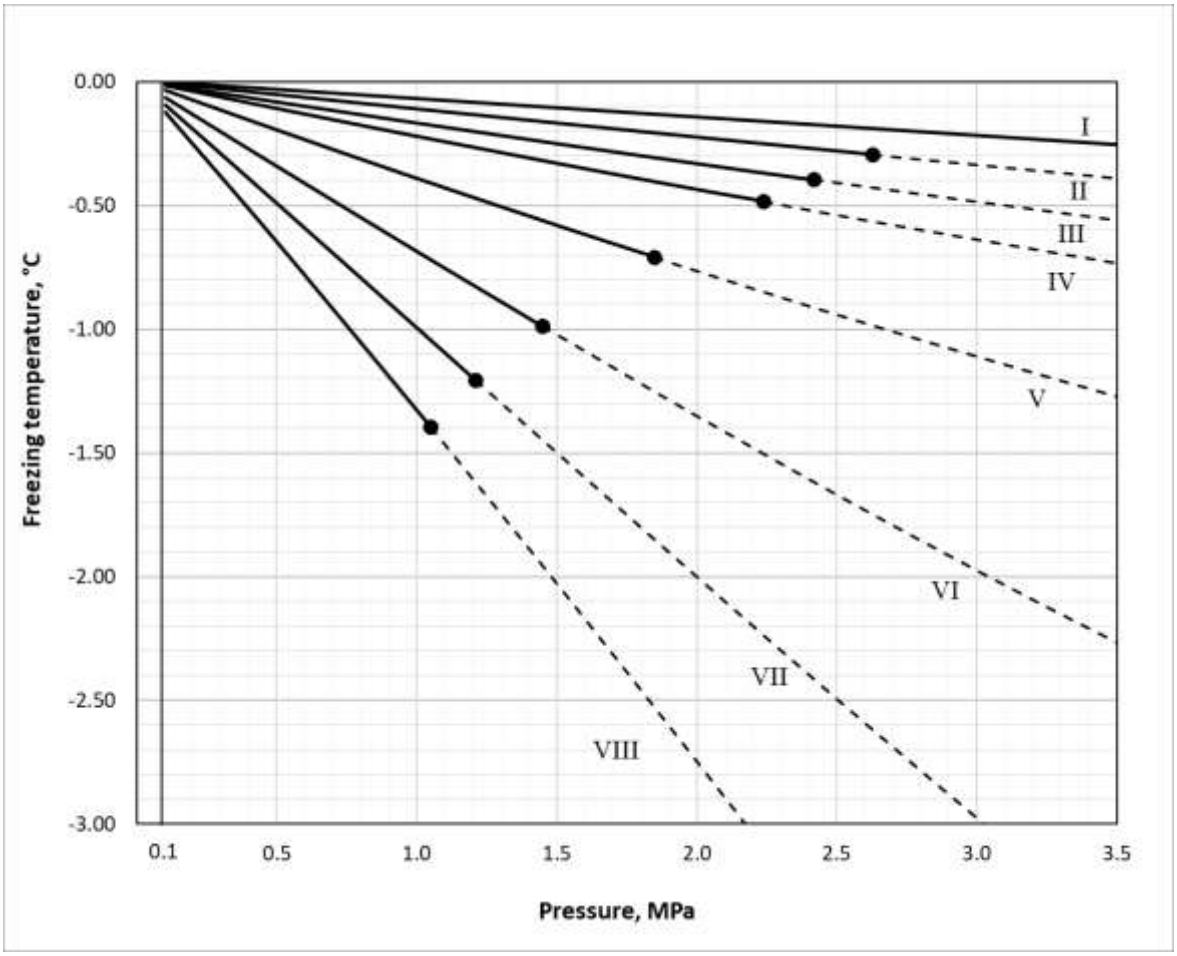

Figure 4.5 Pressure-dependent freezing temperature of pore fluids containing dissolved gases (methane, carbon dioxide and their mixtures). Curves from I to VIII are labeled according to fluid phase composition: pure H_2O free from dissolved gases (I), 100 % CH_4 (II), 95 % CH_4 + 5 % CO_2 (III), 90 % CH_4 + 10 % CO_2 (IV), 25 % CH_4 + 75 % CO_2 (V), 50 % CH_4 + 50 % CO_2 (VI), 25 % CH_4 + 75 % CO_2 (VII), and 100 % CO_2 (VIII)

The presence of carbon dioxide in a gas mixture influences markedly the freezing temperature of pore fluids: at 1.0 MPa, a CO_2-bearing pore water fluid freezes up at –1.4 °C. According to the available filed data, pore gas in freezing closed taliks consists mainly of methane and minor carbon dioxide, and the gas pressure does not exceed 2.0 – 2.5 MPa being limited by the onset of hydrate formation. The available published models of gas fracture show that this pressure is far enough to be responsible for the observed cryovolcanism and formation of natural craters. Joint action of gas pressure, solubility of gases (methane and carbon dioxide), and pore water salinity on freezing temperature (Figures 4.6 and 4.7) was calculated using Sechenov's equation [103], taking into account that gas solubility is lower in saline fluids.

Pressure buildup in a freezing closed talik can be modeled in a simplified thermodynamic formulation (without explicit frontal freezing and geomechanics), in order to estimate the effect of a free gas phase on pressure increase upon partial water-to-ice conversion (and shrinking of the unfrozen zone).

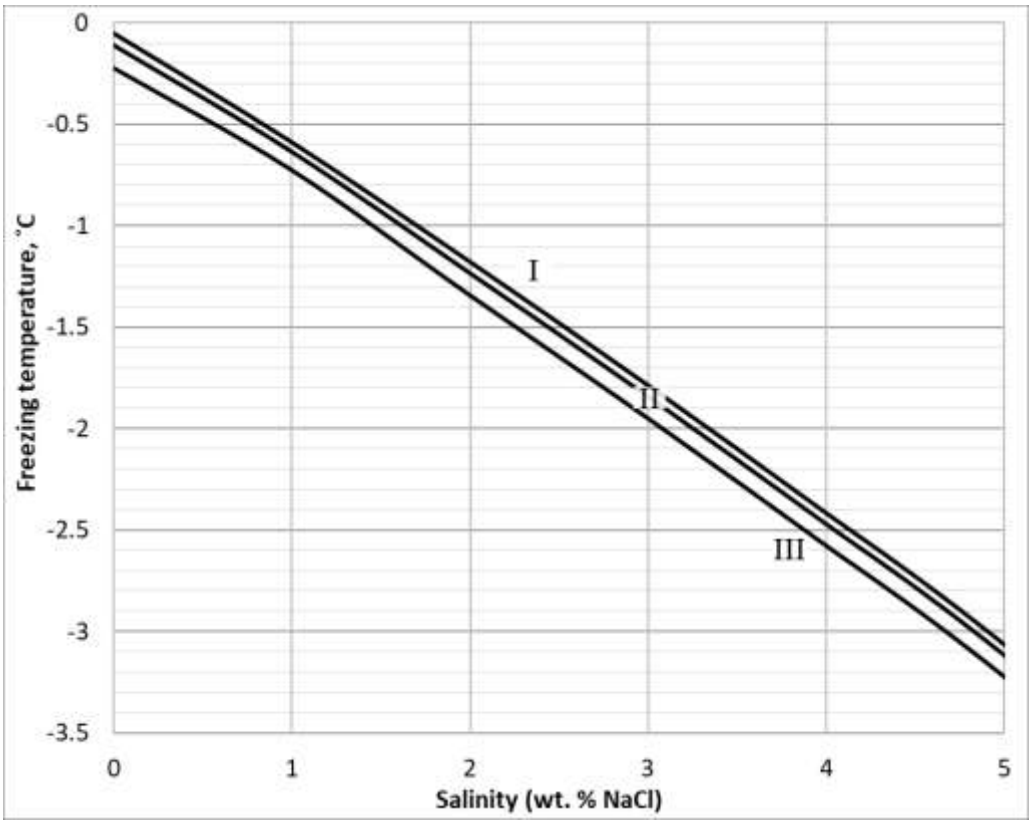

Figure 4.6 Salinity-dependent freezing temperature of methane-bearing solution. Curves I to III are labeled according to gas pressure: 0.5 MPa (I), 1 MPa (II), and 2 MPa (III)

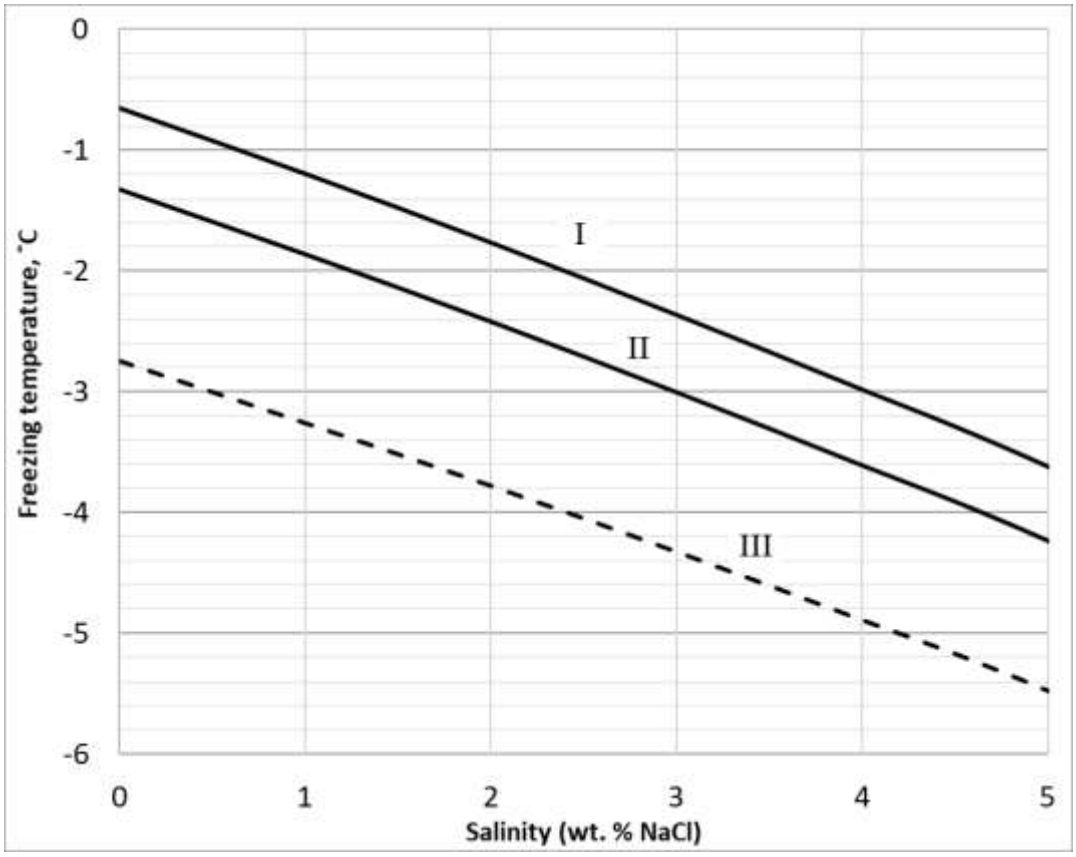

Figure 4.7 Salinity-dependent freezing temperature of solution with carbon dioxide. Curves I to III are labeled according to gas pressure: 0.5 MPa (I), 1 MPa (II), and 2 MPa (III)

At the time when the talik becomes closed and exposed to confined freezing, the system comprises wet soil and methane (hereafter the variables that refer to this system are marked by subscript 1). The unfrozen zone is shrinking with time starting from the volume V_1 at the onset of confined freezing; the pore space is occupied by equilibrated liquid water and gas phases; pore pressure is P_1. Dissolved gas released during water-to-ice conversion (freezing) becomes a free gas phase. The current pressure P depends on the fraction of water converted to ice (δ, u.f.) in the volume V_1. This dependence is found using a mass balance equation (Figure 4.8), assuming a 0.25 MPa starting pressure of gas (methane) in the system. Gas in the unfrozen zone occupies different volume percentages of the pore space (from 1 % to 10%). The system in its initial state (V_1) is assumed to contain both free and dissolved gases; dissolved gases release and become free during freezing. The pressure increase is rapid (the system is rigid) at low initial gas

contents, but slow at high gas contents: it reaches 1.0 MPa and higher upon considerable shrinking of the unfrozen zone.

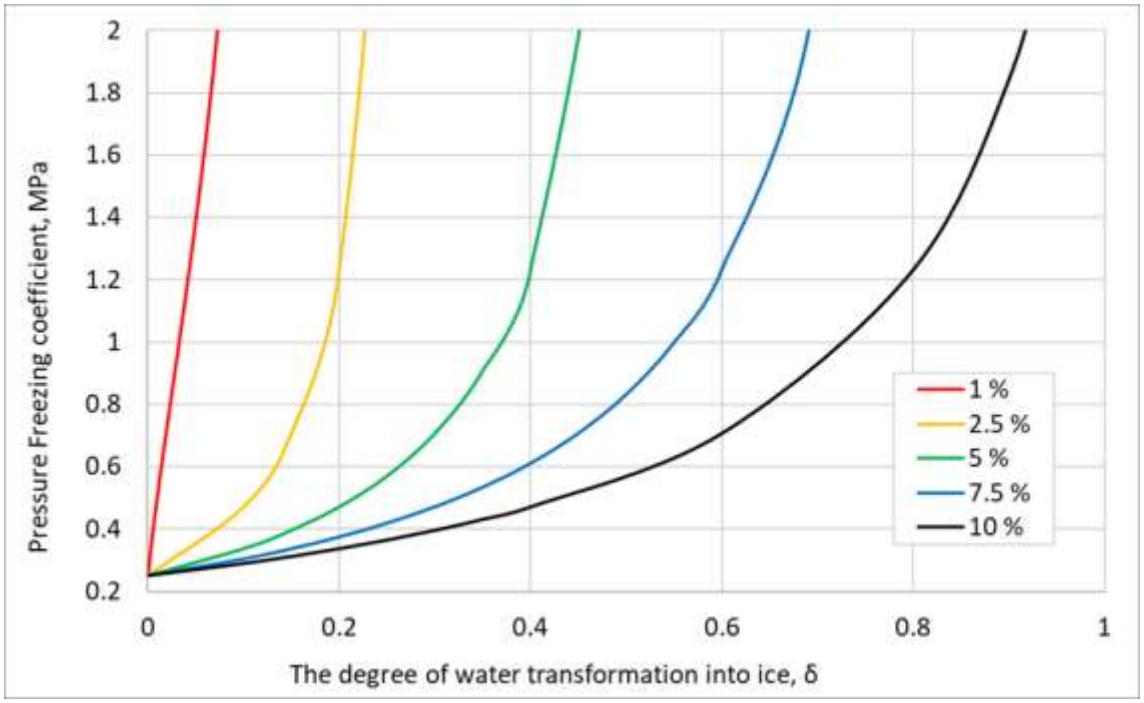

Figure 4.8 Pressure buildup in a freezing methane-bearing closed talik as a function of freezing coefficient

4.3. Influence of gas pressure on unfrozen water content in ice containing soils

The thermodynamic relation (4.6) obtained above also makes it possible to calculate the effect of gas pressure not only on the temperature of the onset of freezing of a gas-saturated pore solution, but also to determine the shift of the entire curve of unfrozen water under gas pressure. Here, as indicated above, two factors influence - the external gas pressure (as hydrostatic pressure) and the gas solubility in pore water. It is easy to see that both of these factors lead to an increase in the content of pore water in the soil with increasing pressure at a given negative Celsius temperature.

Of course, the gas pressure (if the gas is a hydrate forming gas) must be below the hydrate formation line, i.e. three-phase equilibrium "gas – ice – hydrate". If the gas pressure exceeds the equilibrium line "gas – ice – hydrate", then this equilibrium should be considered as metastable.

When the gas pressure exceeds the equilibrium pressure "gas – ice – hydrate", unfrozen water "transforms" into non-clathrate water (see the special study in the next chapter).

The effect of gas pressure on the content of unfrozen water is noticeable for such individual gases as carbon dioxide (due to the high solubility of CO_2 in water) and nitrogen (due to the possibility of increasing nitrogen pressure to 15 MPa without the beginning of hydrate formation), as well as for gas mixtures methane – CO_2, nitrogen – CO_2 and methane – CO_2 – nitrogen.

We calculate the influence of the carbon dioxide pressure on the unfrozen water content for samples of polymineral and kaolinite clay. Curves of unfrozen water content were obtained earlier [91].

It can be seen (Figure 4.9) that, at a given sample moisture content, as the gas pressure of CO_2 increases, the freezing temperature decreases. For instance, at fixed water content of 6.65%, the freezing temperature changed from -5 to -6.5 ^{o}C when the pressure changes from 0.1 to 1 MPa.

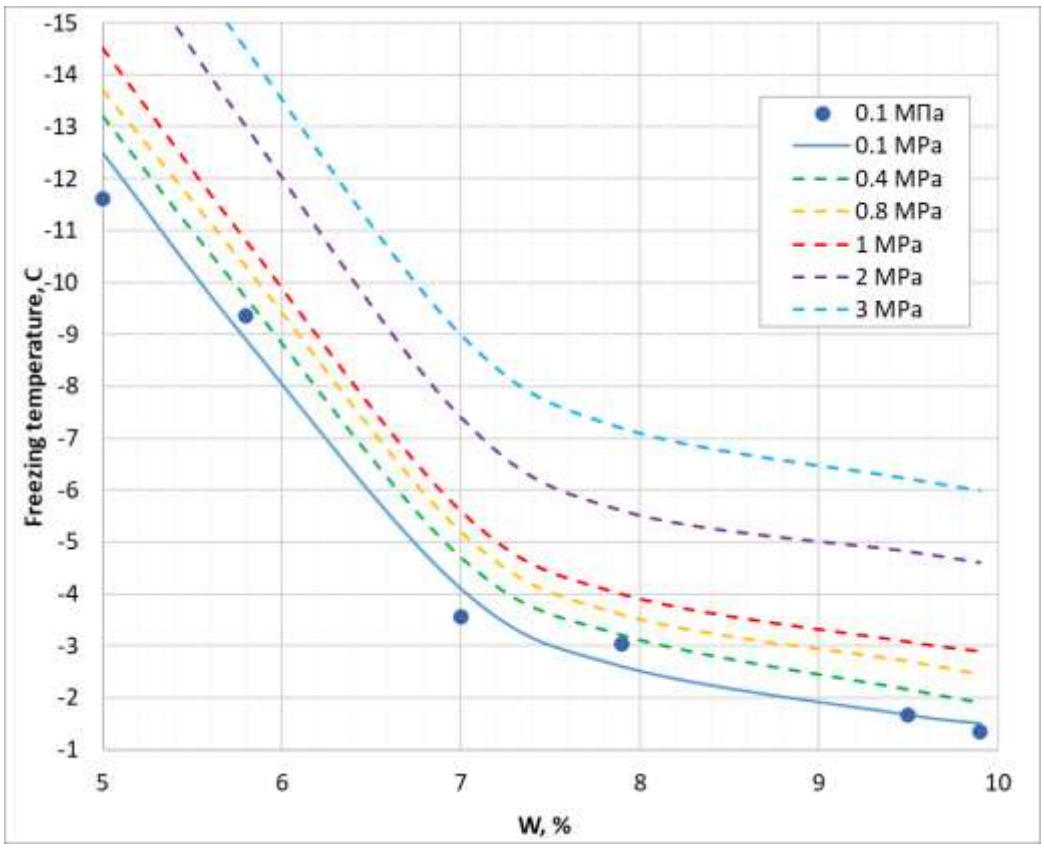

Figure 4.9 Content of unfrozen water in polymineral clay at different pressures of carbon dioxide. Blue dots - experimental data on unfrozen water content at 0.1 MPa; blue line - approximation of experimental data; dotted lines – at different pressures of carbon dioxide

Also, in Figure 4.10 we presented the calculations of unfrozen water content in kaolinit clay at different pressure of carbon dioxide. It can be seen that at a fixed water content in the sample, the freezing temperature strongly decreases with increasing CO_2 pressure. For example, at 15% water content in the kaolinite sample, the freezing temperature (the beginning of freezing) changes from -1 ^oC to -4 ^oC when the CO_2 pressure changes from 0.1 to 2 MPa.

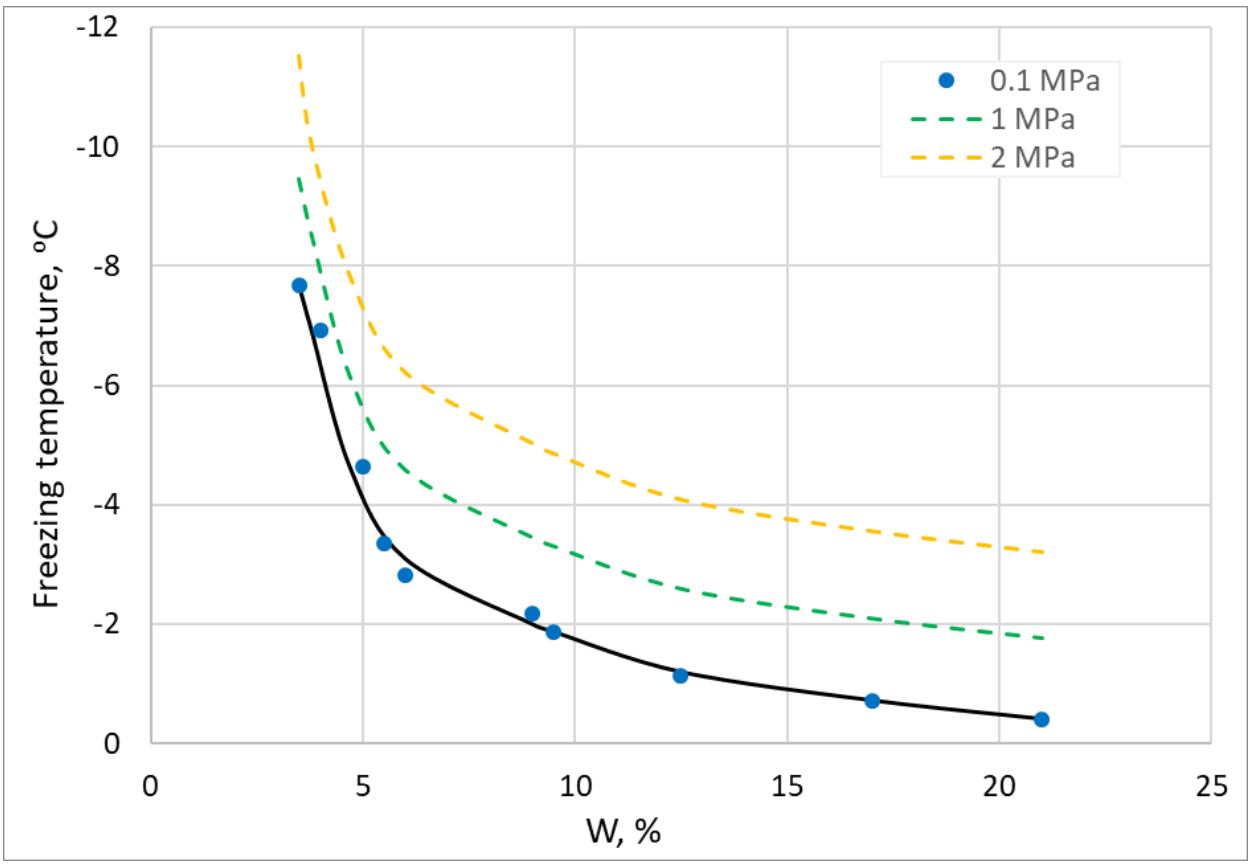

Figure 4.10 Freezing temperature versus water content in kaolinite clay at different carbon dioxide pressures. Blue dots - experimental data on unfrozen water content at 0.1 MPa; black line - approximation of experimental data; dash lines – calculations at different pressures of carbon dioxide

4.4. Conclusions

In the chapter the thermodynamic investigation of gas pressure influence on freezing temperature of pore water in frozen soils as well as the gas influence on the amount of the unfrozen water (shift of the unfrozen water curve by affecting the gas pressure). The general thermodynamic equation was derived. The following factors are taken into account: external gas pressure (the same factor as hydrostatic pressure), gas solubility in pore water, salinity of the pore water. Some model calculations are performed for the freezing temperature of pore fluids containing gases like methane, carbon dioxide, nitrogen, and their mixtures. The model for increasing pressure in freezing talik is also presented as thermodynamic description of new geocryological phenomena.

Chapter 5. Phase equilibria "gas – pore water in soil – gas hydrate". Influence of gas pressure on the pore water content in equilibrium with hydrate

The investigation of gas hydrate's phase equilibria in porous media is great of importance due to the prospects for unconventional energy resource development - gas hydrate deposits. The analysis of publications shows that the direct experimental study of the hydrate formation in porous media (by similar approach as the study of hydrate equilibrium in bulk liquid water and in aqueous solutions in a high-pressure cell) has some serious methodological problems. As a result, the experimental data obtained are mainly qualitative. Drs. Istomin V.A. and Chuvilin E.M. paid attention to this circumstance in 2004-2006. Then the concept of non-clathrate water was proposed in the several papers by Chuvilin E.M., Istomin V.A. et al. (see discussion below). Then the thermodynamic method was developed for pore water content' calculations in equilibrium with hydrate phase depending on gas pressure and temperature. This method is based on experimental measurement of the pore water thermodynamic properties (water potential or water activity depending on pore water content in the sample of porous media). In addition, this authors were proposed a new experimental technique - the direct determination the non-clathrate water content in static condition by contact method.

In this chapter the above research of non-clathrate water in porous media was continued. The main idea of our study is to obtain the analytical dependences on the gas pressure influence on the of non-clathrate water content in the soil systems at a fixed temperature. The obtained relations reveal the qualitative regularities of the gas pressure influence on the non-clathrate water' content as a highly nonlinear dependence.

Research objectives of this chapter are:

1. To propose general thermodynamic formulas, which connect pore water activity with gas pressure in tested soil sample.

2. To obtain some simple correlations, which are convenient for practical calculations of non-clathrate water content from measurement of pore water activity in the soil samples.
3. To proposed the technique for the thermodynamic recalculations of non-clathrate water data from one temperature to another temperature.
4. To reveal connection between unfrozen water and non-clathrate water.

5.1. Phase equilibria of gas hydrates in porous media: brief analysis of the problem

The phase equilibrium problem of gas hydrates in porous media has a long history. Russian scientists first drew attention to this problem in the 1960s of the 20th century during the analysis of hydrate conditions in the oil and gas basins of the Siberian permafrost. The first experimental data concerning the existence of pore hydrate conditions were obtained by Makogon in the mid-sixties of the last century to substantiate natural gas hydrate formations in reservoir rocks [110]. Those results showed that thermobaric conditions for pore hydrates can be different from bulk hydrates. Later, to understand the effect of porous media, a new parameter was added to the thermodynamic model of hydrate existence, which described as pore water in a single capillary of a given radius. In subsequent studies, a porous medium was also considered to be a system with an average capillary radius. As a rule, the value of $\cos(\theta)$ (θ is contact angle) for hydrophilic capillaries was taken to be unity. This model gives the value of the temperature shift of the hydrate formation curve depending on capillary radius (the shift is increased while decreasing the capillary radius). This was followed by numerous attempts of experimental study on gas hydrate conditions in different porous media [111–123], as well as attempts to present theoretical estimations for the description of size distribution and its influence on phase equilibrium in a porous medium [124–136].

Nowadays, the theoretical approach for a real soil system of setting the pore space structure as a certain capillary size distribution and from this distribution calculating the

thermodynamic properties of pore water has only methodological (or theoretical) significance [90]. This is since real porous media (sediments, soils, rocks) can be considered to be systems of capillaries or particle size distribution only on the qualitative level. Such a theoretical scheme has indeed had practical results for specially prepared model porous media with a narrow capillary size distribution, as considered in [124, 90]. Therefore, for soil systems another approach is preferable, in which the thermodynamic properties of pore water in a sample of porous media are measured depending on the water content of the sample. Such experimental data on pore water properties (measurements of pore water activity or unfrozen water content in the samples) make subsequent thermodynamic calculations of pore water content in equilibrium with gas, hydrate, and ice possible. Additional analysis showed that the effect of hydrate-forming gas pressure on nonclathrated water content was not previously covered. Below, our main task is to reveal the effect of pressure of a hydrate-forming gas on pore water content in the sample that is in equilibrium with gas hydrates at the temperature under consideration. Such pore water in soils/sediments is called nonclathrated water. Thus, nonclathrated water is liquid water in a sample of a porous medium (a soil or sediment system) at pressure P, which is in thermodynamic equilibrium with a hydrate-forming gas and a gas hydrate in a bulk phase. Pressure P must be greater than P_{eq}, the equilibrium pressure of hydrate formation (corresponding to equilibrium bulk water or ice–gas–gas hydrate). The term "nonclathrated water" was first introduced in papers [137, 138] by analogy with the concept of unfrozen water. Currently, this term is already used in the literature [5, 139, 140]. In contrast to unfrozen water, the concept of nonclathrated water is applicable to both negative and positive Celsius temperatures.

5.2. Analytical dependences of the gas hydrate-former pressure influence on the equilibrium content of non-clathrate water

For describing the thermodynamic properties of pore water, it is convenient to use water activity $a(T, W)$, which depends on the water content of the sample and temperature

$$a = \frac{p_{wpor}}{p_w}, \tag{5.1}$$

where p_{wpor} is water vapor pressure over the soil sample with water content W (wt% water relative to the dry sample), and p_w is the pressure of saturated water vapor over the bulk water (in MPa or Pa).

The experimental determination of pore water activity $a(T, W)$, depending on water content W in the soil at or close to room temperature, can be carried out by various methods. The most efficient method is to measure the dew point of air brought into equilibrium with a wet soil sample with water content W, followed by a recalculation of the dew-point temperature to water vapor pressure over wet soil and, thereby, water activity. The method for measuring pore water activity is described in detail elsewhere [141].

The activity of pore water in a wet sample W depends on both the water content of the sample and on its temperature, i.e., $a(T, W)$. As a first approximation, the temperature dependence of pore water activity a (at a fixed W) can be neglected. However, this is not the case for low water content in the soil, especially in the presence of a clay component with a sliding framework in the soil (for example, smectite).

Another task was to derive some thermodynamic dependencies connecting pore water activity in the soil (at atmospheric pressure) with the fugacity or pressure of the hydrate-forming gas at a given temperature. At the same time, it was necessary to separately describe positive and negative temperatures due to the existence of unfrozen water at negative Celsius temperatures. Unfrozen pore water in equilibrium with ice also exists at gas pressure, but gas pressure must be below pressure on the gas–ice–hydrate equilibrium line. At pressure P, higher pressure P_{eq}

(pressure at the gas–ice–hydrate equilibrium line), exists instead of ice in the gas hydrate phase (the hydrate phase becomes stabler than the ice phase). Thus, pore water at pressure $P > P_{eq}$ should be nonclathrated water (according to the terminology considered in the introduction).

The consideration of a gas pressure effect on nonclathrated water content begins at positive Celsius temperatures. The soil sample is fixed at temperature $T > 273.15\ K$ (when deriving thermodynamic relations, it is more convenient to set the temperature in Kelvin, while in practical examples, it is more convenient to set the temperature in Celsius). Then, experimental data of pore water activity via the water content of sample W (i.e., dependence $a = a(W)$) were obtained. Then, the hydrate former was chosen (for example, gases such as methane, carbon dioxide, ethane, propane, nitrogen, their mixtures, and natural gas). The line of the three-phase gas–water (in bulk phase)–hydrate equilibrium was assumed either from experimental data or calculated using available software. For instance, in many books analytical approximations of three-phase equilibrium lines (gas and gas hydrates with water/ice) for pure gases were presented [13, 142, 143].

The pressure of hydrate formation P_{eq} at a given temperature T, gas fugacity f_{eq}, and gas compressibility factor z_{eq} were denoted assuming that the activity of pore water in sample $a = a(T, W) < 1$ was known from experimental measurements at atmospheric pressure. Water activity $a = 1$ corresponds to the bulk phase of water. At pressure $P < P_{eq}$, there was no gas hydrate in the system. At $P = P_{eq}$, the amount of nonclathrated water in sample W formally tended to infinity. We were interested in the thermodynamic relation between gas pressure P at the three phase equilibrium gas–pore water–hydrate ($P \geq P_{eq}$) and the activity of pore water $a(T, W) < 1$, as well as the water content W of the soil sample.

A preliminary remark is that from the morphological studies of hydrates [144], the characteristic size of hydrate particles obtained in real soils, as a rule, exceeds 10 microns. It is easy to show that at a characteristic particle size of more than 1 micron, the thermodynamic

properties of pore hydrate particles practically do not differ from their properties in the bulk phase. For further consideration, we excluded nanoporous media, in which the thermodynamic properties of the pore hydrate could significantly differ from the properties of the bulk hydrate phase. The effect of a hydrate particle size of 0.1 microns or less on phase equilibrium requires special consideration.

According to the traditional thermodynamic model of clathrate hydrates by van der Waals–Platteeuw and Barrer–Stuart (see, for instance, [90]), the chemical potential of water $\mu_h(T,P)$ in the hydrate phase is written as follows

$$\mu_h(T,P) = \mu_h^0(T,P_0) - \nu_1 RT\ln(1+C_1 f) - \nu_2 RT\ln(1+C_2 f) + V_h \cdot (P - P_0), \qquad (5.2)$$

or, in an equivalent form

$$\mu_h = \mu_h^0(T,P_0) + \nu_1 RT\ln(1-\theta_1) + \nu_2 RT\ln(1-\theta_2) + V_h \cdot (P - P_0),$$

where T — temperature, K; P — gas pressure, MPa; $P_0 = 0.101325$ MPa; V_h — molar volume of water in hydrate ($22.61\ \mathrm{cm^3/mol}$ for cubic structure I and $23.06\ \mathrm{cm^3/mol}$ for cubic structure II); $\mu_h^0(T,P_0)$ — chemical potential of water in an empty clathrate lattice at pressure P_0 and temperature T; $\mu_h(T,P)$ — chemical potential of water in a clathrate lattice partially filled with guest molecules at pressure P and temperature T; R — universal gas constant, $R = 8.3146\ \mathrm{J/(mol \cdot K)}$; $C_1 = C_1(T)$, $C_2 = C_2(T)$ — Langmuir constants for large and small cavities (depending only on temperature), respectively; θ_1, θ_2 — degrees of filling small and large cavities of the structure, respectively; ν_1 and ν_2 — crystallochemical constants ($\nu_1 = 1/23$ and $\nu_2 = 3/23$ are for Structure I, and $\nu_1 = 2/17$, $\nu_2 = 1/17$ are for Structure II).

Quantities θ, C, and f are related by the Langmuir isotherm $\theta = C\,f/(1+C\,f)$ (the traditional model assumes that gas molecules are sorbed by the clathrate lattice in accordance with the Langmuir isotherm). Hydrate numbers n in the chemical formulas of hydrates $\mathrm{M \cdot}n\mathrm{H_2O}$, where M is a gas molecule (for example, CH_4), are also used below. Hydrate number n is

expressed in terms of the degrees of filling cavities as follows: $n^I = \frac{23}{\theta_1^I + 3\theta_2^I}, n^{II} = \frac{17}{2\theta_1^{II} + \theta_2^{II}}$ for hydrate Structures I and II, respectively.

The chemical potential of water $\mu_w(T, P)$ in a pore solution in a good approximation can be written as follows

$$\mu_w(T, P) = \mu_w^0(T, P_0) + RT\ln(1 - x) + RT\ln a + V_w \cdot (P - P_0), \quad (5.3)$$

where $\mu_w^0(T, P_0)$— chemical potential of pure bulk water at pressure P_0 and temperature T; $\mu_w(T, P)$ — chemical potential of pore water in the soil sample at pressure P and temperature T; x — gas solubility in pore water; a — pore water activity in the soil sample measured at atmospheric pressure (pore water can also be saline); V_w — partial molar volume of water in pore solution, assuming that $V_w = 18.015\ \text{cm}^3/\text{mol}$. Gas solubility in pore water can be approximately equal to solubility in the bulk water phase. In principle, the effect of a porous medium on gas solubility can be estimated by excluding that part of pore water volume, in which the gas does not dissolve (for instance, water in the interlayer space of the sliding frame clays does not dissolve the gas).

Gas solubility in bulk water under gas pressure can be determined by the Krichevsky–Kazarnovsky equation [59] or calculated from the equations of state; experimental data can also be used. For calculations using equations of state, the cubic-plus-association (CPA) equation is recommended and is widely used in commercial software.

The Krichevsky–Kazarnovsky equation [59] for pure gas is

$$\ln\frac{f}{x} = \ln H + \frac{V_g(P - P_0)}{RT}, \quad (5.4)$$

where H, $\text{mol}/(\text{MPa} \cdot \text{cm}^3)$, Henry's coefficient of gas; V_g, partial molar volume of gas in water (cm^3/mol); f, gas fugacity, MPa (fugacity is determined by the equation of state and depends on temperature and pressure). Henry's coefficient H only depends on temperatures up to

a pressure of 20–30 MPa. By knowing Henry's coefficient, gas fugacity f, and the partial molar volume V_g of gas in water, it is possible to determine molar fraction x of gas in water from Equation (5.4). Henry's coefficient is determined from experimental data on gas solubility in water, and the partial molar volume V_g may be determined from experimental data (V_g can also be measured in special direct volumetric experiments). Values of H and V_g for various gases are given in the literature [103].

For a gas mixture, the Krichevsky–Kazarnovsky equation is generalized as follows

$$\ln\frac{f_j}{x_j} = \ln H_j + \frac{V_j(P-P_0)}{RT}, \quad j = 1,\dots N,$$

$$x = \sum_{j=1}^{N} x_j,$$

where N — amount of dissolved gases, x_j — mole fraction of j gas in water; H_j — Henry coefficient of j component of gas mixture; f_j — fugacity of j component of gas mixture, which is determined by the gas equation of state; V_j — partial molar volume of j gas in water.

Phase equilibrium gas–water bulk phase–hydrate at $P = P_{eq}$, $f = f_{eq}$ and a fixed temperature $T > 273.15$ corresponds to the equality of the chemical potential of water in the hydrate phase according to Relation (5.2), and the chemical potential of water in the water bulk phase with dissolved gas according to Relation (5.3) at $a = 1$.

Equating the chemical potentials after some transformations, we obtain

$$\Delta\mu_{hw}^0(T,P_0) - \nu_1 RT\ln\left(1 + C_1 f_{eq}\right) - \nu_2 RT\ln\left(1 + C_2 f_{eq}\right) + \Delta V_{hw}\left(P_{eq} - P_0\right) - RT\ln\left(1 - x_{eq}\right) = 0, \tag{5.5}$$

where $\Delta\mu_{hw}^0(T,P_0) = \mu_h^0(T,P_0) - \mu_w^0(T,P_0)$ — the difference between the chemical potentials of water in the hydrate phase, and liquid water at atmospheric pressure and considered temperature; $\Delta V_{hw} = V_h - V_w$, the difference between molar volumes of water in the hydrate

lattice and in bulk water; $\Delta V_{hw} = 4.595$ and $5.045\ \mathrm{cm}^3/\mathrm{mol}$ for cubic Structures I and II, respectively.

Let us consider phase equilibrium gas–pore water–hydrate at a given sample water content (moisture) W, i.e., at $P > P_{eq}$. In this case, the activity of pore water is equal to a ($a < 1$). Equating the chemical potentials of water in hydrate phase (5.2) and pore water solution (5.3), we obtain

$$\Delta\mu^0_{hw}(T, P_0) - \nu_1 RT\ln(1 + C_1 f) - \nu_2 RT\ln(1 + C_2 f) + V_h \cdot (P - P_0)$$
$$= V_w \cdot (P - P_0) + RT\ln(1 - x) + RT\ln a$$

or

$$\Delta\mu^0_{hw}(T, P_0) - \nu_1 RT\ln(1 + C_1 f) - \nu_2 RT\ln(1 + C_2 f) + \Delta V_{hw} \cdot (P - P_0) - \quad (5.6)$$
$$RT\ln(1 - x) - RT\ln a = 0$$

Subtracting Relation (5.6) from (5.5) after some transformations,

$$\nu_1 RT\ln\left(\frac{1 + C_1 f}{1 + C_1 f_{eq}}\right) + \nu_2 RT\ln\left(\frac{1 + C_2 f}{1 + C_2 f_{eq}}\right) - \Delta V_{hw} \cdot (P - P_{eq}) +$$
$$RT\ln\left(\frac{1 - x}{1 - x_{eq}}\right) + RT\ln a = 0 \quad (5.7)$$

Equation (5.7) relates pore water activity and consequently the water content W of the sample to gas fugacity f and gas pressure P at $P > P_{eq}$. In particular, from Equation (5.7) with $P = P_{eq}$, we obtain $RT\ln a = 0$ or $a = 1$. In Equation (5.7), quantity $\Delta\mu^0_{hw}(T, P_0)$ is excluded, but the value of equilibrium gas pressure P_{eq} is included (in comparison with (5.6)).

Equation (5.7) is easily generalized to the case of a gas mixture (natural or associated petroleum gas etc.); for this, in Equation (5.7) one should replace $C_1 f$ with $\sum_j C_{1j} f_j$ and $C_2 f$ with $\sum_j C_{2j} f_j$, where f_j, C_{1j}, C_{2j} are the fugacity and Langmuir constants of the j-th component of the

gas mixture, respectively. For pure gases (propane, cyclopropane, and isobutane), small cavities of hydrate structure II are not filled, i.e., $\theta_1 = 0$ and $C_1 = 0$. In this case, the first term disappears from the left-hand side of Equation (5.7). The same is true for ethane hydrate, which forms Structure I (in ethane hydrate, the small cavities are also not filled).

At a gas pressure below 6–8 MPa, as an approximation its solubility in water (except for carbon dioxide) and the influence of the Poynting effect can be neglected (i.e., value $\Delta V_{hw}\left(P - P_{eq}\right)$); then, we can obtain the following simplified relationship

$$\nu_1 RT\ln\left(\frac{1 + C_1 f}{1 + C_1 f_{eq}}\right) + \nu_2 RT\ln\left(\frac{1 + C_2 f}{1 + C_2 f_{eq}}\right) + RT\ln a \ = 0 \qquad (5.8)$$

or

$$\left(\frac{1 + C_1 f}{1 + C_1 f_{eq}}\right)^{\nu_1} \cdot \left(\frac{1 + C_2 f}{1 + C_2 f_{eq}}\right)^{\nu_2} = a^{-1} \qquad (5.9)$$

Equations (5.8) and (5.9) can be used for methane, nitrogen, and inert gases at moderately high pressure levels (for CO_2, its water solubility should not be neglected).

Let us analyze the further possibilities of simplifying Relation (5.7) to reduce the necessary parameters for calculating nonclathrated water. For this, let us consider the nature of cavities filling with gas molecules in hydrates of various structures. First, it should be considered that large cavities in clathrate structures are always almost completely occupied (i.e., the degree of the filling of large cavities is always close to unity, $\theta_2 \approx 1$). At temperatures close to 273 K for Structure I, $C_2 f > 10$ and for Structure II, $C_2 f > 50$. This yields the estimate of the large cavities' degree of filling at a temperature of ~273 K: $\theta_2 > 0.9$ for Structure I and $\theta_2 > 0.97 - 0.98$ for Structure II. In addition, in many cases of practical interest (hydrates of methane, natural gases), the degree of the filling of small cavities of hydration structure θ_1 is also close to 1. With increasing temperature (and gas pressure), the degrees of filling approach unity.

Let us consider separately three practically important cases of the filling of clathrate cavities guest molecules: (i) $\theta_1 \approx 1$ and $\theta_2 \approx 1$; (ii) $\theta_1 = 0$, $\theta_2 \approx 1$; and (iii) $0 < \theta_1 < 1$, $\theta_2 \approx 1$.

Let the small and large cavities be almost filled, i.e., $\theta_1 \approx 1$, $C_1 f \gg 1$; $\theta_2 \approx 1$, $C_2 f \gg 1$. This situation is typical for methane and nitrogen gases and inert gases. Thus, we neglect the unit under the logarithm in expressions such as $\ln(1 + \mathrm{C}f)$, i.e., $\ln(1 + \mathrm{C}f) \approx \ln(\mathrm{C}f)$. Equation (5.7) is rewritten as follows

$$\nu_1 RT \ln\frac{f}{f_{eq}} + \nu_2 RT \ln\frac{f}{f_{eq}} - \Delta V_{hw} \cdot \left(P - P_{eq}\right) + RT \ln\left(\frac{1-x}{1-x_{eq}}\right) + RT \ln a \ = 0$$

or

$$(\nu_1 + \nu_2)\ln\frac{f}{f_{eq}} = \frac{\Delta V_{hw} \cdot \left(P - P_{eq}\right)}{RT} - \ln\left(\frac{1-x}{1-x_{eq}}\right) - \ln a \qquad (5.10)$$

For convenience, we introduce into consideration quantities

$$b = a(1-x)\exp\left(-\frac{\Delta V_{hw} \cdot (P - P_0)}{RT}\right),$$
$$b_{eq} = \left(1 - x_{eq}\right)\exp\left(-\frac{\Delta V_{hw} \cdot \left(P_{eq} - P_0\right)}{RT}\right). \qquad (5.11)$$

Let us rewrite (5.10), taking into account (5.11). After some transformations, we obtain

$$(\nu_1 + \nu_2)\ln\frac{f}{f_{eq}} = -\ln\frac{b}{b_{eq}} \text{ or } \ln\frac{f}{f_{eq}} = -\frac{1}{(\nu_1 + \nu_2)}\ln\frac{b}{b_{eq}},$$

and lastly,

$$\frac{f}{f_{eq}} = \left(\frac{b}{b_{eq}}\right)^{-\frac{1}{(\nu_1 + \nu_2)}} \qquad (5.12)$$

Relations (5.11) and (5.12) are the main result of the consideration of the thermodynamics when the filling of both types of cavities in gas hydrate structures is close to 1.

Equation (5.12) allows for the given W and water activity a, and for the known values of P_{eq} and f_{eq}, to calculate the equilibrium gas fugacity f and gas pressure P. At a given gas pressure P, we may determine fugacity f and then the activity of pore water a and W. When calculating nonclathrated water content using Relation (5.12), no information is required on the thermodynamics of an empty clathrate lattice and the Langmuir constants of guest molecules (in contrast to Relation (5.10)).

If the gas is considered to be in the ideal gaseous state, then $f = P$, and Equation (5.12) can be rewritten as

$$\frac{P}{P_{eq}} = \left(\frac{b}{b_{eq}}\right)^{-\frac{1}{(\nu_1+\nu_2)}} \tag{5.13}$$

Since, as a first approximation, $\frac{b}{b_{eq}} \approx a$, then from Equation (5.13), a strong nonlinear relationship between a and $\frac{P}{P_{eq}}$ becomes obvious. Thus, it seems from the obtained relations that, with increasing pressure, the content of nonclathrated water in a porous medium sharply decreases and is in accordance with a power law.

If the gas under consideration is weakly nonideal (for example, for methane up to pressures of about 7–8 MPa), then the approximate thermodynamic formula $f \approx z(P) \cdot P$ should be used, where z is the gas compressibility factor. By using it, Relation (5.12) is rewritten as

$$\frac{P}{P_{eq}} \approx \frac{z_{eq}}{z} \cdot \left(\frac{b}{b_{eq}}\right)^{-\frac{1}{(\nu_1+\nu_2)}}, \tag{5.14}$$

where $z = z(P), z_{eq} = z\left(P_{eq}\right)$ are factors of gas compressibility at pressure P and P_{eq}, respectively.

Let the large cavities be almost filled, $\theta_2 \approx 1$ *(*$C_2 f \gg 1$*)* with empty small cavities, $\theta_1 = 0$. This case is realized for hydrates of propane, isobutane, cyclopropane, ethane, and their mixtures. Taking $\nu_1 = 0$, from Relation (5.12) we obtain

$$\frac{f}{f_{eq}} = \left(\frac{b}{b_{eq}}\right)^{-\frac{1}{\nu_2}} \tag{5.15}$$

For the hydrate of Structure I (for instance, ethane): $\nu_2 = 3/23$, and for hydrates of Structure II (for propane and isobutane): $\nu_2 = 1/17$.

More approximate relationships occur

$$\frac{P}{P_{eq}} \approx \frac{z_{eq}}{z} \cdot \left(\frac{b}{b_{eq}}\right)^{-\frac{1}{\nu_2}} \text{ and } \frac{P}{P_{eq}} = \left(\frac{b}{b_{eq}}\right)^{-\frac{1}{\nu_2}}. \tag{5.16}$$

Let both cavities be filled, and the degree of the filling of large cavities is close to unity, $\theta_2 \approx 1$ ($C_2 f \gg 1$), but the degree of the filling of small cavities θ_1 can vary over a wide range (from 0 to 1). A typical example is carbon dioxide hydrate (and in its mixtures with propane, isobutane, and ethane). In such cases, Expression (5.7) is transformed into the following form

$$\nu_1 RT \ln\left(\frac{1 + C_1 f}{1 + C_1 f_{eq}}\right) + \nu_2 RT \ln\frac{f}{f_{eq}} - \Delta V_{hw} \cdot \left(P - P_{eq}\right) + RT \ln\left(\frac{1 - x}{1 - x_{eq}}\right) + RT \ln a = 0 \tag{5.17}$$

Considering that $\theta = \frac{Cf}{1+Cf}$ and $C = \frac{\theta}{f(1-\theta)}$, after some transformations, we lastly obtain

$$(1 + C_1 f)^{\nu_1} \cdot f^{\nu_2} = \left(1 + C_1 f_{eq}\right)^{\nu_1} \cdot {f_{eq}}^{\nu_2} \cdot exp\left(\frac{\Delta V_{hw} \cdot \left(P - P_{eq}\right)}{RT}\right) \cdot \left(\frac{1 - x_{eq}}{a \cdot (1 - x)}\right) \tag{5.18}$$

Expression (5.18) is less convenient for practical use, since the Langmuir constant C_1 of a small cavity remains. Therefore, the question arises whether it is possible to also use Equations (5.12)–(5.14) for the hydrate of carbon dioxide, substituting stoichiometric value $1/(\nu_1 + \nu_2)$ for

the actual (or effective) hydrate numbers n. In this version, Equations (5.12)–(5.14) are rewritten as follows

$$\frac{f}{f_{eq}} = \left(\frac{b}{b_{eq}}\right)^{-\mathrm{n}} \tag{5.19}$$

More approximately,

$$\frac{P}{P_{eq}} \approx \frac{z_{eq}}{z} \cdot \left(\frac{b}{b_{eq}}\right)^{-n}, \frac{P}{P_{eq}} \approx \left(\frac{b}{b_{eq}}\right)^{-n} \approx \left(\frac{a}{a_{eq}}\right)^{-n}, \tag{5.20}$$

where n is the actual or effective hydrate number on the three-phase gas–bulk phase of water–hydrate equilibrium line.

The simplest Approximation (5.20) may only be used for low pressure levels and low gas solubility in water.

A numerical comparison of approximate Relations (5.18) and (5.19) with general thermodynamic Relation (5.7) showed that it is practically acceptable to use the actual hydrate number n (see below). Moreover, the numerical comparison of (5.7), (5.12), and (5.19) for methane and nitrogen hydrates (the case when both cavities are strongly filled) also showed the benefit of using Equation (5.20). At the same time, for hydrates, in which only large cavities are strongly filled (ethane, propane, isobutane), stoichiometric hydrate numbers ($n = 23/3 = 7.67$ for ethane and $n = 17$ for propane and isobutane), should be used. Thus, the above-obtained approximate Relations (5.12–5.14) can be empirically improved by using Equations (5.19) and (5.20) with an effective hydrate number n (see below for the practical recommendations for choosing the values of n).

As a result, for the equilibrium of gas–pore water–gas hydrate, we obtained approximate Relations (5.12–5.20), which are convenient for practical applications. These relations were considered for positive temperatures in Celsius, but with some modifications they are applicable for temperatures below zero Celsius.

Let us discuss the thermodynamic correlations for calculating nonclathrated water content at temperatures below freezing Celsius. First, if at negative temperatures, the three-phase equilibrium of gas–bulk supercooled water–hydrate is used as a reference line (a continuous continuation of the line of gas–bulk water–hydrate to negative temperatures), then Relations (5.12–5.20) can also be applied for negative temperatures. However, the lines of the metastable three-phase equilibrium of gas–supercooled water–hydrate can be experimentally obtained only for small water droplets in especially organized experiments. Such unique data were obtained in the papers of Melnikov et al. [50, 145] for methane, propane, and carbon dioxide gases. For other gases, up-to-date experimental information is not yet available. However, these lines (including those for ethane, isobutane, and gas mixtures) can be calculated with acceptable accuracy at least up to −15 °C using software by Istomin et al. [146]. In other software, calculations of metastable phase equilibria of gas hydrates as a rule are not provided. Second, the pressure range from P_{eq} to pressure, corresponding to the equilibrium of the gas hydrate with ice (this pressure note by P_{eq}^{ice}), calculated using relations of type (5.12), refers to the zone of nonclathrated water metastability (i.e., to a hypothetical situation, as if ice in a given system did not exist). Strictly speaking, calculations of the content of nonclathrated water at temperatures below 0 °C should be carried out only for pressures $P > P_{eq}^{ice}$ (when there is no ice in the system because the ice is already transformed to hydrate phase).

Therefore, for thermodynamic calculations of nonclathrated water content at negative temperatures, it is preferable to use the gas–ice–hydrate line as reference. The advantage of this reference line is because cages' filling and the hydrate number *n* along this line vary very slightly, with temperatures ranging from −15 to 0 °C. In a soil system, pore water as a fourth phase also exists in the equilibrium with ice, hydrate, and gas (the locus of quadrupole points). At the quadrupole point, according to the above accepted terminology, pore water may simultaneously be considered as unfrozen and nonclathrated water. At this line, the value of pore

water activity $a_{eq} = a_{eq}(t)$ describes the equilibrium between ice and pore water at atmospheric pressure. Thus, a_{eq} decreases with a decreasing negative temperature ($a_{eq}(t) < 1$).

This situation is illustrated in Figure 5.1. Bold lines are the lines of the three-phase equilibrium of gas–water or ice bulk phase–hydrate. Above these lines, there is a zone of nonclathrated pore water. Dotted lines are the equilibrium of gas–hydrate–nonclathrated water with given activity a of pore water (activity measured at atmospheric pressure). For positive Celsius temperatures at $P = P_{eq}$, value $a = 1$ and the amount of nonclathrated water formally become infinite. At $P > P_{eq}$, value $a < 1$, and when gas pressure P increases, pore water activity a and equilibrium water content W in the sample decrease.

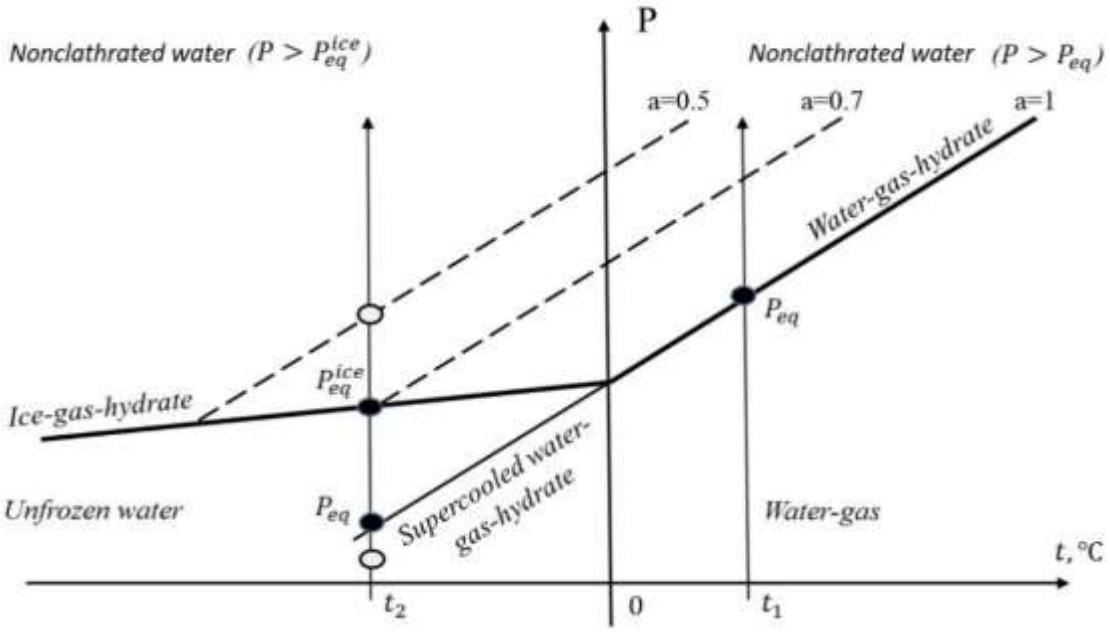

Figure 5.1 Unfrozen and nonclathrated water P-T conditions in porous media. Bold lines: three-phase gas–ice or supercooled water – hydrate equilibrium line; dotted lines: three-phase gas–water – hydrate equilibrium line at given pore-water activity

At a given negative Celsius temperature with gas pressure increasing, the amount of unfrozen pore water (gas–pore water–ice equilibrium) increases up to the quadrupole point (at $P = P_{eq}^{ice}$), but very slowly. During a further increase in pressure ($P > P_{eq}^{ice}$), the content of nonclathrated pore water begins to sharply decrease (according to a power law as established above).

Thus, at temperatures below 0 °C, it is preferable to use the gas–ice–hydrate line as a reference line. Repeating the derivation of Relations (5.7–5.12), instead of Relation (5.12), the modified equation may be obtained. In Relation (5.12), P_{eq} should be replaced by P_{eq}^{ice} and f_{eq} by f_{eq}^{ice}; in Relation (5.11), value b should be replaced by b^{ice}, b_{eq} should be replaced by b_{eq}^{ice}, and ΔV_{hw} by $\Delta V_{hi} = V_h - V_i$, where V_i is the molar volume of ice ($19.65\ \mathrm{cm^3/mol}$).

As a result, using the curve gas–ice–hydrate equilibrium as a reference line, we obtain the following final equation

$$\frac{f}{f_{eq}^{ice}} = \left(\frac{b^{ice}}{b_{eq}^{ice}}\right)^{-\mathrm{n}}, \tag{5.21}$$

where

$$b^{ice} = a(1-x)\exp\left(-\frac{\Delta V_{hi}\cdot(P-P_0)}{RT}\right), a < a_{eq};$$
$$b_{eq}^{ice} = a_{eq}\left(1-x_{eq}\right)\exp\left(-\frac{\Delta V_{hi}\cdot\left(P_{eq}-P_0\right)}{RT}\right),$$

and $\Delta V_{hi} = V_h - V_i = 2.96$ and $3.41\ \mathrm{cm^3/mol}$ for hydrate cubic structures I and II, respectively.

At low pressure, instead of Equation (5.21), the approximation may also be used

$$\frac{P}{P_{eq}^{ice}} \approx \frac{z_{eq}}{z}\cdot\left(\frac{b^{ice}}{b_{eq}^{ice}}\right)^{-\mathrm{n}}, \frac{P}{P_{eq}^{ice}} \approx \left(\frac{b^{ice}}{b_{eq}}\right)^{-\mathrm{n}} \approx \left(\frac{a^{ice}}{a_{eq}}\right)^{-\mathrm{n}} \tag{5.22}$$

A new value a_{eq} appears in the definition of b_{eq}^{ice}, and it is essential that a_{eq} be a function of temperature, i.e., a_{eq} corresponding to the equilibrium of ice–unfrozen water in the soil under consideration (at atmospheric pressure). This means that for the practical application of Equation (5.21), it is necessary to determine the value of a_{eq}, depending on the temperature (negative in Celsius). Such dependence was obtained [147] for unfrozen water calculations (equilibrium of pore water and ice)

$$-RT\ln a_{eq} = 6008\cdot(1-T/T_o) - 38.2\cdot\left[T\ln\frac{T}{T_o} + (T_o - T)\right];$$
$$T_o = 273.15\ \mathrm{K};\ (T < T_o). \tag{5.23}$$

Then Equation (5.23) was transformed into relationship between temperature t (in degrees Celsius) and pore water activity a_{eq} on the pore water–ice equilibrium line [141]

$$t = 103.25 \ln a_{eq} + 5.57 \left(1 - a_{eq}\right)^2. \quad (5.24)$$

Equation (5.24) is used to calculate unfrozen water content from measured water activity when the temperature is set to Celsius. However, for our purposes, a_{eq} needs to be expressed as a function of temperature t (in degrees Celsius). By the approximation of Equation (5.23), we may obtain

$$a_{eq} = 1 + 9.6768 \cdot 10^{-3} \cdot t_{eq} + 4.1769 \cdot 10^{-5} \cdot t_{eq}^2. \quad (5.25)$$

Dependencies (5.23) and (5.25) can both be used in calculating nonclathrated water content at negative temperatures from Relation (5.21). Thus, the final Equation (5.21) is supplemented by Relation (5.23) or (5.25).

5.3. Nonclathrated water content calculations

In the above, some thermodynamic relations were obtained (Equation (5.6), (5.7), (5.13), and (5.19)–(5.25)) that make it possible to calculate nonclathrated water content in a soil sample at a given temperature, depending on the pressure of hydrate-forming gas.

First, the main Equation (5.6) allows for the performance of thermodynamic calculations of equilibrium gas fugacity f and then pressure P at a given temperature, depending on pore water activity a, and thereby pore water content W. However, for the application of Equation (5.6) in practice, we need to know (i) the structure of the hydrate, (ii) the thermodynamic properties of the empty clathrate lattice $\Delta\mu_{hw}^0(T, P_0) = \mu_h^0(T, P_0) - \mu_w^0(T, P_0)$, and (iii) the Langmuir constants of the hydrate-forming gas under consideration. These values can be obtained if the hydrate-phase thermodynamic model's parameterization is published and/or described in the software documentation. For example, such data were presented in Istomin et al. (1996), but for other software they are not documented as a rule.

Equation (5.7) also allows, at a given temperature T, known Langmuir constants C_1, C_2, and the value of P_{eq}, for calculating water activity a depending on gas pressure P under consideration, and thereby determining the content of nonclathrated water W in the sample. Equation (5.7) excludes information about the thermodynamics of the empty hydrate lattice $\Delta\mu_{hw}^{0}(T, P_0)$ but contains additional information on equilibrium gas pressure P_{eq}. However, from a practical point of view Equations (5.6–5.8) are not fully convenient, since the temperature dependences of the Langmuir constants for small and large cavities need to be specified for the considered hydrate-forming gas (these constants must also be consistent with the three-phase equilibrium lines). Thus, relations such as Equation (5.13) look more attractive from a practical point of view, but they are only a good approximation of the main thermodynamic Relations (5.6) and (5.7). Numerical analysis showed that a small additional correction of equations such as (5.13) can be made with the replacement of the limiting hydrate number $\frac{1}{(\nu_1+\nu_2)}$ by its effective value n.

As a result, for the practical calculations of the nonclathrated water content, Relations (5.19) and (5.20) are recommended at temperatures above 0 °C, and Relations (5.21) and (5.23) (or (5.25)) at temperatures below 0 °C. For rough estimations, the replacement of gas fugacity f by $z \cdot P$ in the equation is possible. This approximation may be used for methane up to a pressure of 7–8 MPa.

Hydrate numbers n for different gases are shown in Tables 2.8 and 2.9 (for positive and negative Celsius temperatures, respectively) that were calculated by using software [146]. For C_3H_8 and i-C_4H_{10}, a limited hydrate number may be used.

A variant of the calculation is also possible if the unfrozen water content in frozen soils for different temperature levels ($W_{unf}(t)$) is known from the experiment. Using Equation (5.25), we immediately establish the dependence of pore water activity a on the water content W of the sample. Then, we may calculate the nonclathrated water content as a function of W for any hydrate-forming gas and any temperature (at a negative Celsius temperature according to

Relations (5.21), (5.23), and (5.25) and at a positive Celsius temperature according to Relations (5.19) and (5.20)).

Using the proposed technique, the pressure dependence of the nonclathrated water content was calculated at a temperature of 265.65 K in a kaolinite clay and sand–clay mixture samples (sand plus 14% kaolinite clay and sand plus 25% kaolinite clay). This kaolinite clay was used previously to determine the effect of temperature on nonclathrated water content in porous media [90]. Soil characteristics are presented in Table 5.1.

Table 5.1 Soil characteristics.

Soil Type	Particle Size Distribution (%)							Mineralogy (%)		Salinity (%)
	1–0.5 (mm)	0.5–0.25 (mm)	0.25–0.1 (mm)	0.1–0.05 (mm)	0.05–0.01 (mm)	0.01–0.002 (mm)	< 0.002 (mm)			
Sand	0.2	35.7	62.9	0.8	0.3	0.1		Quartz	> 90	< 0.01
Kaolinite clay	0.7	0.5	0.4	2.9	19.5	34.0	42.0	Kaolinite Quartz Muscovite	92 6 2	0.04

Sand consists of quartz (more than 90%); the prevailing fraction of sand particles 0.1–0.25 mm is reach 62.9%. Kaolinite clay consists mainly of kaolinite (92%), with 95.5% silt-clay size particles, while the percentage of clay particles (<0.002 mm) reaches 42%. Kaolinite clay contains minor amounts of dissolved salts (0.04%). The specific active surface areas of sand and kaolinite clay defined by nitrogen adsorption are 0.2 and 12 m^2/g, respectively.

First, experimental data of pore water activity a at atmospheric pressure via water content W were obtained (Table 5.2).

Table 5.2 Experimental data on the water activity a of kaolinite clay via different water content (W) levels at 298.15 K and atmospheric pressure.

W, %	a	*W*, %	a	*W*, %	a
28.86	0.995	6.41	0.972	2.20	0.897
21.80	0.993	5.42	0.967	1.81	0.866
17.70	0.990	5.12	0.963	1.53	0.830
16.72	0.990	4.07	0.953	1.45	0.813

12.47	0.986	3.55	0.943	1.25	0.753
8.15	0.978	2.79	0.924	1.18	0.720

Pore water activity a was determined with a WP4-T device by a method previously described in detail [90, 141].

Thermodynamic calculations of nonclathrated water were carried out using four methods (Figure 5.2 and Table 5.3):

- Equation (5.7), the most precise method, where the Langmuir constants were obtained from ratio $C = \theta/(1-\theta)/f$, and the degree of cavity filling was calculated using software [146].
- Equations (5.11) and (5.19), where the three-phase methane – supercooled water – hydrate equilibrium line was used as a reference line, $P_{eq} = 1.26$ MPa and $n = 5.75$.
- Equation (5.21) and $n = 5.75$, where the three-phase gas – ice – hydrate equilibrium line was used as a reference line, $P_{eq}^{ice} = 2.00$ MPa and $n = 5.75$.
- Equations (5.21) and (5.25), where the three-phase gas – ice – hydrate equilibrium line was used as a reference line, $P_{eq}^{ice} = 2.00$ MPa, $n = 6.03$.

In Figure 5.2, equilibrium pressure $P_{eq}^{ice} = 2.00$ MPa on the ice – methane – hydrate equilibrium line at a temperature of 265.65 K.

The Equation (5.21) approximation with n = 6.03 gave a very similar result to that of fully correct Equation (5.7). This means that at negative temperatures, it is preferable to use ice – gas – hydrate as a reference line and actual hydrate numbers from Table 2.9. For positive temperatures, Equation (5.19) and actual hydrate numbers from Table 2.8 are recommended.

Table 5.3 Dependence of nonclathrated water content in kaolinite clay on methane pressure at a temperature of 265.65 K by different calculations.

W (%)	P, MPa by Equation (5.7)	P, MPa (Equilibrium Gas–Supercooled Water–Hydrate by Equation (5.19) at n = 5.75)	P, MPa (Equilibrium Gas–Ice–Hydrate by Equation (5.21) at n = 5.75)	P, MPa (Equilibrium Gas–Ice–Hydrate by Equation (5.21) at n = 6.03)
2.79	2.10	2.06	2.07	2.08
2.20	2.56	2.49	2.49	2.52
1.81	3.24	3.13	3.11	3.18
1.53	4.33	4.15	4.10	4.26
1.45	5.01	4.80	4.71	4.93
1.25	9.03	8.60	8.18	8.91

The data (Table 5.3) were calculated using measured water activities for kaolinite clay (Table 5.2). Three methods were used: general (most accurate) Equation (5.7); approximate Equation (5.19), considering (5.11); according to approximate Equation (5.21) using three-phase equilibrium gas–ice–hydrate as a reference line; also according to Equation (5.21) with a hydrate number $n = 6.03$.

A comparison of calculated data with direct experimental data obtained by the contact method (Table 5.4) is shown in Figure 5.2.

Table 5.4 Dependence of nonclathrated water content in kaolinite clay on methane pressure at a temperature

Nonclathrated Water Content (%)	P, MPa (Experimental Data)	P, MPa (Thermodynamic Calculations)
1.36	8.69	6.27
1.43	7.35	5.23
1.47	6.85	4.77
1.51	6.2	4.40
1.52	5.9	4.36

1.69	4.34	3.39
1.97	3.10	2.82
2.38	2.59	2.46

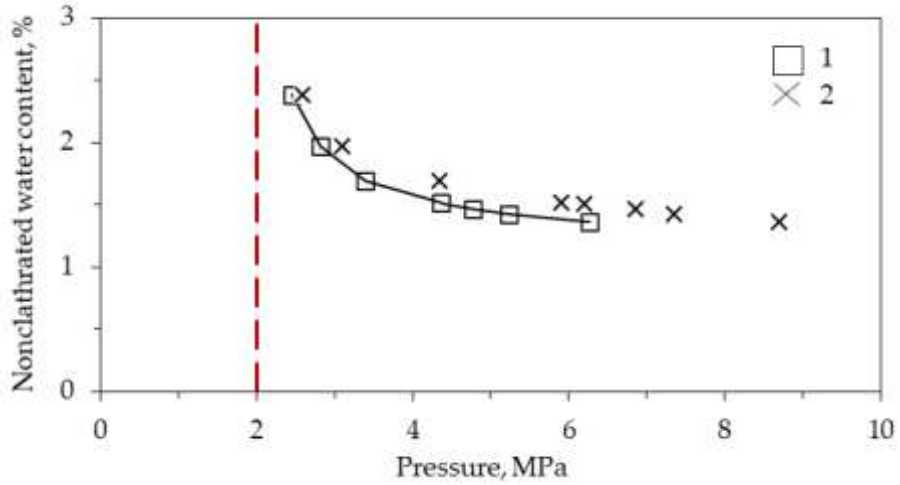

Figure 5.2 Change in nonclathrated water content depending on methane pressure in kaolinite clay at a temperature of 265.65 K. Calculated data represented by squares—1. Crosses, experimental data—2. Solid line—approximation of calculated data; red line—equilibrium "ice – methane – hydrate" at a temperature of 265.65 K

The contact method is a direct technique for nonclathrated water content determination in soil samples. It was proposed earlier in papers [148, 149]. Nonclathrated water content data has a good agreement between that calculated by thermodynamic equations and experimental data obtained by the contact method, the accuracy of which is about 0.1 wt% [90]. The largest discrepancy of ~0.15 wt% in the data was observed in the range of 1.4–1.5 wt%.

Additional experimental data and calculations of nonclathrated water content were obtained for sand–clay mixtures, which consist of quartz sand 14 wt% and 25 wt% of kaolinite clay, respectively (Figure 5.3). These results also demonstrate a good agreement between the calculation and the experimental data. There is a regular increase in the amount of nonclathrated water in model soils with the increase in the content of clay particles. For example, the content of nonclathrated water at 4 MPa gas pressure in sand with 14 wt% kaolinite clay is 0.25%, which is two times lower than that in the sand with 25 wt% clay. The effect of gas pressure on the

nonclathrated water content is weak at pressures above 6–8 MPa. However, the difference depending on the content of clay particles is also preserved under these conditions.

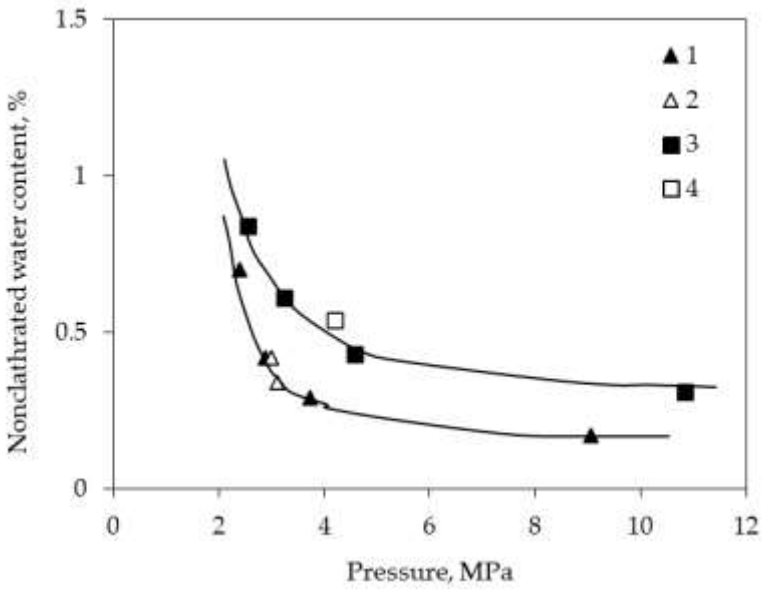

Figure 5.3 Change of nonclathrated water content depending on methane pressure in artificial sediment mixtures: sand with 14% (1, 2) and 25% (3, 4) kaolinite particles at 268.15 K. 1,3—calculated data and 2,4—experimental data, P_{eq} = 2.36 MPa (CH_4).

Thus, the proposed thermodynamic technique for nonclathrated water content calculation allows estimating the effect of hydrate-forming gas pressure on the equilibrium water content in hydrate-bearing soil samples. The comparison showed a sufficiently good agreement between the calculated results by the proposed technique with the direct measurements of nonclathrated water for all investigated soils.

The obtained methodological results make it possible to use the proposed technique during the efficiency estimation of methane hydrate recovery by various production methods. In contrast to the conventional approach, which takes into account only the temperature shift for the assessment of hydrate conditions in porous media, the investigated method takes into account the increase in equilibrium pore water content (non-clathrated water) due to reservoir pressure rise. The information about residual water (nonclathrated water) in hydrate-saturated reservoirs is very important for predicting the efficiency of CO_2 sequestration in a hydrate form under definite temperature and pressure conditions.

5.4. Conclusions

In this chapter, some analytical dependences are proposed that allow to calculate of the non-clathrate water content depending on the pressure of the hydrate-forming gas from the known dependence of the pore water activity via the water content of the sample. Using the obtained relations, the qualitative regularities of the gas pressure influence on the non-clathrate water content at a given temperature (both at positive and negative temperatures) were revealed.

A procedure has been developed for the thermodynamic calculation of the dependence of the nonclathrated water content in the sample on the pressure of the hydrate-forming gas at a fixed temperature. To implement this method of calculation, it is necessary to have data either on the activity of pore water from the water content of the sample, or data on the unfrozen water curve. The performed calculations for hydrate-containing samples of kaolinite clay showed sufficiently good agreement between the results obtained by the proposed method with the direct contact method. The proposed technique can also be used for other hydrate-forming gases and different soil systems.

It should be noted that the obtained analytical dependences can also be used to study the effect of inhibitors on hydrate formation (the dependence of the equilibrium pressure via the concentration of the inhibitor at a given temperature). These questions are discussed in the next chapter devoted to the study of mixed hydrate inhibitors.

Chapter 6. Physical and chemical properties of mixed hydrate inhibitors

As mentioned in the literature review (chapter 2) at daily oil and gas practice methanol and MEG as thermodynamic hydrate inhibitors are ordinary used. Kinetic inhibitors (water soluble polymers like PVP, PVCap etc.) may also apply, especially in offshore conditions. This is due to stable thermodynamic regime of marine pipelines, which is favorable for kinetic inhibitors applications. Sometimes, kinetic inhibitor may be preferable from economic and environmental points of view. As known, kinetic inhibitors are suitable for field application up to $\Delta T \approx 8 - 9$ ℃ (ΔT means the difference between gas hydrate formation temperature and a fluid temperature in pipeline at pressure under consideration). If $\Delta T > 9$ ℃ or so, the hydrate depositing risks become more serious: at least it requires a special hydrate control system to avoid the hydrate plugging. As for Russian Northern regions, the kinetic inhibitors are not used due to severe conditions and varying frequently of the thermobaric regimes. So, if we want to use kinetic inhibitors for Russian conditions, a new approach is needed for hydrate avoiding in field pipelines. One of the fruitful idea is the application of mixed anti-hydrate reagents, which combine different inhibitors for increasing of total effectively.

In this connection one of the task of the chapter is to study some mixed hydrate inhibitors, which may include different components: different compositions of thermodynamic inhibitors like "electrolytes plus methanol (or MEG)", as well as "thermodynamic plus kinetic" inhibitors. The reasons to use such compositions are both economic and ecological (for instance, to reduce methanol consumption). Also, the inhibitor mixtures may include some additives to prevent corrosion and/or scaling (this is so-called complex inhibitors for prevention hydrates, paraffins, scales and corrosion). But complex inhibitors are beyond the scope of this research.

Why are mixtures of some thermodynamic inhibitors interesting for study and for application in practice? When we use of the methanol or MEG for avoiding hydrates in gas wells or gas-gathering systems, such reagents are mixing with the formation mineralization water (formation water like brines at the fields of Eastern Siberia). As well known, the highly

mineralized reservoir water is also a thermodynamic inhibitor. This means that in the gas wells and production gathering pipelines at least two thermodynamic inhibitors "work together"- brine and methanol (or MEG). But a mixing of the concentrated methanol with formation water leads to the risk of halite and other precipitations. As for MEG, its salinization leads to the technological problems in regeneration system and the possibility of precipitation of hardly soluble salts like calcites, barites etc. Thus, additional data on the physicochemical properties of mixed inhibitors are required: densities, viscosities, water activity in the inhibitor solutions, its freezing temperatures etc. First of all, we need to know the shift of hydrate formation temperature, which depends on concentration of each inhibitor in aqueous solutions. Several questions can arise. Is the influence of two thermodynamic inhibitors are additive or not additive? When the salt precipitation can arise if we mix the methanol with formation water? The answers to such questions are required for practical application of the mixed hydrate inhibitors.

As mentioned above, kinetic inhibitors work effectively in a narrow range of supercooling ΔT from the hydrate equilibrium line. If we wish to expand the range of kinetic inhibitors applicability, then mixture of kinetic and thermodynamic inhibitors may be used. To make this, it is necessary to understand how these components interact between each other - simply additively or with some synergetic effect?

Kinetic inhibitor affect primary on the stage of hydrate nucleation (to eliminate or reduce the nucleation). As for salt (electrolyte) solutions, they can be considered simultaneously as thermodynamic and kinetic inhibitors. It was recently published by Istomin et.al. [150] that the electrolyte solutions not only shift of hydrate formation line as thermodynamic inhibitors, but also slow down the growth of hydrate particles as kinetic inhibitor. So, it seems that the mixture of the water soluble polymer with electrolytes may have the cumulative (or synergetic) kinetic effect.

Thus, there are some scientific problems, which need to solve if we want to use mixed compositions as hydrate inhibitors in daily practice. So, the task of the chapter is to study some of the emerging problems.

Research objectives of the chapter are:

1. To propose general thermodynamic formulas, which connect water activity with temperature shift ΔT of hydrate formation in aqueous inhibitor solutions (both for pure and mixed inhibitors).
2. To study experimentally the physicochemical properties of mixed inhibitor "methanol + magnesium chloride" and to establish simple and reliable correlations for its influence on hydrate formation shift.
3. To study experimentally the physicochemical properties of "PVP + NaCl" and "PVP + $MgCl_2$" solutions as mixed hydrate inhibitors. And also to calculate the influence of PVP, "PVP + NaCl" and "PVP + $MgCl_2$" solutions on ΔT - thermodynamic shift of hydrate formation.

6.1. Thermodynamic dependencies of the inhibitor's effect on hydrate formation conditions

First of all, let us discuss the calculations by HydraFLASH software of three-phase equilibrium line "methane – water solution of methanol – hydrate" with different methanol concentration (in the range 0-70 wt% methanol in the solution) in the semi logarithmic coordinates: $\ln P - T$ and $\ln f - T$. From the graph in Figure 6.1(a) (in coordinates "logarithm of pressure versus temperature") it seems that the equilibrium lines are situated as nearly parallel straight lines. And a dash line is a locus of quadruple points (the fourth phase is ice). This dash line is calculated separately (our version of HydraFLASH software not possible to calculate the dash line) by using technique, which was developed in chapter 3 - the equation for freezing of aqueous solution combine with the equation for three phase hydrate equilibrium.

At Figure 6.1(b) the same graphic is presented in the coordinates $\ln f - T$. We see that the lines at Figure 6.1(b) are more straight and they become more equidistant. So the coordinates $\ln f - T$ are better for representing the calculation data by some empirical correlations. The same situation takes place for three phase equilibrium "methane – MEG solutions – hydrate" on Figure 6.2(a,b), as we calculated by HydraFLASH software. So, if need to derive some correlations on hydrate equilibrium shift via inhibitor concentrations, we may take into account that coordinates like $\ln f - T$ are more preferable.

Below the thermodynamic formulas of the inhibitor content's influence on gas fugacity/pressure for hydrate formation conditions at constant temperature, as well as the temperature shift of hydrate formation conditions (at constant fugacity/pressure) are presented. So, we try to get an answer for the following question: how to relate correctly the lines of three phase equilibrium with two different inhibitor concentrations by each other?

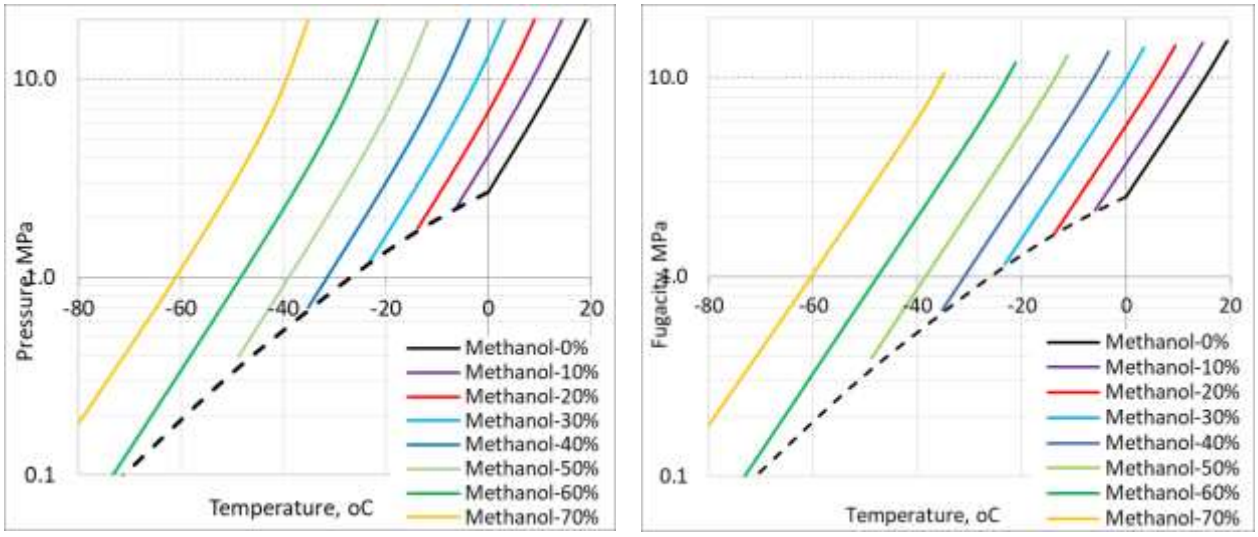

a b

Figure 6.1 Methane hydrate conditions (a) (fugacity-(b)) in equilibrium with aqueous methanol solutions in the range of its concentration 0-70 wt.%

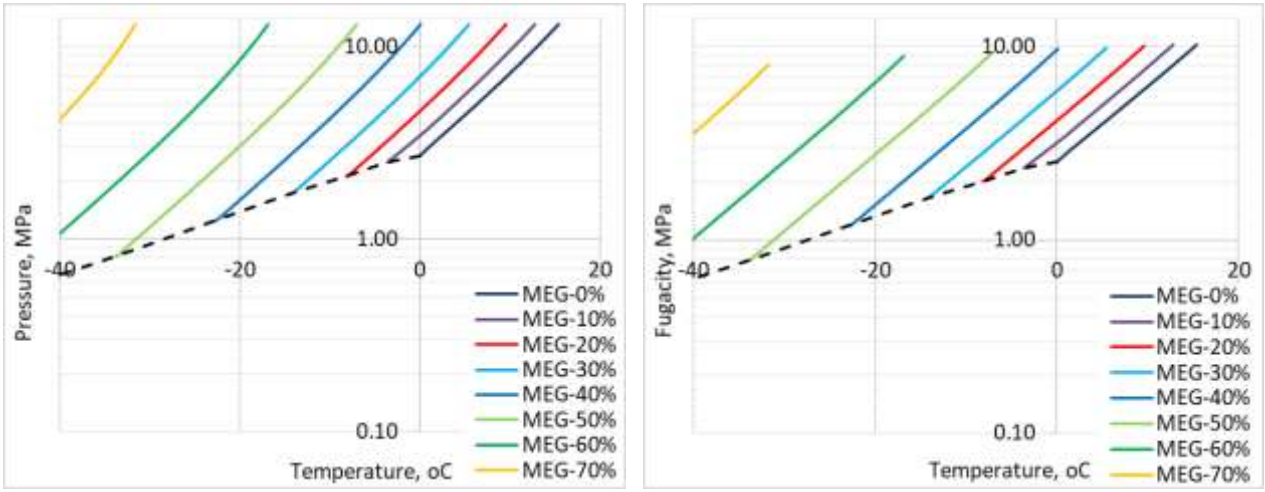

a b

Figure 6.2 Methane hydrate conditions (a) (fugacity-(b)) in equilibrium with aqueous MEG solutions in the range of its concentration 0-60 wt.%

6.1.1. Influence of inhibitor concentration on the hydrate equilibrium pressure shift at constant temperature

In the Chapter 5, the analytical dependencies for influence of gas fugacity/pressure on the non-clathrate water content in a porous medium were obtained. The same dependences with small modifications are also applicable to describe the effect of inhibitor's activity/concentration on the shift in the equilibrium gas pressure/fugacity of hydrate formation at a fixed temperature. Below, we consider the question in more detail.

Let's take two concentrations of the hydrate inhibitor X_1 and X_2 in an aqueous solution at a given temperature T (the activity of water at atmospheric pressure in these solutions is a_1 and a_2, respectively). In particular, if $X_1 = 0$ (pure water), then $a_1 = 1$. The equations, which relate the water activities a_1 or a_2 with the equilibrium gas fugacity f_1 or f_2, can be written as follows (as an analog of the equation (5.5) in Chapter 5)

$$\Delta\mu^0_{hw}(T,P_0) - \nu_1 RT\ln(1+C_1 f_1) - \nu_2 RT\ln(1+C_2 f_1) + V_h\cdot(P_1-P_0) = \\ = V_w\cdot(P_1-P_0) + RT\ln(1-x_1) \ + RT\ln a_1 \qquad (6.1)$$

and

$$\Delta\mu^0_{hw}(T,P_0) - \nu_1 RT\ln(1+C_1 f_2) - \nu_2 RT\ln(1+C_2 f_2) + V_h\cdot(P_2-P_0) = \\ = \ V_w\cdot(P_2-P_0) + RT\ln(1-x_2) \ + RT\ln a_2 \qquad (6.2)$$

Subtracting expression (6.1) from (6.2), we obtain an analog of equation (5.6) from Chapter 5

$$\nu_1 RT\ln\left(\frac{1+C_1 f_2}{1+C_1 f_1}\right) + \nu_2 RT\ln\left(\frac{1+C_2 f_2}{1+C_2 f_1}\right) - \Delta V_{hw}\cdot(P_2 - P_1) + RT\ln\left(\frac{1-x_2}{1-x_1}\right) + RT\ln\frac{a_2}{a_1} = 0, \quad (6.3)$$

where: a_1, a_2- water activities in solutions, $x_1, x_2 -$ gas solubility in water, $\Delta V_{hw} -$ the difference between the molar volumes of water in the hydrate lattice and in bulk water.

The modification of formula (6.3) can also be obtained when the degree of filling of small cavities θ_1 may be varied in the wide range, while θ_2 is close to 1

$$\nu_1 RT\ln\left(\frac{1+C_1 f_2}{1+C_1 f_1}\right) + \nu_2 RT\ln\frac{f_2}{f_1} - \Delta V_{hw}\cdot(P_2 - P_1) + RT\ln\left(\frac{1-x_2}{1-x_1}\right) + RT\ln\frac{a_2}{a_1} = 0. \quad (6.4)$$

Relations (6.3) and (6.4) give a solution of the problem. As for the relation (6.4), it may be applied in practice for methane and carbon dioxide, because in the chapter 3 we find the correct value of θ_1 directly from the experimental data for hydrates of these gases. For the application of (6.3) and (6.4), the activities of water in aqueous solutions of inhibitors (depending on inhibitor's concentration) are required.

It seems more preferable for practice the following equation (as analog of equation (5.10) from the Chapter 5)

$$\frac{f_2}{f_1} = \left(\frac{b_2}{b_1}\right)^{-n}, \quad (6.5)$$

where

$$b_1 = a_1\,(1 - x_1)\exp\left(-\frac{\Delta V_{hw}\cdot(P_1 - P_0)}{RT}\right),$$

$$b_2 = a_2\,(1 - x_2)\exp\left(-\frac{\Delta V_{hw}\cdot(P_2 - P_0)}{RT}\right). \quad (6.6)$$

At special simplified case for $a_1 = 1$, $x_1 = 0, x_2 = 0$ and $\Delta V_{hw} = 0$ of the dependence (6.5) was previously presented (without derivation and any discussion) in the book by Istomin and Kwon [21].

Equations (6.5) - (6.6) allow to connect the equilibrium line of three-phase equilibrium with one concentration of the inhibitor to a line with another concentration. Also, the equations

(6.5) - (6.6) give possibility to extrapolate the valuable experimental data to higher pressure or fugacity. Besides, from the precise experimental data on three phase hydrate equilibria with different concentrations of the inhibitor, it is possible to calculate the water activity in the inhibitor solution as a function of its concentration and a temperature.

6.1.2. Temperature shift of hydrate formation conditions (at constant gas fugacity or pressure)

As we see in the graphs at Figures 6.1 and 6.2 the temperature shift ΔT is a monotonic dependence of the inhibitor's concentration (in this context, the value ΔT means the difference between hydrate point for inhibitor concentration inhibitor X_1 and hydrate point at concentration X_2 at fixed pressure or fugacity). It should be pointed that the monotonic dependence is fully correct for inhibitors, which molecules are not included into cavities of clathrate hydrate phase. For instance, this assumption is fully correct for electrolyte inhibitors (except, NH_4F aqueous solution). But this is not true for isopropanol as a hydrate inhibitor due to molecules of isopropanol is included into large cavities of hydrates structures. Thus, isopropanol plays a dual role: on the one hand, it reduces the water activity and thereby inhibits the process of hydrate formation, and on the other hand, it participates in the formation of a hydrate structure. For such inhibitors, there is a limit of inhibitor action and the value of ΔT tends to a constant with increasing concentration of the inhibitor. As for methanol, it also can be incorporated into large cavities of the hydrate structure (only at high concentration of methanol in the solution), but the influence of this factor on the ΔT value is very small. The molecules of other hydrate inhibitors like MEG or electrolytes are not included to hydrate phase. Below we are studying the case, when inhibitor' molecules not included into clathrate cages.

Hammerschmidt [10] was the first who proposed an empirical correlation between ΔT and inhibitor concentration X for some inhibitors (at low its concentrations). The next step was presented by Pieron [151]. He considered the process of hydrate formation as a chemical

reaction, and gas hydrate as a chemical compound of constant composition. He neglected the solubility of gas in water, and did not take into account the Pointing effect. Also, he made the additional assumption that the enthalpy of hydrate dissociation is not depends on P, T and inhibitor concentration. The equilibrium "gas – aqueous inhibitor solution – hydrate" was considered at a fixed gas pressure and at two inhibitor concentrations in an aqueous solution X_1 (at temperature T_1) and X_2 (at temperature T_2) and $\Delta T = T_2 - T_1$. As a result of thermodynamic consideration, Pieron obtained the following relationship

$$nR \ln(\frac{a_2}{a_1}) = \Delta H \, (\frac{1}{T_2} - \frac{1}{T_1}) = \Delta H \frac{\Delta T}{T_1 \cdot T_2}, \quad (6.7)$$

where n – hydrate number, ΔH – enthalpy of hydrate decomposition.

From (6.7) in the case $a_1 = 1$ and low inhibitor concentration we have a more simple correlation:

$$\Delta T \approx A \ln a \text{ at } P = \text{const}, \quad (6.8)$$

where A - is empirical parameter, which may be estimated from experimental data.

It should be noted that Pieron published the paper before the development of hydrate's statistical thermodynamic model (this model was developed later, in 1957-1958). But up to now there are no publications where formulas like (6.7) derive from statistical thermodynamic model of hydrates. Therefore, it is of interest to derive relations for ΔT using van der Waals et al. thermodynamic model without some Pieron's assumptions.

Let's consider the equilibrium "gas – aqueous inhibitor solution – hydrate" at two different temperatures T_1 and T_2 and fixed gas fugacity f. It should be borne in mind that $f = idem$ and the gas pressure somewhat changes at these two temperatures. The concentrations of the inhibitor at these temperatures are X_1 and X_2 and, accordingly, the activity of water in the inhibitor solution a_1, a_2 (referred to atmospheric pressure).

Chemical potential of water in a hydrate phase (by the example of a hydrate with filling two types of cavities)

for temperature T_1

$$\mu_h(P_1,T_1) = \mu_h^0(P_0,T_1) - \nu_1 RT_1 \ln(1 + C_1(T_1)f) - \nu_2 RT_1 \ln(1 + C_2(T_1)f) + V_h \cdot (P_1 - P_0)$$

and for temperature T_2

$$\mu_h(P_2,T_2) = \mu_h^0(P_0,T_2) - \nu_1 RT_2 \ln(1 + C_1(T_2)f) - \nu_2 RT_2 \ln(1 + C_2(T_2)f) + V_h \cdot (P_2 - P_0)$$

Chemical potential of water in aqueous solution (containing inhibitor and dissolved gas) at temperature T_1 and T_2, accordingly

$$\mu_w(P_1,T_1) = {\mu_w}^0(P_0,T_1) + RT_1 \ln\left(1 - x_{g,1}\right) + RT_1 \ln(a_1) + \bar{V}_w \cdot (P_1 - P_0)$$

$$\mu_w(P_2,T_2) = {\mu_w}^0(P_0,T_2) + RT_2 \ln\left(1 - x_{g,2}\right) + RT_2 \ln(a_2) + \bar{V}_w \cdot (P_2 - P_0).$$

Phase equilibrium at temperature T_1 between water in hydrate and water in aqueous solution means $\mu_h(P_1,T_1) = \mu_w(P_1,T_1)$ or

$$\Delta\mu_{hw}^0(P_0,T_1) - \nu_1 RT_1 \ln(1 + C_1(T_1)f) - \nu_2 RT_1 \ln(1 + C_2(T_1)f) + V_h \cdot (P_1 - P_0) =$$

$$= RT_1 \ln\left(1 - x_{g,1}\right) + RT_1 \ln(a_1) + \bar{V}_w \cdot (P_1 - P_0) \quad (6.9)$$

where $\Delta\mu_{hw}^0(P_0,T_1) = \mu_h^0(P_0,T_1) - {\mu_w}^0(P_0,T_1)$.

Phase equilibrium at temperature T_2 between water in hydrate and water in aqueous solution means $\mu_h(P_2,T_2) = \mu_w(P_2,T_2)$ or

$$\Delta\mu_{hw}^0(P_0,T_2) - \nu_1 RT_2 \ln(1 + C_1(T_2)f) - \nu_2 RT_2 \ln(1 + C_2(T_2)f) + V_h \cdot (P_2 - P_0) =$$

$$= RT_2 \ln\left(1 - x_{g,2}\right) + RT_2 \ln(a_2) + \bar{V}_w \cdot (P_2 - P_0) \quad (6.10)$$

where $\Delta\mu_{hw}^0(P_0,T_2) = \mu_h^0(P_0,T_2) - {\mu_w}^0(P_0,T_2)$.

It should be pointed that $\Delta\mu_{hw}^0(P_0,T)$ is known as function of T from the parametrization of empty hydrate lattice thermodynamic model.

Subtracting expression (6.10) from (6.9), we obtain

$$[\Delta\mu_{hw}^0(P_0,T_1) - \Delta\mu_{hw}^0(P_0,T_2)] - \nu_1 RT_1 \ln(1 + C_1(T_1)f) - \nu_2 RT_1 \ln(1 + C_2(T_1)f)$$

$$+ \nu_1 RT_2 \ln(1 + C_1(T_2)f) + \nu_2 RT_2 \ln(1 + C_2(T_2)f) + V_h \cdot (P_1 - P_2) =$$

$$RT_1 \ln\left(1 - x_{g,1}\right) - RT_2 \ln\left(1 - x_{g,2}\right) + RT_1 \ln(a_1) - RT_2 \ln(a_2) + \bar{V}_w \cdot (P_1 - P_2) \quad (6.11)$$

Equation (6.11) is a general equation, which give the solution of the problem under consideration.

Let's analyze the terms in this expression.

$\Delta V_{hw} \cdot (P_2 - P_1) = V_h \cdot (P_2 - P_1) - \bar{V}_w \cdot (P_2 - P_1)$ this term in many cases can be neglected because the pressures P_1 and P_2 are quite close, and the value ΔV_{hw} is small.

With small error, this can be done for

$$RT_2 \ln(1 - x_{g,2}) - RT_1 \ln(1 - x_{g,1}) \approx 0$$

and $[\Delta\mu^0_{hw}(P_0, T_1) - \Delta\mu^0_{hw}(P_0, T_2)]$ is known value.

Also the assumption $\ln(1 + C(T)f) \approx \ln C\ (T) + \ln f$ may be used for some hydrates.

To further simplify the expression, it is necessary to take the form of the temperature dependence of the chemical potential differences and the temperature dependence of the Langmuir constants. The temperature dependence of the Langmuir constants in a good approximation is described by the following expression: $C_1 = A_1 \exp \frac{B_1}{RT}$ and $C_2 = \mathrm{A}_2 \exp \frac{B_2}{RT}$.

Similar expressions are also valid for the chemical potential difference

$$[\Delta\mu^0_{hw}(P_0, T_1) - \Delta\mu^0_{hw}(P_0, T_2)]$$

Substituting these values, we may obtain the following relation, which is generalized the Pieron formula (6.7)

$$\ln(\frac{b_2}{b_1}) = \tilde{A}\ (\frac{1}{T_2} - \frac{1}{T_1}) \text{ at fixed } f\,, \qquad (6.12)$$

where $\tilde{A} -$ complex parameter (we recommended the empirical estimation of it directly from experimental data);

$$b_1 = a_1(1 - x_1) \exp\left(-\frac{\Delta V_{hw} \cdot (P_1 - P_0)}{RT_1}\right),\ b_2 = a_2(1 - x_2) \exp\left(-\frac{\Delta V_{hw} \cdot (P_2 - P_0)}{RT_2}\right).$$

Thus, we have obtained the new relation (6.12), which is very close to Pieron' formula (6.7). It may be considered as modification of Pieron' formula from the statistical thermodynamic model of clathrate hydrate phase. We may recommend the relation (6.12) for description of

experimental data. Sometimes it is possible to use a rougher approximation, when *P*=const is used instead *f*=const.

6.2. Experimental data and empirical correlations of the temperature shift for hydrate formation the mixed inhibitor "methanol + magnesium chloride"

For application of mixed thermodynamic inhibitors we need to know how affect such mixture on hydrate equilibrium lines if is known only the influence of each component. A mixed inhibitor "methanol + magnesium chloride" was chosen due to its promising for practical applications (it is more effective than methanol and magnesium chloride separately). This mixed composition is the difficult case for thermodynamic description, because at the same weight percentage magnesium chloride is significantly superior methanol as a thermodynamic inhibitor. For another composition (like "methanol + NaCl" or "methanol + $CaCl_2$" etc.) such correlations is more easy to obtain. For thermodynamic analyses we used our experimental data for hydrate formation conditions of methane in aqueous solutions "magnesium chloride – methanol". These data were obtained during performance of a joint project Skoltech and Russian Oil and Gas State University named after I.M. Gubkin (the project with Gazprom PJSC). The experiments were carried out on a hydrate rig at the Gubkin university. The experimental data are presented in the Appendix 2. Below these data are analyzed to obtain semi-empirical correlations.

Experimental data on the hydrate formation conditions in mixed inhibitors were presented as the dependence of the shift in the temperature of hydrate formation ΔT (with respect to the hydrate formation curve for pure water) on the mass concentrations of each component (magnesium chloride and methanol) in aqueous solutions. The concentration of methanol in the solution is varied from 0 to 50 wt%, magnesium chloride - from 0 to 22 wt%, and in the mixed inhibitor - up to 20 wt% of methanol and up to 16 wt% of magnesium chloride.

Preliminary, it was tested the simplest additive formula: $\Delta T_{calc} = \Delta T_{CH_3OH} + \Delta T_{MgCl_2}$, where ΔT_{CH_3OH} a contribution of methanol at considered concentration (known from the studies

of the aqueous methanol solution as inhibitor), ΔT_{MgCl_2} – a contribution of $MgCl_2$ (known from the studies of the aqueous $MgCl_2$ solution as inhibitor). We established, that this formula leads to an error in the value of ΔT more than 20%, especially at high concentrations of the components (mainly the value ΔT is overestimated in comparison with the experimental data). It means that in this mixed inhibitor the synergistic effect take place by action of both components.

Thus, it is impossible to recommend a simplest additive formula for the practical application due to its significant errors. It should be obtained more correct semi empirical correlations. Analyzing the situation, we have proposed and tested two rather simple correlations, which may be convenience for practical applications: i) modified additive formula, where anti-hydrate activity of each inhibitor component take into account by using its effective concentrations; ii) the application of modified Zdanovsky's rule.

6.2.1. The first correlation for antihydrate activity of a mixed inhibitor CH_3OH+$MgCl_2$ (contributions of each inhibitor component by using its effective concentration).

At this correlation, we want to formally apply an additive formula, in which the effective concentrations of the components in an aqueous solution instead of actual concentrations are used.

Let us introduce the concept of the effective concentrations of each component $\tilde{X}_i$ in the mixed inhibitor. The effective mass concentration of each individual component in the mixed inhibitor is defined by formulas

$$\tilde{X}_i = \frac{X_i}{X_i + X_{H_2O}} \cdot 100\%, \tag{6.13}$$

where $\tilde{X}_i$ means the concentration of each inhibitor if there were no the another inhibitor in the solution.

So, for ΔT of mixed inhibitor, the following formula may be used

$$\Delta T = \sum \Delta T_i(\tilde{X}_i), \tag{6.14}$$

where $\tilde{X}_i$ – effective concentration of *i*-component (instead its real concentration X_i in an aqueous solution).

The comparison of our experimental data (see Appendix 2) for pure and mixed inhibitor with calculation by formulas (6.13) and (6.14) is presented in the Table 6.1. In relative units, the experimental error (reduced difference $(\Delta T - \Delta T_{calc})/\Delta T$ is not more than 4% for all experimentally studied samples of mixed inhibitors.

Table 6.1 The comparison of the first correlation for mixed inhibitor "methanol + $MgCl_2$" with experimental data

Experimental data for mixed inhibitor ΔT_{exp}					The calculated data by the correlation for mixed inhibitor ΔT_{calc}				
X_{CH3OH}, % wt.	X_{MgCl2}, % wt.	T_{eq}, °C (at P = 8 MPa)	ΔT_{exp}, °C (at P = 8 MPa)		$\tilde{X}_{CH3OH}$, % wt.	ΔT_{CH3OH}, °C	$\tilde{X}_{MgCl2}$, % wt.	ΔT_{MgCl2}, °C	ΔT_{calc}, °C
5.00	5.00	6.30	4.69		5.26	2.25	5.26	2.32	4.57
10.01	5.01	3.49	7.49		10.54	4.70	5.57	2.48	7.18
19.99	5.00	-2.71	13.70		21.04	10.48	6.25	2.87	13.35
30.00	5.00	-10.63	21.62		31.58	17.44	7.14	3.42	20.86
5.00	9.39	2.98	8.01		5.52	2.36	9.88	5.46	7.83
10.00	9.39	-0.22	11.21		11.04	4.94	10.43	5.94	10.89
20.00	9.39	-7.99	18.98		22.07	11.12	11.74	7.19	18.31
30.00	9.38	-16.94	27.92		33.11	18.51	13.40	9.01	27.52
5.00	16.40	-6.02	17.01		5.98	2.57	17.26	14.42	16.99
10.00	16.40	-10.47	21.45		11.96	5.41	18.22	16.07	21.47
20.00	16.39	-20.53	31.52		23.92	12.28	20.49	20.58	32.87

From the comparison (Table 6.1), it follows that the correlation is consistent fully with experimental data within the experimental error up to a value of ΔT ~28 °C. Moreover, dependencies (6.14) with an acceptable for practice error can be applicable up to ΔT at a level of ~35 °C. This range covers the possible values of ΔT, which needs for hydrate inhibiting the gas gathering systems at Russian gas and gas-condensate fields.

6.2.2. The second correlation for calculation the shift of hydrate formation conditions in mixed inhibitors (modified Zdanovsky's rule)

Also, we proposed and analyzed a second correlation for the shift of the conditions of hydrate formation, based on the generalization of the Zdanovsky rule for determining the activity of water in multicomponent electrolyte solutions from experimental data of binary aqueous solutions. Note that Zdanovsky's rule was introduced only for determination of the water activity in mixed solutions of electrolytes (salt systems). The essence of the rule is the very similar assumption: if mixing electrolyte solutions with the same water activity (but different compositions) in any proportion, then the water activity of the mixed solution does not change. For saline solutions like formation waters of gas and gas condensate fields (even with high salinity), this rule gives a small and quite acceptable error in the value of water activity at the level of 1 %. For formation waters at East Siberian gas condensate fields (highly mineralized brines) the level of errors less of 1.0 % is expected from our estimations.

Let us generalize the Zdanovsky' rule (initially formulated for the water activity in aqueous electrolyte solutions) to a shift ΔT in the temperatures of hydrate formation. We may formulate the modified rule as follows: "If it takes two solutions of different hydrate inhibitors with the same shift ΔT of the hydrate formation curve and mix the solutions in any proportions, then the resulting solution of the mixed inhibitor will have the same ΔT value". We call this new rule as a modified Zdanovsky rule for hydrate-forming systems. Also, we may use this rule not only for electrolyte solution.

From general thermodynamic consideration, the proposed modified Zdanovsky' rule should be correctly valid for mixed solutions of electrolytes (mixed salt inhibitors). But in our case there is a more complex solution, consisting of water, magnesium chloride and methanol. Therefore, such modified Zdanovsky' rule needs for testing using our experimental data on methane hydrate formation in a mixed inhibitor "methanol + magnesium chloride".

Comparison of the modified Zdanovsky' rule with the experimental data are presented in Table 6.2. In contexts of our consideration we called the proposed modified Zdanovsky' rule as a second correlation for calculation the shift of hydrate formation conditions in mixed inhibitors. For the comparison convenience in Table 6.2 also were included the calculations by the first correlation and by HydraFLASH software.

Table 6.2 Comparison of the modified Zdanovsky rule for mixed inhibitor "methanol + $MgCl_2$" with experimental data

Experimental data				Calculation by effective concentrations	Calculation by Modified Zdanovsky rule	Calculation by HydraFLASH
X_{CH3OH}, % wt.	X_{MgCl2}, % wt.	T_{eq}, °C (at P = 8 MPa)	ΔT_{exp}, °C (at P = 8 MPa)	ΔT, °C	ΔT, °C	ΔT, °C
5.00	5.00	6.30	4.69	4.57	4.72	4.71
10.01	5.01	3.49	7.49	7.18	7.74	7.47
19.99	5.00	-2.71	13.70	13.35	14.58	13.66
30.00	5.00	-10.63	21.62	20.86	22.56	21.13
5.00	9.39	2.98	8.01	7.83	8.19	7.97
10.00	9.39	-0.22	11.21	10.89	12.08	11.36
20.00	9.39	-7.99	18.98	18.31	20.70	19.37
30.00	9.38	-16.94	27.92	27.52	30.42	29.82
5.00	16.40	-6.02	17.01	16.99	17.80	17.28
10.00	16.40	-10.47	21.45	21.47	23.46	22.74
20.00	16.39	-20.53	31.52	32.87	35.55	36.90

Analysis of the data in Tables 6.1 and 6.2 shows that our second correlation (modified Zdanovsky' rule) may be acceptable up to $\Delta T = 20 - 25$ ℃ for the system under consideration, but the error is higher in comparison with the first correlation. Also, a comparison with results on HydraFLASH software show that the first simple correlation works practically the same as this software (which are commonly used in some complicated thermodynamic models for hydrate phase, aqueous solutions etc.)

It should be pointed that we checked our correlations on the most complicated case: the mixed inhibitor "$MgCl_2$ + methanol". It means that such correlations also correctly work for another mixed inhibitor like "$CaCl_2$ + methanol", "NaCl + methanol" and "brine + methanol". Here, the brine may be considered as "united inhibitor component".

Thus, two correlations were proposed and analyzed, which can be used in calculations of the specific consumption of the mixed inhibitors. First correlation based on the effective concentrations of the mixed inhibitor' components is primary recommended for practical use. At the next chapter our first correlation is used in practice for Yarakta gas-condensate field, namely for "methanol + brine" mixed inhibitor during calculations of methanol consumption.

6.3. Experimental data on water activity in the mixed inhibitors "PVP + NaCl" and "PVP + $MgCl_2$" and empirical correlations of the hydrate formation temperature shift

The next step of our consideration is another types of mixed inhibitors, which include both thermodynamic and kinetic inhibitors. One of the interesting system is water soluble polymer (as a kinetic inhibitor) plus salt solution (as a thermodynamic inhibitor). This is due to possible double kinetic effect: polymer affect primary on nucleation and the electrolyte primary affects on the growth stage of hydrate particles.

The simplest systems are: "PVP + NaCl" and "PVP + $MgCl_2$" aqueous solution. It should be noted that in the literature practically no any experimental data on physical and chemical properties of such systems. So, first of all, we need to study the physical properties (density, viscosity, etc.) of such mixed solutions. We obtained the experimental data of the physical properties by using the equipment of Skoltech laboratory (the results presented at Appendix 3).

Below we mainly pay attention on the experimental study of the water activity in "PVP + NaCl + water" and "PVP + $MgCl_2$ + water" systems. In literature there is no water activity data in aqueous polymeric solutions, excluding the high concentrations of polymer (>25-30 % wt.) because only with high concentrations the water activity in polymer solutions becomes

significantly less than one. Also, there is no any data on water activities in mixed aqueous solutions of polymer and salts.

The WP4C dew point potentiometer (Decagon Devices) was used to measure water activity. To obtain reliable results, the device was first calibrated according to the procedure described in [152]. A standard solution of KCl was chosen for this procedure. At 25 ºC the deviation of water activity for the solution equals ±0.001.

At the second step, we calculate the water activity in sodium chloride solution using HydraFLASH software for comparison with obtained data by using WP4C device (see Figure 6.3 and Table 6.3). The calculation and experimental data are fully coincided at concentrations up to 10-15 %wt., but slight different at higher concentrations. It means that instead of calculations by HydraFLASH software it is more correctly for concentrated solutions (higher than 12-15 wt% of salt) to use the experimental data for single-component aqueous solution and to use these data for further semi-empirical correlations for water activity in mixed inhibitor solutions.

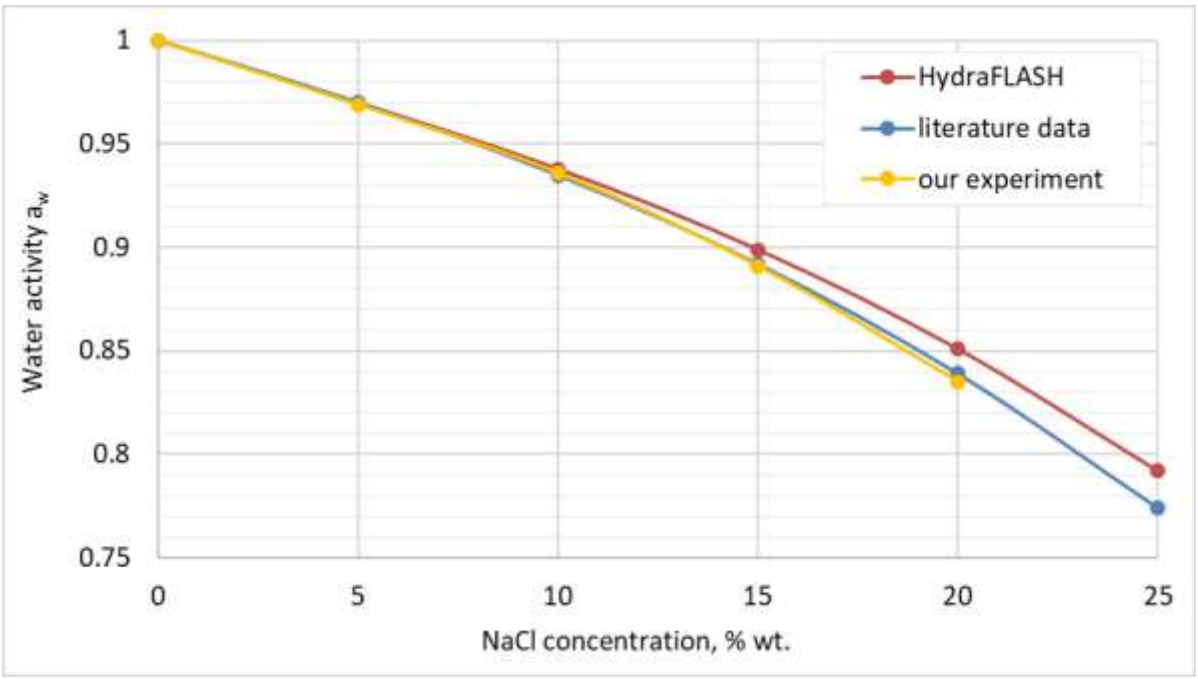

Figure 6.3 Water activity in NaCl solutions data from experiments and from calculations 25 ºC

Table 6.3 Comparison of experimental and calculated water activities for sodium chloride solution at 25 °C

NaCl concentration, wt%	a_w, our experiment by WP4C	a_w, by HydraFLASH	a_w, by [153]
0	1.000	1.000	1.000
5	0.969	0.970	0.970
10	0.936	0.938	0.935
15	0.891	0.899	0.892
20	0.835	0.851	0.839
25	-	0.792	0.774

Our measurements of water activity in the PVP + NaCl and PVP + $MgCl_2$ aqueous solutions by WP4C are given in Tables 6.4 and 6.5

Table 6.4 Experimental data for water activity in the PVP + NaCl solution at 25°C

# of solution	X_{pvp}, wt%	X_{NaCl}, wt%	a_w
0	0	0	1.000
1	5	0	0.999
2	10	0	0.999
3	15	0	0.998
4	20	0	0.996
5	25	0	0.994
6	0	10	0.936
7	10	10	0.919
8	30	0	0.991
9	35	0	0.988
10	40	0	0.982
11	45	0	0.970
12	50	0	0.957
13	0	15	0.891
14	20	10	0.895

15	50	10	0.737
16	20	15	0.828
17	45.5	13.6	0.734

Table 6.5 Experimental data for water activity in the PVP + $MgCl_2$ solution at 25°C

# of solution	X_{water}, wt%	X_{PVP}, wt%.	X_{MgCl2}, wt%	a_w
0	100	0	0	1.000
1	80.0	20.0	0	0.9967
2	75.0	25.0	0	0.9960
3	70.0	30.0	0	0.9923
4	60.0	40.0	0	0.9828
5	50.0	50.0	0	0.9595
6	52.8	42.3	5.0	0.9088
7	54.3	38.0	7.6	0.8756
8	56.0	33.6	10.5	0.8368
9	73.9	21.1	4.9	0.9568
10	76.0	16.3	7.6	0.9340
11	78.3	11.2	10.5	0.9057
12	50.0	40.0	10.0	0.8128
13	50.0	35.0	15.0	0.7022
14	50.2	29.9	19.9	0.5800
15	70.0	20.0	10.0	0.8935
16	70.0	15.0	15.0	0.8169
17	70.0	10.0	20.0	0.7224

Figure 6.4 shows curves of water activity in aqueous solutions of sodium chloride and polyvinylpyrrolidone. As can be seen that water activity does not really change in polymer solution with concentration under 15 % wt. It means that polymeric kinetic inhibitors practically not affect on hydrate thermodynamics.

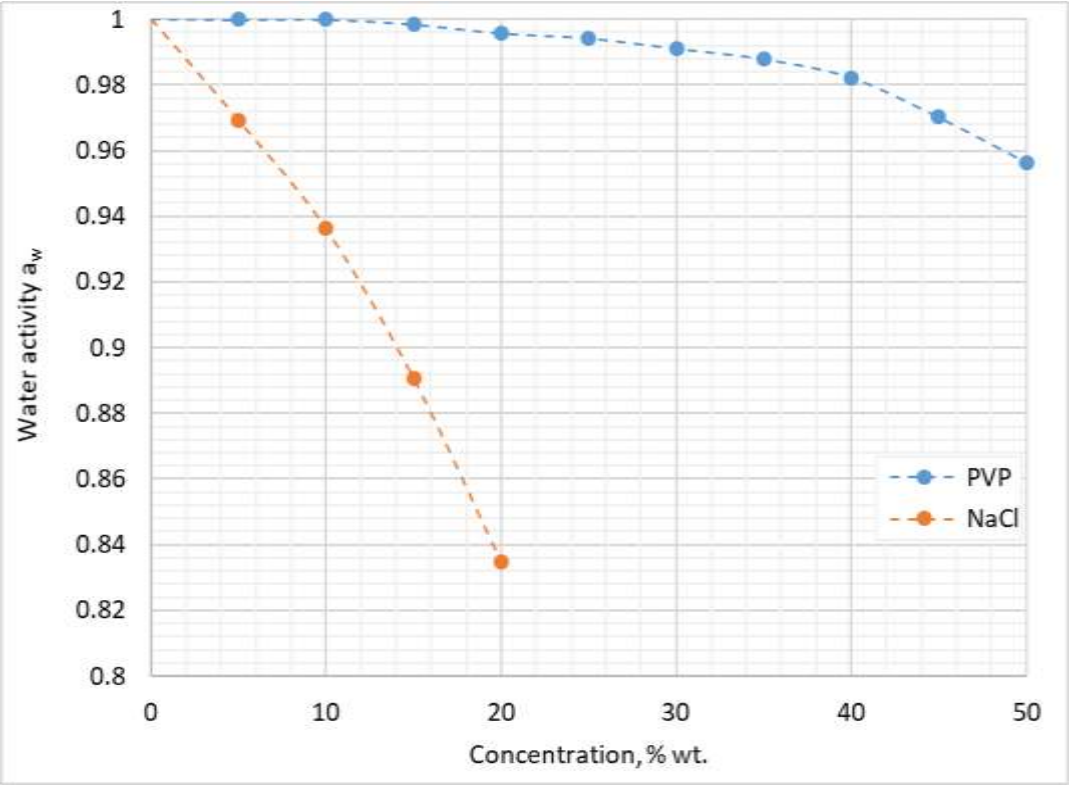

Figure 6.4 Dependence of water activity for PVP and NaCl solutions via concentrations

It's important to check the applicability of above mentioned Zdanovsky' rule for such system. This rule is known for describing the relationship between electrolyte solutions' properties. According to it, that the mixing of two or more isopiestic electrolyte solutions with any proportions (‘isopiestic’ means solutions having equal water vapor pressures under solution or in other words - the same water activity) leads to the same water activity in mixed solutions (the electrolyte systems like formation water up to brine obey this rule).

Graphic representation of this rule for our system "PVP + NaCl" is shown in Figure 6.5. Water activity data for pure PVP and NaCl aqueous solutions are blue and red, respectively. Water activity of their combined solutions is purple line. We see that Zdanovsky’ rule work well for such mixed inhibitors.

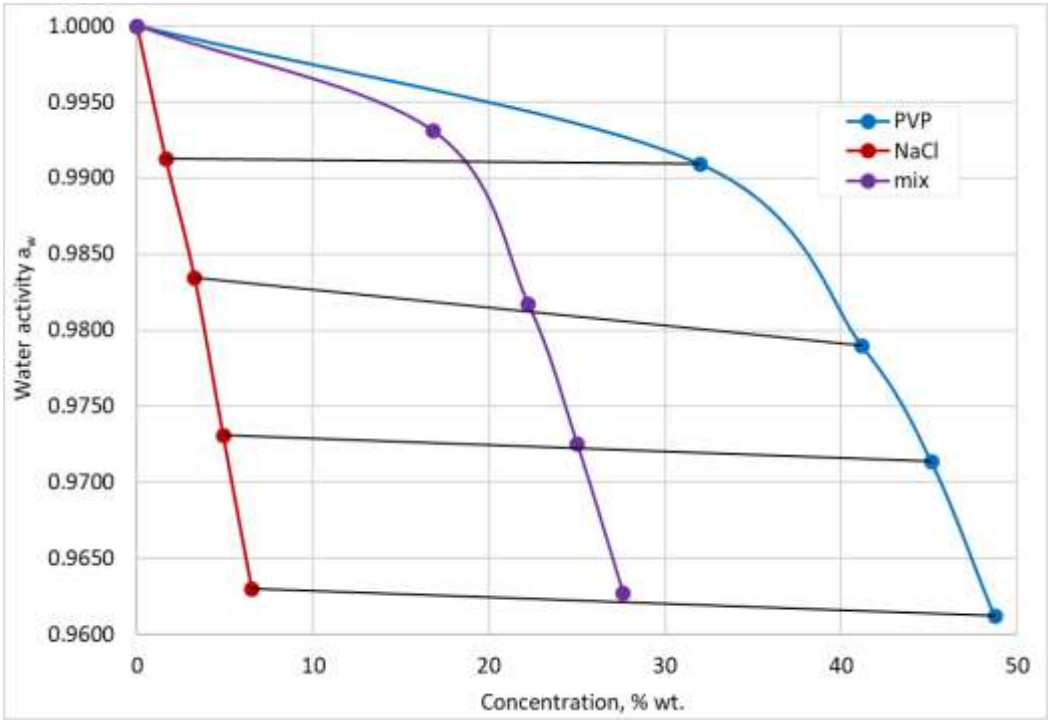

Figure 6.5 Verification of Zdanovsky' rule for the system "PVP + NaCl"

A similar investigation was done for studying the water activity for a mixture of PVP and magnesium chloride.

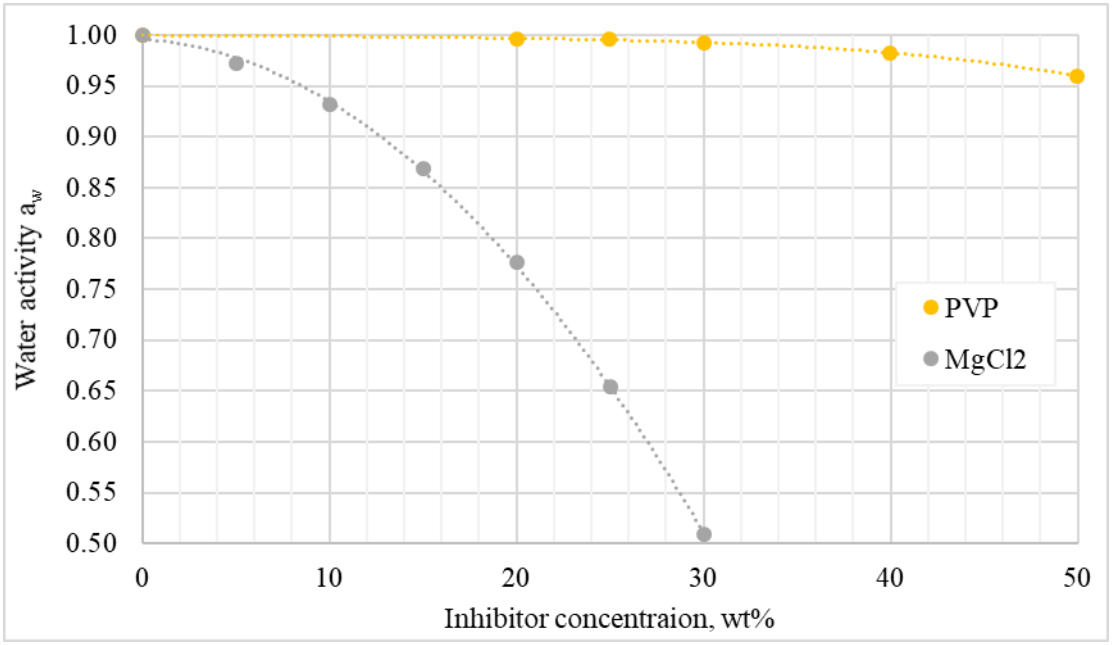

Figure 6.6 Water activity data for aqueous solutions of PVP and $MgCl_2$ via concentrations

The idea of obtaining water activity is assumption that a_w is the multiplicativity of partial activities of water a_{PVP} and a_{MgCl2} in binary solutions PVP – water and $MgCl_2$ – water with effective concentrations of the components in binary solutions, i.e. The correlation for water

activity by our experimental data for $MgCl_2$

$$a_w = a_{PVP} \cdot a_{MgCl2}.$$

So, the main task is to calculate the effective activities a_{PVP} and a_{MgCl2}. It means to use appropriate formulas (6.13) for effective mass concentration of PVP or $MgCl_2$ in aqueous binary solutions from mass concentration in triple PVP – $MgCl_2$ – water solutions.

Based on the obtained experimental data (Table 6.5), an analytical formula was derived for the activity of water in a PVP solution

$$a_{\mathrm{PVP}} = 1 - 0.00050928367 \cdot X_1 + 0.000032414936 \cdot {X_1}^2 - 0.000000767608 \cdot {X_1}^3.$$

The next step is to take data on the activity of water in a solution of magnesium chloride from software HydraFLASH (Table 6.6).

Table 6.6 Water activity of $MgCl_2$ depending on mass concentration at 25 °C (calculations by HydraFLASH program and literature data [154])

$MgCl_2$, wt%	a_{MgCl2} (HydraFLASH)	Literature data [154]
0	1	-
5.2	0.9706	0.97
9.9	0.9330	0.93
15.3	0.8646	0.86
20.3	0.7703	0.76
24.6	0.6650	0.66
30.3	0.5003	0.50
34.8	0.3644	0.36

Analytical formula for the activity of water in a magnesium chloride solution according to calculations, presented in Table 6.6

$$a_{\mathrm{MgCl2}}(T) = 1 - 0.0015819078125001 \cdot X_2 - 0.0004899860267857 \cdot {X_2}^2,$$

where X_2 is mass concentration of $MgCl_2$ in solution.

The resulting comparison is presented in the Table 6.7. As we can see from the comparison, this method works reliably at low concentrations of PVP.

Table 6.7 Comparison of calculated water activity with experimental water activity

# of solution	Composition	$\tilde{X}_1$	a_1	$\tilde{X}_2$	a_2	Water activity from experiment	Calculated water activity from correlation
12	H_2O (50%) – PVP (40%) – $MgCl_2$(10%)	16.67	0.8382	44.44	0.9740	0.8128	0.8164
13	H_2O (50%) – PVP (35%) – $MgCl_2$ (15%)	23.08	0.7032	41.18	0.9804	0.7022	0.6894
14	H_2O (50%) – PVP (30%) – $MgCl_2$ (20%)	28.57	0.5545	37.50	0.9860	0.5800	0.5468
15	H_2O (70%) – PVP (20%) – $MgCl_2$ (10%)	12.50	0.9038	22.22	0.9963	0.8935	0.9004
16	H_2O (70%) – PVP (15%) – $MgCl_2$ (15%)	17.65	0.8203	17.65	0.9969	0.8169	0.8177
17	H_2O (70%) – PVP (10%) – $MgCl_2$ (20%)	22.22	0.7236	12.50	0.9972	0.7224	0.7216

From the Table 6.7 we can see that this correlation for calculating water activity works well approximately up $a = 0.65$, which is sufficient for practical purpose.

Therefore, we may calculate water activities in any triple "PVP – $MgCl_2$ – water" solutions and then to calculate the hydrate formation curves of such mixed inhibitors. As mentioned above, HydraFLASH software cannot calculate water activity and hydrate formation curves for any polymer solutions such as PVP + water as well as for "PVP – $MgCl_2$ – water" solutions.

Three mixed inhibitor compositions with different mass concentration ratios were selected as a further research: $MgCl_2$-PVP (1:2), $MgCl_2$-PVP (1:1), $MgCl_2$-PVP (2:1). First, the

effective concentrations were calculated. And by using the proposed correlation, water activities were calculated (Figure 6.7).

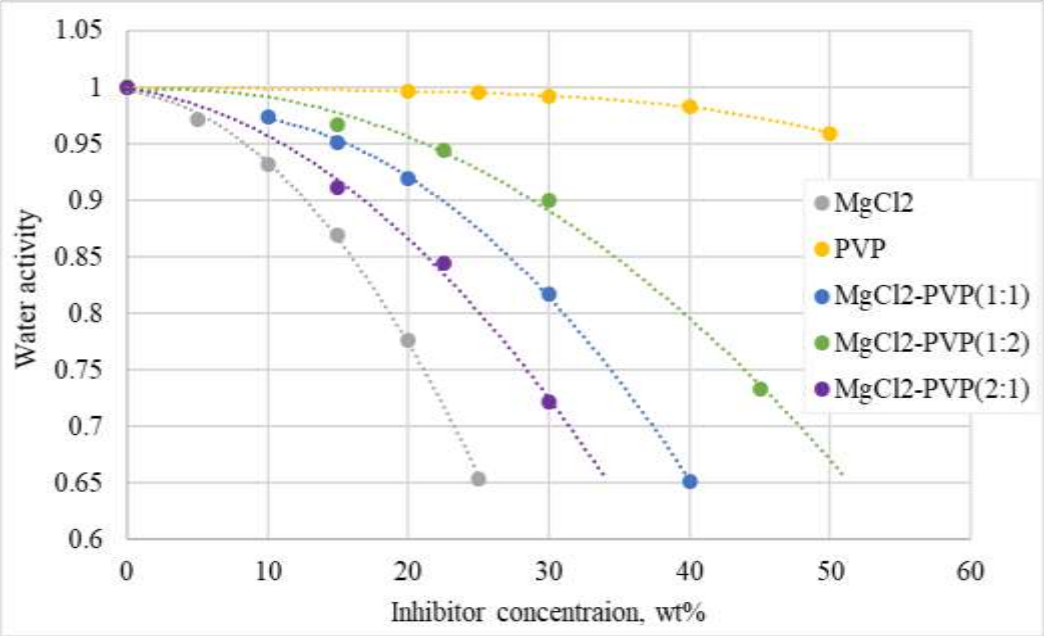

Figure 6.7 Calculated water activity in mixed inhibitors (with different mass ratio) in dependence of total inhibitor concentration (PVP + $MgCl_2$) at temperature 25°C

So, we may calculate water activities at any component concentration of "PVP – $MgCl_2$ – water" solutions (at its water activity $a > 0.65$). Further it would be desirable to develop the method for thermodynamic calculation the hydrate formation curves of such mixed inhibitors.

In context of our further discussion the following question is important: How to obtain the hydrate's equilibrium conditions for different gases (methane etc.) in polymeric and polymer + salts solutions? It should be pointed that there is no possibility to calculate gas hydrate curves in water-polymer and polymer + salts + water solutions by using any program software (including HydraFLASH). Also, it is very difficult to measure such hydrate curves by experiment. This is due to strong influence of polymer additives on hydrate kinetics what interferes with the measurement of the hydrate formation equilibrium conditions.

We have a two alternative ways for developing thermodynamic technique for such calculations.

The first way is to use the previous correlation (6.14) for total hydrate shift ΔT, which we

already used for H_2O + CH_3OH + $MgCl_2$ system. For the system H_2O + PVP + $MgCl_2$, which is now under consideration, $\Delta T = \Delta T_{PVP} + \Delta T_{MgCl2}$, where ΔT_i are calculated at the effective mass concentration of each individual component in the mixed inhibitor (by formula (6.13)). The value ΔT_{MgCl2} may be taken from the experimental data or calculated by HydraFLASH program. But for the value ΔT_{PVP} there are no experimental data, and we have to use the correlation like $\Delta T = A \ln a$. The parameter A may be calibrated from similar systems (at the same gas hydrate-former and salt solution, for instance, for methane $A \approx 72 - 75$).

The second way is to use directly the correlaton between water activity and the shift of hydrate formation $\Delta T = A \ln a$ or more complication formula $\ln(\frac{b_2}{b_1}) = \tilde{A}\,(\frac{1}{T_2} - \frac{1}{T_1})$ (see above discussion). So, at the second way we need to use experimental data and/or correlations on water activity for mixed solutions. As for correlations on water activity for mixed solutions, we may apply the Zdahovsky' rule (second type correlation) or use the first correlation, in which the water activity in mixed solution is calculated by multiply the water activities in binary solutions using its effective concentration in solutions.

Firstly, let's calculate the curves of hydrate formation of methane in $MgCl_2$ solutions by HydraFLASH (see Table 6.8 and Figure 6.7).

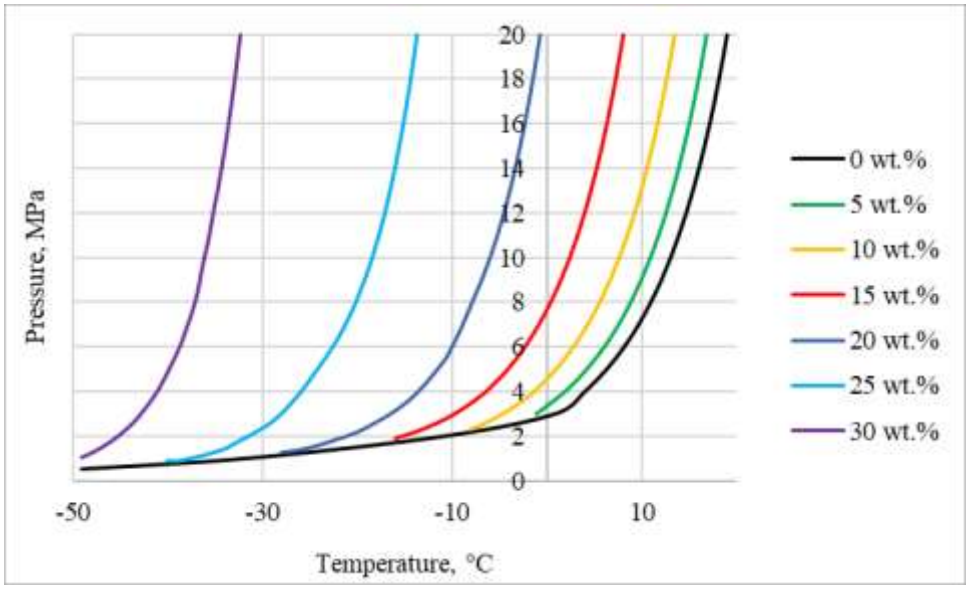

Figure 6.8 Conditions for hydrate formation of methane in aqueous solutions of $MgCl_2$

Table 6.8 Calculation of the equilibrium conditions of hydrate formation for $MgCl_2$ solutions of various concentrations by HydraFLASH

Pressure, MPa	Hydrate formation temperature (°C)					
	$MgCl_2$ (0 wt.%)	$MgCl_2$ (5 wt.%)	$MgCl_2$ (10 wt.%)	$MgCl_2$ (15 wt.%)	$MgCl_2$ (20 wt.%)	$MgCl_2$ (25 wt.%)
3	1.01	-1.17	-13.80	-28.44	-49.41	-29.10
4	4.02	1.85	-1.32	-6.42	-42.49	-26.31
5	6.31	4.14	0.96	-4.18	-37.24	-24.23
6	8.14	5.97	2.79	-2.39	-10.52	-22.61
7	9.66	7.49	4.29	-0.91	-9.11	-21.29
8	10.95	8.77	5.56	0.33	-7.92	-20.19
9	12.06	9.88	6.66	1.40	-6.91	-19.27
10	13.03	10.85	7.62	2.33	-6.03	-18.47
11	13.89	11.71	8.47	3.15	-5.25	-17.77
12	14.67	12.48	9.23	3.89	-4.56	-17.15
13	15.37	13.18	9.92	4.56	-3.94	-16.60
14	16.00	13.82	10.54	5.16	-3.37	-16.09
15	16.59	14.40	11.12	5.72	-2.85	-15.63

Further, using the correlation $\Delta T = A \cdot \ln a$, where ΔT is a temperature shift of hydrate formation, and the coefficient $A = 75.04$, which was found from the known curves of hydrate formation of methane in $MgCl_2$ solutions.

Next, we proceed to the calculation of the curves of hydrate formation of the studied mixed inhibitors. For example, we will investigate a solution with a water content of 70 wt. % and a mixed inhibitor concentration (total PVP + $MgCl_2$) of 30 wt.%. The calculations of the curves of hydrate formation are presented in Table 6.9 and Figure 6.8. So, the developed approach give us possibility to calculate the anti-hydrate properties of mixed inhibitor PVP + $MgCl_2$.

Table 6.9 Hydrate formation conditions of methane in mixed inhibitor PVP + $MgCl_2$

Pressure, MPa	Hydrate formation temperature (°C)														
	H_2O	H_2O (70 wt.%) - Inhibitor (total amount 30wt.%)					H_2O (75 wt.%) - Inhibitor (total 25 wt.%)					H_2O (80 wt.%) - Inhibitor (total 20 wt.%)				
		PVP (30 wt.%)	$MgCl_2$ (15 wt.%)-PVP (15 wt.%) (1:1)	$MgCl_2$ (10 wt.%)-PVP (20 wt.%) (1:2)	$MgCl_2$ (20 wt.%)-PVP (10 wt.%) (2:1)	$MgCl_2$ (30 wt.%)	PVP (25 wt.%)	$MgCl_2$ (12.5 wt.%)-PVP (12.5 wt.%) (1:1)	$MgCl_2$ (8.33 wt.%)-PVP (16.67 wt.%) (1:2)	$MgCl_2$ (16.67 wt.%)-PVP (8.33 wt.%) (2:1)	$MgCl_2$ (25 wt.%)	PVP (20 wt.%)	$MgCl_2$ (10 wt.%)-PVP (10 wt.%) (1:1)	$MgCl_2$ (6.67 wt.%)-PVP (13.33 wt.%) (1:2)	$MgCl_2$ (13.33 wt.%)-PVP (6.67 wt.%) (2:1)	$MgCl_2$ (20 wt.%)
5	6.31	5.73	-8.79	-1.56	-18.18	-44.31	6.01	-3.68	1.01	-9.69	-25.53	6.06	0.00	2.86	-3.64	-12.63
6	8.14	7.57	-6.96	0.28	-16.34	-42.48	7.85	-1.85	2.85	-7.86	-23.70	7.90	1.83	4.69	-1.81	-10.80
7	9.66	9.08	-5.44	1.79	-14.83	-40.96	9.36	-0.33	4.36	-6.34	-22.18	9.41	3.35	6.21	-0.29	-9.28
8	10.95	10.37	-4.16	3.08	-13.54	-39.68	10.65	0.95	5.65	-5.06	-20.90	10.70	4.63	7.49	0.99	-8.00
9	12.06	11.48	-3.05	4.19	-12.43	-38.57	11.76	2.06	6.76	-3.95	-19.79	11.81	5.74	8.60	2.10	-6.89
10	13.03	12.45	-2.07	5.16	-11.46	-37.60	12.73	3.04	7.73	-2.98	-18.81	12.78	6.72	9.57	3.08	-5.92
11	13.89	13.31	-1.21	6.02	-10.60	-36.73	13.59	3.90	8.59	-2.11	-17.95	13.64	7.58	10.44	3.94	-5.05
12	14.67	14.09	-0.44	6.80	-9.82	-35.96	14.37	4.67	9.37	-1.34	-17.18	14.42	8.35	11.21	4.71	-4.28
13	15.37	14.79	0.26	7.50	-9.12	-35.26	15.07	5.37	10.07	-0.64	-16.48	15.12	9.05	11.91	5.41	-3.58
14	16.00	15.43	0.90	8.14	-8.48	-34.62	15.71	6.01	10.71	0.00	-15.84	15.76	9.69	12.55	6.05	-2.94
15	16.59	16.01	1.49	8.72	-7.90	-34.03	16.29	6.60	11.29	0.59	-15.25	16.34	10.28	13.14	6.64	-2.35

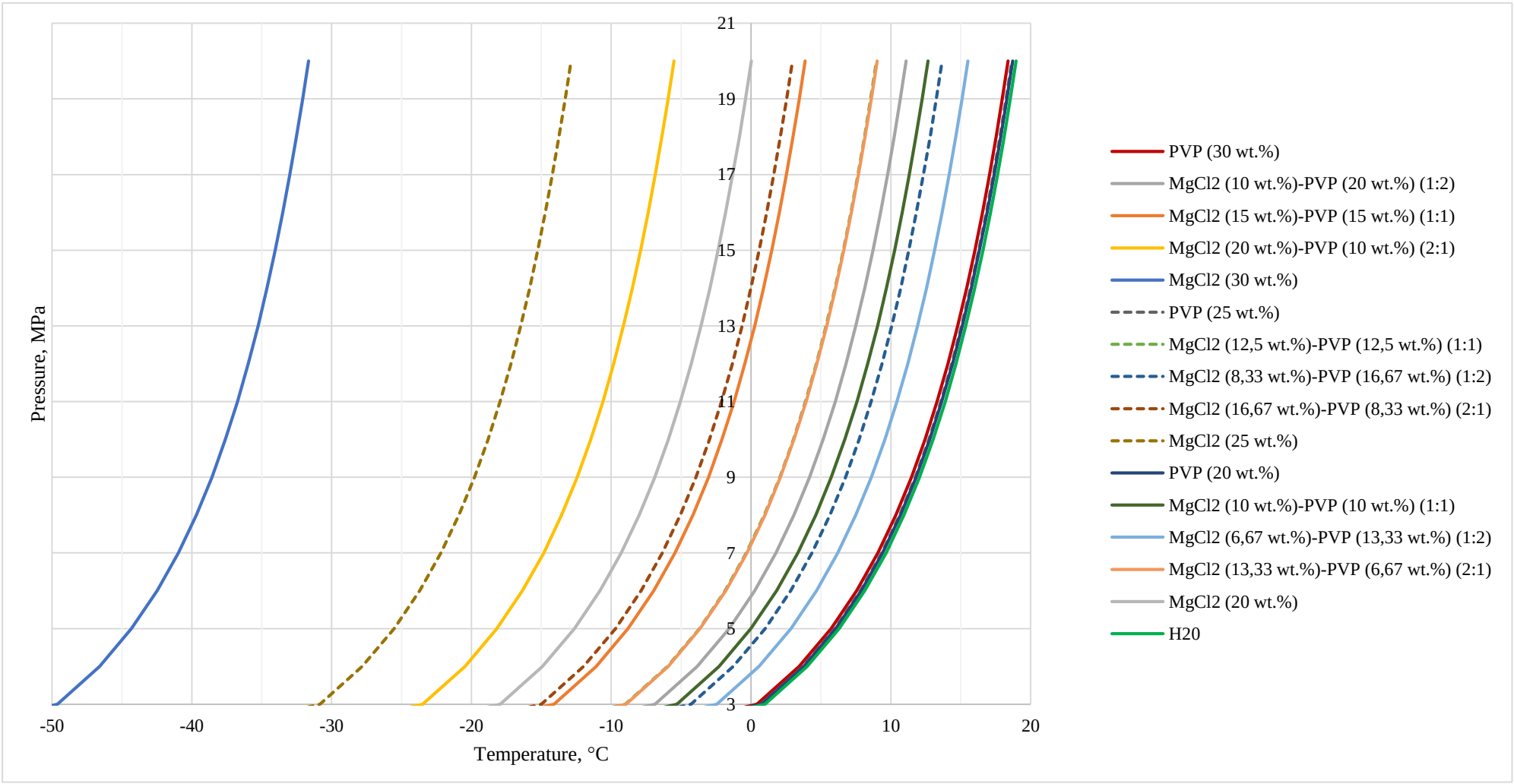

Figure 6.9 Hydrate formation conditions of methane in aqueous solutions of PVP + $MgCl_2$

6.4. Conclusions

The theoretical and experimental results of the chapter are as follows.

It has been developed more general correlations than early known (formulas (6.5-6.6) and (6.12)), which connect water activity with the temperature shift ΔT of hydrate formation in aqueous inhibitor solutions (at fixed fugacity/pressure) as well as the pressure shift of hydrate formation (at fixed temperature). These thermodynamic correlations may be use for several ways:

- to extrapolate the experimental data on inhibitor affect from one gas or gas mixture to another gas (for instance, from methane to natural gas or carbon dioxide);
- to extrapolate the experimental data for hydrate equilibrium in inhibitor solutions for more (than experimental) thermobaric area, i.e. for more high pressures and for lower temperatures.

The properties of mixed inhibitor "methanol + magnesium chloride" were experimentally studied, including methane hydrate formation conditions in this composition (see Appendix 2 and 3). This composition is a promising inhibitor for the gas gathering systems of Western Siberia gas fields (for inhibition pipelines from hydrates/ices). On the base of experimental data two simple and reliable thermodynamic correlations on ΔT for mixed inhibitors like "methanol + salts" are proposed. The first correlation is based on the formally additive contribution of inhibitor components on ΔT by using their effective concentrations in the solutions. And the second correlation is based on the modified Zdanovsky' rule. For mixed inhibitor "methanol + magnesium chloride" the both correlations may be used in practice, but the first correlation is better and work up to $\Delta T \cong 30 - 35$ K. Also such correlations may be used for another mixed inhibitor (methanol + $CaCl_2$ and methanol + formation brine etc.). In the chapter 7 the first correlation is used for methanol + brine consumption calculations.

The water activities, viscosity and density of mixed "kinetic + thermodynamic" inhibitor for "PVP + NaCl" and "PVP + $MgCl_2$" solutions were experimentally studied. Also, for mixed "PVP + salt" inhibitors were discussed two previous thermodynamic correlations for water activity. It was established that for such mixed inhibitors these correlations work very good. It gave us possibility to propose the technique for calculation of hydrate formation conditions in mixed "PVP + salt" inhibitors.

Chapter 7. New features of hydrate formation in gas and gas-condensate fields in Russia and flow assurance studies

Gas hydrates are one of the serious problem during gas recovery at Northern regions due to pluggings, which causes in pipelines or field equipment blockage.

For hydrate appearance low temperatures and high pressures are required. The methods of hydrate control are reducing gas pressure or gas heating for changing conditions to avoid hydrate stability condition. Another approach to prevent hydrate depositing in the field gas gathering and gas treatment systems is to use chemical compounds which change hydrate thermobaric conditions, or prevent hydrate particles nucleation and agglomeration. Now, hydrate inhibitors are classified as thermodynamic inhibitors (like electrolytes, methanol, glycols) and rather new - so called low dosage hydrate inhibitors (LDHI). LDHI are divided to kinetic inhibitors (water soluble polymers), and anti-agglomerants (surface activity substances). Methanol and monoethylene glycol (MEG) are commonly used in production operations for avoiding gas hydrates.

The thermodynamic inhibitor - methanol is currently the most popular reagent at Russian Siberia's gas and gas condensate fields. MEG is implicated only at Lunskoe and Kirinskoe gas condensate fields, which are in offshore conditions. The application of traditional inhibitors such as methanol and monoethylene glycol sometimes lead to additional technological problems like salt deposition (scaling), corrosion, etc. Such problems recently appeared in Russia during the development of new regions of oil and gas production: shelf fields and fields in Eastern Siberia.

In this chapter, we analyze some features of hydrate/ice formation and their prevention: i) at new gas condensate fields of Eastern Siberia in the initial period of their development; ii) at a late stage in the development of gas fields in Western Siberia.

The Chayandinskoye and the Yaraktinskoye oil and gas condensate fields were selected as typical fields in Eastern Siberia. The features of the methanol applications as hydrate inhibitor are considered, taking into account the serious risks of scaling in gas-condensate wells. As for old gas fields in Western Siberia, the object of our study is the system of in-field gas gathering systems of the Cenomanian gas deposits at a late stage of their development.

Research objectives of this chapter are:

1. To identify the mechanisms of hydrate formation in gas production wells at the Eastern Siberia fields.

2. To develop the model and carry out some calculations of the concentrated methanol consumption and its aqueous solutions, taking into account the possibility of hydrate precipitation directly from the vapor phase (Chayandinskoye field for example), and taking into account the risks of halite deposits, when gas wells also produce the formation water (Yarakta field as example).

3. To reveal the operation features of the in-field pipelines of the Yamburgskoye field and to analyze the possibilities of pipeline operation in the presence of a layer of ice or hydrate in the inner wall of pipeline due to extreme climatic conditions.

7.1. Gas hydrate formation mechanism and the hydrate prevention in exploitation wells of gas condensate fields in Eastern Siberia

Gas condensate fields in Eastern Siberia of Russia are located in the Irkutsk region and in the southern part of the Republic of Yakutia (Sakha), they are partially located in the permafrost zone. A number of gas condensate fields are already being exploited (Sredne-Bobuobinskoye, Otradnenskoye, Yarakta fields etc.). The well-known Chayandinskoye field is currently under initial stage of development, and the Kovykta field will be brought into development in the nearest future.

The specific features of these gas bearing deposits are as follows:

1. Abnormally low geothermal gradient and, as a consequence, abnormally low reservoir temperature: 9-14 ^{o}C - at the Chayandinskoye field, 37 ^{o}C - at the Yarakta field and 55 ^{o}C - at the Kovykta field. In comparison, gas and gas condensate deposits of Western Siberia at comparable depths of 1.5-2.5 km have temperatures of 15-30 ^{o}C higher. This leads to the hydrate formation condition in the operating modes of wells (even for the Kovykta field). Whereas under certain conditions the process of hydrate formation is possible in the bottomhole formation zone (at Chayandinskoye and Sredne-Bobuobinskoye fields).

2. High salinity of formation water (300-400 g/l and more), mainly to sodium, potassium, calcium and magnesium chlorides. Due to the high salinity there are no gas hydrates in reservoir deposits, even on the coldest deposits (Botuobin deposit of the Chayandinskoye field) with a formation pressure of 12-14 MPa and temperatures of 9-12 ^{o}C. In fact, such deposits are "hydrate self-prevention" deposits due to residual highly mineralized water in the reservoir, which is an effective hydrate inhibitor.

3. All deposits are gas condensate with a relatively low C_{5+} content (in comparison with gas condensate fields in Western Siberia). The content of C_{5+} hydrocarbons in reservoir gas is 15-50 g/m^3, methane - 85-87 mol.%, ethane content is quite high (~5%), all deposits are helium-bearing (0.3 ... 0.6% of helium), high nitrogen content (from 2 to 12%). There is a slight undersaturation of the reservoir systems for C_{5+} hydrocarbons. In some cases, the oil rims can be existing. The presence of helium and highly nitrogen content complicates the processing technologies for natural gas recovery.

4. Judging by the thermobaric conditions, the process of hydrate formation is possible in the wells in their operating modes. Note that such phenomenon was not previously observed in production wells of Cenomanian deposits in Western Siberia (this is taken place only for over-

Cenomanian horizons – Turonian horizons of the Yuzhno-Russkoye field). It should be emphasized that in the Eastern Siberia fields there are two complicating factors: hydrate formation in the wellbores (sometimes directly from water vapors) and salt deposition (primary, halite scaling).

7.1.1. Gas hydrate formation in exploitation wells of the Chayandinskoye field

The Chayandinskoye oil, gas and condensate field is one of the largest fields in Eastern Siberia of Russia. The field forms the backbone of the Yakutia gas production center and serves as a resource base for the "Power of Siberia" gas main (along with the Kovykta field in the Irkutsk Region).

The features of the Chayandinskoye field are: very low thermobaric characteristics (the reservoir temperature is 9-12 ^{o}C, the pressure is ~13 MPa) and the presence of trap magmatism and the halite salts as a cementing material of the rock. Oil and gas deposits were discovered in botuobinsky, khamakinsky and talakhsky productive horizons. The botuobinsky horizon is the most productive. It was revealed that the salinization of the pore space is partial and distributed in the volume of the rock locally, therefore, the reservoirs retained relatively high filtration properties.

When gas flows in the wellbore, its pressure and temperature are decreasing: pressure from 13 MPa to 9 MPa and temperature from 10-12 ^{o}C to minus 3... minus 7 ^{o}C at the wellheads. The wellbore (lift pipe) can be divided into two zones:

1. The lower zone of the lift pipe, where there is no any water condensation from the gaseous phase. This is due to the fact that in reservoir conditions, natural gas is in thermodynamic equilibrium with highly saline residual water in the reservoir. So the water vapor in natural gas is unsaturated in relation to pure liquid water phase.

2. The upper zone of the lift pipe is the cold zone, where hydrate formation is possible from the gaseous phase – hydrates may condensate directly from water vapor. There is an analogy with the formation of frosty fog (ice microcrystals) in extremely cold air at temperatures of minus 50 ºC in Yakutia's winter season.

So, an extraordinary mechanism for hydrate forming process from water vapor in the wellbore is realized. As a rule, the hydrate forming process occurs from liquid water phase and gas hydrate-former. Three phase equilibrium "gas – water (or aqueous solution) – hydrates" take place during gas hydrates form at pipelines and equipment. Models and software for calculations of three phase hydrate equilibria are well known and available. But in the case under consideration the thermodynamic model of two phase equilibria "gas with water vapor – gas hydrate" is needed for description the process, because there is no liquid water in the system.

The equation, which describe this two phase equilibrium, is

$$f_{h,\,H2O} = f_{g,\,H2O}, \tag{7.1}$$

where $f_{h,\,H2O} = \exp\frac{\mu_h,(T,P)-\mu_h^0(T,P_0)}{RT}$ is a water fugacity in hydrate phase and $f_{g,\,H2O}$ - a fugacity of water vapor in gaseous phase (natural gas, methane etc.).

The value $\Delta\mu = \mu_h,(T,P) - \mu_h^0(T,P_0)$ is known (see, for instance, [155]). The fugacity of water vapor $f_{g,H2O}$ is a function of a total gas pressure and water vapor content $y_{g,H2O}$ in the gas ($y_{g,H2O}$ is a molar fraction of the water vapor in the gas phase). The value $f_{g,H2O}$ may be calculated by using an appropriate equation of state from known *P*, *T* and $y_{g,H2O}$.

So, the question is: "How to find $y_{g,H2O}$?" It may be possible if we know the conditions of the Chayandinskoye field (the botuobinsky horizon): formation pressure/temperature and salinity content of formation water (residual water mineralization reaches 350 g/l). If salinity content of formation water and salt composition are known we may measure or calculate the water activity a in

salt solution and then to calculate $y_{g,H2O}$ by using formula $y_{g,H2O} = a \cdot y^{(0)}_{g,H2O}$, where $y^{(0)}_{g,H2O}$ is water content in equilibrium of compressed gas with pure water. For calculation of $y^{(0)}_{g,H2O}$ there are monograms, empirical correlations and equation of states may be used.

It should be noted that the equilibrium water content of the reservoir gas of the Chayandinskoye field is quite low - at the level of 100 g/1000 m^3 of gas, which is a five times lower than in the formation gas of the Cenomanian deposits of the Western Siberia fields (comparison was made at the initial period of their development).

Let's consider the operating mode one of the well with a horizontal completion of Chayandinskoye field. The well length is 2745.8 m, and the absolute mark corresponds to minus 1421 m, the effective vertical thickness of the formation is 9.6 m, the permeability coefficient is 520 mD. With a pressure depression at a level of 0.4 MPa, the well production rate is 572.0 thousand m^3/day. The thermobaric regime of the well is calculated at its operating mode of 400 thousand m^3/day and is shown in Figure 7.1. The figure also shows the curves of hydrate formation corresponding to the two-phase equilibrium "gas – hydrate" in the wellbore.

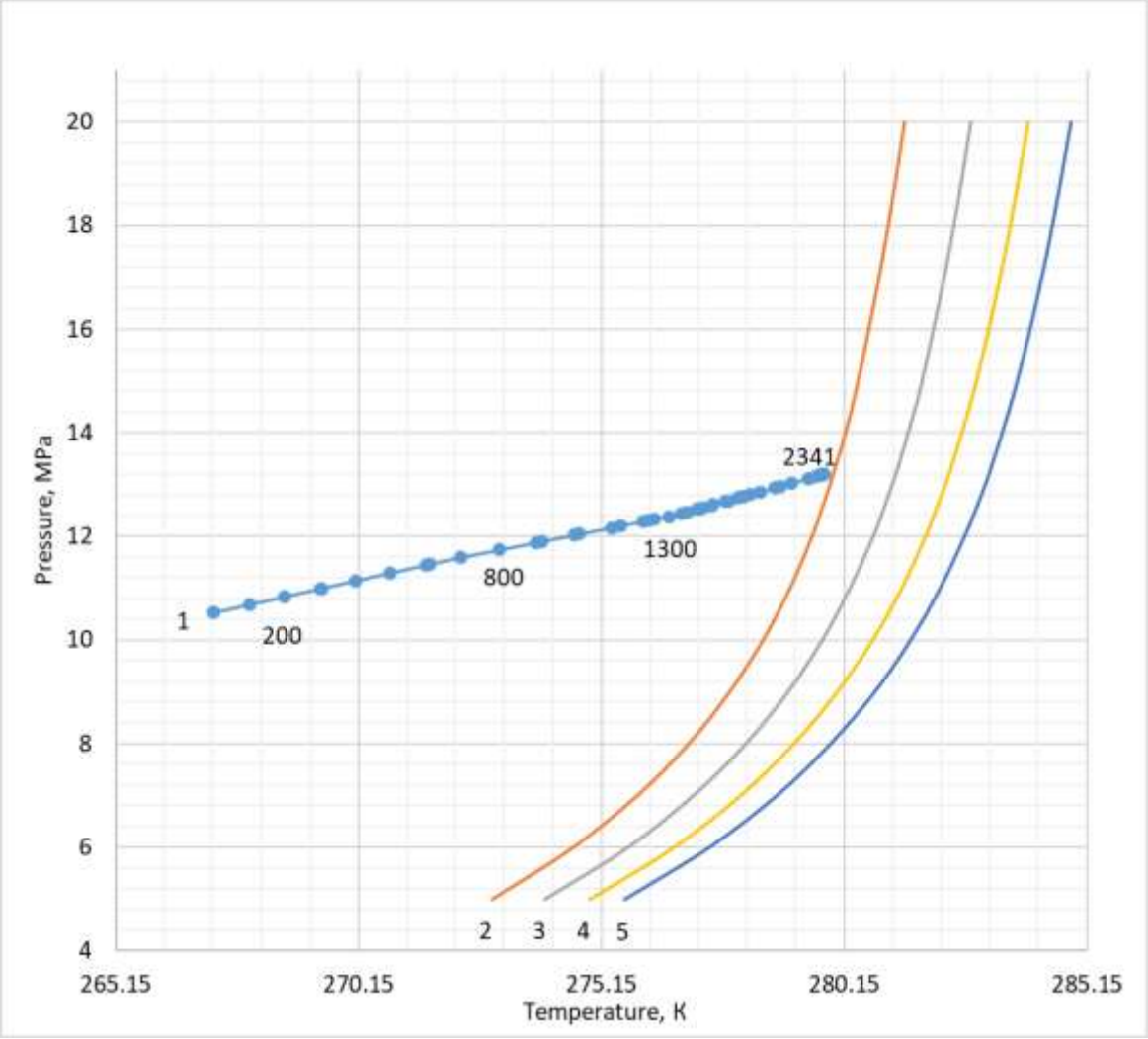

Figure 7.1 Thermobaric regime of the well at a flow rate of 400 thousand m^3/day and gas hydrate lines, corresponding to different salinity of formation water

1 - thermobaric well operation mode (numbers along the curve 1 - distance from the wellhead along the wellbore), 2 - equilibrium curve "gas-hydrate" with formation water salinity equal 350 g/l, 3 - equilibrium curve "gas-hydrate" with formation water salinity equal 300 g/l, 4 - equilibrium curve "gas-hydrate" with formation water salinity equal 250 g/l, 5 - equilibrium curve "gas-hydrate" with formation water salinity equal 200 g/l.

As follows from Figure 7.1, at the most probable salinity of formation water equal to 350 g/l the hydrate formation zone is almost the entire vertical part of the wellbore. Whereas, when the

formation water salinity is below 300 g/l, the entire wellbore from the bottom to the wellhead enters the hydrate formation zone.

To prevent hydrate formation in the wellbores of the Chayandinskoye field, the concentrated methanol is applied. Its specific consumption was calculated based on the temperature regime at the wellhead and the water content of the gas in reservoir conditions. It was ~0.6 kg/1000 m^3.

More details of methanol consumption for the inhibition of the exploitation wells at Eastern Siberia fields are presented in the next section at the Yarakta field as example.

7.1.2. Gas hydrate control in the exploitation gas wells of the Yarakta oil and gas field

Several oil and gas condensate deposits have been identified at the Yarakta field. Currently, six gas wells are in operation. Average flow rates of gas wells are 400 - 500 thousand m^3/day. The characteristic features of the field are a high initial reservoir pressure (up to 25.4 MPa) and a rather low reservoir temperature (37 °C), which leads to hydrate regime at wells working flow rates. At the Yarakta field, the hydrate formation process in the bottom hole zone of wells is impossible due to high reservoir temperature. Gas temperatures at the wellheads, depending on their flow rate, vary in the range of 3 - 10 °C and a wellhead pressure of 11-13 MPa (after the choke). The pressure up to the wellhead choke is 14.7-18.6 MPa. At present, all gas production wells operate without producing of formation water. But at least three gas wells carried out formation water at certain technological modes (it was established by well testing).

Let's briefly discuss the mechanism of hydrate formation in the lift pipes of the Yarakta field' gas wells. This mechanism significantly differs from the hydrate forming mechanism (above discussed) in the wellbores of the Chayandinskoye field.

When gas flows at the production wellbore, its pressure and temperature are decreasing. And the lift pipe can be divided into three zones:

1. The lower zone of the lift pipe, where there is no any water condensation from the gas;

2. Middle zone of the lift pipe, where pure water liquid droplets are condensed from the gas. The water droplets with a characteristic radius of 50-100 microns move together with the gas flow;

3. The upper cold zone of the lift pipe, where water droplets are transformed into hydrate particles, partially settling on the walls of the lift.

The reason why water condensation does not occur in the lower zone is the undersaturation of water vapor in natural gas in relation to pure liquid water. In reservoir conditions natural gas is in thermodynamic equilibrium with highly saline residual water in the reservoir and as a consequence the water vapor undersaturation in relation to pure water take place.

Thus, only the upper part of the wellbore of the Yarakta field is in hydrate regime. In this case, methanol injection to the well bottom is a quite acceptable technology for hydrate prevention. It is advisable to use concentrated methanol (90 wt% and higher), but if the dilute aqueous methanol solutions are used, the required specific consumption is increased.

It should be noted that at high depression on the reservoir and especially at the late stage of development, the wells will begin to carry the saline formation water. So, the physical picture of the hydrate formation process in lift pipes will be changing, because the highly saline formation water is also a hydrate inhibitor. In this case the condensation water process starts directly from the bottom of the well, it means the pure water condensation leads to dilution of the salt concentration of water droplets. At the upper zone of the well, the salt concentration in the water droplets may be insufficient to prevent gas hydrate formation. So the methanol consumption to the well bottom is needed.

Note that the concentrated methanol cannot be used because of the scaling when concentrated methanol is mixed with formation water. Estimates show that in order to prevent scaling (halite formation), it should be used a dilute methanol solution as hydrate inhibitor (at the level of 65-70 wt.% of methanol). Also, the special case take place when amount of formation water is sufficient to prevent fully the hydrate formation process. This situation we name as "self-inhibition" of the well by formation water.

Thus, to prevent hydrate formation in the wells of the Yarakta field, it is necessary to inject methanol or its aqueous solutions to the bottom of the well.

7.1.3. Phase equilibria of gas hydrates at the Yarakta field

First of all, it is necessary to calculate the of hydrate formation conditions for natural gas of Yarakta field with non-saline water, saline water (a mixture of formation and condensation water), and with aqueous solutions of methanol. The component compositions of gases were used according to the analysis data of the testing laboratory of oil products of LLC INK. The lines of three-phase equilibrium "gas – water – gas hydrates of structure II" were determined. The calculations were performed using the HydraFlash software. The results are shown in Figure 7.2. The figure also shows the influence of methanol concentration on the hydrate condition. The error in calculating the temperature is at the level of 0.5 degrees (at a given gas pressure). The water in this case does not contain salts.

The conclusions can be drawn from the calculations. With wellhead pressure varying in the range of 17 - 20 MPa (before the choke), the temperature of hydrate formation varies in a narrow range from 22 to 23 °C. At a wellhead pressure of 11-13 MPa (after the choke), the temperature of hydrate formation is 19-20 °C. Thus, taking into account the wellhead's gas temperature the exploitation well actually operates in a gas hydrate thermobaric mode.

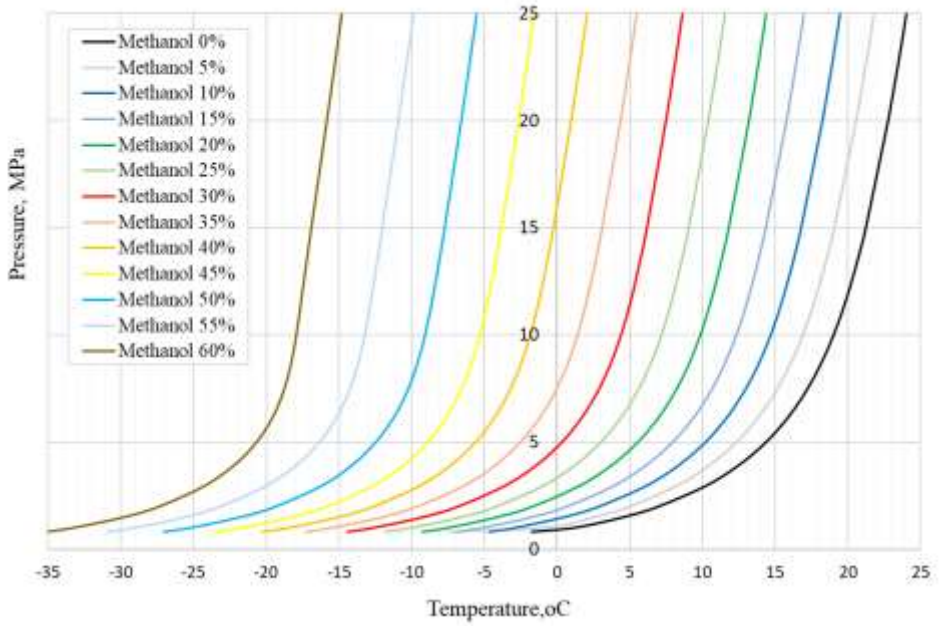

Figure 7.2 Three-phase equilibrium lines for natural gas hydrate formation of the Yarakta field at various concentrations of methanol in an aqueous solution (in the range of 0 – 60 wt.%)

The shift of the hydrate formation temperature ΔT depending on the methanol concentration X (in wt%) at a fixed pressure (in the pressure range of 10 - 20 MPa) can be described by the simplified equation, which is convenient for practice

$$\Delta T = -A \ln \frac{100-X}{100-X\left(1-\frac{M_W}{M_M}\right)}, \quad (7.2)$$

where M_w = 18.015 M_M = 32.04 - molar masses of water and methanol, respectively, g/mol; A is an empirical parameter obtained from the results of calculations. Parameter A weakly depends on X and gas pressure (it can be taken constant in the range of pressure and methanol concentration of interest). According to the calculations, parameter A is taken equal to 70.

The next stage of the calculations is the effect of water salinity on the hydrate formation. The average composition of formation water is shown in Table 7.1.

Table 7.1 Average composition of the formation water

	Ionic composition of water, mg/l							
Water density, kg/m^3	Cl^-	Br^-	SO_4^{2-}	$HCO3^-$	Ca^{2+}	Mg^2+	Na^+	K^+
1280	253069	4067	98.74	64	110175	12730	12132.8	4310

The salinity of the formation water is on average 31.10 wt%, but when gas moves in the wellbore, the formation water is diluted by water condensation from natural gas during its cooling. The degree of dilution depends on the specific amount of formation water entering to the well. Therefore, the calculations of the hydrate formation conditions were carried out for various water salinity from 10 to 31.1 wt% with the retention of the ionic composition. The calculation results are shown in Figure 7.3.

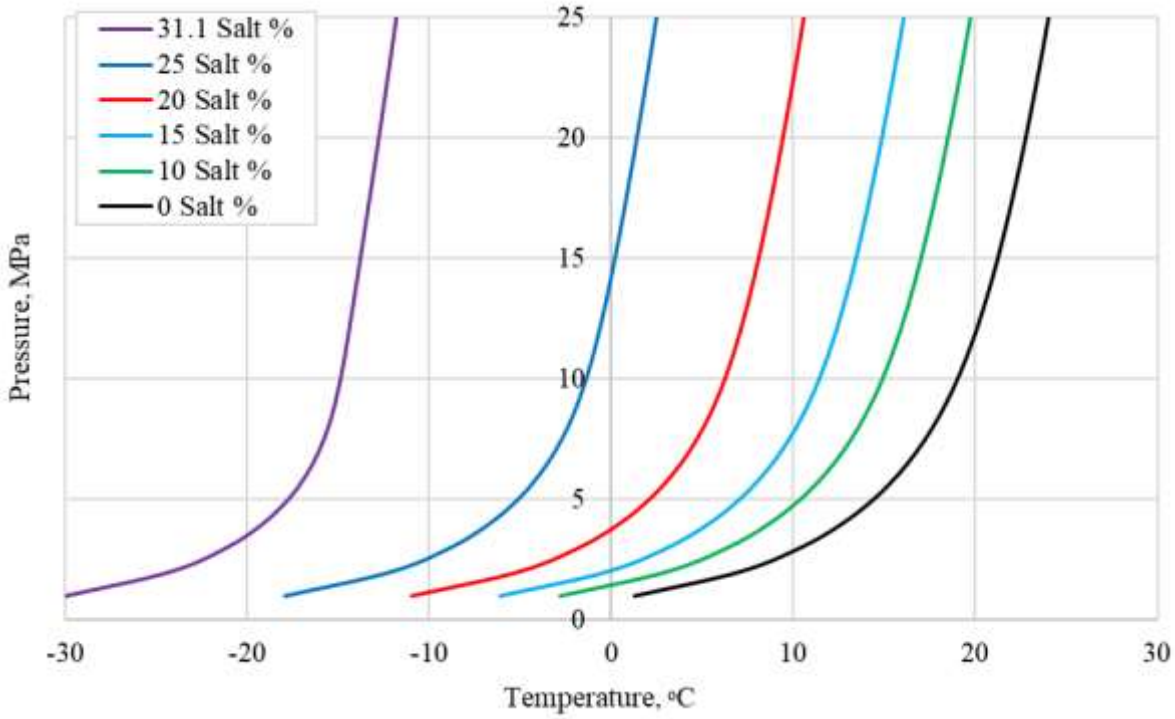

Figure 7.3 Three-phase equilibrium lines for natural gas hydrate formation of the Yarakta field in water solutions of different salinity (salinity of water varying in the range from 0 to 31.1 wt.%)

Based on the calculations, the analytical dependence of the of hydrate formation temperature shift ΔT in saline water relative to the temperature of hydrate formation in pure water was obtained

$$\Delta T = -A \ln a, \tag{7.3}$$

where $A = 73.5$ K, $a = 1 - 0.00155 \cdot m - 0.00034 \cdot m^2$ and m is the concentration of salt in a mineralized aqueous solution, wt. % (the ionic composition is presented in Table 7.1).

It should be emphasized that the calculations of the hydrate inhibition process require approximate analytical dependences of both methanol and saline water combined effect on the shift in the hydrate formation conditions ΔT.

For this purpose, we can use the formula for mixed inhibitor $\Delta T = \Delta T_1 + \Delta T_2$ or $\Delta T \approx -A \ln a_1 \cdot a_2$, where *A*~71; ΔT_1, a_1 and ΔT_2, a_2 - are effective contributions of the methanol and the salinity of the solution, respectively. A detailed technique for the contributions estimation and its experimental verification are given in the previous chapter (the first correlation for mixed inhibitor is used).

7.1.4. Calculations of the methanol and its aqueous solutions consumption to prevent hydrate formation of the Yarakta wells

To calculate the methanol consumption for inhibition of the Yarakta wells, analytical dependences mainly may be used according to the regulatory document [156]. But in our case additional correlation of the methanol solubility in compressed natural gas up to pressures of 20-25 MPa is needed. Also, it should be noted that when gas wells carry out the formation water, the balance relations, which given in [156], are not fully correct. So, for calculating the specific consumption of aqueous methanol solutions we have to use simultaneously three material balance relations separately for water, methanol and salts.

The calculation of the methanol consumption for gas wells, operating without formation water, are shown in Figure 7.4. It can be seen that the specific consumption of concentrated methanol is quite large (0.5 g/m^3 and more), which is due to the high solubility of methanol in gas phase in the pressures of interest. When an aqueous methanol solution is used as hydrate inhibitor, the methanol consumption (in recalculation for pure methanol loses) increases. With decreasing in the methanol concentration from 100 to 70 wt% the pure methanol consumption increases by 5-30 % depending on the wellhead temperature. With a further decrease in the methanol content in its aqueous solution, the specific consumption increases significantly, especially for low wellhead temperatures. So, for this case, we recommend preferable to use the concentrated methanol as hydrate inhibitor. But the methanol solution from 65 wt% or higher concentration also may be used without any additional risks.

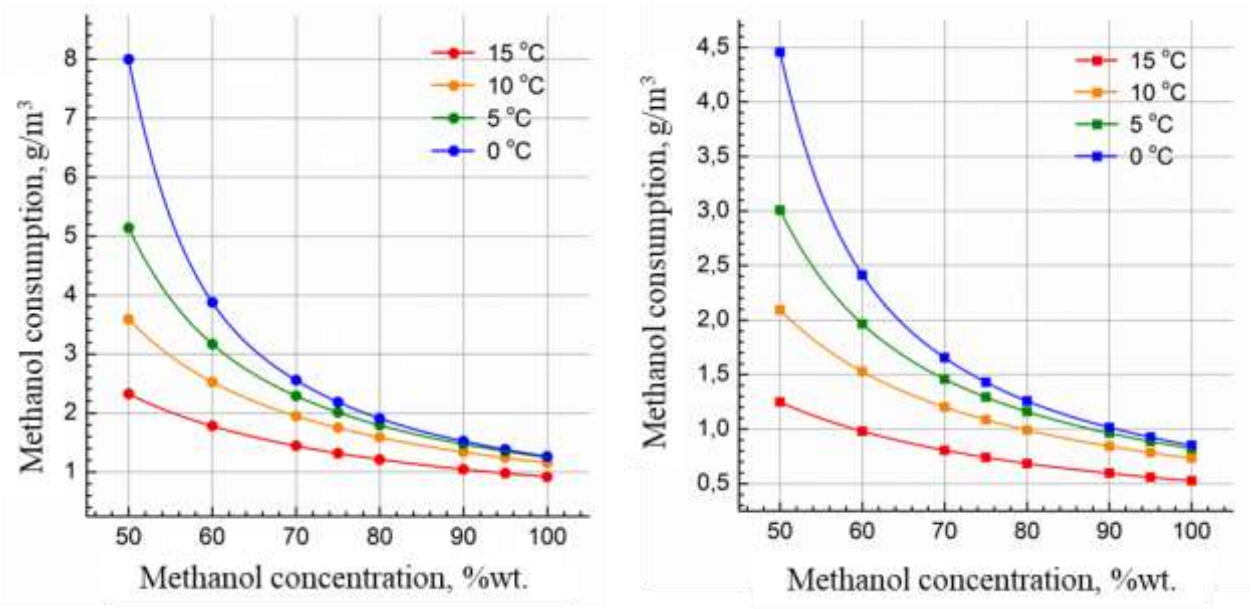

(a) (b)

Figure 7.4 The flow rate aqueous solution of methanol with concentration from 50 to 100 wt. % injection to the bottom of the well for temperatures from 0 to 15 ˚C and pressures of 20 MPa (a) and 14 MPa (b) at the wellhead

As for gas wells with formation saline water producing, the application of concentrated methanol is unacceptable due to the risks of halite deposition. It was established that for such wells it is necessary to use aqueous methanol solutions with optimal concentration in the range of 60-70 wt%.

Firstly, let's consider the possibility of the well inhibition by own formation saline water. The situation is illustrated in Figure 7.5. At this figure the dashed vertical lines show the limiting temperature, at which the "self-inhibition" of the well by means of formation water is still possible (accordingly, for 20 wt% salt in formation water - the right vertical line, and for 25 wt% in formation water - the left vertical line).

For the current operating modes of gas wells with the producing of formation water, for prevention of hydrate formation it is necessary to inject aqueous solutions of methanol to the well's bottom. An example of calculation is shown in Figure 7.6. Note that the calculation is presented formally in the entire range of methanol concentrations in its aqueous solutions, but, as pointed above, it is necessary to use methanol solutions with a concentration in a range of 65-70 wt% (without any risk of scaling).

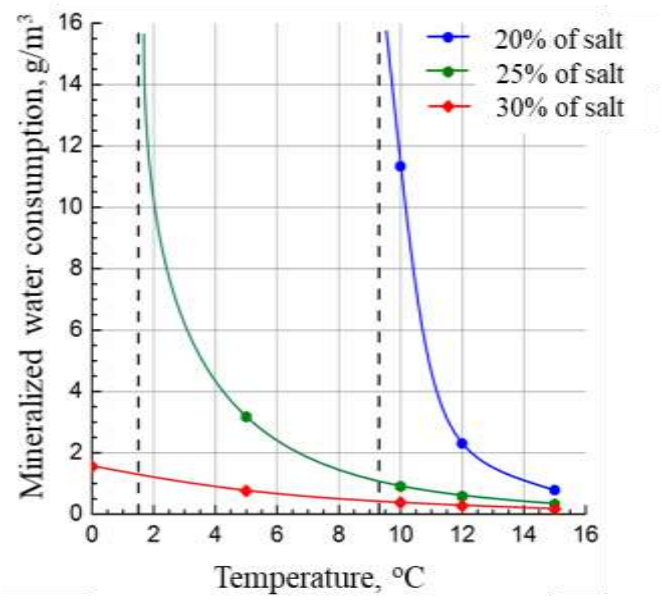

Figure 7.5 The minimum saline water consumption for hydrate inhibiting depending on the wellhead temperature (at wellhead pressure of 20 MPa).

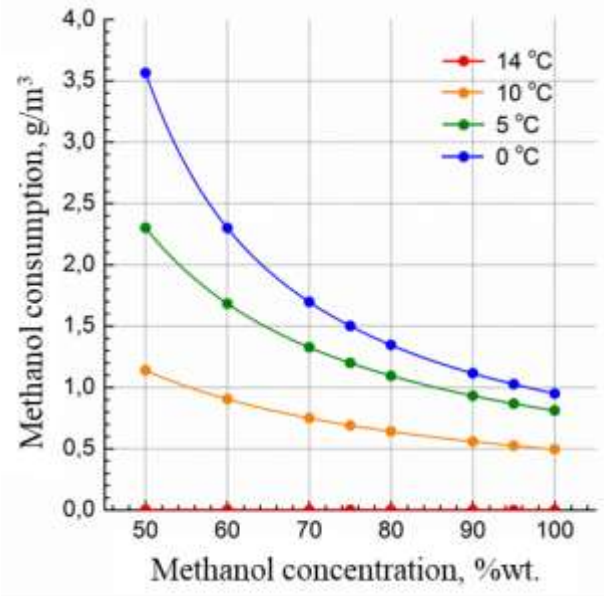

Figure 7.6 The methanol solution consumption depending on the concentration of methanol (taking into account the producing of formation water with a salinity of 30 wt% and in an amount of 0.2 g/m3) for a wellhead pressure of 20 MPa and wellhead temperatures in the range of 0-15 ˚C

Thus, we have developed a technique and carried out some technological calculations of the of methanol and its aqueous solutions specific consumption to prevent hydrate formation in the

wells, taking into account the risks of scaling associated with high salinity of formation waters. The performed calculations allow to optimize the of inhibition technology for gas producing wells of the Yarakta oil and gas condensate field.

7.2. The gas hydrate or ice depositions in gas-gathering pipelines of the Yamburg field (Senomanian horizon)

Raw natural gas is transported from well clusters to field gas plant by horizontal large-diameter in-field pipelines installed above the ground surface on low pillars. Pipelines are thermally insulated with polyurethane or polystyrene shells, covered aluminum sheets (Figure 7.7). Wellhead gas temperature is 5-15 ºC. Gas temperature at the end of in-field pipeline depends on several factors: wellhead gas temperature, pipeline length, quality of thermal insulation and variations of air temperature. So, at the cold season the considerable flow temperature drop along pipeline is observed.

The gas temperature at the end of infield pipeline changing in winter in a wide range: from -5 up to -25 ˚C (Figure 7.8). A major part of infield pipelines works with ice/hydrate formation risks. Despite sufficient methanol supply, low flow velocity and liquid accumulations do not except the ice/hydrate formation on cold inner wall of the pipe. The presence of stagnant liquid zones in certain lower pipe sections contributes to the freezing of high volumes of liquid if the air temperature is negative. This process may be identified by the increase of the pressure drops between well clusters and gas plant.

Figure 7.7 (Photo) Large diameter in-field pipelines in one technological corridor

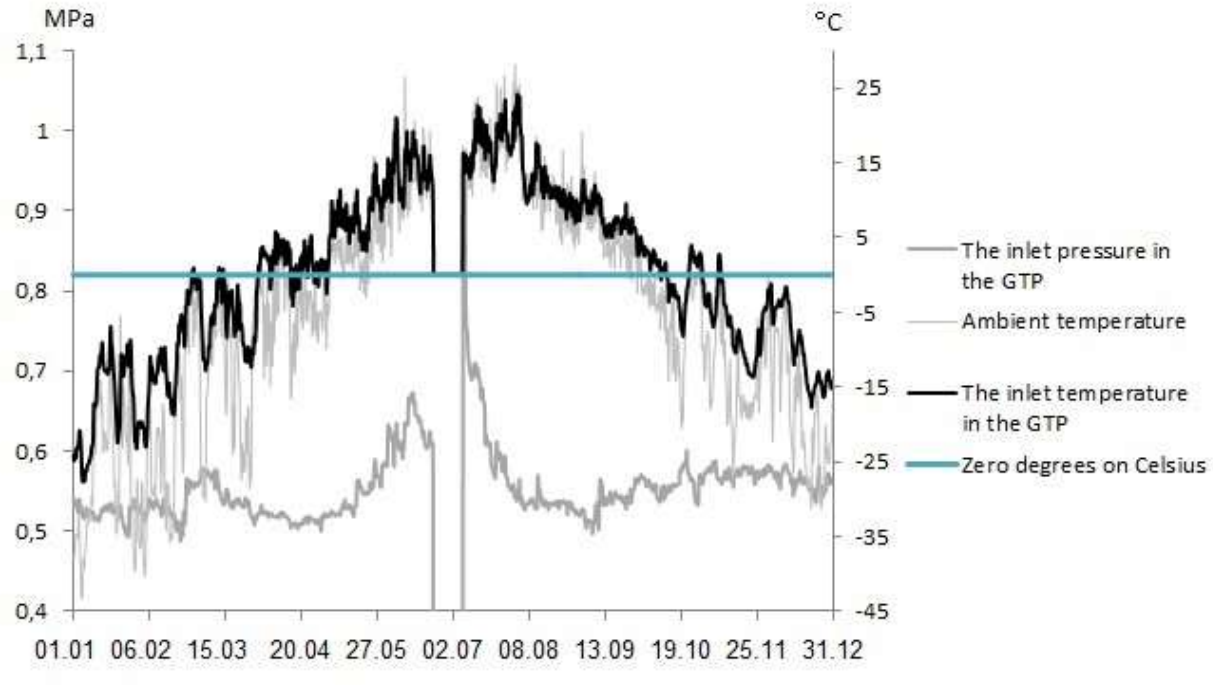

Figure 7.8 Thermobaric parameters for one of the infield pipe of Cenomanian deposits (during the 2015 year as an example)

During winter season, the alternation of extremely low air temperatures with more warm periods is inherent to Far North climate. Sometimes, abrupt temperature changes (up to a range of 20 degrees) can take place within one day. The experience of Yamburg field exploitation indicates

the reduction of gas gathering system performance during extremely cold periods, as well as on decline of liquid phase volumes in inlet separator. At the same time, the warm periods are described with spontaneous spikes of liquid masses entering to inlet separators, which can cause serious complications of normal technological systems operation [157]. Thereby, the oscillations in air temperature directly affect on formation and melting of ice or hydrate deposits in pipelines, which may lead to sudden liquid plug moving from the pipeline.

The analysis of gas gathering systems of Yamburg field reveals the principal difference between the formation of hydrate and ice plugs.

Hydrates formation is characterized by heat and mass transfer. As a rule, gas hydrates are formed at the water-gas boundaries. Hydrate deposits can be transferred by fluid flow and remain in local resistive sites: temperature compensators and pipe diversions, blocking and regulating reinforcements, transitions to reduced pipe's diameter and lifting sections of the pipeline route [158].

On contrary, ice formation is determined by only the heat transfer and the main site of ice formation is a cold inner wall of the pipeline. This explains why at low air temperatures the stagnant fluid zones with the significant amount of liquid are the most critical sites for ice depositions (greatly blocking the pipe cross section).

At the initial period of the development of the Yamburgskoye field of high pressures and temperatures at the wellheads, the thermodynamic parameters of the operation of the pipelines could only be in the hydrate formation mode. However, under reducing the gas production, the thermobaric parameters of the pipeline in the winter season gradually move to the ice formation mode. This is due to the fact that the gas pressure in the pipeline turns out to be lower than the hydrate formation pressure, while the gas temperature at the end of the pipeline may reduce below 0 °C. An operation analysis of the in-field pipelines shows that at the Yamburg field currently ~75% of the total number of in-field pipelines operate in the winter season only in the mode of possible ice

formation, ~10% can be in both the ice formation mode and hydrates, and only 15% can be in the mode of hydrate formation. Methanol is used both as hydrate and ice inhibitor.

At low velocity of gas flow and the accumulations of liquid in the pipeline and the supply of the calculated amount of methanol, the formation of ice deposits on the cold wall of the pipeline is not excluded. So, the ice formation on the cold inner wall of a pipeline may occurs at a low positive temperature of the gas stream in the core of the stream in the absence of methanol supply (see discussion below). As for hydrate formation at the inner wall of the pipeline, it seems also possible when the temperature of gas stream core is slightly above the hydrate formation mode.

Thus, in the winter season, ice (or hydrates) may be deposited on the inner wall of the field pipeline of an overhead laying at low negative ambient temperatures, even if the specific consumption of the methanol is sufficient. This is due to the calculating technique for methanol consumption is based on ensuring a hydrate-free mode of operation only for the core of the gas flow and do not take into account the possibility of ice or hydrate deposits on the cold inner wall of the pipeline (especially in the sites where the thermal insulation is broken). Therefore, the determination of the thickness of the hydrate (ice) layer on the inner wall of the pipeline depending on the flow characteristics, ambient temperature, type and quality of thermal insulation is an important task that determines the temperature and hydraulic modes of the pipeline operation.

Below, a simple computational model of the thickness of the hydrate (or ice) layer depending on the operating mode of the field pipeline with the raw gas (methane) flow is considered. The model takes into account the heat exchange between the gas and the inner wall of the field pipeline, the thermal insulation of the pipeline and the heat exchange with the environment. After a layer of hydrate (or ice) appears on the pipe wall, its insulating properties are taken into account, as well as heat exchange between the gas flow and the hydrate (ice). In this case, the low thermal conductivity of the hydrate was taken into account. The thermal conductivity coefficient of the hydrate is

approximately five times lower than the thermal conductivity of ice, i.e. the layer of hydrate growing on the inner wall of the pipeline is a fairly good heat insulator (in contrast to the ice layer).

Convective heat transfers between the inner wall of the pipe and the gas flow was determined by criterion relations, given, for example in [159]. Only the heat problem was considered, i.e. it is assumed that water in the gas-liquid flow along the pipeline is sufficient to form hydrates or ice.

The schematic of the model is shown in Figure 7.9 (in the section of the pipe).

A calculation formula was obtained (Appendix 4), in which a relationship is established between the heat flux and the conditions of heat transfer in each of the above processes, through which heat transfer through the heat-insulated wall (in a quasi-stationary state) is carried out.

The formula for determining the stationary temperature T_1 on the inner surface of the pipe as a multilayer cylindrical wall, taking into account the deposits of hydrates or ice, is written as follows

$$\frac{T_0-T_4}{T_0-T_1} = 1 + \frac{0.023\cdot\lambda_{CH4}\cdot w^{0.8}\cdot d^{1.6}}{(d-2\cdot x)^{1.8}\cdot\alpha_1{}^{0.43}\cdot\nu_{CH4}{}^{0.37}}\cdot(R-x)\left(\frac{\ln\left(\frac{R}{R-x}\right)}{\lambda_{hyd}}+\frac{\ln\left(\frac{R+\delta}{R}\right)}{\lambda_{pipe}}+\frac{\ln\left(\frac{R+\delta+y}{R+\delta}\right)}{\lambda_{th}}\right), \qquad (7.4)$$

where $\lambda_{hyd}, \lambda_{pipe}, \lambda_{th}$ – the thermal conductivity coefficients of hydrate (or ice), the steel pipe and the thermal insulation; y, δ – pipe wall thickness and thermal insulation thickness, respectively; x – hydrate thickness; R – pipe radius; w – average inlet flow velocity (in the area where there are no deposits); T_0 – the flow temperature; T_1 – the temperature of hydrate formation at a given gas pressure in the pipeline; T_2 – the temperature of the hydrate – wall of the pipe; T_3 – the temperature of the pipe – thermal insulation; T_4 – environment temperature.

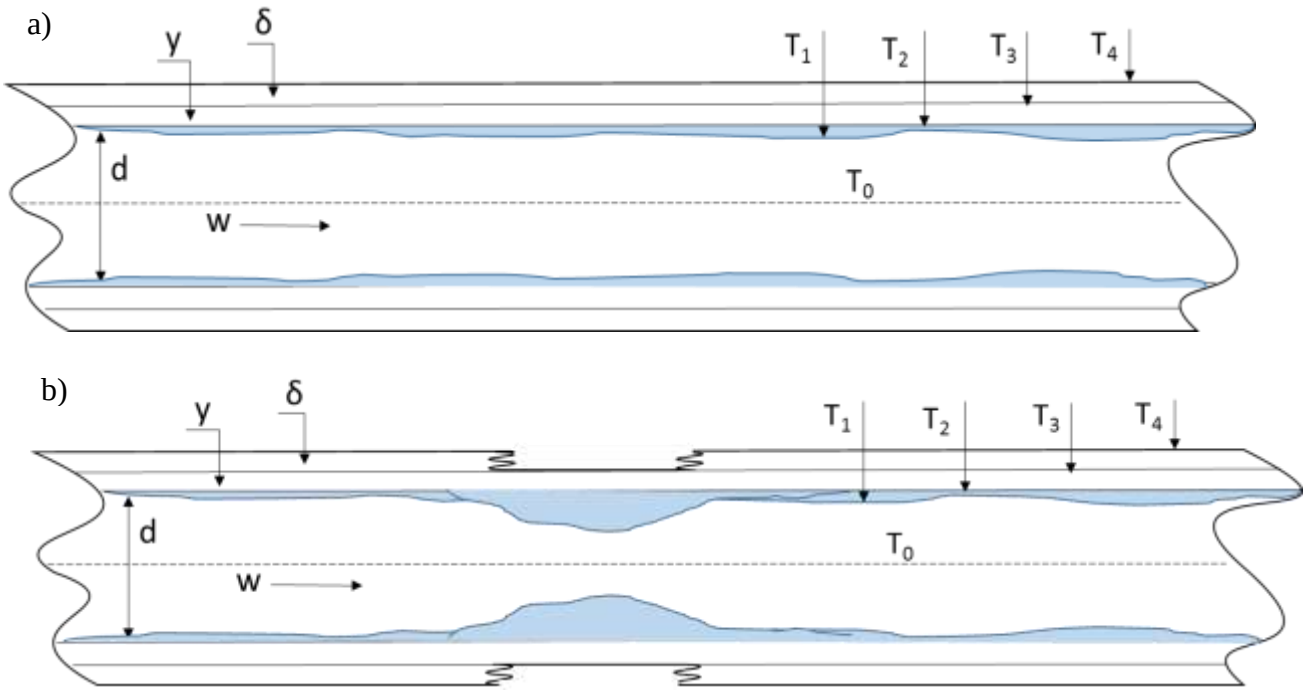

Figure 7.9 Section of the field pipeline, a) heat-insulated pipe b) damaged thermal insulation layer on the pipe

The formula (7.4) makes it possible to calculate the thickness of the stationary hydrate layer from the condition that the hydrate layer on the inner wall of the pipeline grows until the temperature at the hydrate-gas interface T_1 becomes equal to the temperature of hydrate formation at the considered pressure of the hydrate-forming gas (methane). And when injecting methanol to the pipeline, it is necessary to consider the curve of hydrate formation in equilibrium with an aqueous solution of methanol of a certain concentration (at the considered point along the pipeline route). Similarly, when ice is formed, the ice thickness is determined from the condition $T_1 = 0$ ˚C (and if methanol is injected, then instead of the condition $T_1 = 0$ ˚C, it should take into account the freezing point of an aqueous solution of methanol with the methanol concentration at the considered point of the pipeline routes.

The calculations were carried out for pipelines of two outer diameters 0.273 m and 0.53 m, the wall thickness of which is 0.008 m and 0.013 m, respectively. Natural gas (methane) flows through the pipeline, the gas velocity is 5 and 10 m/s. The thermal conductivity coefficients of the materials were considered constant (35 W/m·˚C for steel, 0.5 W/m·˚C for hydrate and 2.22 W/m·˚C for ice). Thermal insulation of the pipeline was set by two values of thermal conductivity coefficient: 0.04 W/m·˚C - the initial thermal insulation, 0.1 W/m·˚C - the "wet" thermal insulation. The case was also considered when the thermal insulation is absent for some reason at all (the thermal insulation is damaged - "bare section of the pipeline"). Table 7.2 shows the properties of methane gas at different pressures and temperatures, taken from the NIST database [160].

Table 7.2 Methane properties at various thermobaric conditions

		Hydrate		Ice
Pressure	MPa	10	5	1.5
Temperature	˚C	12	7	0
Flow temperature	˚C	13	8	1
Heat capacity of methane	J/kg·˚C	3166.6	2622.6	2291.6
Density of methane	kg/m^3	82.57	38.532	10.945
Methane viscosity	Pa·s	$1.3777 \cdot 10^{-5}$	$1.1665 \cdot 10^{-5}$	$1.0602 \cdot 10^{-5}$
Thermal conductivity of methane	W/m·˚C	0.04419	0.03628	0.0321

First, consider the case where the pipe section is not insulated (no insulation).

Figure 7.10 shows the dependence of the thickness of the hydrate layer on the environment temperature for two flow rates (5 and 10 m/s) and two pipe diameters (27.3 and 53 cm) at a gas pressure of 5 MPa.

The flow temperature differs from the hydrate formation temperature by 1 ˚C, i.e. the temperature of hydrate formation is 12 ˚C for a pressure 10 MPa (flow temperature is 13 ˚C), the temperature of hydrate formation is 7 ˚C for 5 MPa (flow temperature is 8 ˚C).

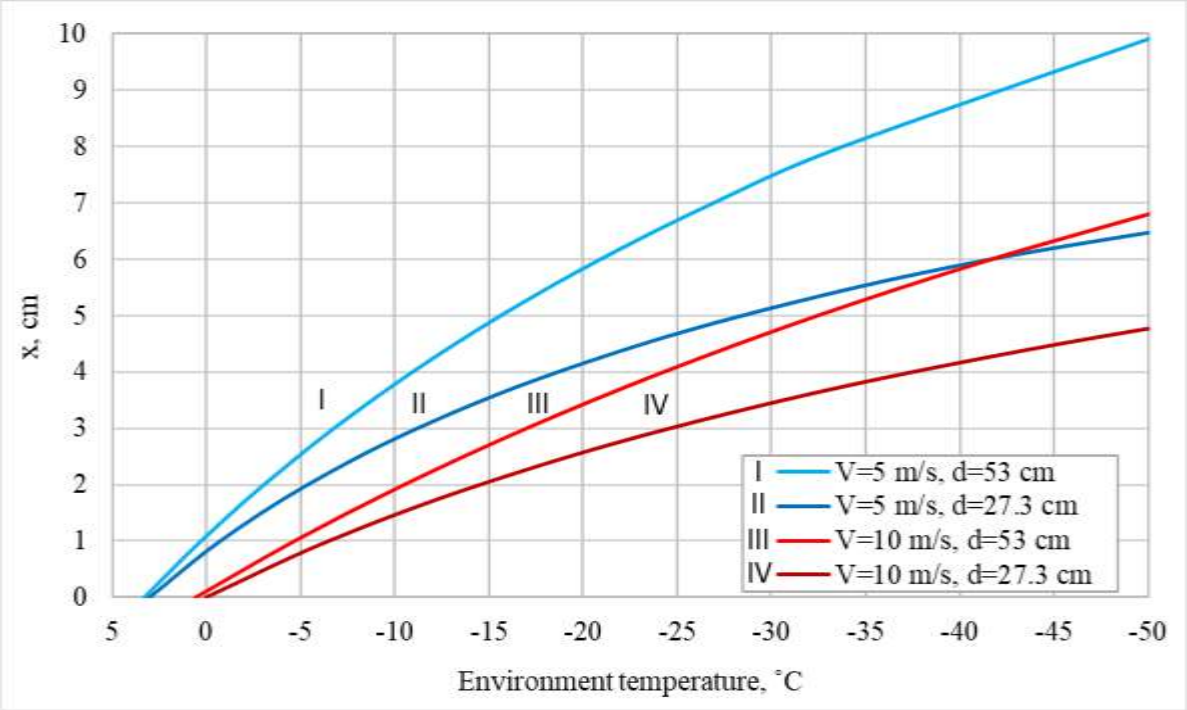

Figure 7.10 The thickness of the hydrate layer depending on the environment temperature for P = 5 MPa, T_1 = 7 ˚C, T_0 = 8 ˚C

From the graph shown in Figure 7.10, it can be seen that the thickness of the hydrate layer is nonlinear, and its growth slows down with decreasing environment temperature. This is due to the fact that as the hydrate layer grows on the inner wall of the pipeline, the thermal resistance between the flow and the pipe wall increases, because additional "hydrated" thermal insulation appears. The thickness of the hydrate layer is in the range of 6–8.7 cm for gas velocities of 5–10 m/s at an environment temperature -40 ˚C for a large-diameter pipe (d=53 cm). In the case when the environment temperature is positive (≥0 ˚C), the thickness of the hydrate layer is about 1 cm at low flow rates (5 m/s) and almost absent at a flow rate of 10 m/s (Figure 7.10).

In the previous case, the flow temperature differed from the hydrate formation temperature by 1 ˚C. Let us consider the effect of the flow temperature on the size of the hydrate layer. The thickness of the hydrate layer increases significantly with a decrease of difference between the flow temperature and the temperature of hydrate formation. This indicates the need for reserve in the consumption of the inhibitor.

On Figure 7.11 the graph of the dependence of the thickness of the hydrate layer x on the environment temperature at a flow temperature of 12.2 ˚C and a gas pressure of 10 MPa is shown below. It can be seen that the thickness of the hydrate layer is ~ 8.1 cm at a flow rate of 10 m/s for a small pipe diameter. In this case, the cross-sectional area free for flow movement has significantly decreased and is ~ 14% of the cross-sectional area of the pipe. The thickness is about 9.5 cm with an inlet flow velocity of 5 m/s and a cross-sectional area ratio of 6.8%.

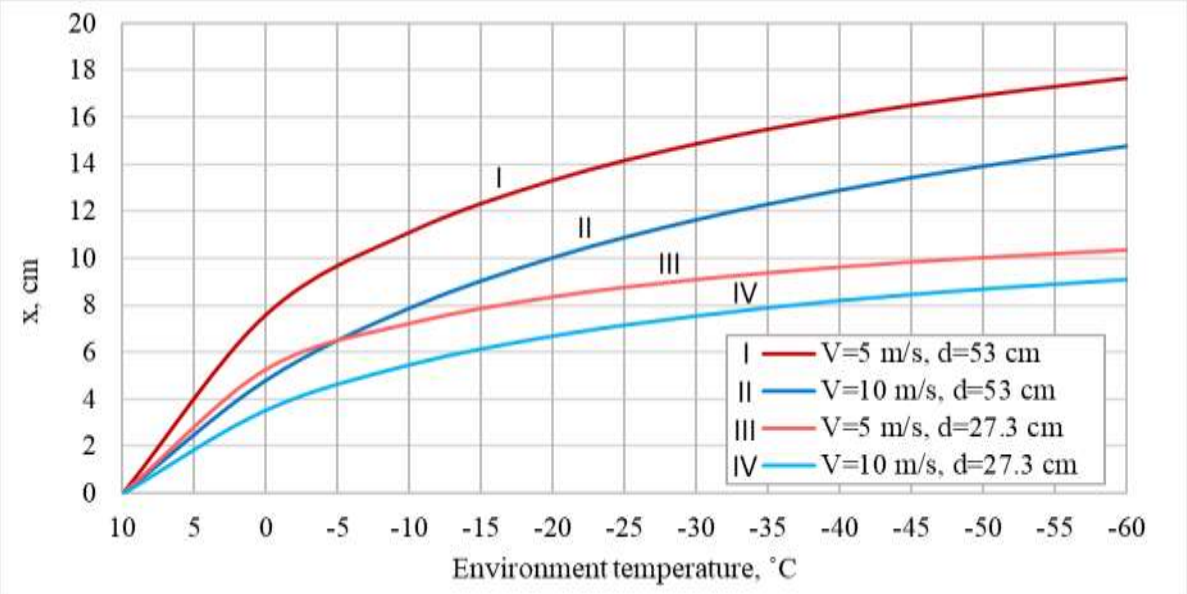

Figure 7.11 Dependence between the thickness of the hydrate layer and the environment temperature for P=10 MPa. T_{flow} =12.2 ˚C

The analysis of the influence of thermal insulation parameters on the size of the hydrate layer is carried out. A heat-insulating layer with a thickness of 6 cm, the thermal conductivity of which is

0.04 (factory excess) and 0.1 W/m˚C (insulation, with deteriorated thermophysical properties) was added to the previous calculations. Figure 7.12 shows the calculations for a gas velocity of 5 m/s at the inlet. For comparison with the previous examples, curves are obtained in the absence of thermal insulation are plotted in the graphs.

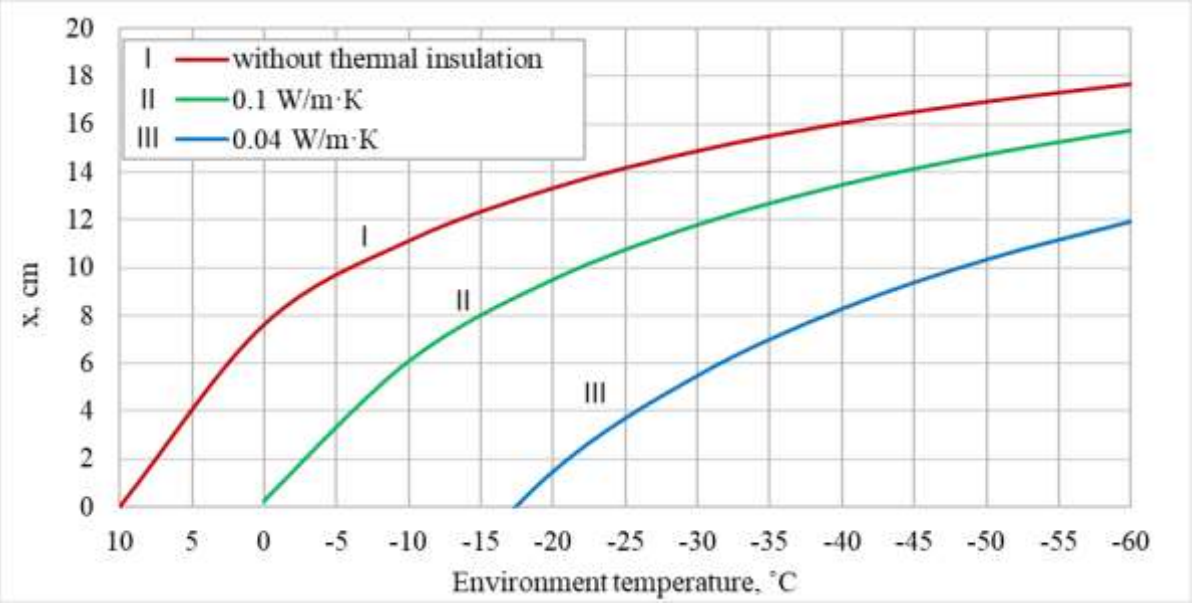

Figure 7.12 Dependence between the thickness of the hydrate layer and the environment temperature for different thermal insulation at V=5 m/s, d=53 cm, P=10 MPa. T_{flow} =12.2 ˚C

It can be seen from the graph that at -50 ˚C with wet thermal insulation (0.1 W/m˚C) the amount of hydrate layer is about 14.5 cm and 10 cm with thermal insulation 0.04 W/m˚C, the cross-sectional area free for the flow increases from 18% to 36% of the total pipe cross-sectional area.

Figure 7.13 presents an estimate of the minimum permissible flow temperature, at a fixed temperature of hydrate formation T_{hyd} = 12 ˚C, at which no hydrate is formed (x = 0 cm); 1 cm; 2 cm; 5 cm; 10 cm. The thickness of the hydration layer (x) is constant along the lines in Figure 7.13. Using this graph, fixing the environment temperature, it is easy to estimate what temperature in the flow should be maintained, so that the thickness of the hydrate layer does not exceed the specified value.

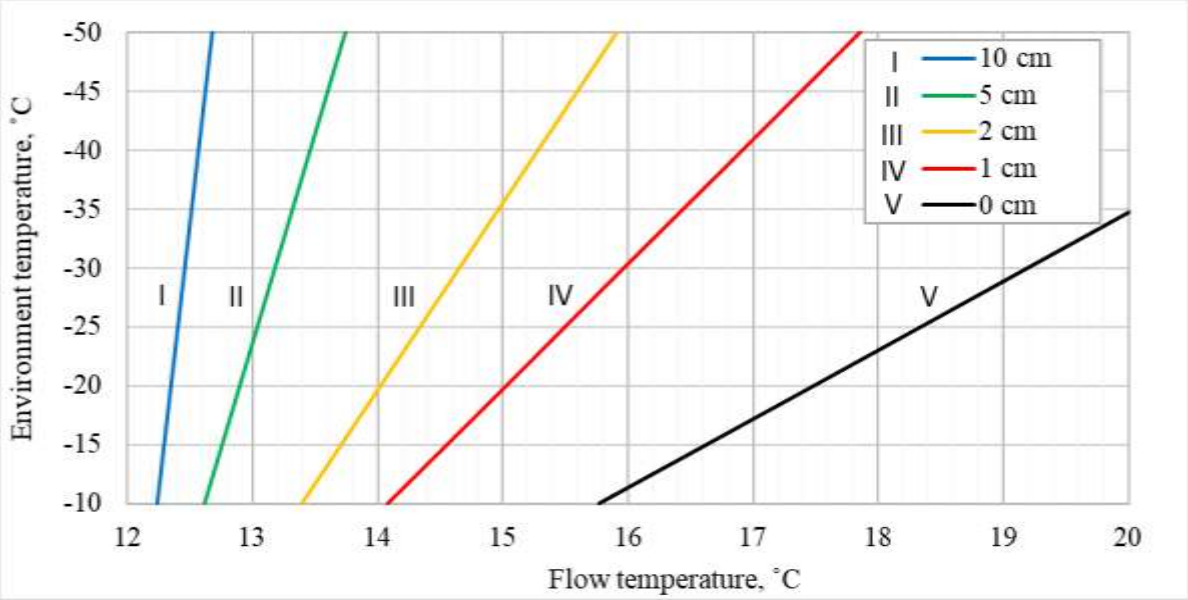

Figure 7.13 Dependence of the flow temperature on the environment temperature at a fixed thickness of the hydrate layer, V=5 m/s, P=10 MPa, d=53 cm

At a methane pressure of 1.5 MPa and a flow temperature of 1 °C, ice deposits are possible on the inner wall of the pipe (hydrate does not form under these conditions). As you know, ice forms at 0 ˚C, its thermal conductivity is 2.22 W/m˚C. To estimate the thickness of the ice layer, we take a pipe with a radius of 53 cm.

Independent of the flow rate, the ice layer is thick (Figure 7.14). At an environment temperature of -40 ˚C it is x=16 or 19 cm at 10 and 5 m/s, respectively. Even at a temperature of -20 ˚C, the size of the ice layer is x=12 and 15 cm at the corresponding speeds.

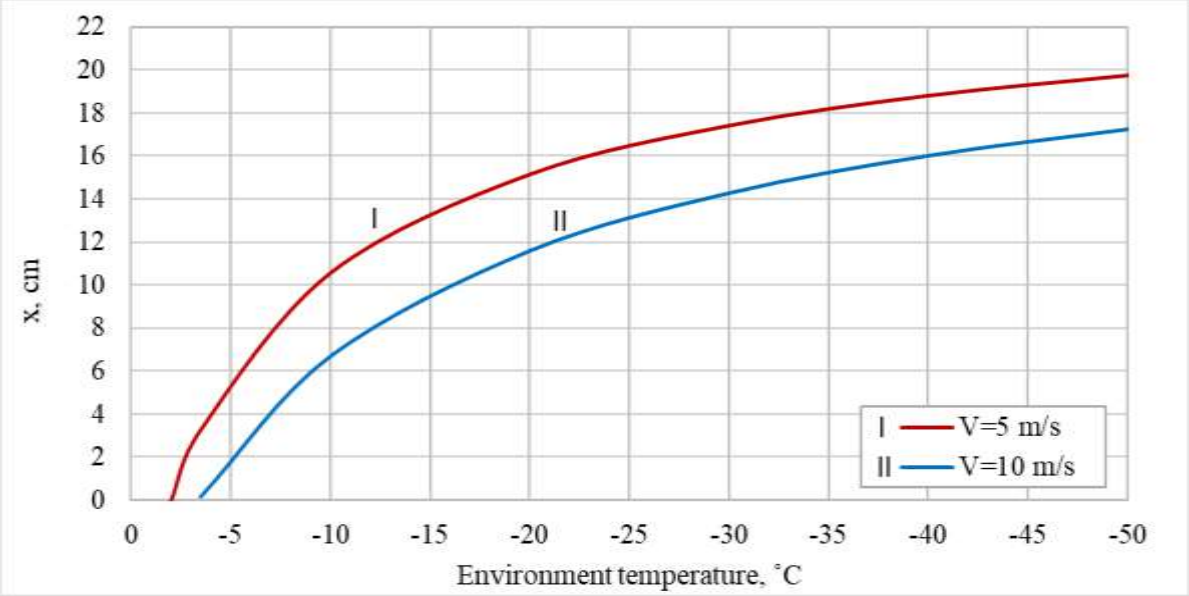

Figure 7.14 Dependence between the thickness of the ice layer and the environment temperature at T_{ice} =0 ˚C, P=1.5 MPa, d=0.53 cm

Figure 7.15 provides an estimate of the minimum allowable flow temperature, at which ice does not form (x =0 cm); the thickness of the ice layer is 1 cm; 2 cm; 5 cm; 10 cm. Along the lines in Figure 7.15, the thickness of the ice layer (x) is constant.

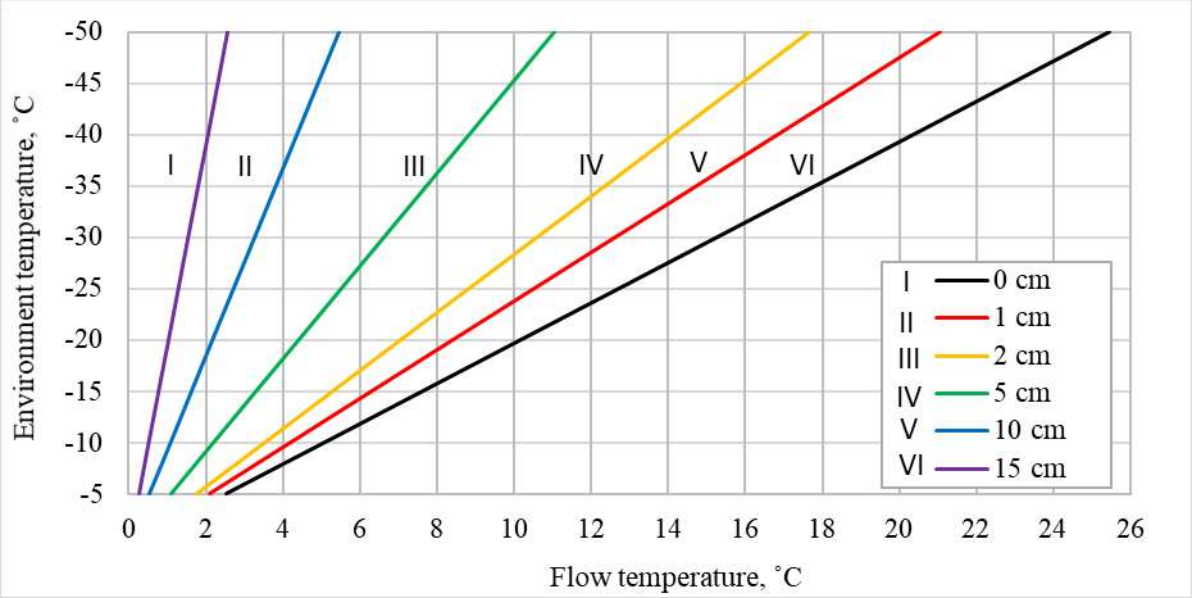

Figure 7.15 Dependence of the flow temperature on the environment temperature at a fixed thickness of the ice layer, V=10 m/s, P=1.5 MPa, d=53 cm

Thus, the results of the performed calculations show that the thickness of the hydrate or ice layer on the inner wall of the pipeline depends on the flow rate, its temperature, ambient temperature, on the diameter of the pipeline and the quality of thermal insulation.

The performed thermophysical calculations show the importance of compliance with a number of requirements during the operation of a field pipeline:

- implementation of technical and technological solutions to ensure the removal of fluid from the pipeline;

- the use of thermal insulation with low water absorption (polyurethane, expanded polystyrene) or taking measures to reduce its water absorption;

- timely restoration of damaged thermal insulation, elimination of gaps at the joints of parts of thermal insulation, as well as between the thermal insulation and the pipe wall.

The obtained data of the formation of a hydrate layer or ice layer on the wall of the pipeline for various pressures, temperatures and flow rates, as well as the diameters of pipelines can be used

to assess the operation of pipelines, including deciding on the need to supply an inhibitor. Under the operating modes of gas pipelines, it is rational to allow the formation of hydrates or ice on the inner wall. This will lead to additional thermal insulation in critical areas of maximum heat exchange with the environment.

7.3. Conclusions

In the chapter were considered the features of hydrate control at the Chayandiskoe and Yarakta oil and gas condensate fields, located in East Siberia. An analysis of the temperature and pressure modes of producing wells is given. It was noted that at the gas and gas condensate fields of Eastern Siberia, there are some new features of the hydrate formation process in the field systems.

A technique for calculating the methanol consumption, taking into account the possibility of producing formation high salinity water by the wells, has been developed. The risks of scaling in the wellbores due to halite precipitation when mixing concentrated methanol with formation water have been analyzed. The application of aqueous methanol solutions with methanol concentrations at the level of 60-70 wt% eliminate any risks of halite deposition.

Technological calculations of the specific methanol and its aqueous solutions consumption were carried out, taking into account the risks of scaling associated with high salinity of formation water. The results obtained make it possible to optimize the technology for hydrate inhibiting by methanol in the wellbores and gas-gathering systems of the gas-condensate fields of Eastern Siberia.

Also, the heat-insulated in-field pipeline operation of the Yamburg gas field (Cenomanian horizons) in the winter season is discussed. The cases are revealed when there is no ice or hydrate operation regime inside the gas stream, nevertheless, ice or hydrate depositing are possible at the internal wall of the pipe. This is due to the above-ground laying of pipelines and the temperature of

inner wall of the pipe may be below then the temperature of ice or hydrate formation. It is shown, that the effect under consideration is existed primary at ambient temperatures below -20 °C, especially in the sites of the pipeline where the thermal insulation has broken. The calculations of the stationary thickness of ice or hydrate layers in the inner wall of pipeline are presented.

Summary of the Research

1. Literature review was performed on physicochemical properties of gas hydrates primary on the thermodynamic aspects. It was mentioned that there are some issues, which are needed to further development. Firstly, it concerns the hydrate equilibria in porous media (with pore water in the soils and sediments) where direct experimental methods are difficult to realize and in many cases they give significant errors in detecting of the equilibrium conditions. The second problem is necessarily of the hydrate prevention technique improving, especially for the novel gas–condensate fields at East Siberia. There is some specific characteristic of the fields: specific gas compositions, low thermobaric conditions of reservoirs and high salinity of formation water. The current actual question is how to optimize the hydrate inhibitor applications for such conditions? One of the considered solutions is to apply so called mixed inhibitors, which include some components of thermodynamic and kinetic actions.

2. The experimental data on hydrate three-phase equilibria of some hydrate-forming gas was analyzed in detail. It was established that frequently the experiments are not fully reliable near 273 K and especially in the temperature range 260-273 K. We obtained a new thermodynamic correlation between three phase equilibria with ice and with supercooled water at temperatures below 273 K. This correlation may be used for ethane, propane, isobutane, nitrogen and methane hydrates. Also, we proposed a new technique for checking the thermodynamic consistency and smoothing of the experimental data for such hydrate-forming gases. For several gas hydrates the recommended reference data of the equilibria "gas – ice – hydrate" and "gas – liquid water – hydrate" were obtained. These data may be used for further more correct calculations of hydrate decomposition enthalpies to ice and to liquid water as well as hydrate number and the quadruple points positions.

3. The thermodynamic research of gas pressure influence on freezing temperature of pore water in frozen soils as well as the gas influence on the amount of the unfrozen water (the shift of the unfrozen water curve by affecting the gas pressure) was presented. The following factors were taken into account: external gas pressure (the same as hydrostatic pressure), gases solubility in pore water and salinity of the pore water. Some model calculations were performed for the freezing temperature of pore fluids containing gases like methane, carbon dioxide, nitrogen, and their mixtures. The thermodynamic model for increasing pressure in freezing of closed gas-saturated talik (as new geological phenomena) was presented.

4. The analytical relations are derived for non-clathrate water content depending on the gas pressure from the known data on of the pore water activity in the soil samples. Using the obtained relations, the qualitative regularities of the gas pressure influence on the non-clathrate water content at a given temperature (both at positive and negative temperatures) were revealed. The performed calculations for hydrate-containing samples of kaolinite clay showed a sufficiently good agreement between the results obtained by the proposed technique and with the experimental contact method. The technique can be also used for different gases and different soil systems.

5. The following part of the thesis deal with some methodic questions on the application of different hydrate inhibitors. It has been developed more general correlations than early known, which connect water activity with the temperature shift ΔT of hydrate formation in aqueous inhibitor solutions (at fixed fugacity/pressure) as well as the pressure shift of hydrate formation (at fixed temperature).

6. The mixed thermodynamic inhibitors like "methanol + brine" are considered as appropriate reagents for wellbores and gas-gathering systems at the gas-condensate field of Eastern Siberia. The properties of mixed reagent "methanol + magnesium chloride" (as promising hydrate inhibitor) were studied by experimental and calculation methods. The new experimental data for this

mixed inhibitor were obtained for methane hydrate formation. On the base of experimental data, it was established two simple and reliable for practice correlations. The first correlation is based on the formally additive contribution of inhibitor components by using their effective concentrations in the aqueous solutions. And the second correlation is based on the modified Zdanovsky rule. The both correlations may be applied in practice, but the first is better and work up to $\Delta T \cong 30\text{-}35$ K. Such correlations may be also used for another mixed inhibitor ("methanol + $CaCl_2$" and "methanol + formation brine").

7. The properties of mixed "kinetic + thermodynamic" inhibitors on the example of "PVP + NaCl ($MgCl_2$)" solutions were studied. The main attention was paid to experimental research of water activity in "PVP + NaCl ($MgCl_2$)" solutions. It was estimate the influence of PVP and "PVP + NaCl ($MgCl_2$)" solutions on ΔT - the thermodynamic shift of hydrate formation. The "polymer + brine" inhibitors may be interesting for further studies due to its possible double kinetic effect both to nucleation and growth of hydrate particles.

8. The hydrate control at the Chayandiskoe and Yarakta oil and gas condensate fields located in East Siberia were considered. An analysis of the temperature and pressure modes of producing wells was given. It was shown that at the gas and gas condensate fields of Eastern Siberia, there are some new features of the process of hydrate formation in the in-field systems. A technique for calculating the methanol consumption, taking into account the producing formation water by the wells, has been developed. The risks of scaling in the wellbores due to halite precipitation when mixing concentrated methanol with formation water have been analyzed. It was noted that when using aqueous methanol solutions (instead pure methanol) with concentrations at the level of 60-70 wt%, the risks of halite deposition were minimized.

9. The Yarakta field is considered as an example for the technological calculations of the specific methanol consumption and its aqueous solutions were carried out to prevent hydrate

formation, taking into account the risks associated with high salinity of field formation waters. The results obtained make it possible to optimize the technology for hydrate inhibiting by methanol in the wellbores and gas-gathering systems of the gas-condensate fields of Eastern Siberia. Also, the heat-insulated in-field pipeline operation of the Yamburg gas field (Cenomanian horizons) in the winter season was discussed. The cases were revealing when there is no ice or hydrate operation regime inside the gas stream, nevertheless, ice or hydrate deposits are existing at the internal wall of the pipe. This is due to the above-ground laying pipelines and the temperature of inner wall of the pipe is below then the temperature of ice or hydrate formation in winter season.

Recommendations for future research

There are several important and principal research directions for the near future investigations:

1. It is desirable to check the proposed simple thermodynamic correlations for the temperature shift of hydrate equilibrium in mixed inhibitors using experimental data for mixed thermodynamic inhibitors like "methanol + calcium chloride", "methanol + sodium chloride".

2. Applying the proposed thermodynamic models for the gas pressure effect of on the unfrozen and non-clathrate water content in saline soils systems.

3. Development of Stefan like models of freezing sediments in closed gas-saturated taliks, taking into account the effect of pressure increase on phase equilibria and the possibility of the hydrate formation during freezing.

4. Development of more detailed thermodynamic models for the consistency of experimental data on the phase equilibria of gas hydrates, including gas mixtures and aqueous solutions of hydrate inhibitors.

5. Further experimental studying of "salt + water-soluble polymer", especially the hydrate formation kinetics in such mixed inhibitors.

Bibliography

1. Claussen, W.F., 1951, J. Chem. Phys., v. 19, 259-267.
2. Pauling L., Marsch R.F., 1952, Proc. Nat. Acad. Sci., v. 38, 112-115.
3. Muller H., Stackelberg M., 1952, Naturwiss., BD. 39. S. 20-27.
4. McMullan, R.K., Jeffrey, G.A., 1965, Polyhedral clathrate hyrates. IX. Structure of ethylene oxide hydrate, Journal of Chemical Physics 42(8), 2725–2732.
5. Hansen, T.C., Falenty, A., Kuhs, W.F., 2016, Lattice constants and expansivities of gas hydrates from 10 K up to the stability limit. The Journal of Chemical Physics, 144(5), 054301(1-11).
6. Mastepanov A.M., 2014, Gas hydrates: a 250-year journey (from laboratory research to a place in the global energy balance), M.: EC "Energia", 272 p. (in Russian).
7. Gilbert, B., 1965, Gmelins Handbuch Der Anorganischen Chemie, 8. Auflage, System-Nummer 9, Teil B - Lieferung 2, 1960, 757 p., Verlag Chemie, GMBH, Weinheim/Bergstrasse, West Germany. Israel Journal of Chemistry, 3(3), 120–120. https://doi.org/10.1002/ijch.196500032.
8. Davy H., 1811, Phil. Trans. Roy. Soc. 101, 30.
9. Faraday M., 1823, Quart. J. Sci. Lit. Arts 15, 71.
10. Hammerschmidt E. G., 1934, Formation of gas hydrates in natural gas transmission lines, Industrial and Engineering Chemistry, v. 26(8), 851-855.
11. Ginsburg G.D., Soloviev V.A., 1994, Submarine gas hydrates, SPb: VNIIokeangeologiya, 199 p.
12. Vasiliev V.G., Makogon Yu.F., Trebin F.A., Chersky N.V., Trofimuk A.A., 1970, Register of Scientific Discoveries of the USSR, 75.
13. Istomin V.A., Yakushev V.S., Natural gas hydrates, 1992, Nedra, Moscow, 236 pp. (in Russian).
14. Deaton, W.M., and Frost, E.M., Jr., 1946, Gas Hydrates and Their Relation to the Operation of Natural Gas Pipelines, U.S. Bureau of Mines Monograph 8.
15. Sloan, E.D. Koh, C.A., 2008, Clathrate Hydrates of Natural Gases, third edition, v. 119. Boca Raton, Florida: Chemical Industries, CRC Press.
16. Yamamuro, O., Suga, H., 1989, Thermodynamic studies of clathrate hydrates, Journal of thermal analysis, v. 35, 2025–2064.

17. Handa Y.P., 1986, Calorimetric determinations of the compositions, enthalpies of dissociation, and heat capacities in the range 85 to 270 K for clathrate hydrates of xenon and krypton, The Journal of Chemical Thermodynamics, v. 18(9), 891-902.
18. Istomin V.A., Yakushev V.S., Kvon V.G., 2008, The role of VNIIGAZ scientists in modern research of gas hydrates, Prospects for the development of the mineral resource base of the gas industry in Russia: Sat. scientific. tr. M.: OOO "VNIIGAZ", 17-32.
19. Istomin V.A., Yakushev V.S., Kvon V.G., Chuvilin., E.M., Dolgaev S.I., 2009, Directions of modern research of gas hydrates. Gas chemistry, 1(5), 56-63.
20. Istomin V.A., Yakushev V.S., 1998, The main directions and results of research on gas hydrates in VNIIGaz, in the collection: "Science of natural gas. Present and future", M., VNIIGaz, 198-213.
21. Istomin V.A., Kwon V.G., 2004, Prevention and elimination of gas hydrates in gas production systems, M., IRTs Gazprom, 556 p. (in Russian).
22. Carroll J., 2020, Natural Gas Hydrates: A Guide for Engineers, Gulf Professional Publishing, 4th edition edition, p. 392, ISBN-10: 0128217715.
23. Kelland, M.A., 2014, Production Chemicals for the Oil and Gas Industry, 2nd ed.; CRC Press: Boca Raton, FL, https://doi.org/10.1201/b16648.
24. Kelland M.A., 2006, History of the development of low dosage hydrate inhibitors. Energy Fuels, 20, 825–847.
25. Kelland M.A., 2018, A review of kinetic hydrate inhibitors from an environmental perspective. Energy Fuels 32, 12001–12012.
26. Waite W.F., Santamarina J.C., Cortes D.D., Dugan B., Espinoza D.N., Germaine J., Jang J., Jung J.W., Kneafsey T.J., Shin H., Soga K., Winters W.J., Yun T.S., 2009, Physical properties of hydrate-bearing sediments, Reviews of Geophysics, 47(4), RG4003. https://doi.org/10.1029/2008RG000279.
27. Gabitto, J. F., Tsouris, C., 2010, Physical Properties of Gas Hydrates: A Review. Journal of Thermodynamics, 1–12., https://doi.org/10.1155/2010/271291.
28. Stoll R. D., Bryan G. M., 1979, "Physical properties of sediments containing gas hydrates, " Journal of Geophysical Research, v. 84, no. B4, 1629–1634.

29. Ershov E.D., Lebedenko Yu.P., Istomin V.A., Yakushev V.S., Chuvilin E.M., 1989, Problems of hydrate formation in the permafrost zone, in collection: "Geocryological research", Moscow, Publishing house 1.3. Moscow State University, 50-63.
30. Yakushev V.S., Istomin V.A., Gas Hydrates Self-Preservation Effect, in: "Physics and Chemistry of Ice", ed. by N. Maeno and T.Hondoh, Hokkaido Univ Press, Sapporo, Japan, 1992, pp.136-140. (June 2-6, 1996, Toulouse, France), Toulouse, 1996, 399-406.
31. Handa Y.P., 1986, Compositions, enthalpies of dissociation, and heat capacities in the range 85 to 270 K for clathrate hydrates of methane, ethane, and propane, and enthalpy of dissociation of isobutane hydrate, as determined by a heat-flow calorimeter, The Journal of Chemical Thermodynamics, v. 18(10), 915-921.
32. Yakushev V.S., Istomin V.A., 1990, Features of the existence of gas hydrates in rocks at negative temperatures, Geokhimiya, no. 6, 899-903.
33. Istomin V.A., 1998, Overheating of gas hydrates and ice, in the collection: "Prospects for the discovery and development of gas, condensate and oil fields on the shelf of the seas of Russia", Moscow: VNIIGaz, 131-140.
34. Istomin V.A., 1999, On possibility of superheating of natural gas hydrates and other hydrogen-containing crystalline structures, Russian Journal of Physical Chemistry. v. 73(11), 1887-1890.
35. Istomin V.A., 2000, On the possibility of the effect of self-preservation of gas hydrates at temperatures above Celsius, in the collection: "Gasification. Natural gas as a vehicle fuel. Gas preparation, processing and use. Energy saving" No. 10-11, 15-20.
36. Istomin V.A,. 2001, Metastability in the processes of gas hydrates formation and dissociation, VIII International Semonal on inclusion compounds (ISIC-8), Barsaw (Popowo), Poland, Sept 105, Program and Abstracts, T5-02.
37. Yakushev V.S., Istomin V.A., 1987, Causes of gas emissions in frozen rocks of the Yamburgskoye gas condensate field, in collection: "Features of the development of gas wells in difficult geocryological conditions", M., VNIIGaz, 119-127.
38. Yakushev V.S., Istomin V.A., 1989, Features of the existence of hydrates of hydrocarbon gases in reservoir rocks at negative temperatures, in collection: "Geology and gas content of oil and gas producing regions", M., VNIIGaz, 159-169.

39. Ershov E.D., Lebedenko Yu.P., Chuvilin E.M., Istomin V.A., Yakushev V.S., 1991, Features of the existence of gas hydrates in the permafrost zone, Reports of the USSR Academy of Sciences, v. 321(4), 788-791.
40. Istomin, V.A., Yakushev, V.S., 1992, Natural Gas Hydrates; Nedra, Moscow, Russia, p. 236 (In Russian).
41. Yakushev V.S., Istomin V.A., Kolushev N.R., 1994, Near-Surface Natural Gas and Gas Hydrates Accumulations in Permafrost, Russia. Proceedings of the AAPG Hedberg Research Conference "Near-Surface Expressions of Hydrocarbon Migration", April 24-28, 1994, Vancouver, British Columbia, Canada.
42. Chuvilin E.M., Kozlova E.A., Kudashov V.A, Petrakova S.Yu., 2005, Estimation of frozen hydrate containing sediment metastability, Third Russian Conference on Geocryology, Moscow, Russia, v.1, 292-300.
43. Istomin V.A., Yakushev V.S., Kwon V.G., Makhonina N.A., Chuvilin E.M., 2006, Self-preservation phenomenon of gas hydrates, - Gas Industry of Russia, Digest No 4, 16-27.
44. Melnikov V.P., Nesterov A.N., Podenko L.S., Reshetnikov A.M., Shalamov V.V., 2011, Metastable states of gas hydrates at pressures below the ice-hydrate-gas equilibrium pressure, Earth's Cryosphere, v. 15(4), 80-83.
45. Vlasov V.A., Drachuk A.O., Zavodovsky A.G., Madygulov M.Sh., Molokitina N.S., Nesterov A.N., Podenko L.S., Reshetnikov A.G., 2014, Metastable states of gas hydrates at subzero temperatures: stability and mechanisms of decomposition, Abstracts of the conference "Gas hydrates in the ecosystem of the Earth 2014" Novosibirsk: INH SB RAS, p. 23.
46. Sizikov A.A., Stoporev A.S., Manakov A. Yu., 2018, Self-preservation of methane hydrate obtained from oil-water emulsions, Actual problems of oil and gas, 3(22), 1-9.
47. Istomin V.A., Kwon V.G., Durov V.A., 2006, Metastable states of gas hydrates, - Gas Industry of Russia, Digest No 4, 13-16.
48. Istomin V.A., Kwon V.G., 2006, Metastable Equilibria of Gas Hydrate at Subzero Temperatures, International Comference Sedimente-hosted Gas Hydrates: New Insights on Natural and Synthetic Systems, 25-26 January, London, Geological Society, 2 p.
49. Mel'nokov V.P., Nesterov A.N., Reshetnikov A.V., Istomin V.A., Kwon V.G., 2010, Stability and growth of Gas Hydrates below the ice-hydrate-gas-equilibrium line on the P-T- phase diagram, Chem. Eng. Sci, v.65, 906-914.

50. Mel'nokov V.P., Nesterov A.N., Reshetnikov A.V., Istomin V.A., 2011, Metastable state during dissociation of carbon dioxide hydrates below 273 K, Chem. Eng. Sci., v.66, 73-77.
51. Sloan E.D., 1997, Jr. Clathrate Hydrates of Natural Gases. Second Edition, Revised and Expanded. N.Y., Basel, Hong Kong:Marcel Dekker, Inc., 705 p.
52. Falenty A, Hansen T.C, Kuhs W.F., 2014, Formation and properties of ice XVI obtained by emptying a type sII clathrate hydrate, Nature, 516 (7530), 231-233.
53. Dyadin Yu.A., Belosludov V.R., Chekhova G.N., Lavrentiev M.Yu,, 1987, Clathrate Thermodynamics for the Unstable Host Framework, Journal of Inclusion Phenomena 5, 195-202.
54. Belosludov V.R., Lavrentiev M.Yu., Dyadin Yu.A., Syskin S.A., 1990, Dynamic and thermodynamic properties of clathrate hydrates, Journal of inclusion phenomena and molecular recognition in chemistry v. 8, 59–69.
55. Belosludov V.R., Lavrentiev M.Yu., Dyadin Yu.A., 1991, Review Article Theory of Clathrates, Journal of Inclusion Phenomena and Molecular Recognition in Chemistry 10:399 422.
56. Istomin V.A., 1987, A Model for Gas Hydrates Taking into Account the Guest-Guest Interactions: Russ. J. Phys. Chem. 61, 732 -734.
57. Zele S.R., Lee S.Y., Holder G.D., 1999, A Theory of Lattice Distortion in Gas Hydrates J. Phys. Chem. B 103, 46, 10250–10257 https://doi.org/10.1021/jp9917704.
58. Belosludov R.V., Subbotin O.S., Mizuseki H., Kawazoe Y., Belosludov V.R., 2009, Accurate Description of Phase Diagram of Clathrate Hydrates at the Molecular Level, J. Chem. Phys. v. 131, 244510.
59. Krichevsky I.R., Kazarnovsky Ya.S., 1935, On thermodynamics of equilibrium gas - gas solution in liquid, Journal of Physical Chemistry, v. 6(10), 1320-1324.
60. Istomin V., Kulkov A., Kolushev N., Kwon V., 1996, Prevention of gas hydrate formation at field conditions in Russia, Proc. of 2nd Int. Conf. on Natural Gas Hydrates, Toulouse, 1996, 399 – 406.
61. http://www.hydrafact.com/index.php?page=software HydraFLASH, version 3.4.0.0, Heriot-Watt University, Hydrafact ltd.
62. https://gashydrates.nist.gov/HydrateViewer/ Clathrate Hydrate Physical Property.

63. Roberts O. L., Brownscombe E. R., Howe L. S., 1940, Constitution diagrams and composition of methane and ethane hydrates, Oil & Gas J., 39(30), 37-43.
64. Chueh P. L., 1973, Arctic pipeline natural gas water content, [Online]. Available: https://gashydrates.nist.gov/HydrateViewer.
65. Falabella B. J., 1975, A Study of Natural Gas Hydrates, PhD. Chemical Engineering Dissertation, University of Massachusetts.
66. Makogon T. Y., Sloan E. D., 1994, Phase Equilibrium for Methane Hydrate from 190 to 262 K, J. Chem. Eng. Data, 39, 351-353.
67. Hachikubo, A., Miyamoto, A., Hyakutake, K., Abe, K., Shoji, H., 2002, Phase Equilibrium Studies on Gas Hydrates Formed from Various Guest Molecules and Powder Ice, The Fourth International Conference on Gas Hydrates, Yokohama, Japan, 19-23, 357-360.
68. Song K. Y., Kobayashi R., 1989, Final hydrate stability conditions of a methane and propane mixture in the presence of pure water and aqueous solutions of methanol and ethylene glycol, Fluid Phase Equilib, 47, 295.
69. Adisasmito S., Frank R. J., Sloan E. D., 1991, Hydrates of Carbon Dioxide and Methane Mixtures, J. Chem. Eng. Data, 36(1), 68-71.
70. Deng Y., Xu X., Zhang L., 1993, A Primary Study on Composition of Methane Hydrate, Permafrost Sixth International Conference, Beijing, China, July 5-9.
71. Dickens G., Quinby-Hunt M., 1994, Methane hydrate stability in seawater, Geophysical Research Letters, 21(19), 2115-2118.
72. Hutz U., Englezos P., 1996, Measurement of Structure H Hydrate Phase Equilibrium and the Effect of Electrolytes, Fluid Phase Equilib, 117, 178-185.
73. Mei D., Liao J., Yang J. T., Guo T. M., 1996, Experimental and Modeling Studies on the Hydrate Formation of a Methane + Nitrogen Gas Mixture in the Presence of Aqueous Electrolyte Solutions, Ind Eng Chem Res, 35(11): 4342–4347.
74. Nixdorf J., Oellrich L. R., 1997, Experimental determination of hydrate equilibrium conditions for pure gases, binary and ternary mixtures and natural gases, Fluid Phase Equilib., 139, 325-333.
75. Smelik E., King H. E., 1997, Crystal-growth studies of natural gas clathrate hydrates using a pressurized optical cell, American Mineralogist, 82, 88-98.

76. Nakamura T., Makino T., Sugahara T., Ohgaki K., 2003, Stability boundaries of gas hydrates helped by methane - structure-H hydrates of methylcyclohexane and cis-1,2-dimethylcyclohexane, Chem. Eng. Sci. 58, 269-273.
77. Gayeta P., Dicharrya C., Mariona G., Graciaaa A., Lachaisea J., Nesterovb A., 2005, Experimental determination of methane hydrate dissociation curve up to 55MPa by using a small amount of surfactant as hydrate promoter, Chem. Eng. Sci., 60, 5751-5758.
78. Sergeeva D., Istomin V., 2018, Thermodynamics of methane hydrate, Proceedings of the Skoltech Energy PhD Seminar, Moscow, 30-38.
79. Istomin, V.A., Chuvilin, E.M., Makhonina, N.A., Bukhanov, B.A., 2009, Temperature dependence of unfrozen water content in sediments on the water potential measurements. Earth's Cryosphere 13 (2), 35-43 (in Russian).
80. Yasuda K., Ohmura R., 2008, Phase Equilibrium for Clathrate Hydrates Formed with Methane, Ethane, Propane, or Carbon Dioxide at Temperatures below the Freezing Point of Water, Cite this: J. Chem. Eng. Data 53, 9, 2182–2188, https://doi.org/10.1021/je800396v.
81. Nema Yu., Ohmura R., Senaha I., Yasuda K., 2017, Quadruple point determination in carbon dioxide hydrate forming system, Fluid Phase Equilibria, v. 441, 49-53.
82. Nema, Y., Ohmura, R., Senaha, I., Yasuda, K., 2017, Quadruple point determination in carbon dioxide hydrate forming system. Fluid Phase Equilibria, 441, 49–53. doi:10.1016/j.fluid.2016.12.014.
83. Semenov A.P., Mendgaziev R.I., Stoporev A.S., Istomin V.A., Sergeeva D.V., Ogienko A.G., Vinokurov V.A., 2021, The pursuit of a more powerful thermodynamic hydrate inhibitor than methanol. Dimethyl sulfoxide as a case study, Chemical Engineering Journal, v. 423, 130227, https://doi.org/10.1016/j.cej.2021.130227.
84. Ershov E.D., Danilov I.D., Cheverev V.G., 1987, Petrography of frozen rocks. M., Publishing house of Moscow State University, 311s. (in Russian).
85. Ershov E.D., 1999, Osnovy geokryologii, Ed. E. D. Ershova. M., Moscow State University Publishing House. Part 5. Engineering geocryology, 518 p. (in Russian).
86. Ershov E.D., 1995, Osnovy geokryologii, Ed. E. D. Ershova. M., Moscow State University Publishing House. Part 1. Physical and chemical foundations of geocryology, 368 p. (in Russian).

87. Ershov E.D., 1996, Osnovy geokryologii, Ed. E. D. Ershova. M., Moscow State University Publishing House. Part 2. Lithogenetic geocryology. 399 p. (in Russian).
88. Komarov I.A., 2003, Thermodynamics and heat and mass transfer in dispersed frozen rocks. M., Nauch. mir, 608 p. (in Russian).
89. Cheverev V.G., 2004, The nature of cryogenic properties of soils. M.: Scientific world, 234 p. (in Russian).
90. Istomin, V.A., Chuvilin, E.M., Bukhanov, B.A., Uchida, T.A., 2017, Pore water content in equilibrium with ice or gas hydrates in sediments. Cold Region Science and Technology 137, 60-67. https://doi.org/10.1016/j.coldregions.2017.02.005.
91. Istomin, V.A., Chuvilin, E.M., Bukhanov, B.A., 2017, Fast estimation of unfrozen water content in frozen soils. Earth's Cryosphere 21(6), 134–139. https://doi.org/10.21782/KZ1560-7496-2017-6 (134-139) (in Russian).
92. Are, F.E., 1998, Emission of deep gases into atmosphere. Earth's Cryosphere 2 (4), 42–50 (in Russian).
93. Bogoyavlensky, V.I., 2014, Threat of catastrophic gas blasts from permafrost in the Arctic. Craters in the Yamal and Taimyr Peninsulas. Drilling and Oil 9, 13–18 (in Russian).
94. Kizyakov A.I., Sonyushkin A.V., Leibman M.O., Zimin M.V., Khomutov A.V., 2015, Geomorphological conditions for the formation of a gas outburst funnel and the dynamics of this form in Central Yamal // Earth's Cryosphere, v. XIX, no. 15-25 (in Russian).
95. Olenchenko, V.V., Sinitsky, A.I., Antonov, E.Yu., Eltsov, I.N., Kushnarenko, O.N., Plotnikov, A.E., Potapov, V.V., Epov, M.I., 2015, Results of geophysical researches of the area of new geological formation "Yamal crater". Earth's Cryosphere 19 (4), 94–106 (in Russian).
96. Buldovicz S.N., Khilimonyuk V.Z., Bychkov A.Y., Ospennikov E.N., Vorobyev S.A., Gunar A.Y., Gorshkov E.I., Chuvilin E.M., Cherbunina M.Y., Kotov P.I., Lubnina N.V., Motenko R.G., Amanzhurov R.M., 2018, Cryovolcanism on the Earth: Origin of a Giant Crater in the Yamal Peninsula (Russia). Scientific reports,
97. Lipenkov, V.Ya., Istomin, V.A., 2001, On the stability of air clathrate–hydrate crystals in subglacial lake Vostok, Antarctica. Glaciological research materials 91, 138–149 (in Russian).
98. Lipenkov, V.Ya., Istomin, V.A., Preobrazhenskaya, A.V., 2003, Gas regime in sub-ice Lake Vostok: A case study. Arctic and Antarctic problems 74, 66-87 (in Russian).

99. Chuvilin E.M., Ebinuma T., Kamata Y. et al., 2003, Eff ects of temperature cycling on the phase transition of water in gas–saturated sediments, Can. J. Phys., v. 81, 1–8.
100. Chuvilin E.M., Kozlova E.V., Makhonina N.A., Yakushev V.S., 2003, Experimental investigation of gas hydrate and ice formation in methane-saturated sediments, Proc. of 8th Intern. Conf. on Permafrost (July 21–25, 2003). Zurich, Switzerland, 145–150.
101. Mel'nikova V. P., Nesterova A. N., Podenko L. S., Reshetnikova A. M., 2014, Influence of Carbon Dioxide on Melting of Underground Ice. Doklady Earth Sciences, v. 459, Part 1, 1353–1355.
102. Bridgman, P.W., 1912, Thermodynamic properties of liquid water to 80° and 12.000 kgm. Proc. Am. Acad. Arts Sci. 48, 309-62.
103. Namiot, A.Yu., 1991, Gas Solubility in Water. Moscow Nedra, (in Russian).
104. Bogorodsky, V.V., Gavrilo, V.P., 1980, Ice. Physical Properties. Modern Methods of Glaciology. Gidrometeoizdat, Leningrad (in Russian).
105. Petrenko, V.F., Whitworth, R.W., 2002, Physics of Ice. Oxford University Press, Oxford
106. Mackay, J., 1998, Pingo growth and collapse, Tuktoyaktuk PeninsulaArea, Western Arctic Coast, Canada: A long-term field study,Geogr. Phys. Quat., 3, 271–323.
107. Kuzin, I.L., 1999, Extent of natural gas emission in West Siberia. Reports of RGO 131 (5), 90–96 (in Russian).
108. Bondarev, V.L., Mirotvorsky, M.Yu., Zvereva, V.B. Oblekov, G.I., Shaidullin, R.M., Gudzenko, V.T., 2008, Supra-Cenomanian deposits in the Yamal Peninsula: Gas geochemistry. Geology, Geophysics and Production of Oil and Gas Fields 5, 22–34 (in Russian).
109. Sigunov, Yu.A., Samylova, Yu.A., 2006, Dynamics of pressure increase in a freezing closed volume of water with dissolved gas. Applied math and technical physics 47 (6), 85-92 (in Russian).
110. Makogon, Y.F., 1974, Hydrates of Natural Gases; Nedra: Moscow, Russia, 208p. (In Russian).
111. Handa, Y.P., Stupin, D.Y., 1992, Thermodynamic properties and dissociation characteristics of methane and propane hydrates in 70-. ANG.-radius silica gel pores. J. Phys. Chem. 96, 8599-8603, https://doi.org/10.1021/j100200a071.
112. Uchida, T., Ebinuma, T., Ishizaki, T., 1999, Dissociation condition measurements of methane hydrate in confined small pores of porous glass, J. Phys. Chem. B 103, 3659-3662.

113. Seo, Y., Lee, H., Uchida, T., 2002, Methane and carbon dioxide hydrate phase behavior in small porous silica gels: Three-phase equilibrium determination and thermodynamic modeling. Langmuir 18, 9164-9170, https://doi.org/10.1021/la0257844.
114. Anderson, R., Llamedo, M., Tohidi, B., Burgass, R.W., 2003, Experimental measurement of methane and carbon dioxide clathrate hydrate equilibria in mesoporous silica. J. Phys. Chem. B. 107, 3507-3514.
115. Uchida, T., Ebinuma, T., Takeya, S., Nagao, J., Narita, H., 2002, Effects of pore sizes on dissociation temperatures and pressures of methane, carbon dioxide and propane hydrate in porous media. J. Phys. Chem. B 106, 820-826, https://doi.org/10.1021/jp012823w.
116. Uchida, T., Takeya, S., Chuvilin, E.M., Ohmura, R., Nagao, J., Yakushev, V.S., Istomin, V.A., Minagawa, H., Ebinuma, T., Narita, H., 2004, Decomposition of methane hydrates in sand, sandstone, clays and glass beads. J. Geophys. Res. 109, B05206, https://doi.org/10.1029/2003JB002771.
117. Kang, S.P., Lee, J.W., Ryu, H.J., 2008, Phase behavior of methane and carbon dioxide hydrates in meso- and macro-sized porous media. Fluid Phase Equilibria, 274, 68-72, https://doi.org/10.1016/j.fluid.2008.09.003.
118. Smith, D.H., Seshadri, K., Uchida, T., Wilder, J.W., 2004, Thermodynamics of methane, propane, and carbon dioxide hydrates in porous glass. AICHE J. 7, 1589-1598, https://doi.org/10.1002/aic.10141.
119. Chong, Zh. R., Yang, M., Khoo, B. Ch., Linga, P., 2016, Size effect of porous media on methane hydrate formation and dissociation in an excess gas environment. Ind. Eng. Chem. Res. 55, 7981-7991, https://doi.org/10.1021/acs.iecr.5b03908.
120. Zarifi, M., Javanmardi, J., Hashemi, H., Eslamimanesh, A., Mohammadi, A.H., 2016, Experimental study and thermodynamic modelling of methane and mixed C1 + C2 + C3 clathrate hydrates in the presence of mesoporous silica gel. Fluid Phase Equilibria 423, 17-24, https://doi.org/10.1016/j.fluid.2016.03.018.
121. Park, T., Lee, J.Y., Kwon, T.H., 2018, Effect of pore size distribution on dissociation temperature depression and phase boundary shift of gas hydrate in various fine-grained sediments. Energy Fuels 32, 5321-5330, https://doi.org/10.1021/acs.energyfuels.8b00074.

122. Em, Y., Stoporev, A., Semenov, A., Glotov, A., Smirnova, E., Villevald, G., Lvov, Y., 2020, Methane hydrate formation in halloysite clay nanotubes. ACS Sustain. Chem. Eng. 8, 7860-7868, https://doi.org/10.1021/acssuschemeng.0c00758.
123. Zaripova, Y., Yarkovoi, V., Varfolomeev, M., Kadyrov, R., Stoporev, A., 2021, Influence of water saturation, grain size of quartz sand and hydrate-former on the gas hydrate formation. Energies 14, 1272, https://doi.org/10.3390/en14051272.
124. Clarke, M.A., Pooladi-Darvish, M., Bishnoi, P.R., 1999, A method to predict equilibrium conditions of gas hydrate formation in porous media. Ind. Eng. Chem. Res. 38, 2485-2490, https://doi.org/10.1021/ie980625u.
125. Klauda, J.B., Sandler, S.I., 2001, Modeling gas hydrate phase equilibria in laboratory and natural porous media. Ind. Eng. Chem. Res. 40, 4197-4208, https://doi.org/10.1021/ie000961m.
126. Wilder, J.W., Seshadri, K., Smith, D.H., 2001, Modeling hydrate formation in media with broad pore size distributions. Langmuir 17, 6729-6735.
127. Mel'nikov, V.P., Nesterov, A.N., 2001, Gas hydrate formation from porous mineralized water. Earth's Cryosphere 1, 61-67 (In Russian).
128. Smith, D.H., Wilder, J.W., Seshadri, K., 2002, Methane hydrate equilibria in silica gels with broad pore-size distributions. AICHE J. 2, 393-400.
129. Li, X.S., Zhang, Y., Li, G., Chen, Z.Y., Yan, K.F., Li, Q.P., 2008, Gas hydrate equilibrium dissociation conditions in porous media using two thermodynamic approaches. J. Chem. Thermodyn. 40, 1464-1474, https://doi.org/10.1016/j.jct.2008.04.009.
130. Chen, L.T., Sun, C.Y., Chen, G.J., Nie, Y.Q., 2010, Thermodynamics model of predicting gas hydrate in porous media based on reaction? adsorption two-step formation mechanism. Ind. Eng. Chem. Res. 49, 3936-3943, https://doi.org/10.1021/ie901878p.
131. Lee, S., Seo, Y., 2010, Experimental measurement and thermodynamic modeling of the mixed CH4+C3H8 clathrate hydrate equilibria in silica gel pores: Effects of pore size and salinity. Langmuir 26, 9742-9748, https://doi.org/10.1021/la100466s.
132. Liu, H., Zhan, S., Guo, P., Fan, S., Zhang, S., 2018, Understanding the characteristic of methane hydrate equilibrium in materials and its potential application. Chem. Eng. J. 349, 775-781, https://doi.org/10.1016/j.cej.2018.05.150.

133. Zhou, J., Liang, W., Wei, C., 2019, Phase equilibrium condition for pore hydrate: Theoretical formulation and experimental validation. J. Geophys. Res. Solid Earth 124, https://doi.org/10.1029/2019JB018518.
134. Liang, W., Zhou, J., Wei, C., 2021, Uniqueness of the equilibrium relationship among temperature, pressure and liquid water content in hydrate-bearing soils. J. Nat. Gas Sci. Eng. 88, 103820, https://doi.org/10.1016/j.jngse.2021.103820.
135. Azimi, A., Javanmardi, J., Mohammadi, A.H., 2021, Development of thermodynamic frameworks for modeling of clathrate hydrates stability conditions in porous media. J. Mol. Liq. 329, 115463, https://doi.org/10.1016/j.molliq.2021.115463.
136. Zhang, Y., Taboada-Serrano, P., 2020, Model for gas-hydrate equilibrium in porous media that incorporates pore-wall properties. Phys. Chem. Chem. Phys. 22, 10900-10910, https://doi.org/10.1039/D0CP01263G.
137. Chuvilin, E.V., Istomin, V.A., Safonov, S.S., 2011, Residual nonclathrated water in sediments in equilibrium with gas hydrate, Comparison with unfrozen water. Colds Reg. Sci. Technol. 68, 68-73, https://doi.org/10.1016/j.coldregions.2011.05.006.
138. Chuvilin, E., Istomin, V., 2012, Temperature dependence of the equilibrium pore water content in gas hydrate contained sediments. Proc. Tenth Int. Conf. Permafr. 2, 57-60.
139. Yakushev, V.S., 2019, Experimental modeling of methane hydrate formation and decomposition in wet heavy clays in Arctic regions. Geosciences 9, https://doi.org/10.3390/geosciences9010013.
140. Sell, K., Quintal, B., Kersten, M., Saenger, E.H., 2018, Squirt flow due to interfacial water films in hydrate bearing sediments. Solid Earth 9, 699-711, https://doi.org/10.5194/se-9-699-2018.
141. Istomin, V.A., Chuvilin, E.M., Bukhanov, B.A., 2017, Fast estimation of unfrozen water content in frozen soils. Earth's Cryosphere 21, 116-120, https://doi.org/10.21782/EC1560-7496-2017-6(116-120).
142. Sloan, D.E., 1990, Clathrate Hydrates of Natural Gases; Marcel Dekker: New York, NY, USA, 641 p.
143. Broseta, D., Ruffine, L., Desmedt, A., 2017, Gas Hydrates 1: Fundamentals, Characterization and Modeling; Wiley-ISTE, London, UK, 302 p.

144. Luo, T., Li, Y., Sun, X., Shen, S., Wu, P., 2018, Effect of sediment particle size on the mechanical properties of CH4 hydrate-bearing sediments. J. Pet. Sci. Eng. 171, 302-314, https://doi.org/10.1016/j.petrol.2018.07.054.
145. Mel'nikov, V.P., Nesterov, A.N., Reshetnikov, A.V., Istomin, V.A., Kwon, V.G., 2010, Stability and growth of gas hydrates below the ice-hydrate-gas-equilibrium line on the P-T-phase diagram. Chem. Eng. Sci. 65, 906-914, https://doi.org/10.1016/j.ces.2009.09.041.
146. Istomin, V., Kwon, V., Kolushev, N., Kulkov, A., 1996, Prevention of gas hydrate formation at field conditions in Russia. In Proceedings of the 2-nd International Conference on Natural Gas Hydrates, Toulouse, France, 2-6 June, 399-406.
147. Istomin, V.A., Chuvilin, E.M., Makhonina, N.A., Bukhanov, B.A., 2009, Temperature dependence of unfrozen water content in sediments on the water potential measurements. Cryosphere Earth 13, 35-43 (In Russian).
148. Chuvilin, E.M., Gureeva, O.M., Istomin, V.A., Safonov, S.S., 2008, Experimental method for determination of the residual equilibrium water content in hydrate-saturated natural sediments. In Proceedings of the 6th International Conference on Gas Hydrates (ICGH 2008), Vancouver, BC, Canada, 6-10 July, p. 5490.
149. Chuvilin, E.M., Istomin, V.A., Safonov, S.S., 2010, Method for Determination of Pore Water Content in Equilibrium with Gas Hydrate in Dispersed Media. U.S. Patent 2010/0139378 A1, 10 June 2010.
150. Istomin V.A., Dolgaev S.I., Dzhedzherova A.A., Kvon V.G., Nefedov P.A., 2014, Kinetics of Methane Hydrate Formation in Highly Mineralized Water Solution, Proceedings of the 8th International Conference on Gas Hydrates (ICGH8-2014), Beijing, China, 28 July - 1 August, 7 p.
151. Pieron A.P., 1955, Gas hydrates - approximate relations between heat of formation, composition and equilibrium temperature lowering by inhibitors "Recueil. Trav." - Chem. Phys.-Bas, v.74, 6-9, 995-1002
152. «WP4C Dew Point Potentiameter - Operator's Manual», 2010
153. Chirife, J., Resnik, S. L., 1984, Unsaturated Solutions of Sodium Chloride as Reference Sources of Water Activity at Various Temperatures, Journal of food Science, v.49, 1486-1488.
154. Mikulin G.I.(ed.), 1968, Questions of physical chemistry of electrolyte solutions, Chemistry publishing house, 420 p.

155. Handa Y. P., Tse J. S., 1986, Thermodynamic properties of empty lattices of structure I and structure II clathrate hydrates J. Phys. Chem. 90, 22, 5917–5921 https://doi.org/10.1021/j100280a092.
156. STO Gazprom 3.1-3-010-2008. 2009, Methodology for calculating the chemicals consumption for gas producing enterprises of JSC "GAZPROM", Moscow, 45 p.
157. Efimov V.V., Khaliulin D.V.., 2014, Designing of Early Detection and Prevention Measures for Large Volume of Fluids in a Form of High-Porous Icy Sediments in Gas Gathering Field Network at the Late Stage of Northern Fields Operation. "Plug-type injection" of Methanol into Gas/Fluid Flow. Gathering, preparation and transportation of hydrocarbons. 5:19-28.
158. Istomin V.A., Kvon V.G., Troynikova A.A., Nefedov P.A., 2016, Some features of ice and gas hydrates prevention in gas-gathering systems at the development latest stage of Cenomanian fields in western Siberia. Transport and storage of oil products and hydrocarbons. v.2, .25–30.
159. Mikheev M.A., 1966, Calculation formulas for convective heat transfer, Izv. Academy of Sciences of the USSR. Energy and transport, No. 5, p. 96-105.
160. Setzmann, U., Wagner, W., A New Equation of State and Tables of Thermodynamic Properties for Methane Covering the Range from the Melting Line to 625 K at Pressures up to 1000 MPa.In: NIST Chemistry WebBook, NIST Standard Reference Database Number 69. National Institute of Standards and Technology, Gaitherburg, MD 20899, http://webbook.nist.gov/chemistry/fluid/.
161. Semenov A.P., Medvedev V.I., Gushchin P.A., Kotelev M.S., Yakushev V.S., Stoporev A.S., Sizikov A.A., Ogienko A.G., Vinokurov V.A., 2017, Phase equilibrium for clathrate hydrate formed in methane+water+ethylene carbonate system, Fluid Phase Equilib. 432, doi:10.1016/j.fluid.2016.10.015.
162. GmbH P., «DMA™ 4200 M density meter» [In the Internet]. Available: https://www.anton-paar.com/in-en/products/details/dmatm-4200-m/, [date of the application: 18 May 2020].
163. Hai-Lang Z., Shi-Jun H., 1996, «Viscosity and Density of Water + Sodium Chloride + Potassium Chloride Solutions at 298.15 K» Journal of chemical and engineering data, v. 41(3), p. 516 – 520.
164. Fundamentals of Heat and Mass Transfer, 7th Edition, 2011, T.L. Bergman, A.S. Lavine, F.P. Incropera. J. Wiley & Sons, Incorporated, ISBN: 9781118137253, p. 544(1076).

Appendix 1. Continuous temperature function is designed to verify and reconcile experimental data on the three-phase equilibrium of gas hydrates

Let's analyze the relationships of the gas hydrates thermodynamic model on relation of two three phase equilibria: "gas – water – hydrate" and "gas – ice – hydrate".

The difference between the chemical potentials of water in hydrate phase and in the ice is written as follows (a discussion of the notice of chemical potentials is presented in more detail in the chapters 4 and 5)

$$\Delta\mu_{hi}^{0}(T) = \nu_1 RT\ln(1 + C_1 f) + \nu_2 RT\ln(1 + C_2 f) + \Delta V_{hi}(P - P_0) \qquad \text{(A1.1)}$$

and the difference between the chemical potentials of water in liquid water rich phase and water in hydrate phase

$$\Delta\mu_{wh}^{0}(T) = \Delta\mu_{wi}^{0}(T) - \Delta\mu_{hi}^{0}(T) = -\nu_1 RT\ln(1 + C_1 f) - \nu_2 RT\ln(1 + C_2 f) - \Delta V_{wh}(P - P_0) - RTln(1 - x)$$

$$\Delta\mu_{hi}^{0}(T) = \Delta\mu_{wi}^{0}(T) + \nu_1 RT\ln(1 + C_1 f) + \nu_2 RT\ln(1 + C_2 f) + \Delta V_{wh}(P - P_0) + RT\ln(1 - x) \qquad \text{(A1.2)}$$

where $\Delta\mu_{wi}^{0}(T) = 6008 \cdot \left(1 - \frac{T}{T_0}\right) - 36.93 \cdot \left(T \cdot \ln\frac{T}{T_0} + (T_0 - T)\right)$.

Further let's consider the typical cases of the filling degree of the cavities in hydrate structures.

When the filling degrees of large and small cavities are close to unity ($C_1 f \gg 1$, $C_2 f \gg 1$) from (A1.1) and (A1.2) can be obtained

$$\begin{aligned}\Delta\mu_{hi}^{0}(T) &= \nu_1 RT\ln(C_1 f) + \nu_2 RT\ln(C_2 f) + \Delta V_{hi}(P - P_0) \\ &= \nu_1 RT\ln C_1 + \nu_1 RTlnf + \nu_2 RTlnC_2 + \nu_2 RT\ln f + \Delta V_{hi}(P - P_0) \\ &= RT(\nu_1 \ln C_1 + \nu_2 lnC_2) + (\nu_1 + \nu_2)\, RT\ln f + \Delta V_{hi}(P - P_0)\end{aligned}$$

and

$$\Delta\mu_{hi}^{0}(T) = \Delta\mu_{wi}^{0}(T) + \nu_1 RTln(1 + C_1 f) + \nu_2 RT\ln(1 + C_2 f) + \Delta V_{wh}(P - P_0) + RTln(1 - x)$$

$$= \Delta\mu_{wi}^{0}(T) + RT(\nu_1 lnC_1 + \nu_2 \ln C_2) + (\nu_1 + \nu_2)RT\ln f + \Delta V_{wh}(P - P_0)$$

$$+ RT\ln(1 - x)$$

Let's introduce a new coordinate

$$m = \frac{\Delta\mu_{hi}^{0}(T)}{(\nu_1+\nu_2)RT} - \frac{(\nu_1 \ln C_1+\nu_2 \ln C_2)}{(\nu_1+\nu_2)},$$

then

$$m = \ln f + \frac{1}{(\nu_1+\nu_2)RT}\Delta V_{hi}(P - P_0), T < 273.15\ K, \quad \text{(A1.1a)}$$

$$m = \ln f + \frac{1}{(\nu_1+\nu_2)RT}(\Delta\mu_{wi}^{0}(T) + \Delta V_{wh}(P - P_0) + RT\ln(1 - x)), T \geq 273.15\ K \quad \text{(A1.2a)}$$

In the particular case when small cavities remain unfilled, but in large cavities the degree of filling is close to unity ($C_2 f \gg 1$)

$$m = \frac{\Delta\mu_{hi}^{0}(T)}{\nu_2 RT} - \ln C_2$$

from (A1.1) and (A1.2) we can be obtained

$$m = \ln f + \frac{1}{\nu_2 RT}\Delta V_{hi}(P - P_0), T < 273.15\ K, \quad \text{(A1.1b)}$$

$$m = \ln f + \frac{1}{\nu_2 RT}(\Delta\mu_{wi}^{0}(T) + \Delta V_{wh}(P - P_0) + RT\ln(1 - x)), T \geq 273.15\ K \quad \text{(A1.2b)}$$

Appendix 2. Experimental data on the hydrate formation in mixed inhibitor "methanol + $MgCl_2$"

Methanol and $MgCl_2$ were used as received. Refractive index of methanol was 1.328595±0.000006 at 293.15 K measured with an Abbemat 650 (Anton Paar, Austria) at a wavelength corresponding to the D-line of sodium. Aqueous solutions of inhibitors were prepared by means of laboratory balance Pioneer PA 413C (Ohaus, USA) (resolution 0.001 g). Detailed description of setup for phase equilibrium measurements was presented in our work [161]. The heart of the apparatus is a vessel (600 cm^3) made of Hastelloy C276. The vessel is designed for a maximum operating pressure of 35 MPa. The operating temperature range in the autoclave is from 243 K to 333 K. The vessel temperature is controlled by a surrounding jacket filled with MEG – water mixture and by liquid circulating thermostat Ministat 240 (Huber, Germany). Platinum resistance thermometer (Pt 100) and pressure sensor with measurement errors of 0.1 K and 0.2 bar are used to measure the internal temperature and pressure in the vessel. Stirring of the medium in the high pressure cell is performed by a four-blade stirrer connected to an electric motor RZR 2102 (Heidolph, Germany) through a magnetic coupling Premex (Switzerland).

The experimental results on the hydrate formation in mixed inhibitor "methanol – $MgCl_2$" presented in Table A.1.

Table A.1 Gas hydrate formation data in mixed inhibitor "methanol – $MgCl_2$"

Experiment' number	Mass fraction in solution, % wt.		Hydrate CH_4 decomposition		Thermodynamic shift ΔT from hydrate equilibrium with pure water, °C
	CH_3OH	$MgCl_2$	T, °C	P, bar	
1	5	-	-0.32	30.99	2.09
			4.95	52.67	1.95
			7.89	71.88	2
			10.61	97.88	2.09
			12.86	127.66	2.14
2	10.01	-	-2.89	30.13	4.4
			2.25	50.48	4.23
			3.86	59.86	4.28
			5.21	69.03	4.3
			5.9	74.53	4.33
			6.75	81.86	4.35
			8.35	98.16	4.38
			10.53	127.88	4.49
3	20	-	-8.42	29.91	9.86
			-3.32	49.76	9.66
			-1.52	59.88	9.67
			-0.2	69.09	9.72
			0.49	74.34	9.72
			1.3	81.54	9.76
			3.4	103.73	9.81
			5.04	127.06	9.92
4	30.01	-	-15.27	29.52	16.59
			-10.03	49.03	16.23
			-8.15	59.38	16.22

			-6.57	70.09	16.22
			-5.97	74.95	16.25
			-5.21	81.41	16.26
			-3.62	97.77	16.31
			-1.46	127.53	16.45
5	39.99	-	-22.02	30.86	23.75
			-17.46	47.6	23.37
			-15.44	58.42	23.35
			-13.82	69.08	23.34
			-13.14	74.89	23.42
			-12.17	83.46	23.45
			-10.83	97.29	23.48
			-8.67	127.6	23.67
6	44.68	-	-20.4	50.93	26.97
			-17	72.86	27.02
			-14.26	99.76	27.13
			-12.2	129.39	27.32
7	49.99	-	-30.13	29.78	31.53
			-24.73	50.29	31.18
			-23.14	59.36	31.2
			-23.16	59.28	31.21
			-21.74	68.99	31.24
			-20.89	75.17	31.2
			-20.9	75.28	31.22
			-20.44	79.94	31.32
			-18.65	97.61	31.33
			-16.66	127.61	31.66
8	-	5	-0.43	30.7	2.11
			4.7	51.55	1.99
			7.97	72.89	2.05

			10.58	98.09	2.14
			12.84	127.95	2.18
9	-	8.21	-2.07	31.5	3.99
			2.8	51.51	3.88
			6.05	73.26	4.02
			8.57	97.73	4.12
			10.66	125.75	4.21
10	-	16.39	-10.61	31.73	12.6
			-5.93	51.64	12.64
			-2.77	73.26	12.84
			-0.37	98.19	13.1
			1.65	126.8	13.29
11	-	21.85	-21.17	31.42	23.07
			-16.58	51.48	23.26
			-13.6	72.6	23.59
			-11.29	97.17	23.93
			-9.58	124.43	24.36
12	-	26	-26.65	69.99	36.29
			-24.62	92.52	36.83
			-24.06	102.71	37.19
			-22.57	129.32	37.68
13	-	32.78	-	-	-
			-	-	-
			-	-	-
	5	5	-2.69	31.27	4.54
			2.15	51.28	4.49
			5.52	73.31	4.56
			8.07	98.16	4.66
			10.26	128.01	4.77
14	10.01	5.01	-5.59	30.87	7.32

			-4.57	34.22	7.27
			-0.9	49.72	7.23
			1.25	62.58	7.32
			4.73	92.16	7.44
			7.5	128.95	7.59
15	19.99	5	-11.69	32.05	13.77
			-10.87	34.9	13.76
			-7.18	50.59	13.68
			-4.93	63.13	13.59
			-1.46	92.5	13.66
			0.89	127.64	14.11
16	30	5	-19.56	31.71	21.54
			-19.62	31.58	21.56
			-14.67	51.81	21.41
			-11.39	73.4	21.48
			-8.83	99.05	21.64
			-6.88	126.9	21.83
17	40	4.68	-26.4	35.64	29.49
			-22.74	51.35	29.39
			-19.54	73.08	29.59
			-17.1	98.1	29.82
			-15.11	127.7	30.12
	5	9.39	-5.9	31.36	7.78
			-1.1	51.15	7.71
			2.31	74.03	7.86
			4.59	96.89	8.02
			6.87	128.59	8.19
18	10	9.39	-8.68	32.5	10.89
			-4.23	51.55	10.92
			-0.85	74.32	11.05

			1.45	97.63	11.23
			3.67	128.84	11.41
19	20	9.39	-16.51	32	18.58
			-11.89	51.63	18.59
			-8.63	74.29	18.83
			-6.28	98.25	19.02
			-4.16	129.37	19.28
20	30	9.38	-25.62	31.6	27.57
			-21.04	50.28	27.48
			-17.66	73.53	27.77
			-15.34	97.45	28.01
			-13.25	128.93	28.34
21	5	16.4	-14.09	33.16	16.49
			-14.09	33.12	16.48
			-9.99	51.3	16.63
			-6.73	73.86	16.88
			-4.33	98.06	17.05
			-2.39	128.26	17.43
22	10	16.4	-18.99	31.3	20.85
			-14.34	50.99	20.92
			-11.27	72.59	21.25
			-11.27	72.62	21.26
			-9.03	95.72	21.54
			-6.84	129.15	21.94
23	20	16.39	-28.77	31.65	30.74
			-24.59	49.5	30.88
			-21.68	69.57	31.26
			-19.25	94.34	31.63
			-17.07	129.23	32.18

24	5	21.07	-24.07	32.64	26.33
			-24.07	32.52	26.29
			-19.66	52.49	26.53
			-16.64	74.05	26.81
			-14.55	97.67	27.24
			-12.68	128.32	27.73
25	10	21.07	-28.7	34.94	31.6
			-25.3	51.25	31.93
			-22.64	70.7	32.38
			-20.29	95.53	32.78
			-18.28	127.74	33.29

Appendix 3. Properties of mixed inhibitor "PVP + NaCl" and "PVP + $MgCl_2$"

We are experimentally studies some properties of aqueous PVP, PVP + NaCl and PVP + $MgCl_2$ solutions (Table A.2): density**,** viscosity. All experiments are provided in Skoltech laboratory.

Table A.2 Individual solutions

Individual solution	Supplier
NaCl	LLC 'Component-Reaktiv', Moscow, Russia
PVP (polyvinylpyrrolidone)	Acros Organics B.V.B.A., Geel, Belgium
$MgCl_2$	$MgCl_2$·6H2O, "ChDA", GOST 4209-77, manufacturer Russia, CHIMMED

Firstly, we presented the experimental results on "PVP + NaCl" solutions. The PVP concentration is varied in the range of 0-50 % wt, while the concentration of NaCl in the range of 0-15 %wt.

Density was measured on the Anton Paar DMA 4200 M. Using the Anton Paar DMA 4200 M the density was measured at 1 bar and 25 ºC. The accuracy of density is 0.0001 g/cm3. Anton Paar company introduced this technology in 2017 [162].

From Figure A.1 it can be seen that density of polymer solution changes little with concentration comparing to electrolyte solution.

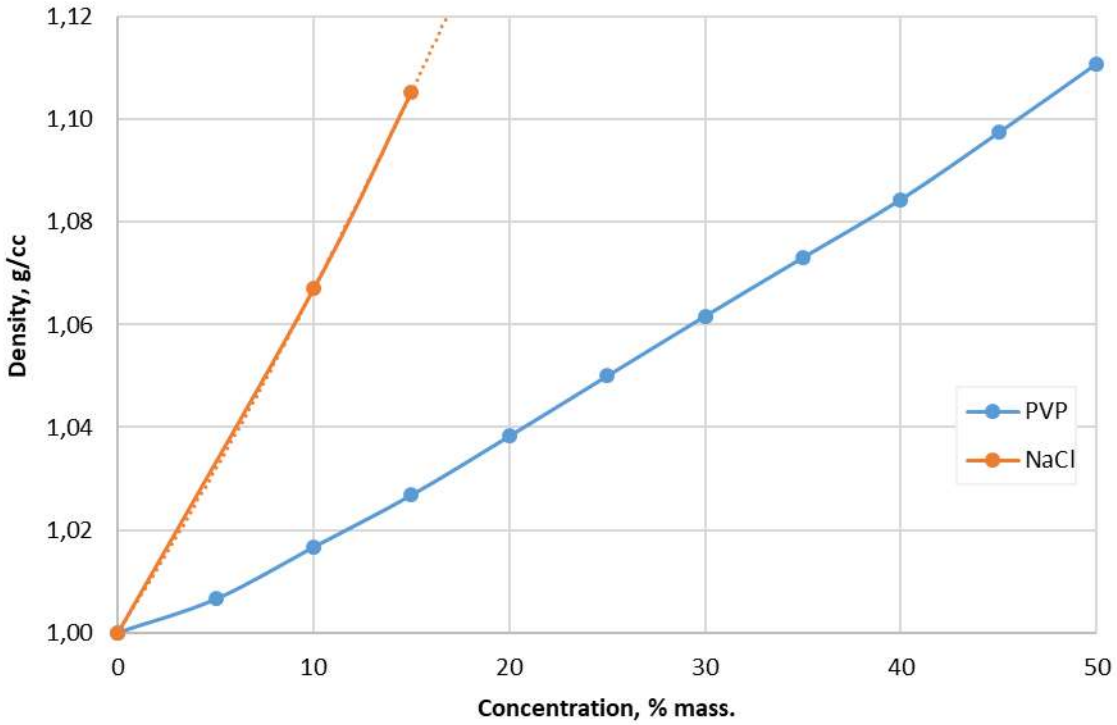

Figure A.1 Density versus PVP and NaCl concentration

On Figure A.2 experimental results of density values are visualized and compared with data from [163]. It can be noted that deviation between these results is slight.

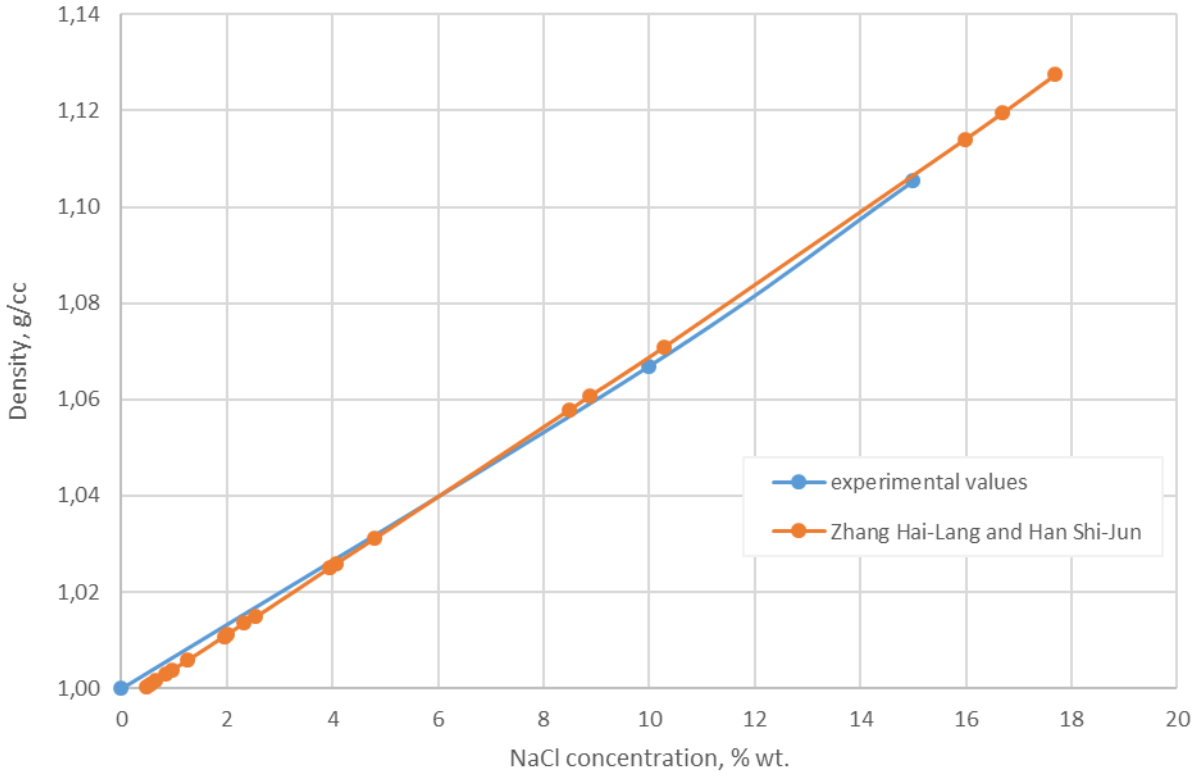

Figure A.2 Literature and experimental data for density of NaCl solutions

The Figure A.3 shows that with an increase in the concentration of polyvinylpyrrolidone in the PVP + NaCl solution, the effect of the electrolyte (10% and 15% NaCl solutions) on the density value weakens.

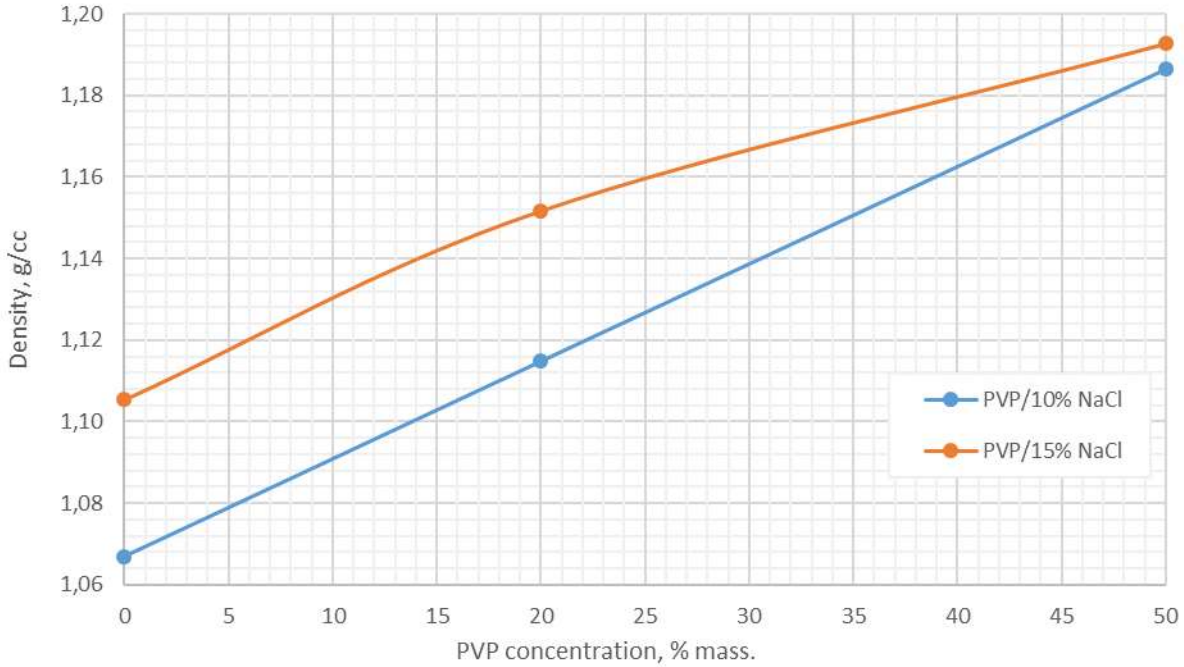

Figure A.3 Density of PVP + NaCl aqueous solutions depending on PVP concentration

Viscosity is another important property of inhibitor solutions. There are dynamic viscosity [Pa·s, 1 Pa·s = 10 poise] and kinematic viscosity [m²/s]. Using an Anton Paar MCR 302 rheometer (instrument error is 0.01 mPa·s) was measured the dynamic viscosity of the PVP, NaCl and PVP + NaCl solutions (Figure A.4).

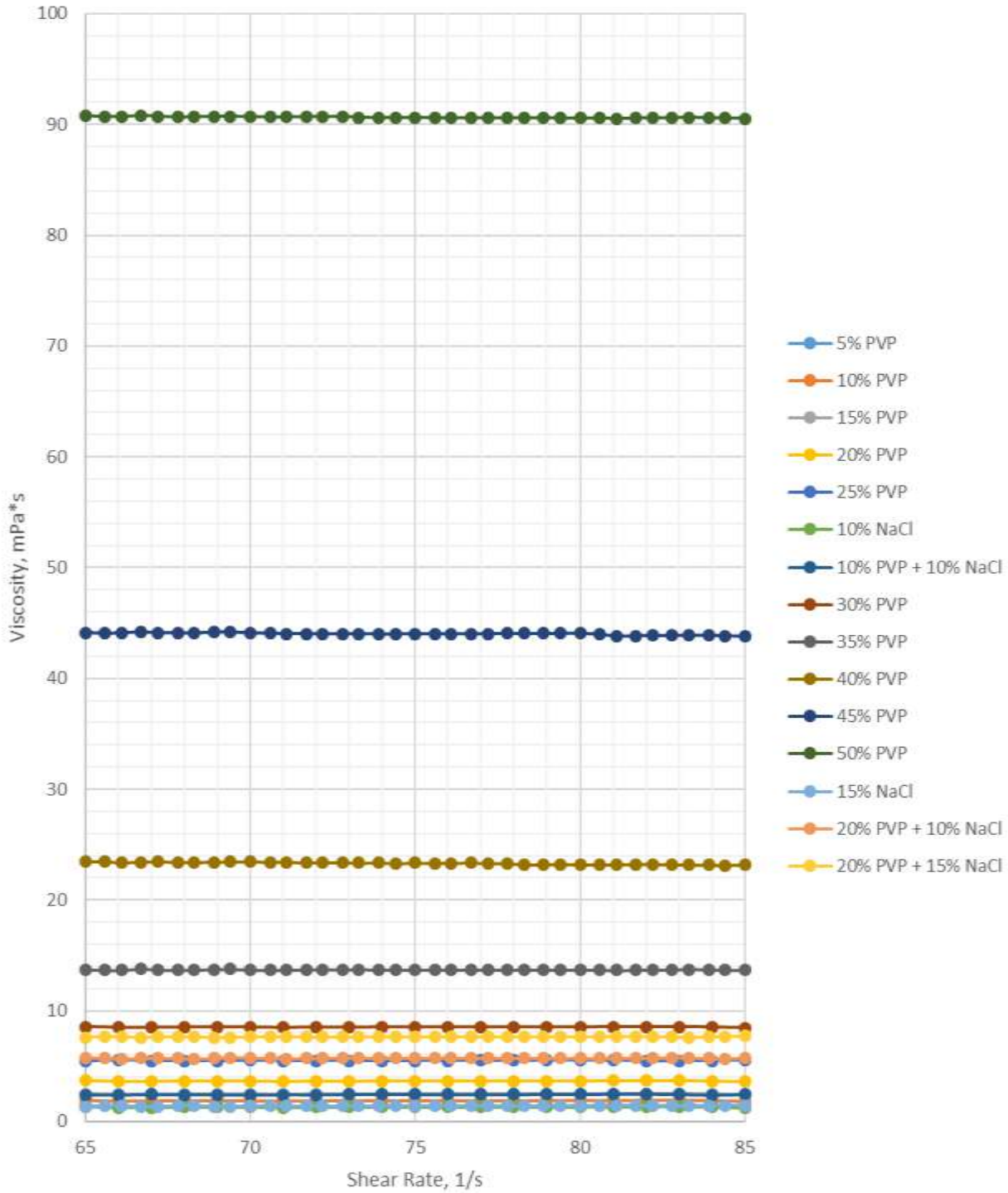

Figure A.4 Viscosity of PVP, PVP + NaCl and NaCl aqueous solutions (Anton Paar MCR 302 rheometer)

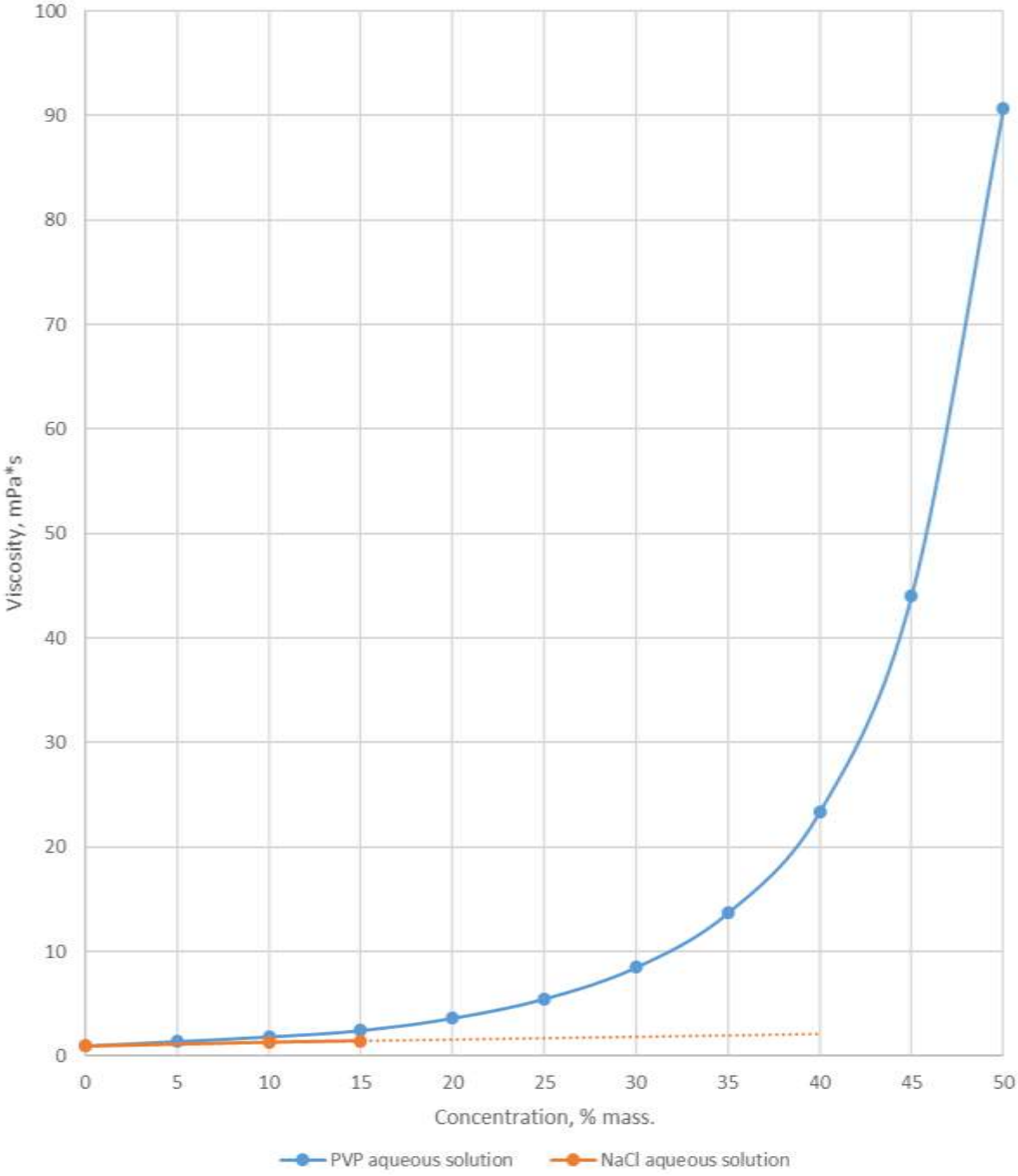

Figure A.5 Data on the viscosity of individual solutions of PVP and NaCl

Figure A.5 shows that viscosity does not change significantly down to 15%, but after this concentration the viscosity growth becomes exponentially for the polymeric solution. The viscosity

of polymeric inhibitors is comparable to the viscosity of water due to such inhibitors are used in low concentration.

Also the similar experimental data were obtained for the PVP + $MgCl_2$ solutions. Magnesium Chloride 6-hydrate ($MgCl_2 \cdot 6H_2O$, "ChDA", GOST 4209-77, manufacturer Russia, CHIMMED) was used for analysis.

Densities and viscosities of PVP + $MgCl_2$ solutions were measured for the selected compositions at temperatures from 5 °C to 25 °C and atmospheric pressure. The results obtained from the analysis of three parameters of solutions are summarized in Table A.3.

Table A.3 Physicochemical properties of PVP (8000g/mol) + $MgCl_2$ at different temperatures

# of solution	c_{Water}, wt%	c_{PVP}, wt%	c_{MgCl2}, wt%	Density, g/cm^3			Dynamic viscosity, mPa·s		
				5°C	20°C	25°C	5°C	15°C	25°C
1	80.0	20.0	0	1.0465		1.0412	10.61	7.58	5.41
2	75.0	25.0	0	1.059		1.0529	17.62	12.22	8.42
3	70.0	30.0	0	1.072		1.065	32.21	21.49	15.06
4	60.0	40.0	0	1.0996		1.0905	126.54	79.70	47.80
5	50.0	50.0	0	1.1287		1.1176	837.23	408.48	267.57
6	52.8	42.3	5.0	1.1572	1.1497	1.147	549.27	308.41	230.87
7	54.3	38.0	7.6	1.1694	1.1621	1.1596	416.14	249.72	180.00
8	56.0	33.6	10.5	1.1862	1.1793	1.1769	303.00	202.44	136.84
9	73.9	21.1	4.9	1.0958	1.091	1.0891	19.27	12.62	9.13
10	76.0	16.3	7.6	1.1083	1.1036	1.1018	13.61	9.42	7.3
11	78.3	11.2	10.5	1.121	1.1165	1.1147	9.15	7.00	5.36
12	50.0	40.0	10.0	1.2016	1.194	1.1914	1435.4	865.44	735.6
13	50.0	35.0	15.0	1.2365	1.2293	1.2267	1951.48	1114.35	676.8
14	50.2	29.9	19.9	1.2715	1.2647	1.2623	2304.08	1398.6	877.15
15	70.0	20.0	10.0	1.1409	1.1356	1.1337	27.58	20.34	13.71
16	70.0	15.0	15.0	1.1749	1.1696	1.1677	24.49	17.49	12.56
17	70.0	10.0	20.0	1.2092	1.204	1.2021	19.12	13.59	11.06

In Figure A.6 the values of densities are plotted as a function of the temperature. With decreasing temperature, the density increases, the dependence is linear: $\rho = A \cdot T + B$, where A and B are the coefficients presented in the Table A.4. The values of the coefficients depend on the concentration of the component composition: the more water, the lower the density.

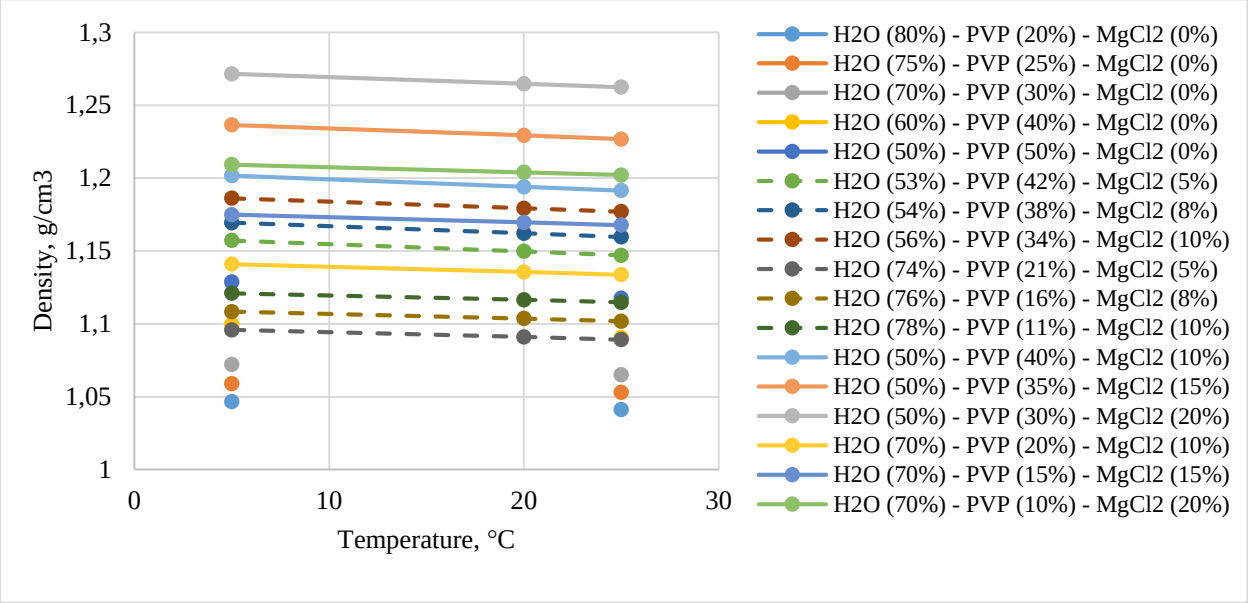

Figure A.6 Temperature dependence of the density of PVP (8000 g/mol) – $MgCl_2$ – water mixtures

Table A.4 Coefficients in equation for describing the experimental density of PVP + $MgCl_2$ solution

# of solution	Water, wt%	PVP, wt%	$MgCl_2$, wt%	A	B
1	80.0	20.0	0	-0.0003	1.0478
2	75.0	25.0	0	-0.0003	1.0605
3	70.0	30.0	0	-0.0004	1.0738
4	60.0	40.0	0	-0.0005	1.1019
5	50.0	50.0	0	-0.0006	1.1315
6	52.8	42.3	5.0	-0.0005	1.1598
7	54.3	38.0	7.6	-0.0005	1.1719
8	56.0	33.6	10.5	-0.0005	1.1885
9	73.9	21.1	4.9	-0.0003	1.0975
10	76.0	16.3	7.6	-0.0003	1.1099
11	78.3	11.2	10.5	-0.0003	1.1226

12	50.0	40.0	10.0	-0.0005	1.2042
13	50.0	35.0	15.0	-0.0005	1.239
14	50.2	29.9	19.9	-0.0005	1.2738
15	70.0	20.0	10.0	-0.0004	1.1427
16	70.0	15.0	15.0	-0.0004	1.1767
17	70.0	10.0	20.0	-0.0004	1.211

Figure A.6 provides an overview of viscosities at three different temperatures. With an increase in the concentration of PVP, the viscosity increases sharply. As can be seen from the graph, an acceptable viscosity (up to 20-30 mPa·s) is achieved with the addition of PVP no more than 20 wt%.

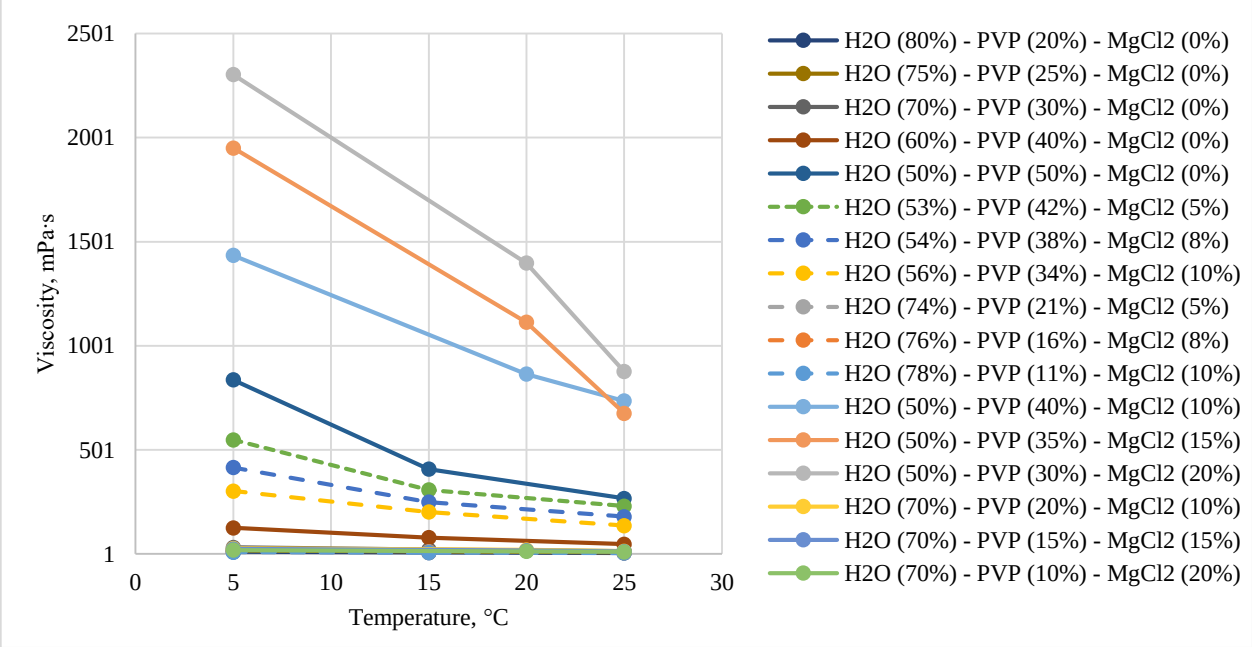

Figure A.7 Temperature dependence of the viscosity of PVP – $MgCl_2$ – water mixtures

The Figure A.7 below illustrates change in water activity depending on the mass concentration of PVP and $MgCl_2$. The higher the concentration of magnesium chloride, the lower the water activity. The main contribution to the change in water activity is made by the presence of

magnesium chloride. Below is the correlation between water activity and the freezing point of the solution. This gives us an indication about its anti-hydrate properties.

Appendix 4. The formula for the thickness of hydrate (ice) layer in the pipe

Thinness estimation of the hydrate (ice) layer on the inner wall of the in-field pipeline depending on the gas flow characteristics, ambient temperature, as well as the type and quality of the thermal insulation is one of the important characteristic. Because it affects on the hydraulic and temperature regimes of the in-field pipeline.

The formula for the amount of transferred heat, W/m^2, where the heat flux is proportional to the temperature difference between the gas and the wall, is given as follows

$$q = \pi d\alpha \cdot (T_0 - T_1), \tag{A4.1}$$

where $T_0 -$ gas temperature, ˚C; $T_1 -$ wall temperature, ˚C; $\alpha -$ heat transfer coefficient, W/(m^2·˚C), $d -$ inner diameter of the pipe, m.

Equation (A4.1) determines the heat transfer per unit area.

The heat transfer coefficient α depends on many factors: the type and characteristics of fluid, its physical properties, the size and shape of the wall, the roughness of the tube. According to the Nusselt criterion, the heat transfer coefficient can be calculated using the following equation

$$\alpha = \frac{Nu \cdot \lambda}{d}, \tag{A4.2}$$

where $\lambda -$ the thermal conductivity coefficient; W/(m·˚C), $Nu -$ the Nusselt number.

To calculate the Nusselt number for turbulent flow in channels the following correlation may be used [164]

$$Nu = 0.023 Re^{0.8} Pr^{0.43}, \tag{A4.3}$$

where $Re = \frac{wd}{v}$ – Reynolds number; $Pr = \frac{\mu C_p}{\lambda}$ – Prandtl number; w – gas velocity, m/s; v – kinematic viscosity, Pa·s; μ – dynamic viscosity, Pa·s; C_p – heat capacity, J/(kg·K).

The inner diameter of the pipe $d(x)$ due to the growth of the hydrate (ice) layer x (m) is written as

$$d(x) = d_0 - 2 \cdot x, \tag{A4.4}$$

and the flow rate $w(d)$ as

$$w(d) = w \cdot \left(\frac{d_0}{d_0 - 2 \cdot x}\right)^2. \tag{A4.5}$$

Eq. (A4.2) can be rewritten as

$$\alpha = \frac{0.023 \cdot \lambda \cdot w(d)^{0.8}}{d(x)^{0.2} \cdot {\alpha_1}^{0.43} \cdot \nu^{0.37}}, \quad {\alpha_1}^{0.43} = \frac{\lambda}{\rho \cdot C_p}, \tag{A4.6}$$

For methane gas in the pipe at given pressure and temperature

$$\alpha = \frac{0.023 \cdot \lambda_{CH4} \cdot w(d)^{0.8}}{d(x)^{0.2} \cdot {\alpha_1}^{0.43} \cdot {\nu_{CH4}}^{0.37}}, \quad {\alpha_1}^{0.43} = \frac{\lambda_{CH4}}{\rho_{CH4} \cdot C_{p\,CH4}}, \tag{A4.7}$$

$\rho_{CH4}, \lambda_{CH4}, \nu_{CH4}, C_{p\,CH4}$ – density, thermal conductivity, viscosity and heat capacity of methane, respectively.

The diagram of the model with the specified parameters is shown in Figure 7.9 (where y – pipe wall thickness; δ – thermal insulation thickness; x – hydrate thickness; R – an inner pipe radius; T_0 – the flow temperature; T_1 – the temperature of hydrate formation at a given gas pressure in the pipeline; T_2 – the temperature of the hydrate - wall of the pipe; T_3 – the temperature of the pipe - thermal insulation; T_4 – environment temperature).

Using the heat transfer formula (A4.1) and the temperature distribution associated with radial conduction through a cylindrical wall, we can derive the temperature difference for each layer as

$$T_0 - T_1 = \frac{q}{2\pi(R-x)\alpha}, \tag{A4.8}$$

$$T_1 - T_2 = \frac{q}{2\pi\lambda_{hyd}} \ln\left(\frac{R}{R-x}\right), \tag{A4.9}$$

$$T_2 - T_3 = \frac{q}{2\pi\lambda_{pipe}} \ln\left(\frac{R+\delta}{R}\right), \tag{A4.10}$$

$$T_3 - T_4 = \frac{q}{2\pi\lambda_{th}} \ln\left(\frac{R+\delta+y}{R+\delta}\right), \tag{A4.11}$$

$\lambda_{hyd}, \lambda_{pipe}, \lambda_{th}$ – the thermal conductivity coefficients of hydrate (or ice) layer, the pipe steel and the thermal insulation.

Summing the right and left part of the equations (A4.8-11), we obtain

$$T_0 - T_4 = q\left(\frac{1}{2\pi(R-x)\alpha} + \frac{\ln\left(\frac{R}{R-x}\right)}{2\pi\lambda_{hyd}} + \frac{\ln\left(\frac{R+\delta}{R}\right)}{2\pi\lambda_{pipe}} + \frac{\ln\left(\frac{R+\delta+y}{R+\delta}\right)}{2\pi\lambda_{th}}\right), \tag{A4.12}$$

From (A4.12) and (A4.8)

$$\frac{T_0-T_4}{T_0-T_1} = 1 + \alpha(R-x)\cdot\left(\frac{\ln\left(\frac{R}{R-x}\right)}{\lambda_{hyd}} + \frac{\ln\left(\frac{R+\delta}{R}\right)}{\lambda_{pipe}} + \frac{\ln\left(\frac{R+\delta+y}{R+\delta}\right)}{\lambda_{th}}\right), \tag{A4.13}$$

Eq. (A4.13) then determines the thickness of the hydrate (ice) layer on the inner wall of the pipeline.